VOLUME 107

THE ASTROPHYSICAL JOURNAL

AN INTERNATIONAL REVIEW OF SPECTROSCOPY AND ASTRONOMICAL PHYSICS

MARCH 1948

THE UNIVERSITY OF CHICAGO PRESS
CHICAGO, ILLINOIS, U.S.A.

March 1948 Vol. 107, No. 2

THE ASTROPHYSICAL JOURNAL

AN INTERNATIONAL REVIEW OF SPECTROSCOPY AND ASTRONOMICAL PHYSICS

The Astrophysical Journal is published bimonthly by the University of Chicago at the University of Chicago Press, 5750 Ellis Avenue, Chicago, Illinois, during July, September, November, January, March, and May. ¶The subscription price is $12.00 a year; the price of single copies is $3.00. Orders for service of less than a full year will be charged at the single-copy rate. ¶Postage is prepaid by the publishers on all orders from the United States and its possessions, Argentina, Bolivia, Brazil, Chile, Colombia, Costa Rica, Cuba, Dominican Republic, Ecuador, Guatemala, Haiti, Republic of Honduras, Mexico, Morocco (Spanish Zone), Nicaragua, Panama, Paraguay, Peru, Rio de Oro, El Salvador, Spain (including Balearic Islands, Canary Islands, and the Spanish Offices in Northern Africa; Andorra), Spanish Guinea, Uruguay, and Venezuela. ¶Postage is charged extra as follows: for Canada and Newfoundland, 42 cents on annual subscriptions (total $12.42); on single copies, 7 cents (total $3.07); for all other countries in the Postal Union, 96 cents on annual subscriptions (total $12.96), on single copies 16 cents (total $3.16). ¶Patrons are requested to make all remittances payable to The University of Chicago Press, in United States currency or its equivalent by postal or express money orders or bank drafts.

The following are authorized agents:

For the British Empire, except North America, India, and Australasia: The Cambridge University Press, Bentley House, 200 Euston Road, London, N.W. 1, England. Prices of yearly subscriptions and of single copies may be had on application.

Claims for missing numbers should be made within the month following the regular month of publication. The publishers expect to supply missing numbers free only when losses have been sustained in transit, and when the reserve stock will permit.

Business correspondence should be addressed to The University of Chicago Press, Chicago 37, Illinois.

Communications for the editors and manuscripts should be addressed to: W. W. Morgan, Editor of The Astrophysical Journal, Yerkes Observatory, Williams Bay, Wisconsin.

Line drawings and photographs should be made by the author, and all marginal notes such as co-ordinates, wave lengths, etc., should be included in the cuts. It will not be possible to set up such material in type.

One copy of the corrected galley proof should be returned as soon as possible to the editor, Yerkes Observatory, Williams Bay, Wisconsin. Authors should take notice that the manuscript will not be sent to them with the proof.

The cable address is "Observatory, Williamsbay, Wisconsin."

The articles in this journal are indexed in the *International Index to Periodicals*, New York, N.Y.

Applications for permission to quote from this journal should be addressed to The University of Chicago Press, and will be freely granted.

Entered as second-class matter, July 21, 1240, at the Post-Office at Chicago, Ill., under the act of March 3, 1879. Acceptance for mailing at special rate of postage provided for in United States Postal Act of October 3, 1917, Section 1103, amended February 28, 1925.

[PRINTED IN U.S.A.]

THE ASTROPHYSICAL JOURNAL

AN INTERNATIONAL REVIEW OF SPECTROSCOPY AND ASTRONOMICAL PHYSICS

VOLUME 107 MARCH 1948 NUMBER 2

ANALYSIS OF THE MILKY WAY IN NORTHERN CASSIOPEIA AND CEPHEUS

ELAINE NANTKES AND ROBERT H. BAKER

University of Illinois Observatory

Received November 14, 1947

ABSTRACT

The analysis of the Milky Way in the region of northern Cassiopeia and Cepheus is based on star counts to magnitude 15, published color excesses of stars, and published counts of extragalactic nebulae. The obscuration is represented by two cloud systems: the first, at the distance of 300–500 parsecs, accounts for most of the patterns seen in the region; the second, at the distance of 800 parsecs, is more nearly uniform in density. Throughout the region the star-density functions decrease with increasing distance from the sun.

The region of the Milky Way to be considered here lies, in general, between galactic latitudes 0° and +30° and between galactic longitudes 75° and 103°. It is a northward extension of the region discussed in a previous paper.[1] Together, these two studies cover a somewhat larger area than did an earlier study made at Harvard of this region of Cassiopeia.[2]

THE STAR COUNTS

The material used in this study was obtained from 11 pairs, each pair having 10 and 60 minutes' exposures, of plates taken with the 4-inch Ross-Lundin camera of Harvard Observatory and from 25 pairs of plates taken with the 4-inch Ross-Fecker camera at the University of Illinois. The pairs are taken on centers about 5° apart. The scale of the plates is 290″ per millimeter.

The method of counting the stars is the same as that described in the previous paper. Magnitude standards for calibrating the reference scale are available on plates containing Selected Areas 1, 2, and 7. These are carried by overlapping plates to the remainder of the region. Magnitudes for stars brighter than 13.0 mag. were taken from the *Bergedorfer Spektral-Durchmusterung*, and for fainter stars magnitudes from the *Mount Wilson Catalogue*[3] were used. No corrections of any kind have been made to the star counts.

In preparation for the analysis of the counts the region was divided into areas, in each of which the surface distribution of stars seems fairly uniform and different from that in the surrounding areas. The region is also divided by parallels of galactic latitude into

[1] *Ap. J.*, 99, 125, 1944.

[2] *Harvard Circ.*, No. 424, 1939.

[3] *Carnegie Inst. Washington Pub.*, No. 402, 1930.

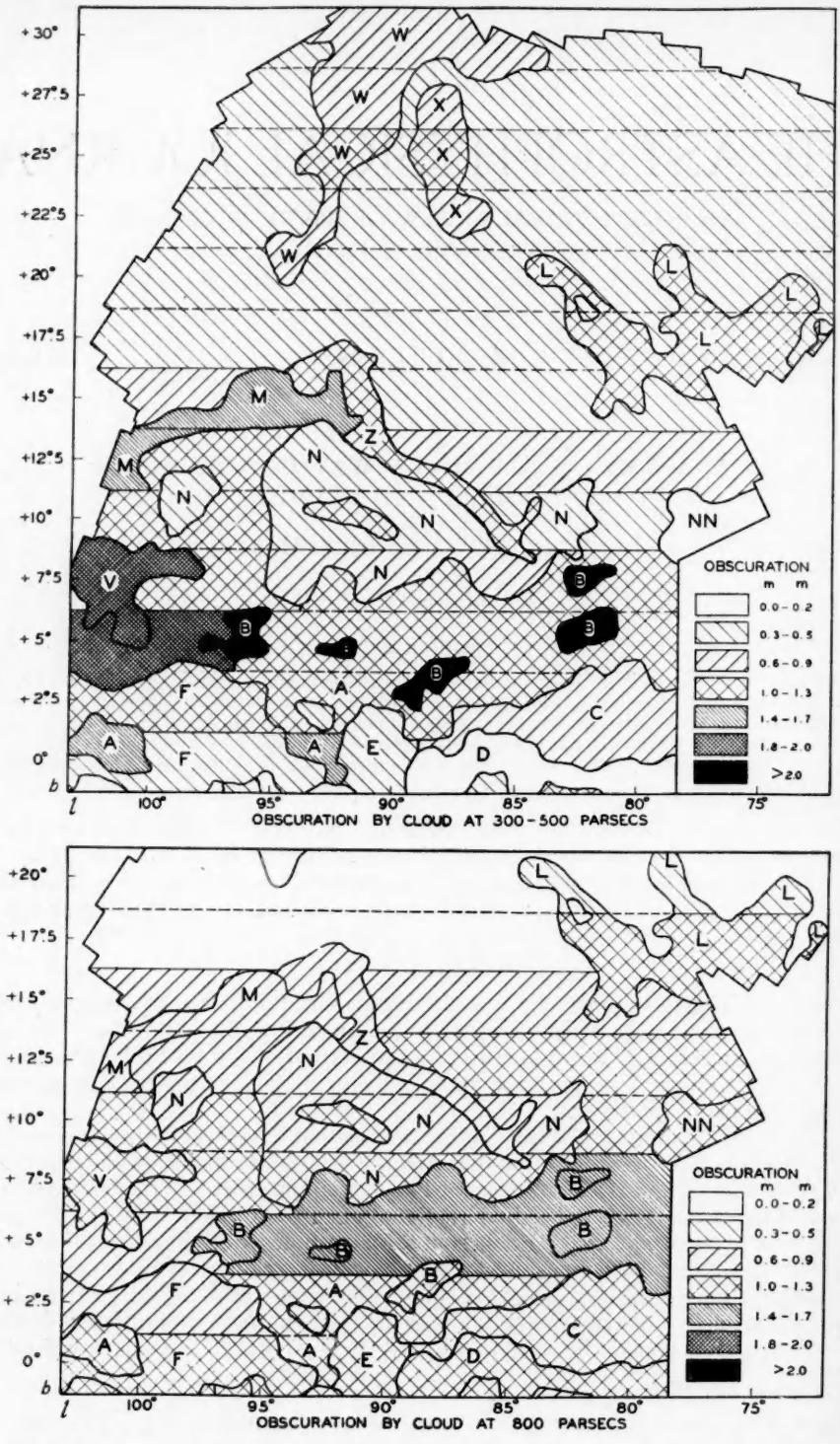

FIG. 1.—Divisions of the Cassiopeia-Cepheus region, showing obscuration at 300–500 and 800 parsecs

zones 2°.5 wide. Figure 1 shows the arrangement of divisions. The areas are designated by the same letters as were used in the Harvard study.

Table 1 shows the values of the mean log $N(m)$ representing the counts in the different divisions, where $N(m)$ is the number of stars per square degree brighter than the apparent photographic magnitude, m. For use in the analysis these are converted to log $A(m)$ at magnitude intervals for $m = 9.5$ to $m = 14.5$, where $A(m)$ is the number of stars per square degree between $m - \frac{1}{2}$ and $m + \frac{1}{2}$.

TABLE 1

MEAN LOG $N(m)$ FOR THE DIFFERENT DIVISIONS

Area	Zone	Longitude of Center*	Limiting Magnitude							Obscuration		
			9.0	10.0	11.0	12.0	13.0	14.0	15.0	At 300 Parsecs	At 500 Parsecs	At 800 Parsecs
A	0°	97°	0.41	0.81	1.23	1.59	1.88	2.18	2.44	.....	1m5	1m1
D	0	83	.69	1.16	1.56	1.96	2.36	2.67	2.88	.....	0.0	1.0
E	0	90	.55	1.00	1.41	1.78	2.10	2.41	2.66	.....	0.5	1.2
F	0	99	.55	0.98	1.41	1.76	2.07	2.38	2.65	.....	0.5	1.2
A	+ 2.5	91	.50	0.86	1.26	1.59	1.89	2.21	2.38	.....	1.2	1.3
C	+ 2.5	82	.52	0.99	1.37	1.73	2.07	2.38	2.57	.....	0.8	1.0
F	+ 2.5	100	.54	0.93	1.28	1.65	1.99	2.37	2.66	.....	1.0	0.7
B	+ 5	89	.12	0.56	0.96	1.28	1.55	1.87	2.06	.....	2.5	1.5
	+ 5	87	.47	0.81	1.17	1.51	1.82	2.11	2.34	.....	1.3	1.5
	+ 5	100	.21	0.53	0.95	1.31	1.68	2.04	2.38	1m8	.....	0.6
N	+ 7.5	89	.45	0.79	1.20	1.57	1.92	2.26	2.58	0.7	.....	1.0
V	+ 7.5	101	.27	0.55	0.95	1.24	1.54	1.86	2.11	2.0	.....	1.1
	+ 7.5	85	.47	0.86	1.19	1.56	1.89	2.14	2.38	.....	1.0	1.5
	+ 7.5	97	.23	0.61	1.00	1.42	1.75	2.06	2.35	1.3	.....	1.0
N	+10	89	.38	0.77	1.22	1.60	1.95	2.27	2.62	0.5	.....	0.8
NN	+10	77	.54	0.98	1.38	1.78	2.08	2.35	.....	.....	0.0	1.2
	+10	80	.55	0.90	1.25	1.65	1.93	2.21	.....	.....	0.5	1.2
	+10	98	.30	0.67	1.01	1.42	1.75	2.05	2.33	1.1	.....	1.0
N	+12.5	89	.32	0.71	1.16	1.51	1.92	2.28	2.59	0.5	.....	0.7
Z	+12.5	92	.27	0.56	0.91	1.32	1.67	2.00	2.34	1.3	.....	0.7
	+12.5	83	.54	0.86	1.18	1.56	1.87	2.14	2.55	.....	0.7	1.0
	+12.5	97	.39	0.62	1.04	1.39	1.73	2.06	2.37	1.1	.....	0.8
M	+15	96	.22	0.50	0.86	1.20	1.51	1.82	2.09	1.6	.....	0.7
	+15	84	.35	0.78	1.18	1.56	1.91	2.18	2.50	.....	0.3	0.7
	+15	99	.47	0.66	1.08	1.43	1.78	2.09	2.39	0.6	.....	0.7
L	+17.5	78	.12	0.53	0.90	1.23	1.55	1.80	2.07	1.1	.....	1.0
	+17.5	93	.35	0.65	1.08	1.45	1.81	2.14	2.49	0.5	.....	0.0
L	+20	78	.22	0.43	0.82	1.19	1.55	1.85	2.11	1.1	.....	0.3
	+20	86	.28	0.69	1.07	1.44	1.78	2.11	2.46	0.4	.....	0.0
W	+22.5	93	.16	0.61	0.92	1.27	1.62	1.94	2.30	0.8	.....	0.0
X	+22.5	88	.22	0.66	0.99	1.32	1.64	1.96	2.23	0.8	.....	0.0
	+22.5	86	.31	0.66	1.07	1.44	1.80	2.12	2.44	0.3	.....	0.0
W	+25	92	.18	0.62	0.92	1.25	1.58	1.88	2.15	1.1	.....	0.0
X	+25	88	.29	0.55	0.92	1.23	1.55	1.86	2.13	1.1	.....	0.0
	+25	85	.34	0.66	1.07	1.46	1.80	2.13	2 42	0.3	.....	0.0
W	+27.5	92	.28	0.60	0.95	1.30	1.59	1.89	2 11	0.9	.....	0.0
	+27.5	85	.22	0.62	1.05	1.44	1.77	2.07	2.29	0.3	.....	0.0
W	+30	90	.28	0.56	0.92	1.26	1.56	1.88	2.15	0.8	.....	0.0
	+30	80	0.17	0.65	1.12	1.40	1.74	2.00	2 21	0.3	.....	0.0

* All galactic co-ordinates in this paper are referred to the conventional pole at right ascension 12h40m, declination +28°.

ANALYSIS OF THE STAR COUNTS

The analysis of the star counts is made with the (m, log π) tables which have been described by Bok.[4] The amount of absorption used in the analysis is attributed to two dust clouds, whose varying densities explain the patterns found in the region. Table 1 shows the amount of obscuration found in each of the different divisions.

The 800-parsec cloud, which appears in the region south of the galactic equator, extends northward, reaching its greatest density in the +5° zone. It then decreases slightly in density through the +15° zone, where it seems to break off quite abruptly. The nearer cloud also extends from the region south of the equator, where it appears at the distance of 500 parsecs from the sun. The extreme eastern part of the +5° zone, areas M, N, and Z, and all parts of the region east of them were found to be more easily analyzed by placing the obscuration at 300 instead of at 500 parsecs. North of the +15° zone the obscuration is also placed at 300 parsecs. This nearer cloud, which is considerably more irregular in density than the other is, accounts for most of the patterns which are seen. Area V and the small B patches are much darker than any of the surrounding divisions. In the latitudes above +20° the cloud is comparatively thin except for two darker patches in the vicinity of the North Pole.

COMPARISONS WITH RELATED DATA

The amounts of obscuration which have been used in the analysis compare, in general, quite favorably with the values of obscurations taken from other sources.

Hubble's[5] counts of extragalactic nebulae indicate an absorption of more than 3.0 mag. from latitude 0° through latitude 10°, for the central part of the +15° zone, and for area L. These values undoubtedly include obscuration at a greater distance from the sun than are the clouds which have been used in the analysis. In the eastern part of the +15° zone Hubble's counts indicate a total absorption of 1.3 mag., which is exactly the value adopted in the analysis. In areas W and X at latitude +25°, Hubble's counts show a value of 0.9 mag. as compared to 1.1 mag. adopted here. In the remainder of the +25° zone we have used a value of 0.3 mag. where the nebulae counts suggest 0.2 mag. In area W +30° we use 0.8 mag., where the nebulae counts suggest 0.6 mag. It is to be expected that in the higher latitudes the values of obscuration determined from Hubble's counts should be more nearly in agreement with the total values used in the analysis, since there is much less likelihood of the existence of obscuring material beyond the range of the star counts in the high, than in the low, latitudes.

Photographic absorptions derived from color excesses determined at the University of Illinois give a total value of 1.0 mag. at 800 parsecs for Selected Area 2. This is exactly the amount used in the analysis of the western part of the +15° zone.

Slocum and Sitterly[6] have found in Selected Area 7 a total absorption of 1.5 mag. at 500 parsecs, as compared to the surrounding region, which they consider unobscured. Selected Area 7 lies in the northern border of area L, where the adopted total values of obscuration at 800 parsecs vary from 1.0 to 1.6 mag. greater than those in the surrounding regions, again giving satisfactory agreement between the two sources.

In Selected Area 1, Stebbins, Huffer, and Whitford[7] have found evidence of an absorbing cloud of 0.3 or 0.4 mag. at a distance of 200–300 parsecs. The results of work by Keenan and Babcock,[8] who have found a cloud of 0.3 mag. at 200–400 parsecs in the vicinity of Selected Area 1, conform very closely with the Stebbins, Huffer, and Whitford results. Seares[9] has shown that within a radius of 10° of the pole there exist small fields in

[4] *The Distribution of the Stars in Space* (Chicago: University of Chicago Press, 1935).

[5] *Mt. W. Contr.*, No. 485, 1934; *Ap. J.*, **79**, 8, 1934.

[6] *Harvard Bull.*, No. 905, 1937.

[7] *Ap. J.*, **90**, 207, 1939.

[8] *Ap. J.*, **93**, 64, 1941.

[9] *Ap. J.*, **98**, 261, 1943.

TABLE 2

ADOPTED VALUES OF UNOBSCURED LOG $A(m)$

ZONE	MAGNITUDE					
	9.5	10.5	11.5	12.5	13.5	14.5
0°0	1.15	1.58	2.00	2.35	2 62	2.83
+ 2.5	1.06	1.53	1.94	2.31	2.59	2.80
+ 5.0	1.00	1.48	1.88	2.21	2.50	2.74
+ 7.5	0.95	1.41	1.70	2.16	2.43	2.69
+10.0	0.96	1.33	1.74	2.08	2.37	2.64
+12.5	0.82	1.25	1.64	2.00	2.24	2.55
+15.0	0.74	1.15	1.52	1.86	2.13	2.42
+17.5	0.64	1 03	1.38	1.74	2 03	2.30
+20.0	0.60	0 98	1.34	1.67	1.94	2.19
+22.5	0.57	0 94	1.32	1.65	1.94	2.18
+25.0	0.57	0.95	1 28	1.64	1.90	2.13
+27.5	0.57	0 94	1.26	1.59	1.83	2.04
+30.0	0.53	0.92	1.20	1.54	1.79	1.97

TABLE 3

DENSITY FACTORS

$D(z)$ FOR HIGHER LATITUDES

z (PARSECS)	b								
	+10°0	+12°5	+15°0	+17°5	+20°0	+22°5	+25°0	+27°5	+30°0
40	0.9	1.0	1.0	1.0	1.0	1.0	1.0	1.0	1.0
60	.9	1.0	0.9	0.9	0.9	1.0	1.0	1.0	1.0
100	.8	1.1	0.8	0.8	0.8	0.9	1.0	1.0	1.0
150	.8	1.1	0.7	0.7	0.8	0.8	0.9	0.9	0.9
250	.8	0.9	0.7	0.8	0.8	0.8	0.9	0.9	1.0
400	.5	0.7	0.6	0 6	0.6	0.8	0.8	0.8	1.0
630	0.5	0.8	0.5	0.6	0.5	0.7	0.8	0.6	0.6

$D(r)$ NEAR THE EQUATOR

r (PARSECS)	b				
	0°0	+2°5	+5°0	+7°5	+10°0
125	1.0	1.0	1.0	1.0	1.0
200	1.0	1.0	1.0	1.0	0.9
300	0.9	0.9	0.9	0.9	0.85
500	0.9	0.9	0.9	0.8	0.7
800	0.75	0.75	0.75	0.7	0.6
1250	0.45	0.45	0.4	0.4	0.35
2000	0.2	0.2	0.15	0.1	0.1
3000	0.03	0.03	0.03	0.03	0.03

which the color excesses of stars indicate slightly more than the small amount of absorption which is found throughout the entire polar cap. Our star counts also have shown patterns near the pole. The amounts of absorption used in the analysis of these areas correspond quite closely to those suggested by the colors. There seems to be quite close agreement among all the results of the various determinations of amounts of obscuration.

THE DENSITY GRADIENTS

Table 2 shows the true values of log $A(m)$ for the different zones, while Table 3 shows the density factors, provided that the correct amounts of absorption have been used in the analysis. The factors $D(z)$ in the upper part of Table 3 represent the star densities in latitudes $+10°$ to $+30°$ relative to the density at the same distance z above the galactic plane at latitude 90°. The unit values used for z = 40–630 parsecs are the values of $D(r)$ for latitude 90°. They are 0.9, 0.8, 0.6, 0.5, 0.3, and 0.16.

The factors $D(r)$ appearing in the lower part of the table show the star densities at distances r from the sun relative to unit density in the sun's vicinity. The density factors above latitude $+20°$ are found to be somewhat higher than the functions in the corresponding southern latitudes. By adding a small amount of absorption in those latitudes, the density factors for the northern and southern regions could be made to be almost identical, thus indicating symmetry between the two.

RADIAL VELOCITIES OF 204 STARS IN THE REGION OF THE HYADES*

RALPH E. WILSON
Mount Wilson Observatory
Received November 14, 1947

ABSTRACT

This investigation completes the determination of the radial velocities of all suggested members of the Taurus cluster brighter than 10.0 visual magnitude, with seven fainter stars. Of the 204 stars recently observed at Mount Wilson for radial velocities, 93, all located within 15° of the cluster center, are classified as definitive members.

The motions of the members of the nearer star clusters, such as the Hyades, Pleiades, and Praesepe, constitute one of the best sets of data available for the determination of stellar distances. If the population is large, the cluster parallaxes in combination with reliable magnitudes and spectral classifications become very useful in studies of the relation between absolute magnitude and spectral type.

The early Groningen photographic surveys of the Hyades,[1] though subject to considerable systematic and accidental errors, suggested a fairly large cluster population. Under the stimulus of L. Boss's classical study[2] of the motions of the brighter stars, a number of investigators have devoted considerable time during the last thirty years to a search for additional members.[3] As a result, by 1941 some three hundred stars were suggested as "certain," "probable," or "doubtful" members of the Taurus cluster. The principal criteria in the selection of these stars were proper motions of about 0".1 per year in the general direction of the Boss convergent. Rather large departures were allowed, especially among the stars listed as "probable" or "doubtful," and among these appear a number of faint early-type stars for which actual cluster membership would entail luminosities not at all in accord with those generally associated with their spectra. The question of cluster membership is further complicated by the proximity of the Taurus convergent to that of Kapteyn's stream I, which is especially pronounced among stars of types A and F, and by the possibility that the cluster itself may share in the motion of the larger stream. It had been clear for some time that the proper motions alone do not suffice to establish cluster membership, especially for stars at considerable distances from the center, and that additional information concerning the radial velocities was highly desirable.

J. H. Moore's catalogue[4] gives radial velocities for 68 cluster stars, a few of them, however, being based on one plate only. In the decade following its publication only ten more velocities were published. In 1941, however, I found in the Mount Wilson files spectrograms of 89 additional stars and decided to complete the determination of the velocities of all the stars in the Hyades list brighter than visual magnitude 10.0. Two plates were deemed sufficient if the measures agreed reasonably well with each other and with the cluster velocity; in all other cases three or more plates were secured. All the plates were

* *Contributions from the Mount Wilson Observatory, Carnegie Institution of Washington*, No. 741.

[1] J. C. Kapteyn and W. de Sitter, *Groningen Pub.*, No. 14, 1904.

[2] *A. J.*, **26**, 31, 1908.

[3] For a history of that period and a complete bibliography see J. M. Ramberg, *Stockholms Obs. Ann.*, Vol. **13**, No. 9, 1941.

[4] *Pub. Lick Obs.*, Vol. **18**, 1932.

taken with a one-prism spectrograph attached to the 60-inch reflector. Two cameras were used, the brighter stars being observed with an 18-inch camera giving a dispersion of 38 A/mm at $H\gamma$, the fainter with a 9-inch camera, dispersion 75 A/mm.

The radial velocities of the 204 stars in Table 1 are based upon 605 plates, 75 per cent of which were secured in the period 1942–1946. All the plates of this epoch were measured by the writer. The headings of the columns of the table are largely self-explanatory. The magnitudes are mainly (*a*) photovisual magnitudes on the International System by Eric Holmberg[5] for stars within 4° of the center, and (*b*) Harvard Draper magnitudes, further from the center. Among the stars observed are seven fainter than the limit set when the program was begun. The classifications of spectra were made by the writer on the Mount Wilson system. The proper motions are compilations by the writer, based upon a number of sources, all of which were roughly reduced to the system of the *Albany General Catalogue*.[6] The probable errors of the radial velocities were computed from the relation

$$r = 0.67\sqrt{\frac{v\,v}{m\,(m-1)}}.$$

Of these stars, 93 are considered to be cluster members, 8 others are probable, and 32 must be considered, mainly on evidence other than the radial velocities, as doubtful. On the basis of the radial velocities alone, 71 of the stars may be eliminated from further consideration as cluster members. Among these are all the faint stars with early-type spectra and nearly all the stars situated more than 15° from the center. The probable spectroscopic binaries number 23, of which only 6, all located near the center, appear to be members; 7 seem to show two spectra. The most interesting of the binaries is BD+16°516 (9.2, G9), which from measures on five plates shows a velocity range of 242 km/sec. The velocities of both components of 5 visual binaries were measured. Only 1 of these, HD 26015, is considered a definitive member, although 3 others—HD 20430–20439, HD 21663, and HD 33204—are probable outliers. Eight of the stars have large velocities (Table 2). Two of these, though widely separated, may have common motion.

A discussion of the motions and absolute magnitudes of the members of the Taurus cluster will appear soon.

[5] *Lund Medd.*, Ser. II, No. 113, 1944.

[6] *Carnegie Inst. Washington Pub.* No. 468, 1938.

TABLE 1

RADIAL VELOCITIES OF 204 STARS IN THE HYADES REGION

BD	HD	(1950) R.A.	(1950) Dec.	m_v	Sp.	μ	θ	ρ r (Km/Sec)	Pl.	Notes
10° 374..	17663	2h47m7	+10° 25′	9.3	G8	0″.144	92°	+ 54.9±1.0	3	
29 503..	.....	54.8	+29 28	9.2	G8	.206	106	+ 25.8±0.5	3	D
11 456..	20278	3 13.2	+11 26	7.9	G1	.193	91	+ 43.6±1.5	4	D
7 493..	20430	14.8	+ 7 29	7.4	G0	.187	92	+ 31.1±0.8	3	P
7 494..	20439	14.9	+ 7 30	7.7	G1	.194	92	+ 31.2±2.0	4	P
19 505..	20600	3 16.6	+19 32	8.4	F9	.102	97	+ 33.0±1.8	3	D
11 462..	20717	17.9	+12 10	7.3	F6	.149	83	+ 44.8±1.8	4	D
8 496..	20727	17.9	+ 8 51	8.3	G3	.301	103	+ 11.1±0.6	3	
25 545..	21168	22.8	+25 41	8.6	F8	.087	116	+ 56: var.	4	1
19 547..	21663A	27.6	+19 56	7.9	G5	.170	109	+ 25.2±1.5	4	P
.....	21663B	3 27.6	+19 56	9.5	K2	.....	.....	+ 28.3±0.5	3	P
23 465..	.....	29.9	+23 31	9.0	K0	.168	102	+ 32.7±0.5	2	P
10 461..	22254	32.6	+11 13	8.3	F9	.180	95	+ 63.4±1.9	3	
19 562..	22328	33.5	+19 54	7.6	F6	.101	114	+ 34.1±0.4	3	D
20 598..	.....	34.6	+21 11	9.0	K0	.159	103	+ 35.4±1.1	3	H
18 514..	.....	3 34.6	+18 27	8.6	F8	.147	96	+ 41.8±1.9	4	H
26 595..	.....	37.1	+26 48	9.1	G8	.156	131	−198.4±0.4	3	
3 512..	22917	38.4	+ 3 25	9.3	F8	.138	86	+ 18.0±1.9	4	
26 601..	23007	39.5	+26 26	7.8	K0	.100	112	+ 33.0±1.9	4	D
27 555..	.....	41.4	+28 03	9.0	G2	.086	134	+ 10.4±1.7	3	
24 550..	23375	3 42.6	+24 19	8.6	A8	.078	132	+ 19.8±1.6	4*	2
25 615..	23488	43.4	+25 43	8.7	A7	.078	152	+ 3.6±2.7	4	
22 550..	23514	43.7	+22 47	9.2	F8	.064	119	+ 12.0±0.4	3	
9 494..	23841	45.8	+ 9 30	7.0	G8	.072	80	− 79.8±2.2	3	
23 556..	23822	46.0	+23 42	6.6	F0	.077	133	+ 18.6±2.1	4	
22 575..	23965	3 47.1	+22 21	7.9	F7	.179	111	+ 11.7±0.8	3	
16 516..	.....	47.4	+17 06	9.2	G9	.104	73	+ 21: var.	5	3
23 571..	.....	48.0	+23 46	9.5	K5	.154	108	+ 38.8±1.7	5	H
21 544..	.....	49.8	+21 50	9.5	G0	.120	126	+ 58.2±2.7	3	4
26 633..	24301	49.9	+26 31	8.0	G1	.163	132	+ 26.6±1.0	3	
27 589..	24365	3 50.7	+27 59	7.8	G5	.094	95	+ 21.7±0.8	3	
16 529..	.....	52.3	+16 51	9.9	K2	.172	102	+ 39.1±1.8	2	H
22 596..	24570	52.4	+23 13	8.6	K0	.103	93	+ 42.9±0.6	3	D
26 645..	24690	53.4	+26 36	9.2	A8	.082	116	+ 8.1±1.0	3	
26 646..	.....	53.9	+27 10	9.1	G9	.090	96	+ 34.2±0.4	2	D
22 608..	24844	3 54.8	+22 47	9.1	K0	.153	78	+ 27.1±0.6	3	
24 603..	24997	56.2	+24 55	9.2	F8	.106	123	− 23.6±0.2	3	
24 605..	25065	56.9	+24 33	8.7	G0	.095	116	+ 26.2±0.3	3	D
13 625..	25153	57.5	+14 10	7.7	F5	.065	101	+ 39.0±1.0	3	D
19 641..	.....	57.7	+20 14	8.6	G2	.157	108	+ 37.6±2.0	2	H
22 626..	25532	4 01.2	+23 16	8.3	F6	.134	128	−113.0±0.3	3	
25 674..	.....	02.9	+25 40	9.0	G8	.137	103	+ 24.0±1.6	4	D
15 582..	25825	03.3	+15 34	7.9	G2	.114	95	+ 35.6±1.5	3	H
14 657..	26015A	04.9	+15 02	5.9	F2	.136	100	+ 34.9±1.7	2*	H
.....	26015B	04.9	+15 02	8.7	G7	.....	.....	+ 40.8±0.3	2	H
13 647..	26091	4 05.5	+13 25	8.8	K1	.074	88	+ 20.3±0.9	3	
28 624..	26090	05.8	+29 03	8.5	G2	.101	99	+ 41.3±1.8	3	D
18 594..	26345	07.8	+18 18	6.6	F6	.120	110	+ 33.6±2.1	2*	H
0 711..	26623	10.0	+ 0 38	9.2	F7	.077	85	+ 25.5±1.5	3	
16 570..	.....	10.3	+16 40	9.1	G2	0.153	109	− 7.3±1.8	3	

TABLE 1—*Continued*

BD	HD	(1950) R.A.	(1950) Dec.	m_v	Sp.	μ	θ	ρ (r) (Km/Sec)	Pl.	Notes
23° 649..	26736	4h11m5	+23° 29′	8.0	G4	0″.129	106°	+ 42.2±2.2	4	H
22 657..	26737	11.5	+22 20	7.0	F4	.101	108	+ 37.9±1.7	4	H
14 673..	26756	11.6	+14 30	8.6	G5	.129	101	+ 37.9±1.3	3	H
12 566..	26767	11.7	+12 20	8.3	G3	.115	92	+ 38.6±1.8	3	H
10 551..	26784	11.8	+10 35	7.1	F7	.125	96	+ 36.6±1.7	3	H
21 608..	.....	4 12.3	+22 11	9.1	K0	.....	.....	+ 22.0±1.1	3	
20 721..	26874	12.8	+20 42	8.1	G6	.121	113	+ 27.7±0.8	3	H:
15 603..	26911	12.9	+15 17	6.4	F5	.123	106	+ 37.0±1.8	4*	H
15 604..	.....	13.1	+15 42	9.5	G9	.078	134	+ 56.4±0.2	3	
21 612..	.....	13.6	+21 47	8.9	G7	.119	109	+ 40.7±0.3	2	H
4 666..	27089	4 14.3	+ 4 25	8.6	F8	.172	87	+ 59.8±0.3	3	
18 613..	.....	14.4	+19 13	9.0	G7	.102	125	+ 4.4±2.7	3	5
17 703..	27149	15.1	+18 07	7.7	G4	.116	112	+ 44.0±2.7	4	6, H
19 694..	27250	16.0	+19 47	8.6	G7	.101	104	+ 40.6±1.6	2	H
17 707..	27282	16.3	+17 24	8.5	G5	.098	98	+ 40.0±0.2	2	H
15 612..	27371	4 16.9	+15 31	3.9	G8	.121	102	+ 38.5±1.4	4*	H
13 662..	27372	16.9	+14 03	7.8	G8	.212	160	− 16.6±0.8	3	
23 675..	27370	17.1	+23 28	7.2	G6	.148	108	+ 8.8±0.8	3	
13 663..	27397	17.1	+13 55	5.6	F1n	.118	101	+ 40: var.	3*	7, H
18 623..	27406	17.3	+19 07	7.7	F9	.125	106	+ 38.7±1.5	3	H
18 624..	27429	4 17.5	+18 37	6.2	F3	.118	114	+ 37.6±0.5	6	8, H
14 682..	27459	17.8	+14 59	5.3	A9n	.113	102	+ 39.7±2.8	3*	H
13 665..	27483	18.1	+13 45	6.3	F4	.118	102	+ 37.0±0.9	6	9, H
18 629..	27534	18.6	+18 18	7.0	F5	.111	108	+ 36.5±2.0	4	H
14 685..	.....	18.7	+14 44	10.1	G3	.135	120	+ 47.5±2.1	4	D
14 687..	27561	4 18.8	+14 18	6.7	F6	.120	103	+ 38.4±0.5	2*	H
5 636..	27610	19.0	+ 5 15	9.0	F3	.072	79	+ 22.4±1.4	4	
13 668..	27628	19.2	+13 58	5.7	A4	.117	102	+ 37.7 var.	4*	H
31 769..	.....	19.9	+32 06	8.8	F8	.104	133	+ 79.4±1.0	3	
16 585..	27685	19.9	+16 40	7.9	G5	.145	106	+ 33.2±1.0	2	H
13 671..	.....	4 19.9	+14 08	10.1	G3	.107	107	+ 39.0±0.4	2	H
21 635..	27732	20.4	+21 16	9.1	G7	.105	115	+ 38.8±1.4	2	H
19 708..	.....	20.4	+19 32	9.1	G7	.094	109	+ 36.4±1.2	2	H
24 654..	27731	20.5	+24 17	7.2	F6	.106	114	+ 33.6±1.2	2*	H
15 616..	.....	20.5	+15 39	10.7	K5	.130	104	+ 48.1±0.3	2	H
14 691..	27771	4 20.7	+14 33	9.3	G8	.107	98	+ 44.2±1.5	2	H
21 641..	27808	21.3	+21 37	8.0	F8	.127	117	+ 33.4±1.0	2	H
14 693..	27836	21.3	+14 39	7.7	G1	.106	102	+ 37.9±0.9	3	H
17 715..	.....	21.4	+17 53	10.0	K4	.111	97	+ 46.9±1.0	3	H
16 589..	27835	21.4	+16 16	8.3	G0	.083	100	+ 38.4±0.6	3	H
17 716..	.....	4 21.5	+17 20	10.0	K0	.028	78	+ 2.1±1.3	3	
16 593..	.....	22.1	+16 52	10.4	K2	.087	101	+ 43.1±1.9	3	H
23 692..	27972	22.8	+23 26	8.9	F8	.082	121	+ 27.7±2.2	3	D
17 721..	27990	22.9	+17 55	9.1	K0	.098	102	+ 38.0±0.5	2	H
17 722..	28007	23.1	+17 20	7.6	F2	.050	107	+ 30: var.	4	10
21 644..	28033	4 23.3	+21 22	7.5	F9	.111	108	+ 42: var.	4	11, H
4 690..	28069	23.3	+ 5 01	7.2	F6	.097	85	+ 31.1±0.3	3	H
16 598..	28068	23.5	+16 44	8.2	G1	.099	99	+ 40.4±2.7	4	H
13 684..	.....	24.6	+14 09	10.6	K5	.118	112	+ 38.7±0.1	2	H
11 614..	28237	25.0	+11 39	7.4	G0	0.138	92	+ 42.2±1.1	2	H

TABLE 1—*Continued*

BD	HD	(1950) R.A.	(1950) Dec.	m_v	Sp.	μ	θ	ρ r (Km/Sec)	Pl.	Notes
13° 685..	28258	4h25m2	+13°46′	9.2	K0	0″.115	93°	+ 42.0±0.6	2	H
19 727..	28291	25.6	+19 38	8.4	G7	.123	114	+ 36.4±0.6	2	H
18 640..	28305	25.7	+19 04	3.8	G9	.118	109	+ 38.1±0.6	3*	H
16 606..	28344	26.0	+17 10	7.8	G2	.105	106	+ 40.5±1.4	3	H
15 633..	28363	26.1	+16 03	6.7	F8	.111	106	+ 45: var.	4	12, H
26 722..	.....	4 26.4	+26 34	9.0	G7	.096	117	+ 37.3±1.9	3	H
17 731..	28394	26.5	+17 26	7.0	F8	.094	107	+ 33.2±2.4	2*	H
17 732..	28406	26.6	+17 45	7.0	F7	.109	104	+ 34.4±0.1	2*	H
17 734..	.....	26.6	+17 47	9.0	G7	.116	107	+ 44.8±0.6	2	H
15 634..	.....	26.7	+16 08	10.5	K5	.097	99	+ 45.3±0.5	2	H
13 688..	28424	4 26.7	+13 48	7.8	G9	.138	99	+ 96.8±1.5	6	
16 609..	28462	27.1	+16 33	9.1	K0	.109	102	+ 41.7±0.1	2	H
15 636..	28485	27.3	+15 32	5.8	A8n	.108	104	+ 27: var.	5*	H
19 731..	28483	27.4	+19 44	7.2	F5	.101	113	+ 37.2±0.8	2	H
15 638..	28545	27.8	+15 38	9.0	G8	.098	104	+ 36.5±0.3	2	H
19 733..	28593	4 28.2	+20 01	8.4	G5	.090	108	+ 40.0±1.3	2	H
10 588..	28608	28.2	+10 38	7.1	F7	.120	91	+ 36.9±1.8	3	H
13 691..	28635	28.6	+13 47	7.9	F8	.093	102	+ 42.4±0.8	2	H
15 645..	28677	29.0	+15 45	6.1	F0n	.110	107	+ 39.0±1.9	4*	H
5 674..	28736	29.4	+ 5 18	6.4	F5	.113	84	+ 40.7±1.5	4	H
15 646..	28783	4 30.0	+15 54	9.1	G9	.111	106	+ 43.4±0.5	2	H
16 620..	28878	30.8	+16 38	9.4	K0	.105	111	+ 43.4±1.3	2	H
15 649..	28888	30.8	+15 52	8.5	G2	.095	131	+ 56.1±0.6	3	
12 608..	28911	31.0	+13 09	6.7	F4	.115	100	+ 34.4±2.3	3	H
15 650..	28977	31.6	+15 43	9.7	K0	.122	103	+ 40.5±1.0	2	H
15 651..	28992	4 31.7	+15 23	8.0	G0	.093	112	+ 41.2±0.6	2	H
27 667..	.....	31.8	+27 56	9.0	F5	.108	122	+ 32.3±1.3	3	D
15 654..	29159	33.2	+15 35	9.4	K0	.104	106	+ 43.5±1.9	2	H
23 715..	29169	33.5	+23 14	6.0	F4	.131	117	+ 41.7±2.0	3*	H
15 656..	29225	33.8	+15 46	6.7	F6	.111	107	+ 33.2±0.6	3	H
14 728..	29310	4 34.7	+15 03	7.7	G1	.106	107	+ 39.7±1.9	3	H
15 662..	29387	35.4	+15 21	9.8	G7	.080	94	+ 43.5±0.9	2	D
12 618..	29388	35.4	+12 25	4.4	A5n	.099	97	+ 45: var.	2*	H
22 721..	29419	35.9	+23 04	8.4	F9	.147	108	+ 39.6±1.1	2	D
13 702..	29461	36.1	+14 00	8.0	G3	.089	100	+ 39.7±1.7	2	H
15 666..	29488	4 36.4	+15 49	4.7	A5n	.089	103	+ 43.8±2.5	2*	H
7 681..	29499	36.4	+ 7 46	5.6	F0	.089	89	+ 42.0±1.1	3*	H
26 732..	.....	36.8	+27 06	9.2	A0p	.....	.....	+ 6: var.	3	13
23 722..	.....	37.1	+23 13	9.0	G9	.093	111	+ 40.0±2.0	3	H
16 640..	29608	37.5	+16 25	9.5	K2	.095	108	+ 41.4±2.5	3	H
23 723..	29621	4 37.8	+23 43	8.8	G5	.095	126	+ 32.3±1.9	3	H
19 754..	.....	38.5	+20 10	9.7	G8	.083	127	+ 31.1±0.6	3	H
28 681..	.....	38.6	+29 07	9.2	K2	.084	126	+ 3.0±2.0	3	
− 1 697..	29789	39.0	− 0 51	8.4	F5	.089	68	+ 35.2±1.9	3	D
19 762..	.....	39.8	+20 07	9.6	A0p	.092	124	− 10: ±4:	3	
18 684..	29836	4 39.9	+18 38	7.1	G3	.142	128	+ 15.0±0.7	3	
21 694..	30169	43.0	+21 12	9.1	G9	.104	105	+ 26.5±1.3	3	
3 664..	30286	43.7	+ 3 13	7.9	G4	.057	61	+ 19.6±1.5	3	
1 819..	30299	43.8	+ 1 15	8.5	F6	.053	80	+ 24.0±0.7	3	
8 759..	30311	44.0	+ 8 55	7.2	G0	0.112	90	+ 39.8±0.4	2	H

TABLE 1—*Continued*

BD	HD	(1950) R.A.	(1950) Dec.	m_v	Sp.	μ	θ	ρ_r (Km/Sec)	Pl.	Notes
17° 786..	30355	4h44m7	+18° 10′	8.2	G4	0".116	119°	+ 42.0±0.7	2	H
24 689..	30418	45.4	+24 40	8.0	F5	.035	147	+ 42.4±0.8	2	
20 823..	.....	45.8	+21 02	9.0	K0	.092	104	+ 42.4±1.6	3	D
24 692..	.....	46.1	+24 44	9.1	K3	.123	119	+ 44: var.	4	14, H
18 736..	30505	46.1	+18 33	8.8	K0	.072	142	+ 42.6±0.8	2	D
3 679..	30544	4 46.1	+ 3 34	7.1	B9	.064	66	+ 33.2±2.3	4	
15 686..	30589	46.7	+15 48	7.9	G0	.086	109	+ 39.7±2.2	4	H
23 747..	30572	46.8	+23 19	8.6	G4	.073	120	+ 32.8±0.8	2	P
16 657..	30676	47.5	+17 07	7.2	F8	.104	114	+ 41.6±0.8	2*	H
14 770..	30712	47.8	+15 00	8.2	G5	.086	102	+ 43.7±0.2	2	H
13 725..	30726	4 47.9	+14 09	8.9	G1	.084	94	+ 31.0±0.7	3	D
15 692..	30738	48.0	+16 08	7.3	F8	.098	101	+ 41: var.	5	15, H
0 873..	.....	48.3	+ 0 30	9.2	F8	.088	79	+102.7±1.7	3	
28 706..	30754	48.4	+28 33	9.0	K5	.124	115	+ 15.8±0.9	3	
− 0 789..	.....	49.1	− 0 10	8.9	G8	.055	46	+ 30: var.	4	16
4 769..	31003	4 49.8	+ 4 15	8.5	F8	.085	107	+ 41.2±2.0	4	D
22 769..	.....	50.6	+22 56	8.8	F8	.083	103	+ 45.2±1.9	2	D
10 668..	.....	51.1	+10 16	8.9	G8	.070	108	− 29.3±1.8	3	
17 807..	31181	51.2	+17 33	9.8	F7	.072	115	+ 40: var.	4	17, D
16 664..	31153	51.2	+16 57	7.1	F8	.080	93	+ 54: var.	4	18
− 1 747..	.....	4 51.2	− 1 15	9.3	G7	.123	61	+ 7.3±0.6	3	
19 811..	31236	52.0	+19 24	6.2	F1	.072	122	+ 41.2±0.8	2	H
5 765..	31354	52.7	+ 5 33	8.2	G0	.112	72	+ 17.5±1.8	4	
13 749..	31609	55.0	+13 56	8.5	G5	.093	113	+ 46.4±1.1	2	H
30 752..	31706	56.1	+30 59	8.0	F6	.055	138	+ 14.2±2.4	3	19
− 0 815..	.....	4 56.1	− 0 47	9.1	G7	.098	67	+ 26.9±1.1	3	
26 771..	31781	56.6	+26 10	8.6	G0	.071	145	+ 16.2±0.7	3	
0 916..	32023	57.8	+ 0 57	9.1	F8	.072	76	+105.3±2.5	3	
− 0 823..	32114	58.2	− 0 34	8.9	A0	.087	64	+ 2: ±6:	3	20
31 846..	.....	58.7	+31 34	8.9	G0	.091	146	+ 74.9±1.8	3	
13 783..	32347	5 00.3	+13 39	9.3	K0	.064	100	+ 43.6±1.8	2	H
27 732..	33204A	06.6	+27 58	6.0	A3	.088	138	+ 41.3±0.9	2*	P
.....	33204B	06.6	+27 58	8.5	G7	.092	....	+ 46.4±0.4	2	P
20 897..	33400	07.8	+20 31	7.8	F5	.051	106	+ 44.8±1.5	3	D
6 865..	33662	09.4	+ 6 47	7.9	K5	.044	85	+ 22.4±1.3	3	
19 876..	34031	5 12.2	+20 00	7.7	G1	.116	109	+ 22.2±1.4	3	
12 756..	.....	13.5	+12 10	8.9	F6	.044	104	− 23.8±0.7	3	
26 806..	.....	16.1	+27 02	9.0	G4	.067	163	+ 10.2±1.2	3	
23 902..	34772pr	17.9	+23 59	8.9	F6	.067	149	+ 18.5±1.5	3	
.....	34772fol	17.9	+23 59	8.9	F6	.....	.....	+ 20.6±1.0	3	
28 783..	34987	5 19.6	+28 42	8.7	F7	.075	147	+ 37.4±0.8	2	D
24 846..	244516	28.9	+24 57	9.2	F7	.090	146	+ 41.6±0.6	2	D
20 978..	.....	29.2	+21 00	9.3	F0	.036	118	+ 37: var.	4	21
29 936..	.....	32.1	+29 14	9.5	G3	.074	148	+ 46.1±2.1	3	D
23 981..	37388A	36.1	+23 16	8.6	F8	.070	141	+ 40.8±1.3	4	D
.....	37388B	5 36.1	+23 16	9.0	F7	.....	.....	+ 44.6:....	1	D
26 899..	246128..	37.7	+26 58	9.0	G1	.087	160	+ 58.4±1.0	3	
26 907..	.....	39.3	+26 54	8.9	F8	.097	155	+ 57: var.	3	22
13 964..	37982	40.2	+13 07	8.9	F5	.061	127	+ 49.6±0.1	2	D
9 970..	.....	46.3	+ 9 52	9.0	K0	0.050	89	+ 51.2±1.0	3	D

TABLE 1—*Continued*

BD	HD	(1950) R.A.	(1950) Dec.	m_v	Sp.	μ	θ	ρ r (Km/Sec)	Pl.	Notes
17°1031..	39117	5h48m2	+17°50′	8.2	F8	0".077	137°	− 26.0±1.5	3	
24 1036..	249499	54.2	+25 00	9.3	K4	.063	151	+ 5: var.	4	23
25 1089..	40895	59.7	+25 53	8.0	F8	.082	150	− 21.4±1.5	3	
25 1105..	41221	6 01.6	+25 11	8.6	F8	0.073	155	−7.6±1.8	3	

NOTES TO TABLE 1

* Other measures available.
H. Member of cluster.
P. Membership probable.
D. Membership doubtful.
1. +56, +59, +37, +70.
2. Two spectra.
3. +143, +99, +38, −76, −99.
4. +51, +60, +64.
5. −4, +9, +8.
6. +49, +46, +30, +51.
7. +51, +41, +30.
8. Two spectra.
9. Two spectra.
10. +43, +11, +28, +40.
11. +51, +23, +58, +38.
12. +49, +37, +52, +40.
13. +14, −28, +32.
14. Two spectra.
15. +65, +26, +38, +41, +38.
16. −13, +42, +50, +42.
17. +30, +28, +53, +48.
18. +46, +50, +58, +60.
19. Two spectra.
20. Two spectra.
21. Two spectra.
22. +44, +60, +66.
23. 0, +21, +4, −3.

TABLE 2

LARGE VELOCITIES IN THE HYADES REGION

Star	m_v	Sp.	ρ	Star	m_v	Sp.	ρ
BD+26°595.....	9.1	G8	−198.4	HD28424.....	7.8	G9	+ 96.8
HD23841.....	7.0	G8	− 79.8	BD+0°873.....	9.2	F8	+102.7
HD25532.....	8.3	F6	−113.0	HD32023.....	9.1	F8	+105.3
BD+31°769.....	8.8	F8	+ 79.4*	BD+31°846.....	8.9	G0	+ 74.9*

* Possible common motion. For BD+31°769, μ = 0".104, θ = 133°; for BD+31°846, μ = 0".091, θ = 146°.

THE STRUCTURE OF THE ATMOSPHERE OF THE K-TYPE COMPONENT OF ZETA AURIGAE*

O. C. WILSON
Mount Wilson Observatory
Received December 1, 1947

ABSTRACT

This investigation is based upon spectrograms of 10.4 A/mm dispersion obtained during the 1939–1940 eclipse.

Curves of growth were constructed for four atmospheric levels observed during ingress and for three during egress. Relative *gf*-values for *Fe* I lines were taken from the laboratory data of King and King. For other elements the relative *gf*'s were calculated from the measures of lines in the solar-flash spectrum made by H. H. Lane.

Doppler widths, $\Delta\lambda_D$, of the theoretical curves of growth which best fit the observations, range from 0.08 A for a height above the limb of 0.8×10^6 km to 0.16 A for a height of 20.6×10^6 km, with corresponding turbulent velocities of 6.5 and 13.0 km/sec, respectively. It appears, therefore, that the turbulence increases with height in the atmosphere.

Excitation temperatures determined by comparison of the populations of the a^5F and a^3F states of *Fe* I with that of the ground state, a^5D, also increase with height. Mean values range from 3780° at $h = 0.8 \times 10^6$ km to 5660° at $h = 13.5 \times 10^6$ km.

Density gradients in the atmosphere are readily evaluated by means of the curves of growth. For all atomic and ionic states included in this investigation the gradients are steepest at the lowest levels and tend to become less steep with increasing height. Moreover, except for *Ca* I in the lowest level, all the density gradients are nearly the same. If the densities are expressed as a function of height by means of the formula $n = n_0 e^{-ah}$, the observations yield a mean value of $a = 2.3 \times 10^{-12}$ cm^{-1}. The observed gradient is compared with those calculated on the assumption of hydrostatic equilibrium. The latter hypothesis leads to gradients of the order of twenty times larger than observed for *H* to one thousand times larger for *Fe* and elements of similar atomic weight. McCrea's theory of turbulent support is also investigated. If the turbulent velocities obtained from the curves of growth are used in McCrea's equation, the resulting gradient is still about ten times too large. It cannot be decided at the present time whether this discrepancy is real or due to an accumulation of errors in the data.

The ionization in the atmosphere of the K-type component is investigated, chiefly at heights of 7×10^6 km and 14×10^6 km, for which the data appear most reliable. Thermodynamic equilibrium is first assumed; the combination of the Boltzmann and Saha equations for *H*, together with the standard ionization equation for *Ca*, then permit an evaluation of the temperature, *T*. The latter is found to be nearly the same as that of the K-type star itself, and the electron density at height 7×10^6 km is 10^9 per cm^3, on the assumption that hydrogen supplies effectively all the electrons. It is next assumed that the ionization of *Ca* is governed by the dilute radiation of the B-type star and Pannekoek's equation is applied. It is shown that the observed ionization of *Ca* requires a higher electron density than appears to be available for *H*, and hence it is unlikely that the B-type star is responsible for the ionization of *Ca* and atoms of similar I.P. This conclusion leads to an investigation of the opacity of the atmosphere of the K-type star as a function of wave length. Menzel's opacity formula is shown to provide ample opacity at $\lambda \leq 2000$ A to screen most of the atmosphere from the ionizing radiation of the companion, while still insuring transparency in the regions ordinarily observed. On the basis of the same equation it is suggested that the eclipses may begin appreciably earlier in the ultraviolet than in the ordinary photographic region. A tentative explanation of the rise of excitation temperature with height is based upon the metastability of the atomic states concerned and the variation of atmospheric opacity with height and wave length.

INTRODUCTION

The eclipsing system Zeta Aurigae consists of a giant K5 star and a much smaller B8 star, which revolve around their common center of gravity in a period of about 972 days. Outside of eclipse the spectrum is composite, dominated in the red by the K-type star and in the violet by the B-type. Earlier work[1,2] has demonstrated that the intensities of

* *Contributions from the Mount Wilson Observatory, Carnegie Institution of Washington*, No. 742.

[1] Christie and Wilson, *Mt. W. Contr.*, No. 519; *Ap. J.*, **81**, 426, 1935.

[2] Guthnick, Schneller, and Hachenberg, *Abh. preuss. Akad. Wiss.*, Phys.-math. Kl., No. 1, 1935.

the two spectra are equal at about λ 4300. As the B star approaches and leaves eclipse, numerous sharp absorption lines which are not present at other times appear in the blue and violet regions of the spectrum. These lines are produced in the light of the B-type companion by atoms in the extensive atmosphere of the K star. This circumstance offers the possibility of analyzing the atmosphere of the K star as a function of height above the photosphere. Such an analysis was made from spectrograms obtained at the last favorable eclipse in December and January, 1939–1940.

OBSERVATIONS

The topics treated in this section include (1) the spectrograms, (2) selection of lines for measurement, (3) measurement of equivalent widths of selected lines, (4) determination of relative *gf*-values; (5) formation of curves of growth; and (6) calculation of heights above the limb of the K-type star.

1. *The Spectrograms.*—The spectrograms were obtained with the coudé spectrograph of the 100-inch telescope. The 32-inch-focus Schmidt camera was used, in the second order of the Wood grating, giving a dispersion of 10.4 A/mm. Eastman 103-O plates were employed throughout. Each plate was calibrated photometrically by means of step slits on either side of the spectrograph slit, illuminated by an auxiliary lamp. Each star spectrum was thus flanked on either side by eight intensity strips, which provided calibration-curves at all wave lengths.

Observations were begun on the night of December 16, 1939, and were carried on almost continuously through succeeding nights until the evening of December 20. Thirty-seven exposures were made during ingress. There were two exposures on the majority of the plates, the exposure times being so chosen that the region from λ 3200 to λ 3900 would have suitable density on the long exposure, the λ 4200 region on the short one. Similar observations were made during egress, although less favorable conditions permitted only twenty exposures to be obtained between the early evenings of January 26 and January 31, 1940.

The labor involved in making photometric measurements on every exposure would have been far too great to justify the returns. Hence fourteen of the exposures (Table 2), well distributed through the time interval of the observations, were selected on the basis of quality; and it is upon microphotometer tracings of these plates that the results of this paper rest. The tracings were made on the photoelectric microphotometer with a magnification of 100.

2. *Selection of lines for measurement.*—In order to derive the maximum amount of information about the atmosphere of the K-type star, it is evident that curves of growth must be plotted for each of the levels observed.[3] For a line to be useful in building up a curve of growth, it should arise from an atomic state which is also the lower state for several other observed lines; in addition, the relative *gf*-values of all the lines originating in the common lower state must be known. A number of lines of *Fe* I which arise from the three states a^5D, a^5F, and a^3F are observed in the lower levels of the atmosphere of the K-type star. For these lines the relative *gf*-values are known from the laboratory investigations of R. B. and A. S. King.[4] Hence these *Fe* I lines, about seventy of which are measurable in the lower levels of the atmosphere, form the backbone, as it were, of the curves of growth and, in addition, provide a measure of the excitation temperatures at the various levels, as will be seen later.

Many more absorption lines than those of *Fe* I appear on the spectrograms, however. On a plate of December 18, for instance, the wave lengths of nearly four hundred lines between λ 3070 and λ 3970 were measured for identification, and it is highly desirable to

[3] To avoid confusion, the word "level" will be used only to refer to levels in the atmosphere. Atomic-energy levels will be referred to as "states."

[4] *Mt. W. Contr.*, No. 581; *Ap. J.*, **87**, 24, 1938.

utilize as many as possible of these lines to fill out the curves of growth. Actual laboratory measures of relative gf's would be highly desirable; but, since these do not yet exist, Dr. Leo Goldberg suggested to the writer that measures of intensity in the solar-flash spectrum would be almost equally good and that the work of H. H. Lane[5] would provide a suitable source of material. A few trials showed that Lane's measures were, in fact, quite satisfactory for deriving gf-values. The following criteria were therefore adopted in the selection of lines (apart from those of *Fe* I) to be measured for intensity on the Zeta Aurigae spectrograms: The line must (1) be a member of a multiplet which provides other suitable lines; (2) be relatively unblended in the Zeta Aurigae spectra; and (3) appear in Lane's list with no evidence of serious blending. The method by which Lane's measures were used to derive relative gf's will be given later. Besides the lines which were measured primarily as a means of obtaining the curves of growth, the equivalent widths of *H* 7, *H* 8, *H* 9, *H* 10, *H* 11, and *H* 12 of hydrogen, H and K of *Ca* II, and 4227 of *Ca* I, were determined wherever possible.

3. *Measurement of equivalent widths of selected lines.*—The absorption lines observed in the spectrum of Zeta Aurigae just before and just after totality are necessarily composite. Except for the hydrogen lines, the spectrum of the B-type star is continuous and merely provides a background from which the atoms and ions of the K-type atmosphere may absorb selectively. Since, however, the normal spectrum of the K-type star contains absorption lines at these same wave lengths, the two spectra are superimposed, and their separation must be considered.

A method for performing this separation, devised by the writer and applied to spectrograms of the 1934 eclipse, is essentially the same scheme as that used by P. Wellmann.[6] The method requires knowledge of two things: (1) the equivalent width of the line in the normal K-type spectrum (found from spectrograms taken during totality), and (2) the ratio, $\alpha = I_{CB}/I_{CK}$, of the two continuous spectra at the wave length in question.

By its definition, α is related to the amplitude of the eclipse in magnitudes by the expression

$$\text{Amplitude} = 2.5 \log (1 + \alpha) , \tag{1}$$

which provides a means of calculating α if the amplitude is known at the desired wave length. The value of α may also be found by combining measures of equivalent widths of lines made during totality (W_K) with those made completely outside of eclipse (W_{BK}) when no chromospheric absorptions are present. In this case the equation is

$$\alpha = \frac{W_K}{W_{BK}} - 1 . \tag{2}$$

The most complete study of the amplitude of eclipse as a function of wave length is that by Guthnick, Schneller, and Hachenberg[2] in 1934. When the values of α found at the same eclipse by Christie and Wilson by application of equation (2) are transformed to amplitudes, as in Figure 4 of the paper of Guthnick, Schneller, and Hachenberg, the agreement is excellent for the range λλ 4000–4300. The results of P. Wellmann, obtained in the same manner as those of Christie and Wilson, show less satisfactory agreement. Neither Wellmann nor Christie and Wilson could carry their determinations of α much farther to the violet than λ 4000 because the B-type spectrum becomes so overwhelming that the quantities W_{BK} rapidly approach values of the same order as the errors of measurement. It is to be noted, however, that the results of Guthnick, Schneller, and Hachenberg show that at λ 3800 the value of α is already in excess of 5 and is apparently rising very rapidly toward shorter wave lengths.

[5] *Harvard Ann.*, **105**, 69, 1937.

[6] *Veröff. d. Sternw. Berlin-Babelsberg*, Vol. **12**, Part IV, 1939.

The equation employed for the 1934 eclipse to separate the chromospheric absorptions from those of the normal K spectrum was

$$W_B = W_{BK} + \frac{1}{\alpha}(W_{BK} - W_K), \tag{3}$$

where W_B is the desired equivalent width produced by the chromosphere; W_{BK} is the measured equivalent width; and α and W_K have been defined above. This equation is especially applicable to spectrograms taken with small dispersion, which is insufficient to produce any measurable distinction between those portions of a line produced by the chromosphere and those due to the underlying K-type spectrum. In fact, such lack of distinction is a requirement for the proper use of the equation which must yield values of $W_B = 0$ above some particular level. On the spectrograms of the 1939–1940 eclipse the dispersion was sufficient, in most instances, to provide a fair separation of the two components of the lines. Before the chromospheric absorptions appeared, the spectrum (to the violet of λ 3900 where most of the work was done) had a slightly "wavy" or "lumpy" appearance. A chromospheric line first appeared as a very sharp narrow component near the bottom of one of the slight waves due to the filled-in lines of the normal K spectrum. Hence there was seldom any question as to what portion of a line was due to the chromosphere, but there was usually considerable uncertainty as to how the measures should be carried out so as to render equation (3) applicable. In view of this situation as well as because of the lack of knowledge of α over the wave-length range used and the difficulty of obtaining accurate values of W_K in the very crowded violet region of the K-type spectrum, it was finally decided not to employ equation (3) except in certain cases noted below. Instead, the "wavy" continuous spectrum was sketched in by hand as accurately as possible, and all measures of chromospheric lines made from the bottoms of the residual K-type lines. If this procedure could be followed with complete accuracy, it would be easy to show that equation (3) should be replaced by

$$W_B = W_{BK} + \frac{1}{\alpha^1} W_{BK}, \tag{4}$$

where

$$\alpha^1 = \frac{\alpha}{r_k}, \tag{5}$$

r_k being the depth of the line in the K-type spectrum.

Since we have seen that α certainly exceeds 5 for the range in which most of the measuring was done and since r_k is probably at least as small as 0.5 for most of the lines considered, this source should produce few errors in excess of 10 per cent in the measured equivalent widths of the chromospheric lines. Accordingly, the measurement of the lines was carried out as described above, and the correction term in equation (4) was neglected entirely. Unfortunately, the residual errors will be systematic in the sense that our values of the chromospheric absorptions will tend to be slightly too small. It is believed, however, that the systematic error has been reduced to a size where it will have very little effect on the conclusions.

The H and K lines of *Ca* II, λ 4227 of *Ca* I, and the hydrogen lines require special discussion. At λ 3933 the spectrum of the B-type star is continuous and the K line of the K-type star is deep and wide; hence for all practical purposes the contribution of the K-type star to the combined spectrum may be taken as zero in the immediate vicinity of this wave length. Thus, as long as the chromospheric K line is weak compared to that in the normal K-type spectrum, its true equivalent width is given directly by the measures without the need of correction. At H and $H\epsilon$ the chromospheric lines lie inside the $H\epsilon$ line of the B star. The latter is used as the background for the measurement of the chromospheric absorptions, and again no correction is required because the strong H line of

the K-type star reduces its contribution effectively to zero. A similar argument applies to λ 4227, though here the filled-in line of the normal K-type spectrum makes more of a showing than at K. The bottom of the residual K-type line is, of course, used as the background for the measurement of the chromospheric λ 4227.

In the lowest observed levels, represented by plates 2199 and 2245, K and λ 4227 are strong, winged lines, and the chromospheric absorptions cannot be separated from those of the K-type star in the above simple manner. For these plates, therefore, equation (3) was used. The values of a were taken from the paper of Guthnick, Schneller, and Hachenberg and reduced by the fractions of the disk of the B star occulted by that of the K star at the times that the two plates were taken. The equivalent widths of K and λ 4227 in the normal K-type spectrum were measured on a plate obtained just before the end of totality.

As noted above, $H\epsilon$ is the most favorable of the Balmer lines because of the presence of the strong H absorption in the K-type star. The hydrogen lines H 8–H 12, inclusive, were, however, measured wherever possible in order to strengthen the data as well as to provide information at the lowest observed levels, where $H\epsilon$ could not be used. In taking the mean values of log N for hydrogen, $H\epsilon$ was given double weight.

Measured equivalent widths are given in Tables 13 and 14 at the end of the paper.

4. *Determination of relative* gf-*values.*—The values of gf were derived from Lane's results in the following manner: Let the upper and lower states for a given line be designated by m and n, respectively. If the line is emitted by a mass of gas (in this case the solar chromosphere) and self-absorption can be neglected, the radiated energy in the line per unit time is[7]

$$E = A_{nm} N_m h\nu \,, \tag{6}$$

where N_m is the population of the upper state. However, f_{mn} is related to A_{nm} by the equation

$$f_{mn} g_n = g_m A_{nm} \frac{m c^3}{8\pi^2 e^2 \nu^2} = \text{const.} \times \frac{g_m A_{nm}}{\nu^2} \,. \tag{7}$$

Eliminating A_{nm} between equations (6) and (7) gives

$$E = f_{mn} \frac{g_n}{g_m} \nu^3 N_m \times \text{const.} \,; \tag{8}$$

and, since

$$N_m = N_0 \frac{g_m}{g_0} e^{\chi_m / kT} \,,$$

$$E = f_{mn} g_n \frac{N_0}{g_0} \nu^3 e^{\chi_m / kT} \times \text{const.} \tag{9}$$

For a given element, N_0 and g_0 may be absorbed into the constant, which is the same for all lines of that element. Thus the relative gf-values are given by the expression

$$\log f_{mn} g_n = \log E + 3 \log \lambda + \frac{5040 \chi_m}{T} \,. \tag{10}$$

The value of T appearing in equation (10) is the excitation temperature of the solar chromosphere. According to L. Goldberg,[8] the appropriate value of this quantity is T = 4200°, which was therefore used in the present calculations. The values of log E were taken directly from Lane's tabulation.

[7] The notation is that of A. Unsöld, *Physik der Sternatmosphären* (Berlin, 1938), chap. ix.

[8] Private communication.

In a curve of growth, the quantity plotted horizontally is $\log N_n f_{mn}$. Since multiplets often arise from a group of lower states having slightly different excitation potentials, it is necessary to correct for the Boltzmann distribution over these states. The correction term is thus of the form

$$\Delta \log N = -\frac{5040\Delta\chi}{T_1},$$

where T_1 is the excitation temperature in the chromosphere of Zeta Aurigae and $\Delta\chi$ is the difference in excitation potential between the state in question and the lowest state of the multiplet. A preliminary determination of T_1 gave also the value 4200°, which was used throughout the reduction. Although it was later found that T_1 was a function of level in the chromosphere, it was not considered worth while to revise the corrections, as the only result would be a slight reduction in horizontal scatter of the points on the curves of growth. Accordingly, the final equation from which the relative values of $\log gf$ were calculated was

$$\log f_{mn} g_n = \log E + 3 \log \lambda + 1.20\chi_m - 1.20\Delta\chi \,. \qquad (11)$$

5. *Formation of curves of growth.*—After the measurements and calculations described above had been completed, curves of growth were formed for each of the observed atmospheric levels in the following manner. On sheets of tracing paper the values of $\log (W \times [3700]/\lambda)$ were plotted against those of $\log gf$ for all lines arising from a common atomic or ionic state. In the lower levels of the atmosphere, *Fe* I provided the greatest number of lines and the three *Fe* I states were combined by making the horizontal shifts necessary to obtain the best over-all fit. Multiplets of other atoms and ions were then added in similar fashion. Up to this point no reference whatever had been made to theoretical curves of growth. A series of theoretical curves for λ 3700 were now computed[9] for various values of $\Delta\lambda_D$,[10] and the observed curves were fitted to them to find the values of $\Delta\lambda_D$ for each level. After this had been done, the observed curves of growth were plotted once more by fitting the groups of lines from each atomic state to the appropriate theoretical curve determined by the first approximation. This procedure tended to decrease the scatter of the observed points to some extent, but had no other effect upon the results.

6. *Calculation of heights above the limb of the K-type star.*—The determination of the height above the limb of the K-type star of the line of sight to the center of area of the B-type star depends primarily upon three quantities: (1) the relative transverse velocities of the two stars during eclipse; (2) the ratio of the radii, k; and (3) the inclination of the orbit plane to the line of sight.

The relative transverse velocities of the stars at egress and at ingress may be calculated from the spectroscopic orbit of the K-type star, provided that the mass ratio of the system is known. The latter quantity, M_K/M_B, is certainly in the neighborhood of 2.0. Published values of the mass ratio, however, range from 1.85 to 2.47. Accordingly, it appears rather doubtful that the mean value is accurate to better than perhaps 10 per cent. In any case it is convenient, however, that the relative transverse velocities at egress and at ingress do not differ by much more than 2 per cent. Hence, if a value for the diameter of

[9] Equations 44.42 and 44.47 of Unsöld's book were used. Since these are derived on the assumption of exponential absorption rather than of scattering, they should be applicable here. Moreover, these equations are for the limiting case $a = \gamma/\Delta\omega_D = 0$, which also should be a reasonable approximation, since for the low densities prevailing in the chromosphere of a supergiant, values of a in excess of 10^{-3} appear very unlikely.

[10] Assuming a Maxwellian velocity distribution, we express the Doppler width, $\Delta\lambda_D$, by

$$\Delta\lambda_D = \frac{\lambda}{c}[\tfrac{2}{3}(V_x^2 + V_y^2 + V_z^2)]^{1/2}.$$

the K star is decided upon and an inclination of 90° is assumed, heights may be computed with sufficient accuracy by a simple proportionality of time intervals.

Although considerable work has now been done on Zeta Aurigae in order to establish accurate values of the constants of the system, rather large uncertainties remain. The situation is illustrated by Table 1, in which the various determinations of the quantities of importance for the present section are listed. Footnotes to the table indicate briefly the methods adopted by the several authors, but the original papers should be consulted for details.

It is evident from the tabulated results that dogmatic statements about any of the listed quantities would not be safe at the present time. Probably, as Kopal notes in his paper, the amplitudes of the eclipse together with the assumption of black-body radiation and reasonable temperatures for the two stars give a much better determination of k than can be found from the duration of partial phase. Even this method is not without uncertainty, however, as Guthnick, Schneller, and Hachenberg found a rapid decrease in apparent temperature of the K-type star to the violet of λ 4600, and Christie and Wilson obtained a similar abnormally low value of T_K in the λλ 4000–4300 region.

TABLE 1

SUMMARY OF DETERMINATIONS OF THE CONSTANTS OF THE SYSTEM OF ZETA AURIGAE

Author	Eclipse	Observations	M_K/M_B	R_K	k^{-1}	i
Christie-Wilson*	1934	Photographic	1.85	192⊙	22.6*	90°*
Guthnick, Schneller, and Hachenberg†	1934	Photoelectric, photographic	2.47	292	73.5†	80.5†
Christie‡	1939–1940	Photographic	.....	.....	28.4‡	90‡
Roach§	1939–1940	Photoelectric	.....	195§	71.5§	78§
Kopal‖	1939–1940	Photoelectric	.....	.....	69‖	77.5¶
Kopal‖	1939–1940	Photoelectric	.....	200**	69‖	~90**

* *Mt. W. Contr.*, No. 519; *Ap. J.*, **81,** 426, 1935; k^{-1}, from duration of partial phase; i, assumed.

† *Abh. preuss. Akad. Wiss.*, 1935; k^{-1}, from amplitudes of eclipse, assumption of black-body radiation, $T_B = 15{,}000°$, $T_K = 3160$. Wave-length range, λλ 4400–6000; i, from duration of partial phase, with $k = 73$.

‡ *Mt.W. Contr.*, No. 635; *Ap.J.*, **92,** 392, 1940; k^{-1}, from duration of partial phase; i, assumed.

§ *Ap.J.*, **93,** 1, 1941; for R_K, k^{-1}, and i, bodily eclipse $T_B = 15{,}000°$ is assumed.

‖ *Ap.J.*, **103,** 310, 1946; from amplitudes in range λλ 4450–6100, assuming black-body radiation, $T_K = 3200$, $T_B = 15{,}000°$

¶ From duration of partial phase, bodily eclipse.

** From analysis based on both atmospheric and bodily eclipse.

The most reliable determination of i is probably that of Kopal, who has developed a more penetrating method of analysis than any used heretofore. In any event, for the purpose of calculating heights above the limb, the writer feels justified in adopting the following rounded values of the essential items:

$$R_K = 200\odot\,, \qquad k^{-1} = 70.0\,, \qquad i = 90°\,.$$

If and when more accurate determinations are available, the calculated heights can be revised if necessary.

In addition to the above data, the following figures are taken from Christie's investigation: Epoch of minimum = JD 2429637.18; duration of eclipse = 39.50 days. It follows that the heights in kilometers are given by the formula

$$h = 2 \times 10^6 + 7.14 \times 10^6 \Delta t\,, \tag{12}$$

where Δt is the time interval in days between the observation and the first or fourth contact for ingress and egress observations, respectively. For those spectrograms for which

Δt is negative (partial obscuration of the disk of the B star by the limb of the K star) the height of the center of area of the visible portion of the disk was calculated. In Table 2 are listed the plates used in the investigation, times of observation, and heights in kilometers computed by equation (12). Where more than one exposure on a given evening was used, the computations were made with the mean time of observation.

RESULTS

The topics treated in this section include: (1) evaluation of turbulence from curves of growth, (2) excitation temperatures from *Fe* I lines, (3) apparent gradients in the chromosphere of Zeta Aurigae, (4) comparison of observed and theoretical gradients, and (5) ionization and excitation in the chromosphere.

TABLE 2

SPECTROGRAMS, TIMES OF OBSERVATION, AND CALCULATED HEIGHTS

Plates Coudé	Date 1939–1940 P.S.T.	JD 2429+	Δt	$h \times 10^{-6}$ km
2181, 2183	Dec. 16, 11:38	614.82	+2.61	20.6
2185, 2188	Dec. 17, 11:36	615.82	+1.61	13.5
2191, 2192, 2194	Dec. 18, 9:23	616.72	+0.71	7.1
2199	Dec. 19, 9:53	617.74	−0.31	0.8
2245	Jan. 27, 7:45	656.66	−0.27	0.9
2248	Jan. 28, 6:50	657.62	+0.69	6.9
2252, 2253	Jan. 29, 9:30	658.73	+1.80	14.8
2254	Jan. 30, 9:52	659.74	+2.81	22.0
2255	Jan. 31, 10:15	660.76	+3.83	29.4

1. *Evaluation of turbulence from curves of growth.*—Curves of growth were constructed for the four levels observed at ingress and for the lower three levels at egress. Since on the plates of January 30 and 31 only a few of the stronger lines remained visible, curves could not be constructed for the corresponding levels.

In Figure 1 are shown the final plots of log Nf against log $(W \times [3700]/\lambda)$ for the egress observations, together with the theoretical curves calculated for the values of $\Delta\lambda_D$ indicated on the figure. The results for ingress, not shown, are quite similar.

The question immediately arises: With what degree of accuracy can the Doppler widths, $\Delta\lambda_D$, be determined from such data? No hard-and-fast rule can be stated. The fitting of theoretical curves of growth to the observations is somewhat of an art and depends not only upon the quality of the measures but also to a considerable extent upon the judgment of the investigator. In an attempt to estimate the accuracy attained, the following experiment was performed. The observations for two selected atmospheric levels, one at egress and the other at ingress, were plotted on theoretical curves whose $\Delta\lambda_D$'s differed by 0.04 A from the values previously found. Every effort was made to force agreement between the observations and the theoretical curves, but in each case without success. The deviations were always large enough to show conclusively that the value of $\Delta\lambda_D$ was incorrect. Hence it seems safe to conclude that the Doppler widths found by the method used here are probably correct to about ± 0.02 A.

The values of $\Delta\lambda_D$ and the corresponding turbulent velocities, V_T, are given in Table 3 as a function of height above the limb.

The first conclusion to be drawn from Table 3 is that the chromosphere of the K component of Zeta Aurigae is quite turbulent, since the observed values of $\Delta\lambda_D$ can scarcely be interpreted as the result of thermal motions. A value of $\Delta\lambda_D$ of 0.10 A corresponds, for instance, to a temperature of 2×10^5 degrees for atomic weight 50. Wellmann[6] came to a similar conclusion, although he derived a turbulent velocity of 22 km/sec for the lower levels of the atmosphere at the 1934 eclipse. There is no reason to suppose that the degree of turbulence is constant; in fact, the known variations in the height of *Ca* II would per-

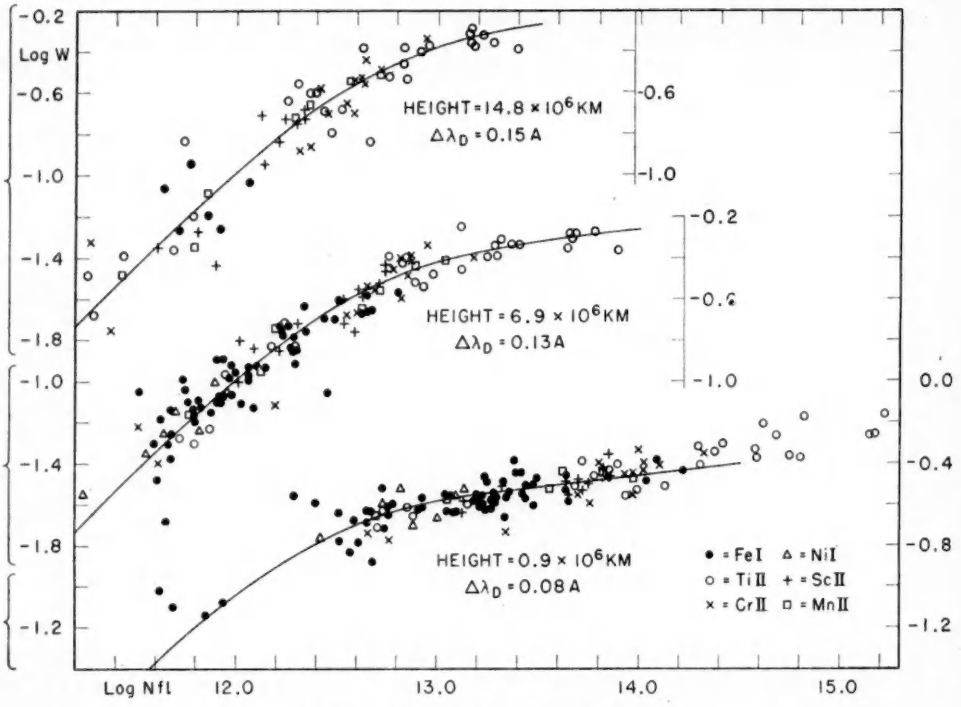

FIG. 1.—Curves of growth for egress

haps imply that it is not.[11] Hence the difference between Wellmann's result and the present one may be real.

Table 3 shows unmistakably that the turbulence increases with height. Even if the estimate of the accuracy of $\Delta\lambda_D$ given above is somewhat optimistic, it is unlikely that an apparent increase in this quantity by a factor of 2 can be attributed to errors of observation. The increase of turbulent velocity with height is probably analogous to that found in lesser degree in the solar chromosphere by D. H. Menzel.[12]

Figure 2 shows the values of $\Delta\lambda_D$ plotted against height. For ingress the relationship may be considered linear, but the egress results show some deviation. Except for one of the egress points, however, the deviations from linearity hardly exceed the estimated allowable error in the determination of $\Delta\lambda_D$. Thus it is not certain that the variation of turbulent velocity with height differed between ingress and egress, although the possibility remains.

[11] A. Beer, *M.N.*, **95**, 24, 1934.

[12] *Pub. Lick Obs.*, Vol. **17**, Part I, 1931.

The conclusion that considerable turbulence exists in the chromosphere is supported by the appearance of the chromospheric absorption lines. Figure 3 is a microphotometer tracing of the H and $H\epsilon$ lines at a height of 14×10^6 km, with the projected spectrograph-slit width indicated for comparison. Both lines are evidently widened, although their sides are steep and there is no indication of wings due to radiation damping. Moreover, the widths of the two lines are certainly very nearly the same in spite of the large

TABLE 3

DOPPLER WIDTH AS FUNCTION OF HEIGHT

Height $\times 10^{-6}$ Km	Doppler Width, $\Delta\lambda_D$	V_T (Km/Sec)
0.8	0.08 A	6.5
0.9*	.08	6.5
6.9*	.13	10.5
7.1	.10	8.1
13.5	.13	10.5
14.8*	.15	12.1
20.6	0.16	13.0

* Egress.

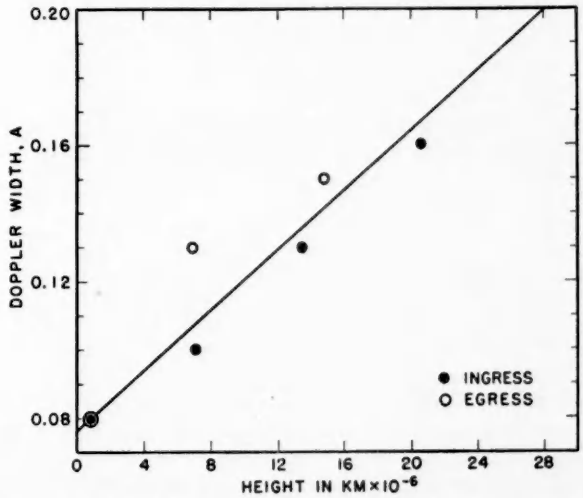

FIG. 2.—Variation of Doppler width, $\Delta\lambda_D$, with height above limb

difference in atomic weight, a result which can hardly be explained on any basis other than macroscopic motions of the absorbing atoms. A study of the contours of the absorption lines with higher dispersion than that used here should be of considerable interest.

2. *Excitation temperatures from* Fe I *lines.*—A number of lines arising from the states a^5D, a^5F, and a^3F were measured in the three lower levels observed at ingress and in the two lower levels observed at egress. The excitation potentials of these three states are 0.000, 0.855, and 1.478 volts, respectively, providing an excellent means of deriving excitation temperatures, through the use of the Boltzmann equation in the form

$$T_{ex} = \frac{5040\,\chi}{\Delta \log N},$$

where $\Delta \log N$ is the horizontal shift required to bring the lines of a^5F or a^3F into agreement with those of a^5D on the curve of growth. Table 4 gives the results.

The values of $\Delta \log N$ and T_{ex} for the lowest levels, both at ingress and at egress, are inaccurate because few of the points for *Fe* I extend down to the linear portion of the curve of growth. This fact presumably accounts for the large discrepancy exhibited by a^5F at $h = 0.9 \times 10^6$ km. Hence it may not be concluded that any real differences ex-

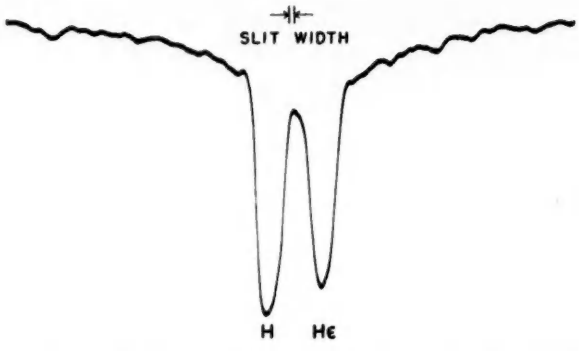

FIG. 3.—Microphotometer tracing of H and $H\epsilon$ at height 14×10^6 km

TABLE 4

EXCITATION TEMPERATURES FROM *Fe* I AS FUNCTION OF HEIGHT

HEIGHT $\times 10^{-6}$ KM	a^5F		a^3F		WEIGHTED MEAN
	$\Delta \log N$	T_{ex}	$\Delta \log N$	T_{ex}	
0.8	1.08	3980	1.81	4100	3780
0.9*	1.35	3190	1.74	4270	
6.9*	1.00	4310	1.60	4650	4450
7.1	0.98	4390	1.63	4560	
13.5	0.77	5590	1.28	5800	5660

* Egress.

isted in T_{ex} between ingress and egress. On the other hand, there can be little doubt that T_{ex} is an increasing function of height in the chromosphere. It is to be noted also that the values of T_{ex} from the a^3F lines are systematically higher throughout than are those from a^5F. The writer regards this effect as probably real, although only about one-fourth as many lines were available from a^3F as from a^5F. The mean relationship between T_{ex} and height is shown in Figure 4, in which the differences between a^5F and a^3F have been ignored and the values from the former given double weight.

3. *Apparent gradients in the chromosphere of Zeta Aurigae.*—The curves of growth provide immediate information on the "apparent gradients" of metallic atoms and ions in the chromosphere. By "apparent gradient" is meant the rate of change with height of the quantity $\log N$, where N is the total number of particles in a column 1 cm square along a given line of sight through the chromosphere. The symbol n will be used to indicate the

numbers of atoms per cubic centimeter; the relationship between N and n depends on the structure of the chromosphere.

In the curves of growth the abscissae are the quantities log Nf, and all the lines of a multiplet are shifted horizontally by the same amount in order to obtain best fit with the theoretical curve. Hence the change in log N between one chromospheric level and an adjacent one may be found simply by reading off the values of log Nf for any one line of the multiplet for the two levels. The difference in the readings is Δ log N for the atomic state concerned. Since the observations appear to be sufficiently accurate to measure the change of excitation temperature with height, it seems best to refer all values of log N, except those for hydrogen, to the ground state of the atom or ion concerned. Hence in all cases the values of log Nf have been increased by the amount

$$\delta \log N = \frac{5040\chi}{T_{ex}},$$

where T_{ex} is the excitation temperature of the level, determined from *Fe* I. The weighted mean values of T_{ex} from Table 4 have been used for this purpose. For the heights 14.8 and 20.6 $\times$ 10^6 km the values 5880 and 6600 were read from the straight line of Figure 4.

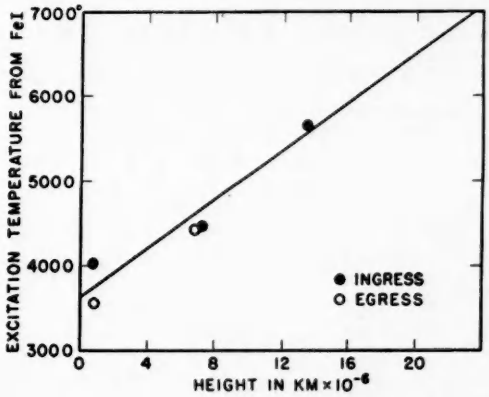

FIG. 4.—Variation of excitation temperature from *Fe* I with height above limb

Table 5 contains the log Nf's corrected for excitation temperature. Inspection of the entries fails to show any unambiguous differences between egress and ingress. In view of this fact, egress and ingress were combined by taking means of adjacent columns in Table 5 to derive apparent gradients, except that the values for ionized elements appearing at height 14.8 $\times$ 10^6 km were not used, in order not to introduce any false differences between neutral and ionized elements.

The resulting apparent gradients are given in Table 6. Comparison of the mean values of $(\Delta \log N)/\Delta H$ shows that the gradient is slightly steeper for neutral than for ionized atoms, which indicates a slow outward increase in ionization. This result is just the reverse of that found by Wellmann.[13] Perhaps more important is the clear indication that $(\Delta \log N)/\Delta H$ is not constant but is, in fact, a decreasing function of height. Wellmann[14] noted a similar trend in the lower chromospheric levels, but it was not nearly so marked as is the variation shown by Table 6.

Values of log N for H, *Ca* I, and *Ca* II are given as functions of height above the limb in Table 7. In the lowest chromospheric levels, where H, K, and λ 4227 are strong winged

[13] *Op. cit.*, Table 12.

[14] *Ibid.*, Fig. 16.

lines, the corresponding N's were calculated by means of the equation

$$W_\lambda = \frac{\lambda^2}{2\pi c}\sqrt{\frac{4\pi^2 e^2}{m c} N\gamma f},$$

with $\gamma_K = 1.55 \times 10^8$ sec^{-1}, $\gamma_{4227} = 1.48 \times 10^8$ sec^{-1}, $f_K = 0.72$, and $f_{4227} = 1.20$.[15] All

TABLE 5

VALUES OF LOG Nf CORRECTED TO GROUND STATE BY BOLTZMANN FACTOR

ATOMIC STATE*		E.P.	HEIGHT×10^{-6} KM						
			0.8	0.9†	6.9†	7.1	13.5	14.5†	20.6
Fe I	a^{5}D (3719.9)	0.000	14.39	14.22	12.80	13.13	12.14	.....	.....
	a^{5}F (3709.2)	0.855	14.50	14.78	13.62	13.19	12.19	.....	.....
	a^{3}F (3815.8)	1.478	15.54	15.33	13.95	14.19	13.17	.....	.....
Ni I	a^{3}D (3414.8)	0.025	13.55	13.12	11.93	12.35	11.56	.....	.....
Ti II	a^{4}F (3361.2)	0.000	15.41	15.15	13.64	13.90	13.30	13.16	13.06
	b^{4}F (3318.0)	0.112	13.98	14.28	13.25	13.66	12.84	12.76	12.37
	a^{2}F (3759.3)	0.571	15.43	15.34	14.33	14.76	13.85	13.67	13.34
Cr II	a^{4}D (3336.4)	2.411	16.64	16.91	15.28	15.46	14.35	14.36	13.90
Sc II	a^{3}D (3372.2)	0.000	13.52	13.82	12.71	12.99	12.42	12.30	11.87
Mn II	a^{5}D (3442.0)	1.768	16.32	16.33	15.04	15.33	14.27	14.23	13.66

* The wave lengths are those of the lines for which the tabulated values of log Nf were read from the curves of growth.
† Egress.

TABLE 6

MEAN APPARENT GRADIENTS, $\frac{\Delta \log N}{\Delta H}$, CM^{-1}, AS FUNCTION OF HEIGHT

ATOMIC STATE		E.P.	MEAN HEIGHT×10^{-6} KM					
			3.92		10.25		17.05	
				Means		Means		Means
Fe I	a^{5}D	0.000	2.18×10^{-12}	.....	1.26×10^{-12}	.....	.....	.....
	a^{5}F	0.855	2.02	2.10×10^{-12}	1.86	1.35×10^{-12}	.....	.....
	a^{3}F	1.478	2.23		1.38		.....	.....
Ni I	a^{3}D	0.025	1.96	.....	0.89	.....	.....	.....
Ti II	a^{4}F	0.000	2.46	.....	0.72	.....	0.34×10^{-12}	.....
	b^{4}F	0.112	1.09	.....	0.95	.....	0.66	.....
	a^{2}F	0.571	1.37	1.73×10^{-12}	1.06	1.06×10^{-12}	0.72	0.66×10^{-12}
Cr II	a^{4}D	2.411	2.30		1.57		0.63	
Sc II	a^{3}D	0.000	1.33	.....	0.66	.....	0.77	.....
Mn II	a^{5}D	1.768	1.85	.....	1.40	.....	0.86	.....

other entries were read from curves of growth and, for hydrogen, the f's calculated by Menzel and Pekeris[16] were used to derive the N's. In each instance the value of $\Delta\lambda_D$ appropriate to the level concerned was used. For the heights 22.0 and 29.4 × 10^6 km, $\Delta\lambda_D$'s of 0.18 and 0.20 A were obtained by extrapolation of the straight line of Figure 2.

A discrepancy should be noted at this point. If the equivalent widths of H and K (excluding plates 2199 and 2245) are taken from Table 14, it is found that the mean ratio is 1.33. On the other hand, the observed equivalent widths, together with the $\Delta\lambda_D$'s deter-

[15] *Ibid.*, p. 56.

[16] *M.N.*, **96**, 77, 1935.

mined from the metallic lines, definitely fix these *Ca* II lines on the transition part of the curve of growth, where K/H should be about 1.1. The probable explanation of this discrepancy appears to be that H has been measured systematically too small. This line lies within the $H\epsilon$ of the B-type star and is slightly blended with the chromospheric $H\epsilon$. Even so, the systematic error in the measurement of H would have to be of the order of 20 per cent, which seems rather large. In any case, in view of the discordant ratio, only the K line was utilized in deriving the log N's of Table 7.

The mean apparent gradients for *H*, *Ca* I, and *Ca* II are given in Table 8 and are shown, together with those of the metals, in Figure 5, in which ingress and egress have been combined, and in which the unit of the ordinate scale corresponds to a ratio of 1:10 in N.

TABLE 7

LOG N AS FUNCTION OF HEIGHT FOR *H*, *Ca* I, AND *Ca* II

ATOM	HEIGHT $\times 10^{-6}$ KM								
	0.8	0.9*	6.9*	7.1	13.5	14.8*	20.6	22.0*	29.4*
H†	16.40	17.22	15.71	15.96	15.20	15.36	14.94	15.09	14.97
Ca I	17.13	16.64	12.46	13.03	11.93	.....	.....	.....	.....
Ca II	18.38	17.52	15.66	16.15	14.86	15.12	14.15	14.40	13.73

* Egress.

† Populations of second state.

TABLE 8

MEAN APPARENT GRADIENTS, $\frac{\Delta \log N}{\Delta H}$, CM^{-1}, FOR *H*, *Ca* I, *Ca* II

ATOM	MEAN HEIGHT $\times 10^{-6}$ KM			
	3.92	10.60	17.8	25.4
H	1.58×10^{-12}	0.78×10^{-12}	0.37×10^{-12}	0.06×10^{-12}
Ca I	6.72	1.25*	.....	.....
Ca II	3.34	1.26	1.01	0.68

* Mean height for this entry, 10.2×10^6 km.

4. *Comparison of observed and theoretical gradients.*—Inspection of Tables 6 and 8 and of Figure 5 shows that the apparent gradients of most of the atoms and ions investigated are remarkably similar. The only exception is *Ca* I, which has a steeper gradient than any of the other particles in the lower portion of the chromosphere. *Ca* II may share in this peculiarity, although not so markedly. Since the method of determining log N for *Ca* I and *Ca* II in the lowest level differed essentially from that used for the other ions and atoms, these apparent differences in behavior may be due, at least in part, to erroneous or inaccurate procedures followed in the reductions, although the writer believes them to be essentially correct. At future eclipses special attention should be directed toward obtaining more exact and reliable gradients in the lowest portions of the chromosphere, where the greatest difficulties and uncertainties arise.

In all the results plotted in Figure 5, the apparent gradients show a consistent tendency to become less steep with increasing height; but, except for *Ca* I and *Ca* II, the changes in gradient are not rapid. For a first comparison with theory we may omit *Ca*,

neglect the other variations with height, and note from Tables 6 and 8 that the mean apparent gradients are of the order of

$$\frac{\Delta \log N}{\Delta h} = 1.0 \times 10^{-12}\,\mathrm{cm}^{-1}.$$

If the chromosphere were in hydrostatic equilibrium at constant temperature, it would be characterized by a density-height relationship of the form

$$n = n_0 e^{-(m\mathcal{G}/kT)h} = n_0 e^{-ah},$$

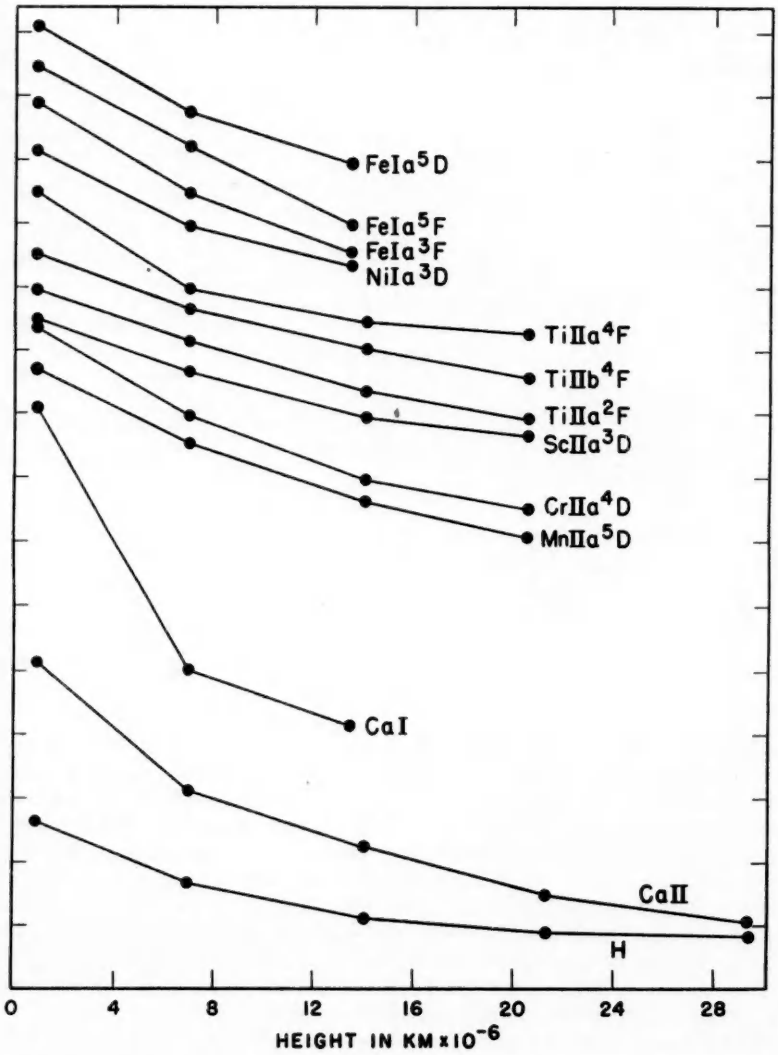

FIG. 5.—Mean apparent gradients in the chromosphere of Zeta Aurigae. The unit of the ordinate scale corresponds to a ratio of 1:10 in N, but the various curves are arbitrarily related to one another.

and the numbers of atoms in the line of sight would be given by[17]

$$N = \left(\frac{2\pi R}{a}\right)^{1/2} n_0 e^{-ah}.$$

For this case the apparent gradient is (natural logarithms)

$$\frac{\Delta ln\, N}{\Delta h} = a = \frac{m g}{kT}.$$

Thus the assumption of hydrostatic equilibrium leads to the prediction of apparent gradients proportional to the atomic weights of the particles, whereas the observations yield practically identical gradients for all constituents, including hydrogen. This result, which in itself clearly rules out the possibility of hydrostatic equilibrium, is not new. It is, however, probably still of interest to make some numerical comparisons.

If we adopt 20 ⊙ and 200 ⊙ as reasonable values for the mass and radius of the K star, respectively, the surface gravity is $g = 13.7$ cm/sec^{-2}. Hence for hydrogen at a temperature of 3300°, $a = 5.0 \times 10^{-11}$ cm^{-1}. By comparison, our adopted mean observed value of $(\Delta \log N)/\Delta h = 1.0 \times 10^{-12}$ cm^{-1} corresponds[18] to $a = 2.30 \times 10^{-12}$ cm^{-1}. Thus the hypothesis of hydrostatic equilibrium yields a gradient for hydrogen about twenty-two times greater than that observed. For elements of atomic weight 50 the discrepancy is fifty times greater.

The approximate equality of apparent gradients for all atomic weights is strongly suggestive of turbulent support in the manner suggested by W. H. McCrea.[19] In fact, Wellmann[6] found excellent agreement between the turbulent velocities required to give the observed gradients and those derived from the mean curve of growth for the lower chromosphere. The present results do not indicate such close agreement between these two quantities.

According to McCrea's theory, for those atoms whose temperature kinetic velocities are less than the turbulent velocities (i.e., all except hydrogen in this instance), the quantity a is given by

$$a = \frac{2g}{V_T^2}.$$

The observed turbulent velocity, V_T, has been tabulated in Table 3 as a function of height. The corresponding a's range from 1.6×10^{-11} to 6.5×10^{-11} cm^{-1}, compared to the observed values of about 1.5×10^{-12} to 4×10^{-12} cm^{-1} derived from the data of Table 6. In other words, the turbulent velocities derived from the curves of growth are inadequate to account fully for the support of the chromosphere of the K star; they lead to gradients about ten times greater than those observed. Even so, McCrea's hypothesis yields results far closer to the observed facts than does that of hydrostatic equilibrium and must almost certainly have some validity. Particularly suggestive are the rise of turbulent velocity and the decrease of gradient with height. Inevitably in a comparison such as this, a number of errors and approximations have been insinuated into the results; perhaps, if all could be eliminated, McCrea's theory would be completely successful. If not, some additional factor of chromospheric support must be sought.

In any case it must not be forgotten in making the above comparison that all the parameters used to describe the physical state of the chromosphere are mean values of some

[17] D. H. Menzel, *Pub. Lick Obs.*, Vol. **17**, eq. 20.30, 1931.

[18] This value of a agrees very closely with that found by F. E. Roach (*Ap. J.*, **93**, 1, 1941) by an application of Menzel's method to the observed light-curve of the 1939–1940 eclipse. Roach finds $a = 2.40 \times 10^{-12}$ cm^{-1}.

[19] *M.N.*, **89**, 718, 1929.

kind obtained by measuring integrated effects along lines of sight perpendicular to the radius of the star. The derivation of the corrections from mean to true values does not appear to be a very simple or direct process, owing to the rather involved way in which the parameters are interrelated, nor does the effort to derive such corrections appear justified unless the variations with height found in this paper are confirmed at future eclipses. Attention, however, is directed to the fact, that since the mean integrated values of turbulent velocity are found to increase with height, the true values are probably less than those given in Table 3. Hence the inadequacy of the hypothesis of turbulent support must be even greater than that noted above.

5. *Ionization and excitation in the chromosphere.*—The study of the ionization in the chromosphere of the K-type component of Zeta Aurigae is beset with numerous difficulties. In the first place, the physical arrangement is not simple. The atoms in the chromosphere are subjected to the radiation from the cool K-type star, which is moderately dilute ($W \sim \frac{1}{2}$), as well as to the much higher temperature and much more dilute radiation from the companion. The latter radiation may be additionally weakened by the opacity of the chromosphere itself, and any such opacity may well be a function of wave length. Moreover, the observations have yielded values of both neutral and ionized atoms only for calcium. It seems evident, then, that a direct frontal attack is not possible and that progress is to be expected only from a trial-and-error procedure. The results of this procedure must be tested as far as possible by comparison with observation, and the validity of the conclusions reached must be judged largely by their general consistency with the facts.

In order to minimize the effects of observational error, all calculations will be restricted to the two chromospheric levels at heights of 7 and 14×10^6 km, since it is for these that the determinations of $N_{Ca\ I}$ and $N_{Ca\ II}$ are most reliable.

Although we are dealing with an assemblage which is probably far removed from a state of thermodynamic equilibrium, it is instructive to begin the discussion by making some calculations based on the assumption that thermodynamic equilibrium prevails. By combining the Boltzmann and Saha equations for hydrogen, the number of hydrogen atoms in the second state is related to the number of hydrogen ions by the formula

$$\log \frac{n_i n_e}{n_2} = -\frac{5040\chi_2}{T} + 1.5 \log T + 14.78, \tag{13}$$

where χ_2 is the "ionization potential" of the second state, 3.38 volts. Equation (13) implies either that thermodynamic equilibrium exists or that the deviations from it are the same for the second state of hydrogen and for the state of ionization. For calcium the ionization equation is

$$\log \frac{n_i n_e}{n_0} = \frac{5040\chi}{T} + 1.5 \log T + 15.98. \tag{14}$$

If the apparent gradients in the chromosphere were constant, the numbers of atoms per cubic centimeter, n, would be related to the numbers in the line of sight by the equation[18]

$$n = N\left(\frac{a}{2\pi R}\right)^{1/2}.$$

We have seen that the chromosphere is characterized by nonconstant gradients, i.e., variable values of a. The variation is not extreme, and, since a enters only to the power $\frac{1}{2}$, it is reasonable to expect that the use of an appropriate mean value will give values of n which are approximately correct. We adopt $a = 2.3 \times 10^{-12}$ cm^{-1} for this purpose, except that for the height 14×10^6 km, the value 1.15×10^{-12} is used for hydrogen in order to make some allowance for the low gradients of this element observed at the higher levels. From the data of Table 7 we find the results in Table 9.

We now make the further assumption, which will be seen to be justified by the results, that practically all the electrons come from hydrogen, i.e., that $n_i = n_e$ in equation (13). Then, eliminating n_e between equations 13 and 14 and inserting the values of log n_2, log $n_{Ca\ I}$, and log $n_{Ca\ II}$ for $h = 7 \times 10^6$ km, we find

$$-\frac{22{,}100}{T} + \tfrac{3}{4} \log T = -3.90\,,$$

from which $T = 3370$. The corresponding electron density computed from equation (13) is log $n_e = 9.04$. A similar computation for $h = 14 \times 10^6$ km yields the results $T = 3070°$ and log $n_e = 8.30$. The foregoing procedure would be correct under conditions of thermodynamic equilibrium. Under the actual conditions it would appear to have merely formal significance, and the close correspondence found between T and the effective temperature of the K-type star would then be merely a coincidence.

The next step is to make the more reasonable assumption that the ionization of calcium is governed by the radiation of the B-type star. A. Pannekoek[20] has derived an

TABLE 9

VALUES OF LOG N AND LOG n FOR H, Ca I, Ca II

$h = 7 \times 10^6$ Km		$h = 14 \times 10^6$ Km	
log N_2 = 15.85,	log n_2 = +3.06	log N_2 = 15.20,	log n_2 = +2.11
log $N_{Ca\ I}$ = 12.74,	log $n_{Ca\ I}$ = −0.05	log $N_{Ca\ I}$ = 11.93,	log $n_{Ca\ I}$ = −0.86
log $N_{Ca\ II}$ = 15.90,	log $n_{Ca\ II}$ = +3.11	log $N_{Ca\ II}$ = 14.86,	log $n_{Ca\ II}$ = +2.07

equation applicable to this situation, which, although only an approximation, is still the best available. His equation is

$$\frac{n_i}{n_0} n_e = W \cdot T_1 T^{1/2} \frac{(2\pi m k)^{3/2}}{h^3} e^{-\chi/kT_1} \cdot 2 \frac{g_1}{g_0}. \tag{15}$$

With the radius of the B star adopted above and the known orbital elements, the dilution factor is $W = 3 \times 10^{-6}$. The temperature of the B star may be taken as $T_1 = 15{,}000°$. When these values are inserted into equation (15), the ionization formula for calcium reads

$$\log \frac{n_i}{n_0} n_e = \tfrac{1}{2} \log T + 12.60\,, \tag{16}$$

where T is the local electron temperature.

Equation (16) may now be used to compute n_e for a series of values of T, and corresponding values of n_e may be calculated from equation (13) for hydrogen. The results are given in Table 10 for $h = 7 \times 10^6$ km.

From Table 10 it is clear that consistency between calcium and hydrogen can be obtained only for very high electron temperatures, of the same order as the assumed surface temperature of the B star. This result is physically improbable; T should undoubtedly be less than T_1. Hence if the ionization of calcium is produced by the radiation of the B star, an electron density considerably higher than that obtainable from hydrogen is apparently required. Since hydrogen is presumably much more abundant than all the remaining atoms combined, the correct conclusion seems to be that the B star is not responsible for the ionization of calcium, and it is necessary to look for a source of opacity which will

[20] *Handb. d. Ap.*, **3**, Part I, 289, 1930.

reduce the ionizing radiation from the companion ($\lambda \sim 2000$ A for *Ca*) throughout most of the chromosphere.

The preceding calculations are strengthened by a consideration of the ionization of iron. On plate Ce 2194, corresponding to $h = 7 \times 10^6$ km, more than four hundred lines were measured for purposes of identification. Among them were several strong lines of *Fe* II, although there were not enough to be useful in forming curves of growth. In any case, however, there is no doubt that at this height n_i and n_o are of the same order of magnitude for iron. If we now use the standard ionization equation and insert the values for $\log n_e$ and T found in similar fashion from *Ca* and *H*, namely, $\log n_e = 9.04$, $T = 3370$, we find $\log n_i/n_o = +0.18$, $n_i = 1.5\, n_o$. If, on the other hand, it is supposed that the B-type star is responsible for the ionization of iron and Pannekoek's equation is employed with $W = 3 \times 10^{-6}$, $T_1 = 15{,}000$, $T = 15{,}000$, $\log n_e = 11.5$ (the latter two values from Table 10 in order to have a solution consistent with both *Ca* and *H*), we find $\log n_i/n_o = 2.30$, $n_i = 200 n_o$. With only one atom of iron in two hundred neutral it is difficult to see how the lines of *Fe* I could predominate as they do.

TABLE 10

COMPUTED VALUES OF LOG n_e FOR $h = 7 \times 10^6$ KM

T	*Ca*	*H*
2,000°	11.09	7.15
3,000	11.18	8.70
4,000	11.24	9.49
5,000	11.29	9.99
6,000	11.33	10.33
8,000	11.39	10.78
10,000	11.44	11.07
12,000	11.48	11.27
18,000	11.57	11.65

If opacity, τ, is effective in reducing the ionizing radiation, the right-hand side of equation (14) should be multiplied by the factor $e^{-\tau}$. For the electron densities derived above, $n_e \sim 10^8$ or 10^9, electron scattering will not suffice, since the scattering coefficient per electron is 7×10^{-25}. Thus for $n_e = 10^9$, $\tau \sim 10^9 \times 10^{13} \times 7 \times 10^{-25} \sim 10^{-2}$ independent of wave length.[21] On the other hand, the source of opacity proposed by Menzel[22] to account for the light-curve of Zeta Aurigae is more promising. Menzel supposes that the opacity arises from the interaction of electrons with positive ions and derives an expression[23] for τ_ν which we may write with ample accuracy as

$$\tau_\nu = \frac{C_o k}{\nu^3 T^{1/2}} \left(\frac{\pi R}{a}\right)^{1/2} e^{h\nu/kT} n_e^2 . \tag{17}$$

In equation (17), which gives τ_ν for the line of sight along which the central electron density is n_e, $C_o = 2.67 \times 10^{24}$, k is the Boltzmann constant, T the local kinetic temperature, and R the radius of the K star. The equation was derived on the assumption of an exponential density law, $n_i = n_e = n_o\, e^{-ah}$, which is not strictly true according to the present results; hence we shall again adopt $a = 2.3 \times 10^{-12}$ cm^{-1} as a reasonable ap-

[21] This argument may be used against the high-electron densities in the second column of Table 10. If the latter were correct, there would be appreciable opacity due to electron scattering at $h = 7 \times 10^6$ km and the eclipse should begin earlier than observed.

[22] *Harvard Circ.*, No. 417, 1935.

[23] *Ibid.*, eq. (8).

proximation. The choice of T is also uncertain. Menzel adopts for T the same value as the effective temperature of the K star, namely, $T = 3200°$. This appears reasonable, especially if most of the chromosphere is screened from the ultraviolet radiation of the B star. To illustrate the effect of varying T, the coefficient of n_e^2 in equation (17) is tabulated for several wave lengths and temperatures in Table 11.

The optical depths of the chromosphere may now be computed by using the values of n_e as calculated for hydrogen from Table 10, together with the coefficients of Table 11. We find the results given in Table 12 for $h = 7 \times 10^6$ km.

Table 12 is very instructive. First, if T lies in the range 3000°–4000°, especially if it is close to the lower limit, the opacity at λ 2000 A is ample to screen most of the chromosphere from the radiation of the B star, which is therefore eclipsed, while for λ > 3000 A

TABLE 11

COEFFICIENT OF n_e^2 FROM EQUATION (17)

λ	$T=2000$	$T=3000$	$T=4000$	$T=5000$
2000 A	3.3×10^{-11}	1.4×10^{-16}	4.1×10^{-19}	1.1×10^{-20}
3000	7.1×10^{-16}	1.8×10^{-19}	3.6×10^{-21}	3.0×10^{-22}
4000	4.2×10^{-18}	1.0×10^{-20}	3.5×10^{-22}	5.5×10^{-23}
5000	2.6×10^{-19}	1.8×10^{-21}	1.5×10^{-22}	3.2×10^{-23}

TABLE 12

τ_ν FOR THE CHROMOSPHERE OF ZETA AURIGAE AT $h=7\times10^6$ KM

λ	$T=2000$	$T=3000$	$T=4000$	$T=5000$
2000 A	6.6×10^{3}	35	3.9	1.1
3000	1.4×10^{-1}	4.5×10^{-2}	3.5×10^{-2}	2.9×10^{-2}
4000	8.4×10^{-4}	2.5×10^{-3}	3.4×10^{-3}	5.3×10^{-3}
5000	5.2×10^{-5}	4.5×10^{-4}	1.4×10^{-3}	3.1×10^{-3}

there is no eclipse, in agreement with observation. Since the ionization of calcium would then be governed largely by the radiation of the primary, the calculations made in the first portion of this section should be essentially correct. Moreover, for $T = 3000°$, the opacity at λ 3000 is about a hundred times greater than that at λ 5000. Such a large difference should be observable if photometric observations at future eclipses can be extended sufficiently far to the violet; the eclipse should begin earlier for the shorter wave lengths. In fact, if such an effect could be measured with sufficient precision, not only would the underlying theory used here be confirmed, but important quantitative results bearing on the conditions in the chromosphere might be expected.

There remains for consideration the excitation temperatures found from the a^5F and a^3F states of *Fe* I (Table 4). These two states are metastable as, indeed, are all those (except the ground states) for which gradients have been derived in this investigation. It is therefore natural to inquire whether metastability can play a role in producing the apparent rise in excitation temperature with height in the chromosphere. According to Rosseland's theorem[24] for a three-state atom subject to dilute radiation of temperature T, if the middle of the three states is metastable and lies close to the ground state, then its population can approach, but not exceed, that of the Boltzmann distribution for the

[24] *Mt. W. Contr.*, No. 309; *Ap. J.*, **63**, 218, 1926.

TABLE 13

VALUES OF LOG ($W \times \frac{3700}{\lambda}$)

Element, Transition, Wave Length	Log gf	Ce 2181 2183	Ce 2185 2188	Ce 2191 2192 2194	Ce 2199	Ce 2245	Ce 2248	Ce 2252 2253	Ce 2254	Ce 2255
FeI										
$a^5D - z^5P^0$										
3440.6	2.20		-1.23	-0.50			-0.78			
3441.3	1.82			-0.69			-0.89			
3443.9	1.27			-0.84						
3465.9	1.89		-1.20	-0.72	-0.50	-0.44	-0.92			
3475.5	1.88			-0.83	-0.32	-0.38	-0.98			
3490.6	1.73			-0.77	-0.51	-0.46	-1.09			
$a^5F - z^3G^0$										
3521.3	2.42				-0.68	-0.84				
3526.2	2.14				-0.50	-0.56				
3565.4	3.14		-1.10	-0.65	-0.55	-0.59	-0.92	-1.26		
3570.1	3.35		-0.77	-0.50	-0.52	-0.47	-0.61	-1.26		
$a^5F - z^5G^0$										
3587.0	2.58				-0.64	-0.52	-0.99			
3589.1	1.70				-0.87	-1.14				
3608.9	3.12			-0.66	-0.58	-0.61	-0.84			
3618.4	3.30			-0.62	-0.56	-0.51	-1.06			
3631.5	3.18			-0.53	-0.52	-0.50	-0.63	-0.94		
3647.8	3.14			-0.60	-0.46	-0.54	-0.85			
$a^5D - z^5P^0$										
3649.5	0.43				-0.86	-1.07				
3679.9	1.78			-0.78	-0.43	-0.58				
3683.0	0.89				-0.53	-0.59				
3705.6	1.98		-1.28	-0.77			-0.93			
3707.8	1.01			-1.15	-0.62	-0.77	-1.28			
3719.9	2.72		-1.02	-0.54	-0.31	-0.43	-0.57	-1.25		
3722.6	1.98		-1.62	-0.76	-0.34		-0.98			
3733.3	1.83		-1.76	-1.00	-0.58	-0.66	-1.10			
3737.1	2.59		-1.07	-0.51	-0.29	-0.38	-0.66	-0.98		
3748.3	2.15		-1.58	-0.69	-0.58	-0.57	-0.78			
$a^5F - y^5P^0$										
3687.5	2.63			-0.99	-0.43	-0.60	-1.15			
3709.2	2.78		-1.70	-0.93	-0.56	-0.57	-0.90			
3727.6	2.76		-1.70	-0.83	-0.37	-0.63	-1.10			
3734.9	3.67									
3743.3	2.59			-0.96	-0.61	-0.72	-1.04			
3749.5	3.50		-1.19	-0.61			-0.66			
3758.2	3.33		-1.15	-0.61	-0.49	-0.51	-0.70			
3763.8	3.10		-1.37	-0.69	-0.43	-0.49	-0.73			
3767.2	2.93		-1.49	-0.85	-0.58	-0.64	-1.13			
3787.9	2.52			-1.16	-0.56	-0.63	-1.37			
3795.0	2.61			-1.00	-0.52	-0.65	-1.10			
$a^3F - y^3D^0$										
3815.8	3.72		-1.14	-0.71	-0.48	-0.54	-0.86	-1.47		
3827.8	3.58		-1.33	-0.85	-0.54	-0.55	-0.94			
3841.0	3.41		-1.60	-1.01	-0.47	-0.63	-1.07			
3888.5	2.93									
3903.0	3.11		-1.66	-0.99	-0.62	-0.61	-1.14			
$a^5F - y^5D^0$										
3820.4	3.49		-0.93	-0.58	-0.52	-0.47	-0.59	-1.03		
3825.9	3.28		-1.09	-0.60	-0.51	-0.55	-0.69	-1.19		
3834.2	3.06		-1.28	-0.74	-0.58	-0.60	-0.73	-1.06		
3840.4	2.78		-1.48	-0.87	-0.39	-0.62	-1.07			
3850.0	2.53		-1.53	-1.06	-0.69	-0.88	-1.26			
3865.5	2.44		-1.55	-1.12	-0.65	-0.68	-1.30			
3872.5	2.46			-1.05	-0.68	-0.78	-1.48			
3878.0	2.50		-1.66	-1.05	-0.69	-0.69	-1.68			
3887.0	2.36		-1.48	-1.15	-0.56	-0.64	-1.05			
3898.0	1.54				-1.00	-1.10				
3917.2	1.47				-0.92	-1.02				
3940.9	1.08				-1.20	-1.14				

TABLE 13—Continued

Element, Transition, Wave Length	Log gf	Ce 2181 2183	Ce 2185 2188	Ce 2191 2192 2194	Ce 2199	Ce 2245	Ce 2248	Ce 2252 2253	Ce 2254	Ce 2255
FeI										
$a^5D - z^5D^0$										
3824.4	1.94		-1.59	-0.87	-0.62	-0.56	-1.11			
3856.4	1.98		-1.38	-0.78	-0.46	-0.60	-0.99			
3859.9	2.54		-1.05	-0.54	-0.49	-0.48	-0.67	-1.28		
3878.6	1.84		-1.60	-0.87	-0.50	-0.56	-1.07			
3886.3	2.14		-1.53	-0.76	-0.55	-0.52	-0.75			
3895.7	1.58		-1.72	-0.98	-0.63	-0.63	-1.30			
3899.7	1.74		-1.72	-0.89	-0.60	-0.62	-1.12			
3906.5	1.15				-0.60	-0.62				
3920.3	1.54			-0.95	-0.65	-0.55	-1.18			
3922.9	1.70			-0.90	-0.62	-0.56	-1.16			
3927.9	1.71			-0.94	-0.59	-0.59	-1.19			
3930.3	1.79			-0.90	-0.68	-0.56	-1.15			
$a^3F - y^3F^0$										
4045.8	3.78		-1.01	-0.70	-0.38	-0.44	-0.76			
4063.6	3.54		-1.14	-0.77	-0.52	-0.58	-0.93			
4071.8	3.43		-1.16	-0.78	-0.55	-0.56	-0.96			
NiI										
$a^3D - z^3F^0$										
3414.8	6.90		-1.08	-0.74	-0.52	-0.56	-1.00			
3458.5	6.55		-1.75	-0.95	-0.61	-0.59	-1.35			
3515.1	6.82		-1.51	-0.96	-0.61	-0.66	-1.24			
$a^3D - z^3D^0$										
3446.3	6.70		-1.85	-0.93	-0.56	-0.70	-1.14			
3472.5	6.24			-1.29	-0.62	-0.76	-1.55			
$a^3D - z^3P^0$										
3493.0	6.64			-0.96	-0.48	-0.52	-1.25			
3524.5	6.95		-1.38	-0.73	-0.47	-0.52	-1.05			
MgI										
$3^3P^0 - 3^3D$										
3829.4	9.79		-0.91	-0.66	-0.42	-0.50	-0.62	-1.02		
3832.3	10.13		-0.88	-0.62	-0.49	-0.50	-0.57	-0.85		-1.45
3838.3	10.32	-0.90	-0.64	-0.43	-0.42	-0.45	-0.42	-0.57	-0.83	-0.71
AlI										
$3^2P^0 - 4^2S$										
3944.0										
3961.5										
CrI										
$a^7S - y^7P^0$										
3578.7	7.02		-1.04	-0.59	-0.48					
3593.5	6.98		-0.87	-0.57	-0.54					
3605.3	6.82		-1.08	-0.63	-0.50					
TiII										
$b^4F - z^4P^0$										
3318.0	7.66	-0.89	-0.58	-0.54	-0.53	-0.51	-0.46	-0.83		
3322.9	7.91	-0.41	-0.41	-0.41	-0.31	-0.34	-0.34	-0.40		
3326.8	7.52	-1.05	-0.66	-0.48	-0.47	-0.43	-0.48	-0.68		
3329.4)										
3329.5)	7.95	-0.52	-0.47	-0.46	-0.37	-0.30	-0.34	-0.37		
3335.17)										
3335.22)	7.84	-0.58	-0.41	-0.43	-0.45	-0.40	-0.39	-0.53		

TABLE 13—Continued

Element, Transition, Wave Length	Log gf	Ce 2181 2183	Ce 2185 2188	Ce 2191 2192 2194	Ce 2199	Ce 2245	Ce 2248	Ce 2252 2253	Ce 2254	Ce 2255
Ti II										
3340.3) 3340.4)	7.83	-0.55	-0.51	-0.41	-0.36	-0.31	-0.34	-0.38		
3343.8	7.47	-1.23	-0.72	-0.58	-0.49	-0.56	-0.54	-0.79		
3346.73) 3346.77)	7.43	-0.97	-0.64	-0.48	-0.49	-0.40	-0.52	-0.69		
$b^4P - z^4S^0$										
3332.1	8.91	-0.89	-0.69	-0.58	-0.58	-0.43	-0.53	-0.75		
$a^2F - z^2G^0$										
3341.8	8.19	-0.39	-0.42	-0.36	-0.29	-0.26	-0.27	-0.36		
$a^4F - z^4G^0$										
3361.2	8.06	-0.40	-0.37	-0.33	-0.26	-0.26	-0.35	-0.31		
3372.78) 3372.86)	8.13	-0.35	-0.37	-0.33	-0.28	-0.16	-0.30	-0.32		
3380.26) 3380.31)	7.53	-0.56	-0.42	-0.32	-0.15	-0.21	-0.25	-0.38		
3383.8	8.07	-0.33	-0.35	-0.32	-0.35	-0.26	-0.28	-0.29		
3387.8	7.73	-0.51	-0.46	-0.39	-0.27	-0.17	-0.31	-0.46		
3394.6	7.66	-0.56	-0.48	-0.42	-0.45	-0.36	-0.39	-0.52		
3407.2	6.69		-0.91	-0.77	-0.50	-0.46	-0.84	-1.20		
3409.8	6.59		-1.08	-0.76	-0.48	-0.51	-0.83	-1.36		
$b^4F - z^4G^0$										
3444.3	7.30	-0.89	-0.66	-0.41			-0.39	-0.55		
3461.5	7.38	-0.80	-0.63	-0.43	-0.47	-0.44	-0.41	-0.60		
3477.2	7.37	-0.83	-0.57	-0.41			-0.42	-0.60		
3489.8	6.26		-1.43	-0.78	-0.69	-0.63	-1.27	-1.48		
3491.1	7.25	-1.01	-0.73	-0.48	-0.35	-0.39	-0.45	-0.64		
3500.3	6.41		-1.25	-0.87	-0.67	-0.66	-1.23			
$b^2G - y^2G^0$										
3504.88) 3504.92)	9.49	-1.16	-0.91	-0.70	-0.59	-0.57	-0.73	-0.98		
3510.8	9.41		-1.11	-0.83	-0.70	-0.62	-0.89	-1.26		
$a^2F - z^4D^0$										
3561.6	7.02		-1.64	-1.34	-0.66	-0.71	-1.30	-1.68		
3573.7	7.17		-1.27	-0.80	-0.73	-0.62	-0.96	-1.39		
3596.1	7.47	-1.33	-0.79	-0.59	-0.58	-0.60	-0.71	-0.83		
$a^2P - z^2S^0$										
3624.8	8.26			-0.71	-0.61	-0.59	-0.76	-0.99		
3641.3	8.41			-0.87	-0.65	-0.74	-0.83			
$a^2F - z^2D^0$										
3685.2	8.31	-0.40	-0.40	-0.39	-0.42	-0.37	-0.36	-0.39	-0.43	-0.42
$a^2F - z^2F^0$										
3759.3	8.09	-0.41	-0.42	-0.36	-0.39	-0.37	-0.28	-0.37	-0.40	-0.38
3761.3	8.08	-0.44	-0.43	-0.39	-0.43	-0.33	-0.29	-0.36	-0.40	-0.39
$a^2G - z^2G^0$										
3900.5	8.48	-1.25	-0.80	-0.56	-0.52	-0.48	-0.60		-1.26	-1.19
3913.5	8.44	-1.26	-0.83	-0.56	-0.58	-0.49	-0.56	-1.08	-1.28	-1.42
Cr II										
$a^4D - y^4P^0$										
3336.4	10.00	-1.29	-0.96	-0.68	-0.57	-0.55	-0.68	-0.88		
3339.8	10.14	-0.84	-0.58	-0.50	-0.50	-0.46	-0.56	-0.70		
3342.6	10.23	-0.75	-0.65	-0.54	-0.50	-0.45	-0.46	-0.65		
3347.8	10.05	-1.13	-0.79	-0.61	-0.50	-0.59	-0.67	-0.86		
3358.5	10.32	-0.70	-0.56	-0.50	-0.42	-0.39	-0.41	-0.56		
3368.1	10.63	-0.46	-0.43	-0.43	-0.41	-0.34	-0.40	-0.34		

TABLE 13 —Continued

Element, Transition, Wave Length	Log gf	Ce 2181 2183	Ce 2185 2188	Ce 2191 2192 2194	Ce 2199	Ce 2245	Ce 2248	Ce 2252 2253	Ce 2254	Ce 2255
Cr II										
$a^4D - z^4P^0$										
3382.7	10.10	-0.97	-0.73	-0.57	-0.53	-0.39	-0.54	-0.58		
3391.4	9.64	-1.51	-1.46	-1.11	-0.78	-0.73	-1.12			
3403.4	10.27	-0.58	-0.57	-0.53	-0.51	-0.44	-0.41	-0.54		
3408.8	10.40	-0.51	-0.48	-0.49	-0.39	-0.40	-0.34	-0.49		
3421.2	10.27	-0.75	-0.68	-0.57	-0.55	-0.55	-0.60	-0.70		
3422.8	10.32	-0.55	-0.55	-0.46	-0.45	-0.43	-0.40	-0.44		
3433.3	10.30	-0.70	-0.61	-0.47	-0.37	-0.33	-0.49	-0.53		
$a^4D - z^6P^0$										
3495.4	9.06			-1.18	-0.83	-0.77	-1.40	-1.75		
3511.8	8.96		-1.34	-1.10	-0.94	-0.74	-1.22	-1.32		
Sc II										
$a^3D - z^3P^0$										
3369.0	7.16		-0.96	-0.76	-0.49	-0.48	-0.76			
3372.2	7.28	-1.13	-0.72	-0.50	-0.46	-0.42	-0.53	-0.75		
$a^3D - z^3D^0$										
3558.5	6.87	-1.56	-0.84	-0.68			-0.72	-1.44		
3567.70)										
3567.74)	6.78	-1.41	-1.28	-0.70	-0.60	-0.51	-0.85	-1.28		
3572.48)										
3572.57)	7.21	-1.00	-0.66	-0.54	-0.53	-0.50	-0.59	-0.73		
3576.33)										
3576.39)	7.11	-1.31	-0.78	-0.64	-0.62	-0.56	-0.72	-0.95		
3580.9	7.31		-0.59	-0.39		-0.35	-0.44	-0.73		
3590.47)										
3590.51)	6.58	-1.45	-1.27	-0.80	-0.62	-0.63	-1.00	-1.35		
$a^3D - z^3F^0$										
3613.81)										
3613.88)	7.31	-0.95		-0.51	-0.45	-0.46	-0.46	-0.68		
3630.74)										
3630.78)	7.18	-1.42		-0.57	-0.55	-0.53	-0.56	-0.84		
3642.78)										
3642.88)	7.10			-0.48	-0.46	-0.49	-0.60	-0.71		
3645.29)										
3645.34)	6.59			-0.70	-0.63	-0.58	-0.80			
3651.8	6.66			-0.82	-0.63	-0.59	-0.84			
Mn II										
$a^5D - z^5P^0$										
3442.0	9.70	-0.71	-0.55	-0.45	-0.50	-0.47	-0.41	-0.51		
3460.3	9.55	-0.77	-0.57	-0.42	-0.47	-0.43	-0.44	-0.54		
3482.9	9.35	-1.05	-0.63	-0.51	-0.52	-0.44	-0.55	-0.66		
3488.7	9.28	-1.15	-0.70	-0.58	-0.57	-0.52	-0.65	-0.72		
3495.8	8.85	-1.40	-1.19	-0.74			-0.74	-1.09		
3496.8	8.42		-1.61	-1.01	-0.66	-0.66	-1.16	-1.48		
3497.5	8.78		-1.37	-0.78	-0.36	-0.57	-0.95	-1.35		
V II										
$a^3F - z^5D^0$										
3517.3	7.78	-1.42	-1.19	-0.96	-0.77	-0.78	-1.12	-1.34		
$a^3F - y^3D^0$										
3530.8	7.68		-1.38	-0.95	-0.73	-0.74	-1.06			
3545.2	7.85		-1.45	-0.99	-0.78	-0.76	-1.05			
3556.8	8.10	-1.20	-0.84	-0.69	-0.53	-0.47	-0.88	-1.10		

temperature T. If this same result may be presumed to apply to a complicated atom like *Fe* I, the fact that the measured excitation temperatures all exceed that of the K-type star leads us to attribute them to the influence of the B star. This point of view can apparently be supported qualitatively, although it does not appear feasible to make numerical comparisons.

If we now suppose that the chromosphere possesses the opacity given by Menzel's formula, it is, of course, completely opaque at all wave lengths when the line of sight is tangent to the limb. If observations could be made at this point, one would expect to find an excitation temperature equal to that of the K star. As the line of sight passes at successively greater heights above the limb, the opacity decreases, the "clearing" taking place first in the red and gradually extending to greater frequencies. At first, the ioniza-

TABLE 14

EQUIVALENT WIDTHS OF H, K, λ 4227, AND *H* 7–*H* 12

Element Line	Ce 2181 Dec. 16	Ce 2185 Dec. 17	Ce 2191, 2194 Dec. 18	Ce 2199 Dec. 19	Ce 2245 Jan. 27	Ce 2248 Jan. 28	Ce 2252 Jan. 29	Ce 2254 Jan. 30	Ce 2255 Jan. 31
Ca II H	0.48	0.52	0.67	.....	.....	0.77	0.67	0.59	0.57
K	.70	.73	.94	7.71*	2.87†	.92	.87	.81	.70
Ca I 4227	.....	.12	.37	2.67‡	1.53§	.28	.....	.....	.....
H *H* 7	.45	.45	.54	.....	.....	.60	.59	.54	.56
H 8	.34	.43	.46	0.35	0.55	.54	.44	.51	.38
H 9	.28	.25	.40	0.32	0.40	.44	.39	.27	.34
H 10	.30	.35	.....	.....	.....	.40	.40	.27	.38
H 11	.24	.28	.29	.....	.....	.40	.36	.28	0.37
H 12	0.22	0.27	0.29	0.40	.....	0.33	0.30	0.24	.....

* $W_{BK} = 9.86$, $W_K = 12.89$, $\alpha = 3.36$, corrected $\alpha = 1.41$.
† $W_{BK} = 6.47$, $W_K = 12.89$, $\alpha = 3.36$, corrected $\alpha = 1.78$.
‡ $W_{BK} = 3.87$, $W_K = 4.46$, $\alpha = 1.17$, corrected $\alpha = 0.49$.
§ $W_{BK} = 3.34$, $W_K = 4.46$, $\alpha = 1.17$, corrected $\alpha = 0.62$.

tion is unaffected, but transitions from the ground state and the low metastable states of *Fe* I and similar atoms to the higher nonmetastable states become increasingly due to the dilute radiation of the companion. The exact effect of these processes on the low metastable states is difficult to determine; but probably there will be an enhancement of their populations which will be reflected in apparently higher excitation temperatures. In fact, the result that a^3F yields consistently higher excitation temperatures than a^5F may possibly be due to the relatively greater metastability of a^3F. To proceed from the latter to the ground state, a^5D, an atom must make an intersystem transition, unless an ionization process is involved and the intersystem lines are, with some exceptions, not very strong.

As the top of the chromosphere is approached, its transparency becomes complete at all wave lengths, and one would expect both ionization and the relative populations of atomic energy states to correspond to the dilute radiations of the B star. Unfortunately, by the time this situation is attained, there are no longer enough metallic atoms in the line of sight to permit the observations necessary to confirm it. In a general way, however, the preceding considerations appear capable of accounting for the behavior of the excitation temperature over its observable range.

SPECTROPHOTOMETRY OF THE F STARS AND OF τ URSAE MAJORIS. I*

JESSE L. GREENSTEIN
Yerkes and McDonald Observatories
Received November 15, 1947

ABSTRACT

This investigation deals with the curves of growth and the abundances of the elements in a group of F stars of a wide range of luminosity. Line intensities of about three hundred and fifty lines have been measured on McDonald coudé spectra (Table 2) in τ UMa, ρ Pup, θ UMa, α CMi, and α Per. A discussion of central intensities shows that the spectrum of τ UMa, a "metallic-line A star," is not of binary composite origin. Hydrogen-line contours show only small dependence on luminosity in the F stars.

The theory of the curve of growth is examined from the point of view of model atmospheres. It is found that the use of a Milne-Eddington model with constant η appreciably changes the curves of growth from the Schuster-Schwarzschild model. An estimate is made, from models of a dwarf F star and of the sun, as to the actual variation of η with optical depth. In a comparison of the F stars with the sun some of these effects of stratification are partially eliminated. The deduced value of the damping constant in the sun and the F stars is much reduced by use of the M.E. model. Deviations from the theoretical curves of growth remain in the best-observed solar curve.

The semiempirical solar-line strengths of K. O. Wright are used to analyze the atmospheres of the five F stars. Similar empirical line strengths are derived from τ UMa. Curves of growth are given in Figures 1–10; the damping constants are low, and turbulence increases in the giant stars. From these curves the apparent abundances of the elements are derived for each star (Table 7). The temperature and pressure at a representative point in the atmospheres are determined by a simultaneous solution giving the correct level of ionization and opacity for some standard elements. This also yields the total pressure and surface gravity. After correction for level of ionization, the abundances relative to the sun of about twenty elements are given in Table 12. No well-established abundance changes by a factor of 2 exist (except in the peculiar star, τ UMa). In the mean the stellar and solar abundances are identical. A slight tendency exists in the supergiants for greater abundances of the heavier elements as compared to the dwarfs. An analysis of the hydrogen lines predicts the observed null-effect and suggests that the hydrogen/metal ratio is the same in the F stars as in the sun.

The present investigation is concerned with the effects of absolute magnitude on stellar spectra and with possible variations of the abundances of the elements from star to star. Even with the highest dispersion now available, the instrumental and physical blending of spectral lines is serious for all stars of types G and later. From a survey of available McDonald coudé spectra, it was found that stars of type F5 were most suitable for this investigation. One particular object of interest is the so-called "metallic-line A star," τ Ursae Majoris; since, in fact, τ UMa is a peculiar F star, a group of stars near F5 was chosen. The stars selected for analysis are standard stars in the Yerkes *Atlas of Stellar Spectra*.[1] The measures of α CMi and α Per were made in the *Photometric Atlas of Stellar Spectra*[2] and will be discussed in more detail by Greenstein and Hiltner[3] in Paper II of this series.

The McDonald coudé plates have a dispersion of 2.8 A/mm at $H\gamma$; the slit width ranges from 0.03 to 0.05 mm; and the resolution is near 30,000. Eastman 103*a*-O emulsion is used throughout. The spectral types and approximate luminosities are listed in Table 1, together with n, the number of measured tracings. Actually, θ UMa was measured on two completely independent microphotometer tracings of the same plate, reduced separately in a study of the accidental errors. Most lines were measured on three

* *Contributions from the McDonald Observatory, University of Texas*, No. 145.

[1] Morgan, Keenan, and Kellman (Chicago: University of Chicago Press, 1943).

[2] Hiltner and Williams (Ann Arbor, 1946).

[3] *Ap. J.*, in press; to be Paper II of this series.

plates in τ UMa; several different plates were used to obtain the intensity tracings in the *Photometric Atlas*[2] of α CMi and α Per, although few lines are measured on more than one plate.

The plates cover only the region $\lambda\lambda$ 4000–4800 A. The calibration, described elsewhere,[2] consists of a wedge-slit spectrogram taken with the coudé spectrograph and developed together with the stellar spectra under standard conditions. The final contrast, as measured on the microphotometer tracings, varies less than 10 per cent from night to night. The variation of contrast with wave length is very slow. A tube-photometer exposure is usually taken as a check on the wedge spectrogram; no systematic difference is found. The tracings obtained with the Yerkes microphotometer (which is of the conventional transmission type), have a dispersion of 35 mm/A. Line depths were measured every millimeter on the tracing, converted into absorptions, and numerically integrated to obtain the equivalent width. Overlap between successive tracings of a plate provided a check on the systematic agreement of individual runs. The extensive measures and reductions, involving about fifty thousand settings, were made with the kind assistance of Miss Gertrude Peterson, Mrs. Wrubel, and Mrs. Greenstein. About three hundred and fifty lines were chosen for measurement. Identifications are based mainly

TABLE 1

STARS MEASURED SPECTROPHOTOMETRICALLY

Star	Abs. Mag.	Type	n	Line Quality
τ UMa	+3:	F6+A3	4	Broadened
α Per	−5	F5 I*b*	1	Very broad
ρ Pup	−3	F6 II	2	Broadened
θ UMa	+1.5	F6 III	2	Sharp
α CMi	+2.5	F5 IV	1	Sharp

on Swensson's study[4] of α CMi but take account of the strengthening of the ionized elements in high-luminosity objects. For use, a line should be substantially unblended in the sun, in α CMi, and in the supergiants. Unfortunately, the increased strength of the lines and the turbulent broadening in α Per, τ UMa, and ρ Pup makes blending serious; many useful lines had to be omitted in α Per. The lines selected had, in general, solar values of the line-absorption coefficient, log X_f, available in an unpublished list by Dr. K. O. Wright, of the Dominion Astrophysical Observatory, who very kindly supplied his data prior to publication. A group of rare-earth and other important lines was added, many of which were weak, blended, or absent in the sun. For some lines new values of the solar log X_f were determined; unfortunately, some could be derived only from the Rowland estimated intensities.

Table 2 gives the spectrophotometric measures of $-\log_{10} W/\lambda$. The wave lengths used are the laboratory values. A symbol p (or a single dot in the figures) indicates that the measurements are affected by blending on the tracings; the symbol P (or a double dot in the figures) indicates serious blending and very low weight. The excitation potentials, E.P., in electron-volts, are given for the lower level producing the line. The value of log $\eta_0(\tau)$ is given for each line in τ UMa; analogous to the solar log X_0, it is the ratio at the center of the line of s_0, the line-absorption coefficient to the continuous-absorption coefficient, κ_ν. The $\eta_0(\tau)$ is read from the theoretical curve of growth of τ UMa, using the measured intensity in that star. While the measured intensities are inferior in accuracy to the solar values and while τ UMa is a peculiar star, these $\eta_0(\tau)$'s have considerable usefulness. In analysis of A and F stars many lines of ionized elements, especially rare

[4] *Ap. J.*, **103**, 207, 1946.

TABLE 2

MEASURED LINE INTENSITIES IN F STARS

$-\log W/\lambda$

λ	Element	τ UMa	ρ Pup	θ UMa	α CMi	α Per	log $\eta_0(\tau)$*	E.P.	Notes
4017.16	*Fe* I	4.44p	.....	.....	4.49	.....	1.52	3.04	
20.90	*Co* I	4.75	.....	.....	4.79	4.84p	0.60	0.43	
22.74	*Fe* I	4.86p	.....	.....	4.75P	.....	0.38	3.27	
28.33	*Ti* II	4.41p	.....	.....	4.50	4.14	1.65	1.88	
33.07	*Mn* I	4.21p	.....	.....	4.24p	4.01P	2.80	0	
34.49	*Mn* I	4.31	.....	.....	4.38	4.08	2.20	0	
35.73	*Mn* I	4.23p	.....	.....	4.29	4.06	2.67	2.13	1
36.78	*V* II	4.69	.....	.....	4.61	4.43p	0.75	1.47	
40.65	*Fe* I	4.29	.....	.....	4.49	4.35P	2.30	3.27	
41.36	*Mn* I	4.35	.....	.....	4.37	4.22P	1.95	2.11	
44.61	*Fe* I	4.35	.....	.....	4.41	4.34p	1.95	2.82	
45.82	*Fe* I	3.83p	.....	3.97	3.88	3.72P	.....	1.48	1
47.32	*Fe* I	5.33P	.....	5.65P	5.09P	5.01P	9.70	2.27	
49.33	*Fe* I	4.76	.....	4.97p	4.88P	.....	0.58	2.58	
50.32	*Zr* II	5.52	.....	5.35	4.81P	.....	9.48	0.71	
55.54	*Mn* I	4.48P	.....	4.61	4.50	4.56p	1.37	2.13	
57.50	*Mg* I	4.30p	4.19p	4.28	4.15	4.19p	2.25	4.33	1
59.39	*Mn* I	5.05	5.31P	5.19P	5.16p	.....	0.08	3.06	
59.73	*Fe* I	4.65p	4.73p	4.87	4.87	.....	0.85	3.53	
62.82	*Pr* II	4.66P	4.91p	5.28p	5.50P	.....	0.82	0.42	1, 2
63.60	*Fe* I	4.18p	4.06p	4.20p	3.97p	3.95P	2.95	1.55	
65.07	*V* II	4.85	4.93	5.15p	4.94P	.....	0.40	3.78	2
65.39	*Fe* I	4.88	4.84P	4.93p	4.57p	.....	0.35	3.42	
67.98	*Fe* I	4.38	4.30	4.55	4.42	4.25	1.80	3.20	
70.77	*Fe* I	4.46p	4.48p	4.69	4.50	4.37p	1.44	3.23	
71.74	*Fe* I	4.11	4.08	4.16	4.10	3.99	3.28	1.60	
72.52	*Fe* I	4.55	4.62	4.80	4.56	4.40	1.13	3.42	
73.48	*Ce* II	4.70P	4.80P	5.38P	5.35P	.....	0.72	0	
77.71	*Sr* II	3.88	3.85p	4.15	4.02	3.75P	4.00	0	1
79.85	*Fe* I	4.58	4.53p	4.72	4.56	.....	1.03	2.85	
82.94	*Mn* I	4.61p	4.57	4.80	4.56	.....	0.95	2.17	
83.23	*Ce* II	4.72p	4.92	5.21p	5.31P	.....	0.67	1.30	
84.50	*Fe* I	4.43	4.43P	4.61	4.43	4.41p	1.56	3.32	
86.72	*La* II	4.61p	4.56P	4.91	4.77	.....	0.95	0	
91.56	*Fe* I	4.95	4.84	4.95	4.94	4.73P	0.23	2.82	3
4109.07	*Fe* I	4.80	4.70p	4.86	4.75	.....	0.50	3.28	3
10.53	*Co* I	4.62	4.80	4.82p	4.92	4.82P	0.92	1.04	3
11.78	*V* I	4.79	4.86p	4.87	4.86	4.86p	0.52	0.30	3
12.35	*Fe* I	5.00p	.....	4.96p	4.96	4.82P	0.15	3.38	3
14.45	*Fe* I	4.59	4.54p	4.70	4.61	4.50	1.00	2.82	3
15.18	*V* I	4.90P	4.87P	5.09P	4.95P	4.81P	0.32	0.28	3
18.14	*Ce* II	4.87P	4.91P	5.27P	5.18P	.....	0.37	0.22	
18.77	*Co* I	4.39P	4.33P	4.49P	4.43P	.....	1.75	1.04	1
20.83	*Ce* II	4.97	5.11p	5.47p	5.61P	4.84P	0.20	0.92	
21.32	*Co* I	4.48	4.43	4.62	4.44	4.37P	1.37	0.92	
23.23	*La* II	4.51p	4.50P	4.89	4.75P	4.38P	1.27	0.32	
26.19	*Fe* I	4.57p	4.43P	4.70	4.53P	.....	1.06	3.32	
26.52	*Cr* I	4.91p	.....	5.29	5.06p	.....	0.30	2.53	
28.05	*Si* II	4.38p	4.35P	4.64P	4.46p	4.15P	1.80	9.79	2, 4
28.74	*Fe* II	4.50p	4.44p	4.82	4.64	4.24P	1.30	2.57	

* When log $\eta_0(\tau)$ is negative it is given in the form log $\eta_0(\tau) + 10$.

TABLE 2—*Continued*

λ	Element	τ UMa	ρ Pup	θ UMa	α CMi	α Per	log $\eta_0(\tau)$	E.P.	Notes
4129.73	*Eu* II	4.38P	4.35p	4.93P	4.77P	4.51P	1.80	0	5
32.06	*Fe* I	4.14p	4.11P	4.28	4.21	.....	3.15	1.60	
32.90	*Fe* I	4.45p	4.40P	4.63	4.45p	.....	1.48	2.82	
33.87	*Fe* I	4.40p	4.40p	4.64p	4.43p	4.34	1.70	3.42	1
36.51	*Fe* I	4.79p	4.74p	4.90	4.54	.....	0.52	3.35	
37.00	*Fe* I	4.40	4.36	4.64	4.46	4.46P	1.70	3.40	
39.93	*Fe* I	4.84	4.78	4.91	4.76	4.73	0.42	0.99	
40.44	*Fe* I	4.80	4.76	4.96	4.75	4.80p	0.50	3.40	
43.42	*Fe* I	4.31	4.24P	4.42	4.39	4.21P	2.20	3.03	
43.87	*Fe* I	4.23	4.16p	4.32	4.26	4.09P	2.67	1.55	
47.67	*Fe* I	4.43	4.36p	4.59	4.46	4.30p	1.56	1.48	
50.97	*Zr* II	4.65	4.58	4.91P	4.89	4.44	0.85	0.80	1
57.79	*Fe* I	4.36	4.34	4.58	4.44	4.27	1.90	3.40	
61.20	*Zr* II	4.51p	4.36p	4.63p	4.53P	.....	1.27	0.71	
61.80	*Sr* II	4.52P	4.45p	4.95p	4.77P	.....	1.23	2.93	
66.00	*Ba* II	4.70	4.93	5.34	5.47P	.....	0.72	2.71	
67.27	*Mg* I	4.38p	4.26p	4.38	4.24p	4.09p	1.80	4.33	
72.75	*Fe* I	.....	.....	4.35	.....	4.17P	.....	0.95	1
74.92	*Fe* I	4.49	4.41	4.60	4.42	4.38P	1.33	1.00	
75.64	*Fe* I	4.37	4.28	4.59	4.36	4.25p	1.85	2.83	
77.54	*Y* II	4.04	4.02	4.27	4.19	3.95p	3.53	0.41	
78.39	*V* II	4.80p	4.90p	5.22p	5.09p	.....	0.50	1.68	
78.86	*Fe* II	4.23P	4.22p	4.55	4.36	3.92P	2.67	2.57	
79.81	*Zr* II	5.32P	4.91	5.37	5.30p	.....	9.71	1.66	
83.44	*V* II	4.56	4.58	4.85	4.55p	4.31P	1.10	2.04	
84.90	*Fe* I	4.40	4.37	4.61	4.54	4.33P	1.70	2.82	
86.60	*Ce* II	4.53	4.54p	4.86p	4.83p	.....	1.20	0.38	
87.04	*Fe* I	4.27p	4.23p	4.43	4.34	.....	2.40	2.44	
87.80	*Fe* I	4.16	4.11	4.36p	4.23P	4.03p	3.05	2.42	
9 7	*Ni* II	4.65	4.87p	4.84p	5.05	4.68P	0.85	4.01	2
99.10	*Fe* I	4.27	4.19	4.47	4.38	4.11P	2.40	3.03	
99.97	*Fe* I	4.76	4.71	4.77p	4.59p	4.74P	0.58	0.09	1
4200.93	*Fe* I	4.51	4.43	4.67P	4.44P	4.37P	1.27	3.38	
03.99	*Fe* I	4.32	4.27	4.52	4.39	4.16p	2.14	2.83	
04.69	*Y* II	4.64P	4.62P	4.87P	4.78P	.....	0.87	0	2
05.05	*Eu* II	4.29p	4.30P	4.62P	4.63P	4.28P	2.30	0	2, 5
06.38	*Mn* II	4.89P	4.99	5.45p	5.35P	.....	0.34	5.37	2
06.70	*Fe* I	4.55p	4.52P	4.59	4.48p	4.29P	1.13	0.05	
07.35	*Cr* II	4.78P	4.93p	5.09p	5.19P	.....	0.54	3.81	2
08.99	*Zr* II	4.85p	4.49P	4.81	4.76p	.....	0.40	0.71	
10.35	*Fe* I	4.33	4.24	4.47	4.42	4.22p	2.07	2.47	
13.65	*Fe* I	4.52	4.43	4.69p	4.56	4.42	1.23	2.82	
15.02	*Gd* II	4.85	5.01	5.06	5.72P	.....	0.40	0.43	2
15.52	*Sr* II	4.03	3.98	4.21p	4.15	3.93p	3.56	0	
16.19	*Fe* I	4.37	4.30	4.48p	4.38	4.24P	1.85	0	
19.36	*Fe* I	4.30	4.22	4.65	4.37	4.24	2.25	3.56	
22.22	*Fe* I	4.35	4.28	4.52	4.45	.....	1.95	2.44	
22.98	*Pr* II	4.98P	5.06p	5.10p	5.28P	.....	0.18	0.05	2
26.73	*Ca* I	4.19P	4.00p	4.07P	3.98p	4.00P	2.90	0	
27.43	*Fe* I	4.21	4.11p	4.34	4.21p	4.10P	2.80	3.32	

TABLE 2—*Continued*

λ	Element	τ UMa	ρ Pup	θ UMa	α CMi	α Per	log $\eta_0(\tau)$	E.P.	Notes
4228.72	*Fe* I	5.35p	5.28P	5.51P	5.45	.....	9.68	3.35	
32.06	*V* II	4.83P	4.84p	5.15p	5.02p	.....	0.44	3.96	2
33.17	*Fe* II	4.19P	4.12P	4.41	4.29	.....	2.90	2.57	1
33.61	*Fe* I	4.31p	4.25P	4.47	4.39	.....	2.20	2.47	
35.94	*Fe* I	4.17	4.12	4.28	4.26	4.05p	3.00	2.42	
38.03	*Fe* I	4.56p	4.46p	4.63	4.57	.....	1.10	3.40	
38.38	*La* II	4.54P	4.74P	5.02P	5.40P	.....	1.16	0.40	
40.37	*Fe* I	4.81p	4.59	4.67	4.56p	4.82P	0.48	3.53	
44.26	*Mn* II	5.33	5.72	5.45	5.85	5.16P	9.70	5.35	
44.80	*Ni* II	4.69	5.02	5.48	5.48	5.00P	0.75	4.02	
45.26	*Fe* I	4.41	4.35	4.47	4.41	4.43p	1.65	2.85	
46.09	*Fe* I	4.48	4.49	4.66	4.65	4.47p	1.37	3.63	
46.83	*Sc* II	4.31p	4.20	4.40	4.33	4.04P	2.20	0.31	
47.43	*Fe* I	4.32	4.29	4.42	4.37	4.13p	2.14	3.35	
48.23	*Fe* I	4.54	4.51p	4.64p	4.51	4.49P	1.16	3.06	
48.68	*Ce* II	4.72	4.92p	4.93P	5.12P	.....	0.67	0.20	2
50.12	*Fe* I	4.29	4.23	4.41	4.38	4.11p	2.30	2.46	
50.79	*Fe* I	4.25	4.16	4.33	4.31	4.06p	2.54	1.55	
51.74	*Gd* II	4.68p	4.83	5.35	5.45	.....	0.77	0.38	2
52.62	*Cr* II	4.41p	4.51	4.82	4.76	4.29P	1.65	3.84	
54.35	*Cr* I	4.20	4.18	4.38	4.37	4.06	2.85	0	
58.62	*Fe* I	5.02p	4.95P	4.85P	4.81P	.....	0.12	2.82	
60.48	*Fe* I	4.19	4.09P	4.29P	4.10P	.....	2.90	2.39	
61.92	*Cr* II	4.32p	4.33	4.59p	4.49p	4.17	2.14	3.85	
63.59	*La* II	4.89p	5.03P	5.32	5.55P	.....	0.34	1.95	2
64.21	*Fe* I	4.83p	4.72p	4.80	4.73	4.69P	0.44	3.35	
64.74	*Fe* I	5.10	4.95p	5.04	4.96	.....	0.00	3.94	
65.26	*Fe* I	4.87	4.73	4.96	4.86	4.76P	0.37	3.91	
67.83	*Fe* I	4.58	4.46	4.58	4.45	4.48	1.03	3.10	
71.16	*Fe* I	4.30	4.23	4.38	4.35	4.13P	2.25	2.44	
71.76	*Fe* I	4.18	4.08	4.19	4.15	4.02P	2.95	1.48	
74.80	*Cr* I	4.24	4.18	4.35	4.26	4.12p	2.60	0	
76.68	*Fe* I	4.84	4.77P	5.01	4.90	4.64P	0.42	3.86	
82.41	*Fe* I	4.29	4.21	4.48	4.41	4.08p	2.30	2.17	
83.01	*Ca* I	4.70	4.32	4.49	4.42	4.20P	0.72	1.88	
83.77	*Mn* II	5.33p	5.52	5.90p	5.68P	.....	9.70	5.35	2
84.21	*Cr* II	4.44	4.44P	4.73	4.58	4.18p	1.52	3.84	
85.44	*Fe* I	4.56	4.45p	4.58	4.55	4.52p	1.10	3.22	
86.01	*Ti* I	5.00P	4.75P	4.64P	4.65p	.....	0.15	0.82	
86.97	*La* II	4.54	4.62	4.62	4.45	.....	1.16	1.94	1
87.40	*Ti* I	5.24	5.00	4.99	4.93	.....	9.81	0.83	
89.07	*Ti* I	5.00P	.....	4.74P	.....	.....	0.15	0.82	
90.93	*Ti* I	4.78	.....	4.52P	.....	4.78P	0.54	0.81	1
91.47	*Fe* I	4.75	4.61	4.77p	4.65	4.63P	0.60	0.05	
94.77	*Sc* II	4.95	4.65	4.69	4.60	.....	0.23	0.60	
96.57	*Fe* II	4.21	4.18	4.46p	4.42	4.03P	2.80	2.69	
98.66	*Ti* I	4.90	4.73P	4.58P	4.78P	.....	0.32	0.82	
4300.05	*Ti* II	4.19p	4.05p	4.30p	4.24p	3.92P	2.90	1.18	
00.82	*Fe* I	4.92p	.....	4.62P	4.64P	.....	0.28	3.97	
01.93	*Ti* II	4.24p	4.17P	4.43P	4.40p	.....	2.60	1.16	

TABLE 2—*Continued*

λ	Element	τ UMa	ρ Pup	θ UMa	α CMi	α Per	log $\eta_0(\tau)$	E.P.	Notes
4302.53	*Ca* I	4.53p	4.23P	4.37P	4.37p	.....	1.20	1.89	1
03.17	*Fe* II	4.30p	4.21p	4.52P	4.43p	.....	2.25	2.69	
03.57	*Nd* II	4.61p	4.71	4.75P	4.93P	.....	0.95	0	
12.86	*Ti* II	4.31	4.21	4.36	4.29	4.06	2.20	1.18	
16.06	*Gd* II	5.11	5.24	5.43	5.79P	4.91P	9.99	0.66	1, 2
16.81	*Ti* II	4.65	4.49p	4.73	4.65	4.16p	0.85	2.04	
17.32	*Zr* II	5.22	4.85	5.02	5.19p	.....	9.84	0.71	
18.65	*Ca* I	4.69	4.36	4.50	4.41	4.14	0.75	1.89	
22.51	*La* II	4.96	5.20	5.43	5.79	4.60P	0.22	0.17	
25.01	*Sc* II	4.48p	4.29	4.37	4.33	4.12p	1.37	0.59	3
25.76	*Fe* I	4.09p	4.01	4.16	4.12	4.13p	3.36	1.60	3
30.26	*Ti* II	4.69P	4.55	4.76P	4.81	.....	0.75	2.04	3
33.28	*Zr* II	5.09p	5.00p	5.29p	5.46P	.....	0.02	2.40	3
33.76	*La* II	4.46	4.57	4.81	5.06p	4.64p	1.44	0.17	3
37.05	*Fe* I	4.51p	4.33P	4.48	4.57	4.48P	1.27	1.55	3
52.74	*Fe* I	4.41	4.34	4.45	4.50	4.43	1.65	2.21	3
54.61	*Sc* II	4.77	4.67p	4.67p	4.66	4.53p	0.56	0.60	3
55.10	*Ca* I	5.10	4.70	4.70	4.56	4.75P	0.00	2.70	3
58.17	*Nd* II	4.80p	4.95	5.22	5.74P	.....	0.50	0.32	
62.10	*Ni* II	4.58	4.71	5.05	4.85	4.55P	1.03	4.01	
69.40	*Fe* II	4.51P	4.45P	4.83p	4.56p	.....	1.27	2.77	
71.28	*Cr* I	4.60	4.64P	4.62p	4.51p	.....	0.97	1.00	
74.46	*Sc* II	4.62P	4.38	4.49p	4.48	.....	0.92	0.62	
74.94	*V* II	4.23	4.18P	4.42P	4.44	.....	2.67	0.41	1, 2
75.93	*Fe* I	4.33	4.32	4.51	4.42	4.19	2.07	0.02	
79.24	*V* I	4.79	4.67	4.65	4.63	.....	0.52	0.30	
82.17	*Ce* II	4.81	4.92	5.16	5.56P	.....	0.48	0.20	
83.55	*Fe* I	4.13	4.06	4.09	4.11	4.14	3.20	1.48	
85.38	*Fe* II	4.23P	4.17P	4.46p	4.36P	.....	2.67	2.77	
87.90	*Fe* I	4.62	4.54p	4.70p	4.63	.....	0.92	3.06	
88.41	*Fe* I	4.48	4.36p	4.60	4.50	.....	1.37	3.59	
89.24	*Fe* I	5.07	4.82	4.89	4.78p	5.00P	0.05	0.05	
89.97	*V* I	4.80p	4.71p	4.72	4.80P	.....	0.50	0.27	
90.58	*Mg* II	4.86P	4.80P	4.87	.....	.....	0.38	9.96	1, 2
92.58	*Fe* I	5.12	4.97P	5.15	4.94P	5.18	9.97	3.86	
94.06	*Ti* II	4.47	4.35	4.50	4.42	4.28	1.40	1.22	
95.03	*Ti* II	4.14	4.09	4.24	4.21	4.00	3.15	1.08	
95.85	*Ti* II	4.54	4.38	4.59	4.50	4.20p	1.16	1.24	
98.02	*V* II	4.47	4.35P	4.73p	4.67	.....	1.40	0.13	
99.77	*Ti* II	4.30	4.23	4.39	4.37	4.05p	2.25	1.23	
4400.36	*Sc* II	4.68p	4.34p	4.43	4.44	4.11P	0.77	0.60	
04.75	*Fe* I	4.18	4.07	4.15	4.16	4.06	2.95	1.55	
06.64	*V* I	4.97	4.94	4.83	5.04P	5.05P	0.20	0.30	
08.84	*Pr* II	4.85P	5.02P	5.21P	5.77P	.....	0.40	0	1, 2
10.52	*Ni* I	4.60p	4.71	4.92P	4.79	.....	0.97	3.29	
11.94	*Ti* II	4.70p	4.56	4.78	4.60	4.21	0.72	1.22	
15.12	*Fe* I	4.16	4.07p	4.26	4.25	.....	3.05	1.60	
15.56	*Sc* II	4.82P	4.36	4.54p	4.51P	.....	0.46	0.59	
16.82	*Fe* II	4.29	4.21	4.52	4.42	4.12	2.30	2.77	
17.72	*Ti* II	4.30	4.21	4.50	4.37	4.09p	2.25	1.16	

TABLE 2—*Continued*

λ	Element	τ UMa	ρ Pup	θ UMa	α CMi	α Per	log $\eta_0(\tau)$	E.P.	Notes
4418.34	*Ti* II	4.55	4.40P	4.63	4.56	.....	1.13	1.23	
21.95	*Ti* II	4.63	4.46	4.69p	4.57	4.29p	0.90	2.05	
24.34	*Sm* II	4.61	4.71	4.83	5.04P	.....	0.95	0.48	1, 2
25.44	*Ca* I	4.69	4.33	4.46	4.42	4.31	0.75	1.87	
27.31	*Fe* I	4.29	4.17	4.34p	4.31p	4.23	2.30	0.05	
28.00	*Mg* II	4.86	4.88P	5.09p	5.16P	4.67P	0.38	9.95	1, 2
30.62	*Fe* I	4.38	4.30p	4.44p	4.40p	.....	1.80	2.21	
31.37	*Sc* II	5.17P	4.99	4.85	4.87	4.67p	9.91	0.60	
32.57	*Fe* I	4.89p	4.80P	4.97	4.83	.....	0.34	3.56	
33.22	*Fe* I	4.48	4.46P	4.58	4.54	4.61p	1.37	3.00	
34.32	*Sm* II	4.76	4.77	5.00	5.04	.....	0.58	0.38	
35.69	*Ca* I	4.42P	4.32p	4.45	4.49	4.35P	1.61	1.88	1
37.57	*Ni* I	4.82	5.00	5.08p	4.81P	5.13	0.46	3.66	
38.35	*Fe* I	4.86	4.83	4.89p	4.78P	5.05p	0.38	3.67	
42.34	*Fe* I	4.36	4.29	4.45	4.44	4.33P	1.90	2.19	
43.80	*Ti* II	4.23	4.17	4.38	4.32	4.20P	2.67	1.08	
47.72	*Fe* I	4.37	4.31	4.48p	4.39	4.29	1.85	2.21	
55.89	*Ca* I	4.62	4.40	4.47	4.41	4.35p	0.92	1.89	
57.43	*Ti* I	4.65	4.52p	4.57p	4.59	4.54p	0.85	1.45	1, 2
62.98	*Nd* II	4.76	4.88	5.02	5.54P	.....	0.58	0.56	
65.81	*Ti* I	5.13p	5.09	5.12	5.29p	5.12P	9.96	1.73	
66.55	*Fe* I	4.30	4.24	4.48	4.42	4.24	2.25	2.82	
67.34	*Sm* II	4.73p	4.92	5.16	5.61P	.....	0.65	0.66	
68.49	*Ti* II	4.24	4.17	4.38	4.30	4.13	2.60	1.13	
72.92	*Fe* II	4.29	4.27	4.50p	4.42p	4.16	2.30	2.83	
76.02	*Fe* I	4.30	4.27	4.43	4.36	4.20	2.25	2.83	
79.61	*Fe* I	4.60P	4.62P	4.85p	4.65P	4.67P	0.97	3.67	
80.14	*Fe* I	4.60p	4.55P	4.67P	4.58P	4.66P	0.97	3.03	
81.13	*Mg* II	3.99	3.97	4.27	4.12	3.90	3.70	8.82	
84.23	*Fe* I	4.51	4.47	4.73	4.64	4.45p	1.27	3.59	
85.68	*Fe* I	4.66	4.62	4.77	4.75	4.59	0.82	3.67	
88.32	*Ti* II	4.41	4.40	4.59p	4.52	4.28	1.65	3.11	
89.18	*Fe* II	4.26	4.24	4.52	4.44p	4.13p	2.47	2.82	
89.74	*Fe* I	4.75p	4.63P	4.70	4.69p	.....	0.60	0.12	
90.08	*Fe* I	4.78	.....	4.84p	.....	.....	0.54	3.00	
91.40	*Fe* II	4.31	4.29	4.59	4.46	4.20	2.20	2.84	
93.53	*Ti* II	4.81	4.83	4.93	4.91	.....	0.48	1.08	1
94.06	*Fe* I	5.04p	5.00P	5.08p	4.99P	.....	0.09	3.97	
94.57	*Fe* I	4.35	4.26	4.44	4.39	4.16	1.95	2.19	
95.97	*Fe* I	4.99	5.00P	5.15P	5.21P	5.08P	0.17	3.64	
4501.27	*Ti* II	4.24	4.18	4.36	4.34	4.16	2.60	1.11	
02.22	*Mn* I	4.91p	4.87	5.04	5.06	.....	0.30	2.91	
04.84	*Fe* I	5.03	4.96	5.00p	5.09P	5.03	0.11	3.25	
06.74	*Ti* II	5.09P	5.07	5.03p	5.06P	.....	0.02	1.13	1
08.28	*Fe* II	4.23	4.22	4.51	4.40	4.04	2.67	2.84	
10.21	*Mn* II	5.19	5.44	5.51p	.....	.....	9.88	10.61	1, 2
12.73	*Ti* I	4.83p	5.00	4.80p	4.98	4.88	0.44	0.83	
15.34	*Fe* II	4.22	4.22	4.50	4.43	4.05	2.74	2.83	
17.53	*Fe* I	4.79p	4.86	4.89	4.89	5.06P	0.52	3.06	
20.23	*Fe* II	4.23	4.24	4.48	4.38	4.10	2.67	2.80	

TABLE 2—*Continued*

λ	Element	τ UMa	ρ Pup	θ UMa	α CMi	α Per	log $\eta_0(\tau)$	E.P.	Notes
4522.63	*Fe* II	4.09	4.10	4.29	4.30	3.95	3.36	2.83	1
28.62	*Fe* I	4.13	4.15	4.25	4.28	4.07	3.20	2.17	1
29.46	*Ti* II	4.32	4.30	4.40	4.38	4.17	2.14	1.56	1
31.63	*Fe* I	4.93	4.92	4.98	4.97	.....	0.27	3.20	
34.78	*Ti* I	4.89p	4.67	4.71	4.71	4.75P	0.34	0.83	
41.52	*Fe* II	4.28	4.26	4.59	4.53	4.20	2.35	2.84	
45.14	*Ti* II	4.59p	4.47p	4.65p	4.72	.....	1.00	1.13	
45.96	*Cr* I	4.62	4.63	4.73	4.68	.....	0.92	0.94	
48.76	*Ti* I	5.17	4.87P	4.87P	4.99	5.06P	9.91	0.82	
51.24	*Ni* I	4.87p	4.92P	5.09P	5.29	5.26P	0.37	4.15	
54.03	*Ba* II	4.14	4.11	4.31	4.38	4.12	3.15	0	
55.02	*Cr* II	4.39	4.38	4.77	4.74	4.37p	1.75	4.05	
58.66	*Cr* II	4.19	4.17	4.50	4.42	4.07	2.90	4.06	
62.36	*Ce* II	4.64	4.75	4.94	5.21	4.61	0.87	0	
63.76	*Ti* II	4.27	4.15	4.43p	4.35	4.05	2.40	1.22	
64.59	*V* II	4.54P	4.60	4.84p	4.80	4.58	1.16	2.26	1
68.31	*Ti* II	5.12	4.80P	4.97	4.84p	.....	9.97	1.22	
71.10	*Mg* I	5.15	4.79	4.76	4.67	4.79p	9.93	0	1
71.97	*Ti* II	4.08	4.06	4.34	4.20	3.94	3.40	1.56	
76.33	*Fe* II	4.34	4.33	4.71	4.53	4.23	2.00	2.83	
78.56	*Ca* I	5.02	4.73	4.67	4.64	4.67	0.12	2.51	
82.84	*Fe* II	4.37P	4.37p	4.72	4.66	.....	1.85	2.83	
83.83	*Fe* II	4.15	4.06	4.40	4.43	4.04p	3.10	2.80	
85.87	*Ca* I	4.96P	4.51p	4.57	4.52	4.48p	0.22	2.52	
86.36	*V* I	.....	4.95P	5.12P	.....	.....	.....	0.04	1
87.13	*Fe* I	4.82	4.85	5.02	4.82	4.91	0.46	3.56	
88.22	*Cr* II	4.27	4.27	4.60	4.47	4.14	2.40	4.05	
91.39	*Cr* I	4.67	4.69p	4.79	4.64	.....	0.80	0.96	
92.09	*Cr* II	4.38P	4.42p	4.84	4.62	.....	1.80	4.06	
96.06	*Fe* I	4.53p	.....	4.76p	.....	.....	1.20	3.59	
96.98	*Gd* II	4.88p	5.02	5.13	5.20P	.....	0.35	0.52	2
97.91	*Gd* II	4.65P	4.68P	4.93P	4.99P	.....	0.85	0.60	2
4602.01	*Fe* I	4.85	4.72	4.85	4.86	4.89	0.40	1.60	
02.94	*Fe* I	4.44	4.36	4.56	4.51	4.29	1.52	1.48	
04.99	*Ni* I	4.47P	4.53p	4.78	4.64	.....	1.40	3.46	
11.28	*Fe* I	4.40	4.37	4.55	4.51	4.46	1.70	0.91	
16.14	*Cr* I	4.60p	4.75p	4.77	4.74	.....	0.97	0.98	
16.64	*Cr* II	4.41p	4.49p	4.91	4.74	.....	1.65	4.06	
17.27	*Ti* I	5.19	5.10	4.99	4.96	5.08P	9.88	1.74	
19.87	*La* II	5.01p	5.34	5.70	5.74	.....	0.14	1.75	2
20.51	*Fe* II	4.45	4.41	4.75	4.72	4.27	1.48	2.82	
25.05	*Fe* I	4.48	4.49	4.70	4.70	4.57	1.37	3.23	
28.16	*Ce* II	4.63	4.82	5.03	5.43	4.75	0.90	0.04	
32.92	*Fe* I	4.63	4.58	4.65	4.64	4.66	0.90	1.60	
34.11	*Cr* II	4.35	4.38	4.68	4.59	4.24	1.95	4.06	
37.51	*Fe* I	4.60	4.52P	4.73	4.69	.....	0.97	3.27	
38.02	*Fe* I	4.56	4.51P	4.70	4.69	.....	1.10	3.59	
42.24	*Sm* II	5.10	5.12	5.49	.....	.....	0.00	0.38	2
43.47	*Fe* I	4.65	4.54	4.79p	4.81	4.67p	0.85	3.64	
46.17	*Cr* I	4.42p	4.38p	4.62	4.66	4.43p	1.60	1.03	

TABLE 2—*Continued*

λ	Element	τ UMa	ρ Pup	θ UMa	α CMi	α Per	log $\eta_0(\tau)$	E.P.	Notes
4647.44	*Fe* I	4.43p	4.38p	4.63	4.63	4.52p	1.56	2.94	
48.66	*Ni* I	4.33	4.33	4.68p	4.59	4.46P	2.07	3.41	
51.28	*Cr* I	4.60p	4.67	4.82	4.85	4.72	0.97	0.98	
52.16	*Cr* I	4.54	4.54p	4.73	4.68	4.51	1.16	1.00	
62.51	*La* II	4.90	4.95P	5.41p	5.41P	4.91P	0.32	0	
68.14	*Fe* I	4.50p	4.44p	4.60	4.62p	4.51P	1.30	3.25	
68.56	*Na* I	4.87p	4.88	5.26p	5.38p	.....	0.37	2.10	1
73.17	*Fe* I	4.60	4.50	4.70	4.62p	4.74	0.97	3.64	
74.60	*Sm* II	4.76p	4.93	5.14	5.41p	.....	0.58	0.18	1, 2
76.91	*Sm* II	5.22	5.19	5.59	5.56	.....	9.84	0.04	2
82.32	*V* II	4.68P	4.55	5.03p	4.86P	.....	0.77	0.41	2
86.22	*Ni* I	4.61	4.67	5.01	4.95	4.98p	0.95	3.58	
94.13	*S* I	4.78	4.77	5.09	5.08p	4.86	0.54	6.50	1, 2
95.45	*S* I	5.05P	4.98P	5.40P	5.31p	5.10P	0.08	6.50	2
96.25	*S* I	5.22P	5.21	5.59	5.63p	5.39	9.84	6.50	2
4702.99	*Mg* I	4.30	4.19	4.32	4.23	4.12	2.25	4.33	
03.81	*Ni* I	4.56	4.71p	5.05	4.86	5.09P	1.10	3.64	
04.96	*Fe* I	4.83p	4.71p	4.95	4.86p	.....	0.44	3.67	
05.46	*Fe* I	5.15	5.13p	5.13	5.22	.....	9.93	3.53	
07.28	*Fe* I	4.39	4.37	4.51	4.48	4.48	1.75	3.23	
10.29	*Fe* I	4.52	4.60	4.70	4.64	4.89p	1.23	3.00	
14.42	*Ni* I	4.24p	4.24	4.52	4.44	4.37	2.60	3.36	
15.78	*Ni* I	4.46	4.53	4.79	4.74	4.72	1.44	3.53	
22.16	*Zn* I	4.43	4.51	4.73	4.68	4.80	1.56	4.01	
30.03	*Mg* I	4.80P	4.72P	4.78P	5.18P	.....	0.50	4.33	
31.44	*Fe* II	4.29P	4.27	4.58	4.51	4.19	2.30	2.88	
33.60	*Fe* I	4.68p	4.65p	4.69	4.78	4.68p	0.77	1.48	
35.85	*Fe* I	4.78	4.73	4.88	4.93	5.04	0.54	4.06	
36.78	*Fe* I	4.34p	4.32p	4.51	4.58p	.....	2.00	3.20	
45.81	*Fe* I	4.70	4.54	4.80	4.80	4.75	0.72	4.09	
48.73	*La* II	4.97p	5.19p	5.31	5.68	5.33P	0.20	0.92	
54.04	*Mn* I	4.48	4.40	4.55	4.53	4.54	1.37	2.27	
55.73	*Mn* II	4.69P	4.74P	5.20P	5.25P	.....	0.75	5.37	1, 2
58.12	*Ti* I	5.38p	5.11	5.16	5.38p	5.47P	9.64	2.24	
59.27	*Ti* I	5.34p	5.19	5.16	5.60p	5.64P	9.69	2.25	
66.43	*Mn* I	4.52p	4.49P	4.63p	4.60	4.58	1.23	2.91	
70.00	*C* I	5.05p	5.36p	5.02p	4.98p	4.87	0.08	7.45	1
79.99	*Ti* II	4.53	4.40	4.61	4.60	4.15	1.20	2.04	
83.42	*Mn* I	4.44p	4.39	4.53	4.49	4.10	1.52	2.29	
4805.10	*Ti* II	4.39	4.25	4.43	4.46	4.15	1.75	2.05	
10.53	*Zn* I	4.43	4.40	4.68	4.68	4.63	1.56	4.06	
12.35	*Cr* II	4.54	4.48p	4.81	4.75P	4.51	1.16	3.85	
23.52	*Mn* I	4.37p	4.25	.....	4.46	.....	1.85	2.31	

NOTES TO TABLE 2

1. The line has very substantial contributions from other elements and is not used in all stars.

2. The solar strength is poor for various reasons. In most cases the strength in τ UMa was used for the analysis of the other F stars.

3. In the wing of a hydrogen line; not used in the curve of growth.

4. Almost certainly not *Si* II; strong in many F stars.

5. The only accessible *Eu* II lines are very badly blended.

earths, are needed. Such lines may be very weak in the sun, e.g., 5 mA, and may reach 50 mA in τ UMa. The blending effects of neutral and ionized elements in τ UMa also more closely resemble those in the A and F stars.

Accidental errors of the photometry are small. From the two independent tracings and reductions of the same plate of θ UMa it was found that the average difference (without regard to sign) was about 5 per cent of the equivalent width for good lines. Thus the total error of the microphotometer, of the drawing of the continuum and the line,

TABLE 3

EQUIVALENT WIDTHS, IN ANGSTROMS, OF LINES MEASURED ON OTHER SPECTROGRAMS

Star	Type	Source	$H\gamma$	$H\delta$	$H\zeta$	$H\eta$	$H\theta$	K
α Lyr	A0 V	CQ	21.4(4)	19.6(4)	14.5(4)	11.1(3)	8.6(3)	0.80(4)
		At	21.5	19.8	.....	.....	.....	.....
α CMa	A1 V	At	17.0	16.2	.....	.....	.....	0.71
		Al	16.4	17.2	.....	.....	.....	.....
γ Gem	A1 V	Al	15.0(2)	14.4(2)	.....	.....	.....	1.05(2)
η Oph	A2 V	CQ	17.5(2)	14.9(2)	12.8(2)	9.7(2)	7.5(2)	2.22(2)
κ Tau	A5 V	CQ	17.5(2)	17.4(2)	10.3(2)	8.8(2)	6.1(2)	4.15(2)
α Car	F0 II	Cd	8.7(2)	8.0(2)	.....	.....	.....	4.9(2)
σ Boo	F2 V	CQ	7.4(3:)	6.7(3:)	5.7(3)	5.8(3)	4.1(3)	5.9(3)
		Hy	.....	6.3	.....	.....	.....	4.4
α CMi	F5 IV	At	7.7	7.4	.....	.....	.....	.....
		Hy	.....	4.4	.....	.....	.....	6.3
α Per	F5 I*b*	At	8.2	6.3	.....	.....	.....	.....
		Hy	.....	.....	.....	.....	.....	7.6
ρ Pup	F6 II	CQ	6.6(2)	4.9	.....	.....	.....	7.1(4)
		Cd	8.4(2)	8.4(2)	.....	.....	.....	.....
		Br	.....	.....	.....	.....	.....	5.5
θ UMa	F6 III	CQ	.....	.....	.....	.....	.....	8.7(1:)
		Cd	5.6	4.6	.....	.....	.....	.....
		Hy	.....	1.8	.....	.....	.....	6.7
		Br	.....	.....	.....	.....	.....	7.5
τ UMa	A+F	CQ	11.1(3)	9.3(3)	7.6(3)	7.1(3)	4.9(3:)	3.39(3)
		Cd	11.0(3)	9.4(2)	.....	.....	.....	.....
		Br	.....	.....	.....	.....	.....	2.8
15 UMa	A+F	CQ	11.4(3:)	8.2(3:)	7.3(3:)	7.2(2)	5.6(2)	3.19(3:)
ζ Lyr A	A+F	CQ	17.1(3)	17.4(3)	10.8(3)	8.5(3)	7.0(3:)	3.83(3)

and of the measurement and reduction is about 3 per cent per plate. A larger error arises from the systematic plate-calibration error. For 60 good lines measured on three different plates of τ UMa, the average deviation of an observation from the mean was 4.7 per cent for strong lines, 5.3 per cent for average, and 7.9 per cent for weak lines. After correction for the errors of measurement we find 5.5 per cent error per plate arising from plate calibration. (Of course, the entire calibration system may be wrong by a large amount, but no evidence for large systematic errors has yet been found.) In stars like θ UMa, α CMi, and α Per, where a single plate was used, a systematic error of about 6 per cent of the equivalent widths is possible, corresponding to ± 0.03 in log W/λ. A systematic error enters nearly linearly into the final value of the turbulent velocity derived and in a larger degree into the opacity, pressure, and surface gravity. These quanti-

ties are less well determined than the other deduced parameters, such as the level of ionization and the relative abundance of the elements.

Certain lines could not be satisfactorily measured on the present coudé plates. Table 3 contains results of my measurements of the hydrogen lines and the K line of *Ca* II on coudé and on other types of plates. The 500-mm camera, with two quartz prisms and Eastman Process plates, was used for the CQ series; hydrogen lines were also measured in the *Photometric Atlas*[2] ("At"), on my own coudé plates ("Cd"), and by Aller[5] ("Al"). Some new measures of relatively low weight were made on Yerkes Bruce plates ("Br"), and some were available by Hynek[6] ("Hy"). In parentheses I give the number of plates used. On short dispersion many metallic lines are included in the measured width of the hydrogen lines; the coudé tracings are also unsuitable for such measurements, since the hydrogen lines are about 6 feet wide. On the whole, the data in Table 3 must be considered of rather low weight. Table 3 also contains measures on certain standard A and F stars and on two other "metallic-line A stars," 15 UMa and ζ Lyr A.

LINE CONTOURS

The dispersion is sufficiently high to permit a study of the contours of strong lines; for moderate lines the instrumental contour requires investigation. Only in α Per is the turbulence large enough to permit a direct estimate of the Doppler broadening; even in this star a special investigation will be required on more suitable fine-grained plates. The apparent line widths decrease in the order α Per, ρ Pup, τ UMa, θ UMa, α CMi, which proves to be the order of decreasing turbulence. The stars are thus nearly free of rotation. Some general considerations on the central intensities may be of interest. In a preliminary analysis let us consider that the instrumental and the true line profile are both of Gaussian form. Let the true absorption, A, at a distance, x, from the center of the true line be

$$A(x) = A(0)\, e^{-(x/\alpha)^2}. \tag{1}$$

Let the instrumental contour be

$$K(x) = \frac{1}{\beta\sqrt{\pi}}\, e^{-(x/\beta)^2}. \tag{2}$$

The observed contour, $A'(x)$ will be

$$A'(x) = \frac{A(0)\,\alpha}{(\alpha^2+\beta^2)^{1/2}}\, e^{-(x^2/\alpha^2+\beta^2)}. \tag{3}$$

The equivalent width is

$$W = \sqrt{\pi}\,\alpha\, A(0). \tag{4}$$

In an investigation[7] of α Car I found that β was of the order of 100 mA; the Doppler broadening and the strength of the line determine α. For very weak lines $\alpha \approx \Delta\lambda_D$, the Doppler width, and ranges from 100 mA to 20 mA for velocities of 10 and 2 km/sec. Now consider lines of equal equivalent width in two stars which have different Doppler broadening, α_1 and α_2. The true central absorptions will be

$$\frac{A(0,1)}{A(0,2)} = \frac{\alpha_2}{\alpha_1}. \tag{5}$$

The observed central absorptions will be

$$\frac{A'(0,1)}{A'(0,2)} = \left(\frac{\alpha_2^2+\beta_2^2}{\alpha_1^2+\beta_1^2}\right)^{1/2}. \tag{6}$$

The effect of Doppler broadening is to make the lines shallower; in stars of very large turbulence, like α Per or ϵ Aur, weak lines will eventually disappear because of low cen-

[5] *Ap. J.*, **96**, 321, 1942. [6] *Ap. J.*, **82**, 338, 1935. [7] *Ap. J.*, **95**, 161, 1942.

tral absorption and increased blending. For example, assume $\beta = 100$ mA, $\alpha_1 = 100$ mA, and $\alpha_2 = 20$ mA; then the apparent central absorption $A'(0, 1) = 0.7$ A$'(0, 2)$, by equation (6).

In all F stars investigated, the apparent central absorption for strong lines (including the hydrogen lines) approaches 0.86. This is also true for τ UMa, the "metallic-line A star." One hypothesis to account for the apparently composite spectrum of τ UMa is that it is an unresolved binary, consisting of an F star and an A star. In such a binary we should expect to observe a central absorption, $A''(0)$ in a line of the F star given by

$$A''(0) = \frac{A(0, F)L(F)}{L(F) + L(A)}, \tag{7}$$

if $L(F)$ and $L(A)$ are the luminosities of the F and the A stars at the given wave length. Since $A''(0)$ (without correction for instrumental blurring) is 0.86, $1.00 > A(0, F) > 0.86$. From (7) we derive $L(A)/L(F) < 0.16$. Consider the superposition of an A-star spectrum in which the K line is absent on an F-star spectrum in which it has equivalent width $W(K)$. The apparent equivalent width in the composite spectrum would be

$$W''(K) = \frac{W(K)L(F)}{L(F) + L(A)}, \tag{8}$$

which involves a maximum possible reduction of less than 14 per cent of $W(K)$. According to Table 3, the K line in τ UMa is about 50 per cent as strong as in a normal F6 star. We may then conclude that no superposition of two spectra can be responsible for the metallic-line A-star spectrum.

Plotting the observed central absorption, $A'(0)$, against equivalent width in several stars gave the statistical relation between $A'(0)$ and W. No significant difference exists for these relations in α CMi and in τ UMa; since the former was measured on direct-intensity tracings[2] made at the University of Michigan and the latter on the Yerkes transmission microphotometer, the agreement shows that the photometric reductions are consistent in scale. For example, the values of W at which $A'(0) = 0.50$ are given in the accompanying tabulation in various wave-length regions. Note that the increase

	λ 4050	λ 4250	λ 4550
α CMi	115 mA	133 mA	146 mA
τ UMa	115	131	171

in W required to obtain $A'(0) = 0.50$ arises mainly from the prismatic dispersion; in fact, if we express the absorption in equivalent millimeters, the required W actually decreases about 20 per cent from λ 4050 to λ 4550.

The hydrogen-line contours are almost unaffected by the instrumental contour, except for scattered light. The extreme wings are easily lost when the continuum is drawn in. Smoothed contours for $H\gamma$ and $H\delta$ in the F stars are given in Table 4. The most striking feature is their similarity, over a range of 8 mag. in absolute luminosity; only small differences of $A'(0)$ or W exist between α CMi and α Per. The observational accuracy is not high, but a similar comparison at type A0 would show differences in W by a factor of 5. It is known that the strong negative luminosity effect in the A stars arises from the decrease of Stark broadening. On the other hand, in giant G and K stars the hydrogen lines are observed to be strengthened. Thus a null-effect in the F stars is not unexpected; more observational data on the hydrogen lines in F, G, and K stars is needed to explore these effects. We shall see in the last section of this paper that the strength

of the hydrogen lines and the existence of extended wings in supergiant F stars is in accordance with theoretical expectation. The star τ UMa has stronger hydrogen lines than is normal for an F star but weaker than a normal A star. The star θ UMa has weak metallic lines and has the weakest hydrogen lines as well. Although he has not given a complete theoretical explanation, we may note that Hynek[6] has shown that some late F and G giants and subgiants have weaker lines than either dwarfs or supergiants have.

THE THEORY OF CURVES OF GROWTH

Theoretical methods for the analysis of the chemical constitution of stellar atmospheres can be divided into two main types. One involves the construction of a curve of growth for the star; since laboratory or theoretical intensities are lacking for most

TABLE 4

SMOOTHED HYDROGEN-LINE CONTOURS
$A'(0)$ IN PERCENTAGES

$\delta\lambda$	$H\gamma$					$H\delta$				
	τ UMa	α Per	ρ Pup	θ UMa	α CMi	τ UMa	α Per	ρ Pup	θ UMa	α CMi
0Å0	87	89	85	86	87	85	87	81	86	89
0.5	68	79	71	58	67	67	69	67	53	74
1.0	57	68	56	44	54	58	58	55	41	60
1.5	52	58	48	37	45	52	50	49	37	50
2	49	53	45	32	42	48	44	45	31	45
3	43	45	38	28	34	42	36	40	24	37
4	38	40	32	24	30	38	29	33	18	29
5	34	35	29	20	26	32	24	30	15	26
6	30	31	26	17	24	29	20	27	12	22
8	24	24	20	13	18	22	14	22	9	16
10	19	20	14	10	16	17	8	18	6	11
12	17	15	12	8	12	13	3	15	4	7
15	12	9	8	5	8	10	0	10	2	2
20	8	0	3	1	1	5	0	3	0	0
25	5	0	1	0	0	1	0	0	0	0
30	2	0	0	0	0	0	0	0	0	0
35	1	0	0	0	0	0	0	0	0	0

metallic lines, a curve of growth of the sun is used to determine semiempirical line intensities for the metallic lines. Another approach is taken in the analysis of the sun by Bengt Strömgren,[8] who obtains a detailed model giving the temperature, pressure, and opacity as a function of optical depth. For those few lines for which laboratory or theoretical f-values and damping constants are known, he computes rigorously the expected line contour and equivalent width for various abundances of the element and of the metals compared to hydrogen. This latter exact approach involves a knowledge of the physical parameters of the star—effective surface gravity and temperature. Since we are interested in many elements which lack f-values and since the gravity and temperature of most of our stars are unknown, we proceed by using a curve of growth. The availability of the exact theory, however, permits us to criticize and partially justify many of the assumptions of the theory of curves of growth.

Chandrasekhar[9] has recently obtained an exact solution for the absorption A_ν in a line as a function of η_ν, the ratio of the line-scattering coefficient to the continuous-

[8] *Pub. Kobenhavns Observatorium*, No. 127, 1940.

[9] *Ap. J.*, **106**, 147, 1947 (Paper XX).

absorption coefficient. The results are valid for the case in which the line is produced in an atmosphere where η is independent of optical depth, τ:

$$\lambda_\nu = \frac{\kappa_\nu}{s_\nu + \kappa_\nu}, \tag{9}$$

$$A_\nu = 1 - \frac{\lambda_\nu^{3/2}}{\frac{1}{3} + \frac{1}{2}\frac{B^{(0)}}{B^{(1)}}} \left(a_2 + \frac{B^{(0)}}{B^{(1)}} \frac{a_1}{\lambda_\nu} + \frac{1-\lambda_\nu}{2\lambda_\nu^{1/2}} a_1^2 \right). \tag{10}$$

The first and second moments, a_1 and a_2, of certain H-functions are tabulated for a set of values of λ. The constants $B^{(0)}$ and $B^{(1)}$ measure the limb darkening; in the usual linear approximation for the temperature as a function of τ,

$$\frac{B^{(0)}}{B^{(1)}} = \frac{8}{3} \frac{kT_0}{h\nu} \frac{\kappa_\nu}{\bar{\kappa}}. \tag{11}$$

Since we plan to use a single curve of growth for all frequencies, we must chose $B^{(0)}/B^{(1)}$ constant; its value is near $0.39\ \kappa_\nu/\bar{\kappa}$ for the sun. To compare with other computed curves of growth, e.g., Strömgren's,[8] we actually adopt $B^{(0)}/B^{(1)} = \frac{2}{3}$, corresponding to the latter's value:

$$\frac{x_0}{n} = \frac{h\nu}{kT_0} \frac{\bar{\kappa}}{\kappa_\nu} = 4.$$

A value of x_0/n near 8 might be preferable, since $\kappa_\nu/\bar{\kappa}$ is near 0.7 for the sun. On the assumptions that η is independent of depth and that the line is formed by scattering, Strömgren obtains

$$A_\nu = \frac{1-\lambda}{1 + \frac{2}{3}\sqrt{3\lambda}}. \tag{12}$$

A comparison of the values of A_ν computed according to these two Milne-Eddington (M.E.) models, equations (10) and (12), is given in Table 5. The ratio in the sense of *Chandrasekhar* divided by *Strömgren*, is in the fifth column. For comparison I also give the value of A_ν for a Schuster-Schwarzschild (S.S.) model in the last column. The S.S. model gives

$$A_\nu = \frac{s_\nu}{1 + s_\nu} \tag{13}$$

and differs in its asymptotic form as $s_\nu \to 0$. To permit a comparison I have adopted $\kappa_\nu = 0.4641$ in the S.S. model, so that $s_\nu = 0.4641\ \eta_\nu$. Then the S.S. model agrees with the Strömgren M.E. model both for small and for large s_ν. In spite of this forced agreement, the deviations reach 20 per cent and are very systematic in nature. We can then expect serious differences in the curves of growth between the S.S. model and the M.E. model. The same remarks are valid for those curves developed by Unsöld, who uses

$$A_\nu = \frac{A\,(0)\ s_\nu}{A\,(0) + s_\nu}. \tag{14}$$

The data in Table 5 could be used to compute a complete curve of growth on the exact M.E. theory. For the present I limit myself to an estimate of the errors produced by the use of equation (12). For very weak lines, with $\eta_0 < 1$, the line absorption is everywhere small, and the exact value of the equivalent width will be about 9 per cent larger than that given by Strömgren. For very strong lines, $\eta_0 \gg 1$, the line is saturated, and

the two expressions agree; in the extreme wings $\eta_\nu < 1$, and a 9 per cent error appears. The equivalent width will be less than 9 per cent in error, of course—probably near 4 per cent. Since the errors vary from 9 per cent for weak lines to 4 per cent for strong, the shape of the curve of growth will be nearly correct. An error of 5 per cent is 0.02 in $\log_{10} W/\lambda$; on the flat part of the curve of growth, where $d \log W/d \log \eta_0$ is about 0.25, errors of 0.08 in $\log \eta_0$ may occur. The curve for the S.S. model is very different in shape, and, if the conventional formula in equation (13) had been used, the strength of weak lines would have been doubled. Consequently, the theoretical curves of growth used by Allen,[10] K. O. Wright,[11] Unsöld,[12] and J. G. Baker[13] in most recent investigations of the solar and stellar curves of growth will not agree with those computed on the exact theory with constant η. In particular, the damping constant is systematically increased by the use of the S.S. model.

TABLE 5

PREDICTED ABSORPTIONS, A_ν

λ_ν	η_ν	Chandrasekhar	Strömgren	Ratio	S.S.
1.0	0.000	0.0000	0.0000	*	0.0000
0.9	0.111	0.0519	0.0477	1.087	0.0464
0.8	0.250	0.1061	0.0984	1.078	0.1040
0.7	0.429	0.1631	0.1526	1.069	0.1659
0.6	0.667	0.2238	0.2112	1.060	0.2363
0.5	1.00	0.2890	0.2753	1.050	0.3170
0.4	1.50	0.3609	0.3468	1.041	0.4104
0.3	2.33	0.4420	0.4288	1.031	0.5199
0.2	4	0.5385	0.5276	1.021	0.6499
0.1	9	0.6660	0.6593	1.010	0.8068
0.05	19	0.7588	0.7550	1.005	0.8981
0.00	∞	1.0000	1.0000	1.000	1.0000

* Note that, as $\eta_\nu \to 0$, the first-order expansion is $A_\nu \approx 0.4641\eta_\nu$ in Strömgren's formula (12). In eq. (10) it is necessary to obtain asymptotic expansions of the moments a_1 and a_2. I have done this only approximately and find $A_\nu \approx 0.4910\eta_\nu$, so that this ratio is 1.058 as $\eta_\nu \to 0$. The expansion of eq. (10) is based on the values of a at $\lambda = 1.0$ and $\lambda = 0.9$, not on the exact expansion at $\lambda = 1.0$. The probable limiting value of the ratio is near 1.096.

For the present analysis we must decide whether, in fact, the M.E. model with constant η is to be preferred to the S.S. model, in which the lines are formed in a layer where the re-emission in the continuum can be neglected. If, in fact, η decreased very rapidly inward, the S.S. model might be preferable. Only a detailed model for each type of line in each star will justify a choice—and if such models were available, the use of curves of growth would become unnecessary. Since we compare an F star with the sun, we wish to estimate the order of magnitude of the error produced in the F star, as compared to the sun, by the approximation η = constant. At present, model atmospheres for the sun[8] and for a bright dwarf F star[14] ($\theta_0 = 0.8$, $\log g = 3.5$) have been published by Strömgren and his collaborators. These models give θ, $\log P_g$, $\log P_e$, and $\log \bar{\kappa}$ as a function of τ, at frequent intervals in τ. Let us assume that the ionization and excitation follow the formulae of Saha and Boltzmann, with equal excitation and ionization temperatures. Then, for any element in a given stage of excitation, the number of active

[10] *Mem. Commonwealth Solar Obs., Canberra*, No. 5, 1934; No. 6, 1938.

[11] *Ap. J.*, **99**, 249, 1944.

[12] *Physik der Sternatmosphären* (Berlin, 1938), Fig. 85 and p. 266.

[13] *Ap. J.*, **84**, 474, 1936.

[14] *Pub. Kobenhavns Observatorium*, No. 138, 1944.

atoms can be computed at each τ; if we know the f-value and the damping, we can compute η_ν and eventually the exact line profile by an integration over τ. I have neglected the increase of damping with depth and have computed the absorption produced by various atoms in the cases, $\eta = 0.1$, $\eta = 1.0$, and $\eta = 10$, at optical depth $\tau = 0.3$. The latter value is a useful representative point in the star; the range of values of η covers both weak and moderately strong lines. The line absorption was computed from

$$A = \frac{1 - \bar{\lambda}}{1 + \frac{2}{3}\sqrt{3}\,\overline{\sqrt{\lambda}}}, \tag{15}$$

where $\bar{\lambda}$ and $\overline{\sqrt{\lambda}}$ are properly weighted averages of λ and $\sqrt{\lambda}$ in the atmosphere. The method of averaging, using a five-point Gaussian division, follows that given by Strömgren.[15] Unfortunately, if λ varies with τ, the points in the atmosphere λ_0, about which the Gaussian division should be taken, should be determined so as to give the most accurate representation. This problem requires further exploration. If we arbitrarily take λ_0 to be the value at the boundary of the star, say at $\tau = 0.01$, we heavily weight the outer layers of the star. This representative point is best for very strong lines and undoubtedly exaggerates the effect of the variation of λ with τ for normal lines. Except in the most luminous stars, broadening of lines by collisions either with electrons or with hydrogen atoms produces an effective increase of η with depth in the wings of a line. Since most of the decrease of η normally arises from the increase of κ_ν, which is proportional to P_e, pressure-broadening tends to make η independent of depth and further reduces the effects revealed in the model that we have adopted.

Typical atoms listed in Table 6 in various states of excitation were chosen. I computed, with $x_0/n = 4$, the absorptions, $A(F)$ in the F star and $A(\odot)$ in the sun. The table also gives $A(\eta)$, from equation (12), computed on the assumption of η = constant, and A(S.S.) according to equation (13). The variations of η are quite large; in the F star, η for metallic lines decreases by a factor of 10 from $\tau = 0.05$ to $\tau = 1.0$, and for the hydrogen lines shows a slow increase. In the sun the resonance *Fe* I, *Fe* II, and *Ca* II lines show larger decreases; the excited *Fe* II lines have constant η, and the hydrogen lines have η increasing by twenty times in the same range. Since Table 6 neglects the pressure dependence of η and overweights the upper layers, it gives line absorptions that lie rather close to the S.S. values. Nevertheless, if we compare the F stars and the sun, we find in the main that the differences are small, i.e., that if two lines have the same η at a representative point in an F star and in the sun, the line absorption will be similar. Variations are of the order of 10 per cent, except for the wings of the hydrogen lines, which are produced at great depths in the sun. (The pressure-dependent Stark broadening will further increase the latter effect.)

A preliminary test was made of the effect of weighting less strongly the upper layers of the atmosphere. For large η this will introduce only small changes in Table 6, since such lines are formed at small τ. However, for $\eta = 1.0$, I chose λ_0 to be the value of λ at $\tau = 0.3$ and made the Gaussian summations about that value of λ_0. The results for the *Fe* II line at 0 volts were $A(F) = 0.293$, $A(\odot) = 0.295$; for the hydrogen lines, $A(F) = 0.288$, $A(\odot) = 0.284$. These absorptions lie close to the value for η = constant, i.e., $A = 0.275$, and show little change from star to star. We may take this evidence and the data in Table 6 as a first attempt to justify the use of curves of growth. In the main the effects of stratification cancel out when we compare the F stars and the sun. Over wider ranges of temperature and pressure this cancellation may not occur. Comparing dissimilar lines in the same star leaves a larger effect. Since changes of the order of 25 per cent occur between the predicted absorptions for different elements in different stages of excitation, similar systematic changes of equivalent width may occur. It is possible that the abnor-

[15] *Ibid.*, No. 127, p. 243, 1940.

mally low excitation temperature indicated in all stars by metallic lines of low excitation potential is connected with the systematic weakness of the excited lines in Table 6. The low opacity of the outer layers produces a rapid decrease of η with increasing depth; at low excitation potential the large boundary value of η gives very strong absorption lines, while for highly excited lines, η may be constant, and the line will be relatively weakened. Lines of high excitation potential may be strengthened by stratification especially if subject to pressure broadening. Different curves of growth for different elements and deviations from a simple theoretical curve of growth may also be expected.

In the actual analysis a set of curves of growth based on the M.E. model with constant η was available from the computations of Pannekoek and van Albada.[16] They have shown that their curves agree within 0.01 in log W with that given by Strömgren. They give the equivalent width in units of the Doppler width, $(A/2b)$, as a function of log s_0/κ (our log η_0) for various values of the ratio, a, of the damping to the Doppler

TABLE 6

COMPARISON OF ACTUAL LINE INTENSITIES IN MODEL ATMOSPHERES AND THE PREDICTED ABSORPTIONS WITH η CONSTANT

ELEMENT	E.P. (VOLTS)	$\eta = 0.1$		$\eta = 1.0$		$\eta = 10.0$	
		$A(F)$	$A(\odot)$	$A(F)$	$A(\odot)$	$A(F)$	$A(\odot)$
Fe II	0	0.055	0.050	0.38	0.35	0.82	0.78
Fe II	3	.048	.049	.34	.31	.78	.72
Fe I	0	.047	.047	.32	.34	.78	.80
Fe I	2	.042	.041	.30	.31	.76	.76
Ca II	0	.059	.049	.39	.32	.83	.78
H I	10	0.050	0.105	0.29	0.30	0.67	0.60
$A(\eta)$		0.043		0.275		0.674	
A(S.S.)		0.044		0.316		0.823	

width. To transform to the notation most used recently, we proceed as follows: The observed curves of growth, in which log W/λ is plotted against log X_f, are slid both horizontally and vertically until a best fit with the theoretical curve is obtained. From these shifts and the value of a, we derive

$$\log \frac{W}{\lambda} - \log \frac{A}{2b} \equiv \Delta \log \frac{W}{\lambda}, \tag{16}$$

$$\log \frac{s_0}{\kappa} - \log X_f \equiv \Delta \log X_f, \tag{17}$$

$$\log V = \Delta \log \frac{W}{\lambda} + 10.18, \tag{18}$$

$$\log \eta_0 = \log X_f + \Delta \log X_f, \tag{19}$$

$$\log \frac{\Gamma}{\gamma_{cl}} = \log a V - 2.92. \tag{20}$$

[16] *Pub. Astr. Inst. Amsterdam*, No. 6, 1946.

The velocity parameter, V, is

$$V = c\,\frac{\Delta\lambda_D}{\lambda} \tag{21}$$

and can be converted into a root-mean-square velocity by multiplication by $\sqrt{3/2}$.

THE OBSERVED CURVES OF GROWTH

The homogeneous nature of the observational data in Table 2 provides an opportunity for a systematic study. However, the interpretation must be based on several assumptions and approximations. We must attempt to derive information as to the physical conditions in the stars and as to the abundances of the elements by indirect means. We assume that the radiative transfer in subordinate lines follows the general lines of that within a resonance line. The distribution of atoms in the excited levels is supposed to follow a Boltzmann formula, with a unique excitation temperature, T_{exc}. The ionization of all elements is supposed to follow a Saha formula, without reference to the detailed ionization and recombination processes, at a single ionization temperature, T_{ion}, and electron pressure, P_e. The ratio of s_ν/κ_ν is taken as independent of optical depth. If turbulence exists, we assume that all atoms possess the same mean peculiar motion, described by a Gaussian distribution with velocity V. We must also permit the effective value of the surface gravity, g_e, of a star to differ from the gravitational value g.

With these assumptions we can proceed to compare the F stars to the sun. Based on the accurate solar intensities of Allen[10] and the Utrecht *Atlas*,[17] many solar curves of growth have been prepared, with either theoretical or laboratory intensities. In the analysis of the sun by K. O. Wright,[11] laboratory intensities are used to obtain a curve-of-growth relation between W and laboratory intensity, log X_f (with arbitrary zero point). Once this curve is established, semiempirical values of log X_f for all solar lines can be obtained. There is a systematic difference between the best-observed solar curve and the theoretical curve based on the S.S. model fitted to it by Wright. He found[11] residuals of about ± 0.17 in log X_f. Unfortunately, a re-analysis with the theoretical curves of the M.E. model does not improve these residuals appreciably. The shape of the observed curve differs from that of either theoretical type.[17a] One important factor may be the omission of the variation of κ_ν over the wave-length range covered by the solar observations; this same omission may partly explain the low solar excitation temperature. A trial fit of Wright's observed curve of growth with the M.E. curves gives

$$\log V = 5.34 \pm 0.04\ ,$$

$$\log a = -1.8\ ,$$

$$\frac{\Gamma}{\gamma_{cl}} = 4.3 \pm 0.5\ ,$$

$$\log \eta_0 = \log X_f + 2.14\ .$$

K. O. Wright found $\Gamma/\nu = 2.61 \times 10^{-6}$, which corresponds to $\Gamma/\gamma_{\text{cl}} = 15$. Our new solar damping constant is only one-third the old. Since it has been pointed out for some time that most stars had apparently excessively large damping constants, this reduction is important. A re-analysis of my curve of growth for α Car,[7] which had $\Gamma/\gamma_{\text{cl}} = 10$ when interpreted with Baker's S.S.-type curves of growth,[13] gives a corrected value of

[17] Minnaert, Mulders, and Houtgast, *Photometric Atlas of the Solar Spectrum* (Utrecht, 1940).

[17a] *Note added in proof:* A redetermination of the solar curve of growth by Pierce and Goldberg (*Quarterly Progress Report, ONR Project M720-5* [Ann Arbor, October, 1947]) results in slightly smaller residuals when a M.E. model is used and when the variation of κ_ν is taken into account. Large discrepancies persist in the damping portion of the curve.

$\Gamma/\gamma_{el} = 5$. All the F stars in this investigation prove to have nearly the classical damping constant. It is worth noting that the collisional damping for λ 3933 of *Ca* II has been derived by Strömgren for the sun.[8] From quantum-mechanical computations the damping is found and is proportional to the total gas pressure; if we evaluate it at a representative point, $\tau_0 = 0.3$, where $\log P_g = +4.80$, we find $\log a = -1.8$, in perfect agreement with the statistically determined value of $\log a$ given above for the neutral metallic lines in the sun. We have not justified in detail the use of a constant value of η for neutral subordinate lines in the sun or in the F stars. However, it is probably still to be preferred to the S.S. model, which corresponds to $\eta = 0$ except at the boundary.

The analysis of the stellar-line intensities proceeded in the conventional manner. The stellar values of $\log X_f$ for a line of excitation potential, χ, were computed for different excitation temperatures from

$$\log X_f'' = \log X_f + 5040\chi\left[\frac{1}{T(\odot)} - \frac{1}{T(*)}\right]. \tag{22}$$

The excitation temperature for the *Fe* I lines was determined by trial and error. Wright's value of $T(\odot) = 4850°$ was adopted for *Fe* I, and it was assumed that in the star all elements had the same excitation temperature. For most ions only partial curves of growth could be prepared. These were shifted horizontally to obtain a fit with the *Fe* I curve; a composite curve of growth for the ions and the neutral elements, excluding *Fe* I, was thus obtained. It was found that in all cases the theoretical curve determined for *Fe* I represented equally well the observed curve for *Fe* I and the composite curve for the other elements. From the measured intensity in the star $\log X_{f,i}''(*)$ was read for each line from the stellar curve of growth. Then the mean shift was determined for element i from

$$S_i = \overline{\log \frac{X_{f,i}''(*)}{X_{f,i}''(\odot)}}. \tag{23}$$

For each star a scale correction, δ, to the $\log X_f''$ of *Fe* I is required, because of the changing abundance of *Fe* I. Define

$$\delta \equiv \log \eta_0 - \log X_f''. \tag{24}$$

The value of $\delta(\odot)$ proves to be $+2.14$; for each other atom or ion,

$$\overline{\log \frac{\eta_{0,i}(*)}{\eta_{0,i}(\odot)}} = S_i + \delta(*) - \delta(\odot). \tag{25}$$

From the definition of η_0, we find

$$\Delta \log \zeta_i(*) \equiv \log \frac{\dfrac{N_i(*)}{\kappa_\nu(*)}}{\dfrac{N_i(\odot)}{\kappa_\nu(\odot)}} = \log \frac{\eta_{0,i}(*)}{\eta_{0,i}(\odot)} + \log \frac{V(*)}{V(\odot)}, \tag{26}$$

where $\Delta \log \zeta_i(*)$ may be considered the apparent relative abundance of the given atom in the star as compared to the sun; it is analogous to (N_iH) in the S.S. type of analysis, the number of atoms above a square centimeter of the photosphere. From equation (26) we determine the relative number of atoms of a given ion per gram of stellar material, in units of the continuous absorption coefficient per gram. In this discussion we shall neglect the small variation of κ_ν over the 750-A range covered.

We may wish to use a value of η_0 in a given star, as predicted from its value in the star τ UMa, for which the observational accuracy was greatest. Since we shall have tabulated the values of $\Delta \log \zeta_i$ in various stars, we use the relation

$$\log \eta_0(*) = \log \eta_0(\tau) + \Delta \log \zeta_i(*) - \Delta \log \zeta_i(\tau) - \log \frac{V(*)}{V(\tau)}. \quad (27)$$

In the sun we read $\log X_f$ from the *observed* curve, while in τ UMa we used the *theoretical* curve of growth. While there is an inconsistency in principle, in practice the stellar data cannot certainly establish a difference. We are thus now able to predict the intensity of a line in a star from its intensity both in τ UMa and in the sun. Different observational errors enter these two predictions; the blending effects in the F stars are in part eliminated by using measures in the same type of star, as observed with the same dispersion. The spectrum and probably the physical conditions in ρ Pup and α Per resemble τ UMa much more closely than they do the sun.

A systematic comparison of the values of $\log X_f''$ and $\log \eta_0(\tau)$ for different elements is of interest. Let us assume a linear relation:

$$\log \eta_0(\tau) = a + b \log X_f'' . \quad (28)$$

We find that b is nearly unity for most elements, except that $b = 1.48$ for *Cr* II and $b \approx 1.4$ for strong lines of *Ti* II. The solar X_f'' are poor for *La* II and *Ce* II, which give $b \approx 0.6$. Thus *Cr* II, and *Ti* II slightly, may show different curves of growth in certain stars, when plotted against solar $\log X_f''$. Aller[18] pointed out what may be an extreme example of this phenomenon in α Cyg, where the curves of growth for *Cr* II and *Ti* II differed substantially from that for *Fe* II. In several of this group of F stars, the curve of growth for *Ti* II is definitely peculiar. There may be physical processes, such as stream motions or variations of η with depth, that actually alter the curves of growth of certain elements in the sun and the stars. The previously noted differences between the solar observed and theoretical curve of growth are also quite significant. Let us read from the new theoretical curve of growth of the sun the values of $\log \eta_0(\odot)$. Then, if we write

$$\log \eta_0(\odot) = \alpha + \beta \log X_f'' , \quad (29)$$

we can choose ranges of $\log X_f''$ where β differs very substantially from unity. For $-1.5 < \log X_f'' < -0.5$, I find $\beta \approx 0.7$; for $-0.5 < \log X_f'' < +0.5$, $\beta \approx 1.0$; for $+0.5 < \log X_f'' < +1.5$, $\beta \approx 1.3$. In the mean, β is near unity.

The final results of the analysis of the various stars are collected in Table 7, which gives the values of $\Delta \log \zeta_i$ for 32 elements. The number of lines used is given in parentheses, with a colon (:) if the determination is poor. The table also contains parameters derived from the curve of growth, the excitation temperature ($\theta_{exc} = 5040/T_{exc}$), and the spectroscopically estimated absolute magnitude, M_s. Other tabulated quantities which will be discussed later are the absorption coefficient, κ_ν, at a mean wave length near 4300 A; the ionization temperature, θ_{ion}, the electron pressure, P_e, the total pressure, P_g, and the surface gravity, g_e and g. The quantities δ are defined in equation (24).

The curves of growth for τ UMa, ρ Pup, and θ UMa are shown in Figures 1–10; the curves for α Per and α CMi will be given in Paper II of this series. They are plotted against $\log X_f''$, the solar values corrected to the excitation temperature shown. The observational scatter is small; the *Fe* I curve has about 115 plotted points, of which only 10 lie more than ± 0.20 in $\log W$ off the theoretical curve in τ UMa (Fig. 1) and only 5 each in ρ Pup (Fig. 4) and θ UMa (Fig. 8). Most discrepant lines show appreciable blending. In Wright's curve of growth for the sun[11] about 5 per cent of the lines also

[18] *Ap. J.*, **95**, 73, 1942.

TABLE 7

UNCORRECTED RATIO OF APPARENT ABUNDANCES, F STAR TO SUN

$\Delta \log \zeta_i$

Element	τ UMa	ρ Pup	θ UMa	α CMi	α Per	Notes
C I	−0.4 (1:)	−0.5 (1:)	+0.3 (1:)	+0.2 (1:)	.....	.....
Mg I	−1.30 (5:)	−0.92 (5)	−0.45 (7)	−0.10 (5:)	−0.9 (4)	.....
Mg II	+1.9+a_1 (3:)	+2.3+a_1 (3:)	+2.5+a_1 (3:)	+2.2+a_1 (2:)	+2.6+a_1 (1:)	1
Si I	+0.25 (2)	+0.49 (3)	+0.25 (3)	+0.17 (3)	+0.48 (3)	.....
Ca I	−1.49 (9)	−0.61 (10)	−0.25 (10)	−0.07 (8)	−0.59 (8)	.....
Ca II	−0.78+a_2 (1:)	−0.18+a_2 (1:)	−0.18+a_2 (1:)	a_2 (1:)	−0.1+a_2 (1)	2
Sc II	−0.58 (8:)	+0.03 (10)	+0.35 (8)	+0.41 (8)	+0.5 (5)	.....
Ti I	−0.74 (12)	−0.57 (10)	−0.14 (13)	−0.43 (8)	−0.57 (9)	.....
Ti II	+0.47 (27)	+0.77 (26)	+0.54 (26)	+0.71 (25)	+0.96 (20:)	.....
V I	−1.14 (5)	−1.02 (6)	−0.73 (6)	−0.93 (5)	−1.3 (3)	.....
V II	+0.56 (4)	+0.63 (4:)	+0.03 (4:)	+0.7 (4)	+0.6 (3)	.....
Cr I	−0.30 (10)	−0.30 (9)	−0.28 (10)	−0.23 (9)	−0.4 (5)	.....
Cr II	+1.20 (9)	+0.88 (10)	+0.49 (9)	+0.57 (10)	+1.24 (8)	.....
Mn I	−0.47 (12)	−0.67 (7)	−0.45 (7)	−0.18 (12)	−0.4 (8)	.....
Mn II	a_3 (4:)	a_3 (6:)	−0.2+a_3 (5)	−0.4+a_3 (3:)	+0.5+a_3 (1:)	1, 3
Fe I	−0.60 (120)	−0.52 (115)	−0.43 (121)	−0.23 (117)	−0.63 (84)	.....
Fe II	+1.20 (21)	+1.06 (22)	+0.56 (21)	+0.98 (20)	+1.37 (16)	.....
Co I	−0.73 (4)	−0.88 (4)	−0.7 (3)	−0.5 (4:)	−1.0 (3)	.....
Ni I	+0.18 (9)	+0.03 (8)	−0.08 (9)	−0.03 (9)	−0.41 (7)	.....
Ni II	+0.9+a_4 (2)	+0.50+a_4 (3)	+0.4+a_4 (3)	+0.2+a_4 (3)	+0.7+a_4 (3)	4
Zn I	+0.35 (2)	+0.14 (2)	+0.05 (2)	0.0 (2)	−0.4 (2)	.....
Sr II	+0.70 (3)	+0.85 (3)	−0.01 (3)	+0.49 (3)	+0.8 (2)	.....
Y II	+0.99 (5:)	+1.07 (5)	+0.45 (5)	+0.55 (5)	+0.9 (1)	.....
Zr II	+0.18 (7:)	+0.69 (6)	+0.15 (7)	+0.36 (7)	.....	.....
Ba II	+0.77 (2)	+0.55 (2)	+0.23 (2)	0.0 (2)	0.0 (1)	.....
La II	+0.97 (10)	+0.73 (7)	+0.34 9)	+0.35 (9)	+0.9 (4:)	.....
Ce II	+0.90 (8)	+0.58 (8)	+0.32 8)	+0.05 (8)	+0.8 (3)	.....
Pr II	+1.0 (3)	+0.8 (3)	+0.4 (3:)	0.0 (2:)	.....	5
Nd II	+1.1 (3)	+0.8 (3)	+0.5 (3:)	−0.1 (2:)	.....	5
Sm II	+1.1 (4)	+0.9 (4:)	+0.5 (4)	+0.4 (3:)	.....	5
Eu II	+1.9+a_5 (2:)	+1.6+a_5 (2:)	+0.5+a_5 (2)	+0.8+a_5 (2:)	+1.2+a_5 (2:)	5
Gd II	+0.9 (4)	+0.6 (4)	+0.4 (4:)	0.0 (4:)	+1.1 (1:)	5
δ(*)	+1.28	+1.25	+1.61	+1.79	+1.06	.....
log V	+5.60	+5.70	+5.44	+5.46	+5.80	.....
Γ/γ_{cl}	1.5	1.2	1.7	1.4	1.5	.....
θ_{exc}	0.91	0.95	0.98	0.96	0.98	.....
Spectrum	F6 II+A3	F6 II	F6 III	F5 IV	F5 Ib	.....
M_*	+3	−3	+1.5	+2.5	−5	.....
log κ_P	−1.62	−1.36	−1.00	−1.18	−1.64	.....
θ_{ion}	0.86	0.83	0.87	0.86	0.82	.....
log P_e	0.0	+0.4	+0.6	+0.5	+0.1	.....
log P_g	+2.7	+3.0	+3.9	+3.6	+2.3	.....
log g_e	+1.6	+2.1	+3.4	+2.9	+1.2	.....
log g	+4.0	+2.5	+3.5	+3.7	+1.7	.....

NOTES TO TABLE 7

1. The high excitation potential of *Mg* II and *Mn* II makes these determinations very uncertain. If there are departures from a simple Boltzmann distribution or if the scale of T_{exc} is incorrect, the comparison of F stars and the sun is difficult. Let the value of log $\eta_0(\odot)$ require an arbitrary correction ($-a_1$ or $-a_3$); then the intercomparison of the F stars can proceed, subject to this zero-point correction.

2. The great strength of λ 3933 of *Ca* II, the only available line, makes this a very poor determination. The measured intensities are taken from different sources. In particular, the damping constant, which is the dominant quantity for strong lines, is poorly determined observationally in the F stars. Two values of log $\eta_0(\odot)$ may be used, one based on the extrapolation of the observed curve of growth (+6.19) and the other on the theoretical curve (+6.82). The latter is exactly Strömgren's collisional-broadening value. If we write log $\eta_0(\odot) = +6.82 - a_2$, we may later try to adjust a_2 for the normal F stars.

3. The identification of *Mn* II is very poor, and only Rowland intensities were available. The arbitrary zero point, a_3, will be set later.

4. A systematic difference between the results for *Ni* I and *Ni* II indicates that a zero-point correction to the solar strengths is required. Both *Ni* I and *Ni* II are at present somewhat unsatisfactory.

5. The rare earths are weak and badly blended in the sun, and Rowland intensities had to be used. Arbitrary zero-point corrections may be needed. In practice the line strengths in τ UMa, $\eta_0(\tau)$, were used to determine the relative abundances in the F stars. The latter comparison is accurate, and the uncertainty appears relative to the sun.

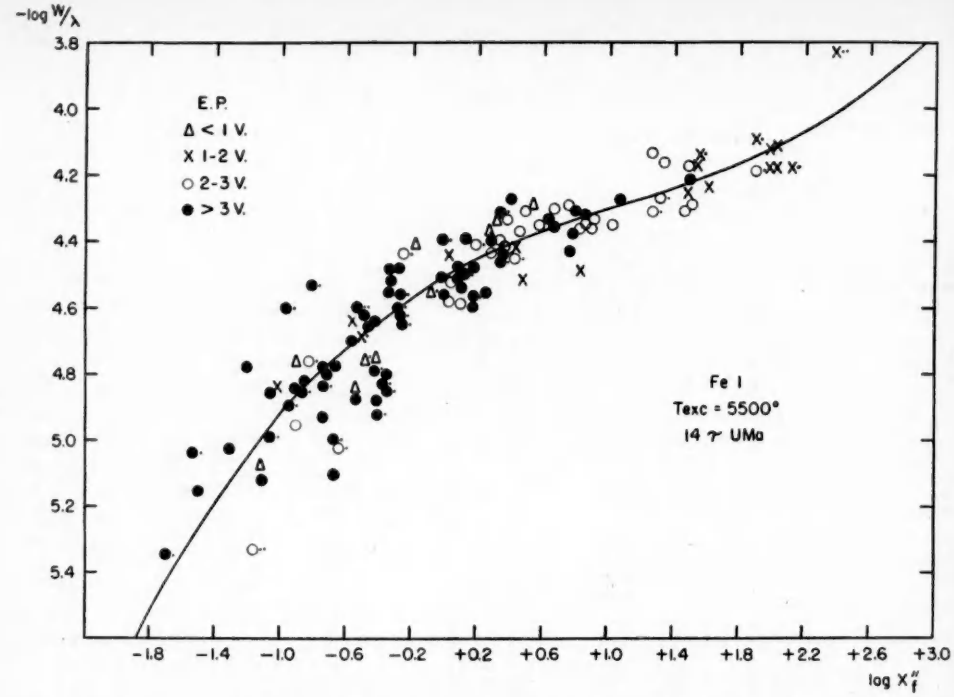

FIG. 1.—The curve of growth of *Fe* I for the metallic-line star, τ UMa. The abscissae are the line-absorption coefficients, X''_f based on the solar values of K. O. Wright. They are derived from the *observed* solar curve of growth, corrected to the excitation temperature of the star. The zero-point shift, $\delta(*)$, is given in Table 7. The theoretical curve of growth is plotted.

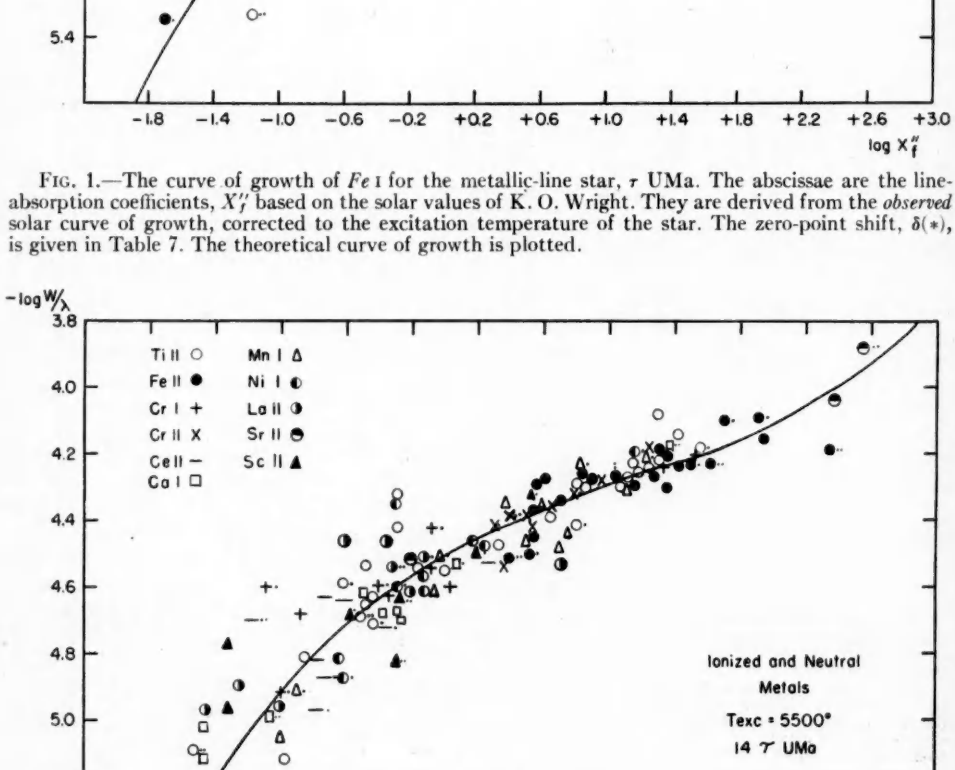

FIG. 2.—The curve of growth for other elements in τ UMa

deviate by ± 0.20 in log W. Since all solar errors reappear in the stellar curves, it seems probable that nearly all the residual scatter can be explained by errors in solar log X_f''-values and by the increased blending in the stars. The curves drawn are the theoretical curves, parameters of which are given in Table 7; the same theoretical curve is used in the plot for *Fe* I and for the other elements.

Figure 3 is a special curve for *Fe* I in τ UMa. Instead of using the solar log X_f'', based on Wright's *observed* solar curve of growth, I redetermined log η_0 ($\odot$), using the *theoretical* solar curve of growth. These η_0 ($\odot$) were corrected to the excitation temperature of τ UMa, giving the revised solar η_0' used in plotting Figure 3. The complicated residuals exemplified in equation (29) reappear in Figure 3 and result in a very peculiar diagram. (The plotted theoretical curve for τ UMa is the same as in Figs. 1 and 2.) The scale of log η_0' is compressed for lines that fall at the transition between Doppler and flat portions of the curve of growth of the star. It is enough expanded near the damping portion to require a damping less than the classical value. No theoretical curve would fit satisfactorily when the scale of log η_0' is used.

If we were to plot the curve of growth of τ UMa against the $\eta_0(\tau)$ given in Table 2, we should have zero residual scatter by the definition of $\eta_0(\tau)$. If we prepare curves of growth for ρ Pup and θ UMa, using $\eta_0(\tau)$ computed according to equation (27), we have a test of the quality of these $\eta_0(\tau)$. Figures 6, 7, and 10 present such curves of growth, together with the original *Fe* I theoretical curve derived for these stars. The residual scatter is considerably reduced in Figure 10, compared to Figure 9, for θ UMa. But the curves for *Fe* I (Fig. 6) and for the other elements (Fig. 7) in ρ Pup show, I believe, less scatter than any previously published curves of growth. No point deviates by ± 0.20 in log W, and only 10 per cent of the lines deviate by more than ± 0.10. Several elements have been omitted from Figures 7 and 10 because their Δ log $\zeta_4(*)$ were poorly determined. (In all these curves it should be remembered that a systematic positive residual in log W is to be expected for very weak lines; they will be absent on plates in which they are accidentally weak; blending also increases log W.)

The curves of growth seem quite normal, and no large systematic deviations are detected for any elements. The rare earths, *Ce* II and *La* II, fit the standard curve quite well, especially when $\eta_0(\tau)$ is used. Certain elements which are greatly weakened in τ UMa, like *Ca* I, *Sc* II, and *Zr* II, still fall on the standard curve. The poor solar X_f'' of *Cr* II and *Ti* II found in the discussion of equation (28) appear to have only small effect. Certain important lines are badly blended, even on this dispersion. The strongest *Fe* I line, λ 4045, is far off the curve, especially in τ UMa (Fig. 1). Examination of the line contour shows that what was measured as *Fe* I, λ 4045.82, actually included lines measured by Swensson[4] in α CMi at $\lambda\lambda$ 4045.39, 4045.64, 4046.01, 4046.42. In supergiant F stars, as λ 4045.82 widens, its intensity is increased very rapidly by such blending. (The great width of the turbulently broadened lines in supergiants probably has a different origin. Much recent work has indicated that line contours in supergiants may be very appreciably broader than those predicted from the turbulence given by the curve of growth.) Some of the excessive strength of λ 4077.71 of *Sr* II compared to λ 4215 has the same origin; the lines at $\lambda\lambda$ 4076.60, 4076.81, 4078.39, and especially λ 4077.35 of *La* II and λ 4077.94 of *Dy* II, blend with *Sr* II. In Figure 2 for τ UMa and Figure 5 for ρ Pup, the *Sr* II doublet deviates in slope from the theoretical curve. In Figure 7, however, where $\eta_0(\tau)$ was used in ρ Pup, the doublet falls close to the curve. These and other blending effects must be important for classification and luminosity criteria on low-dispersion spectra. The intensity of a badly blended line varies rapidly as the blending changes, and many strong features of low-dispersion spectral criteria are such blends. One example is the group of lines at λ 4172, λ 4178, important in F stars. They appear as a strong doublet in the Yerkes *Atlas of Stellar Spectra*;[1] in supergiant stars like ϵ Aur, α Per, and γ Cyg, the λ 4178 component is very strong. Both λ 4172 and λ 4178 contain many lines, but the λ 4172 blend has important neutral-line contributors, while λ 4178 is dominated

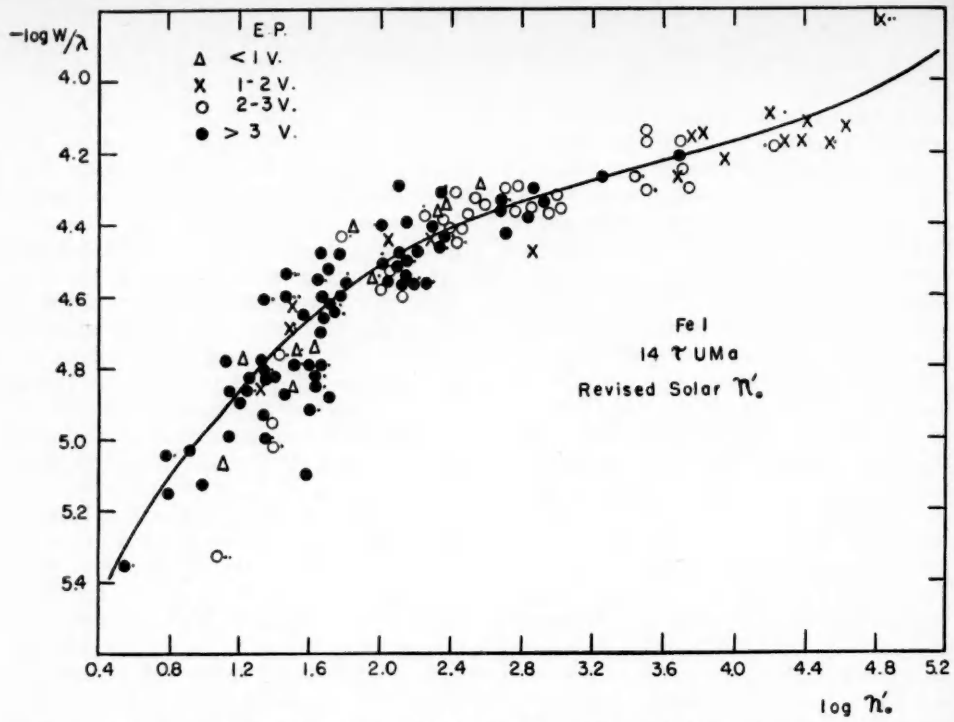

FIG. 3.—The curve of growth for *Fe* I in τ UMa, with the $\eta_0'(\odot)$ as abscissae; these are read from a *theoretical* curve of growth of the sun and are corrected to the excitation temperature of the star. Note the systematic nature of the residuals.

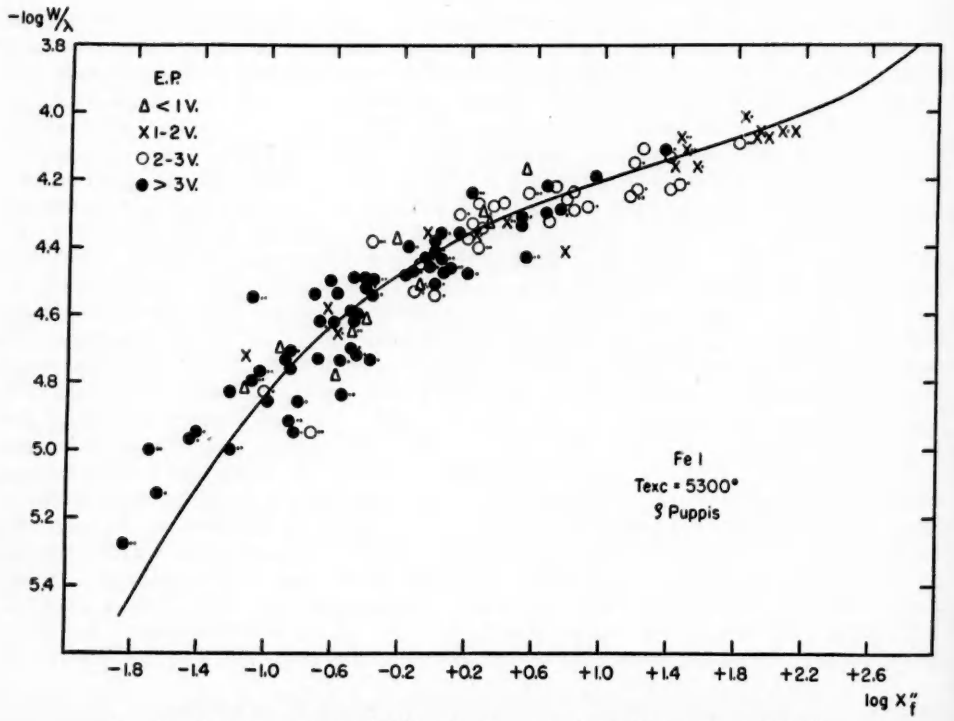

FIG. 4.—The curve of growth of *Fe* I in the supergiant ρ Pup, using solar X''_f

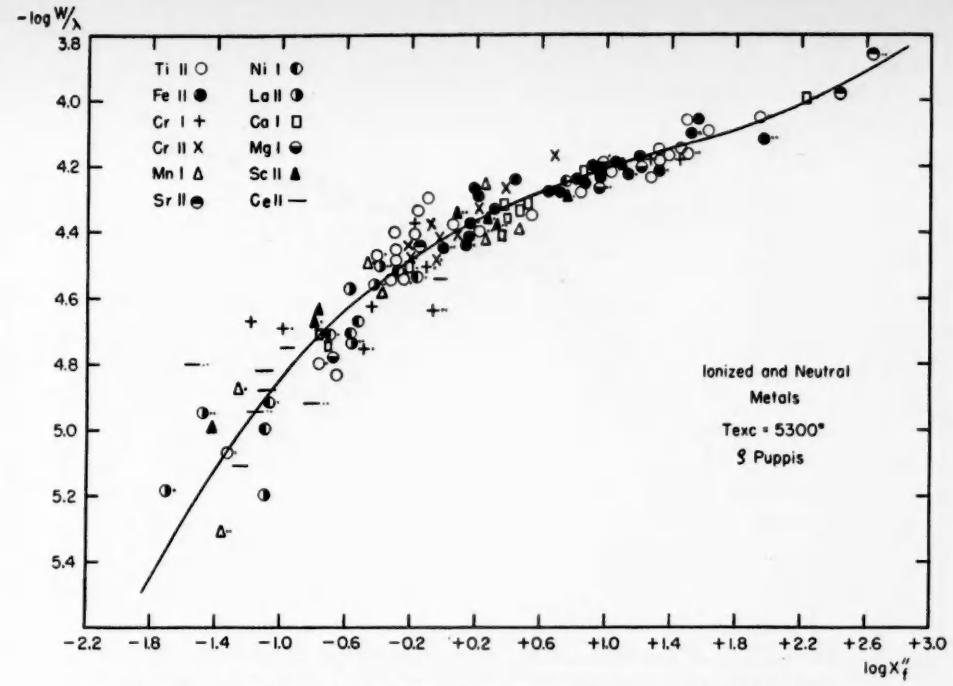

FIG. 5.—The curve of growth for other elements in ρ Pup, using solar X''_f

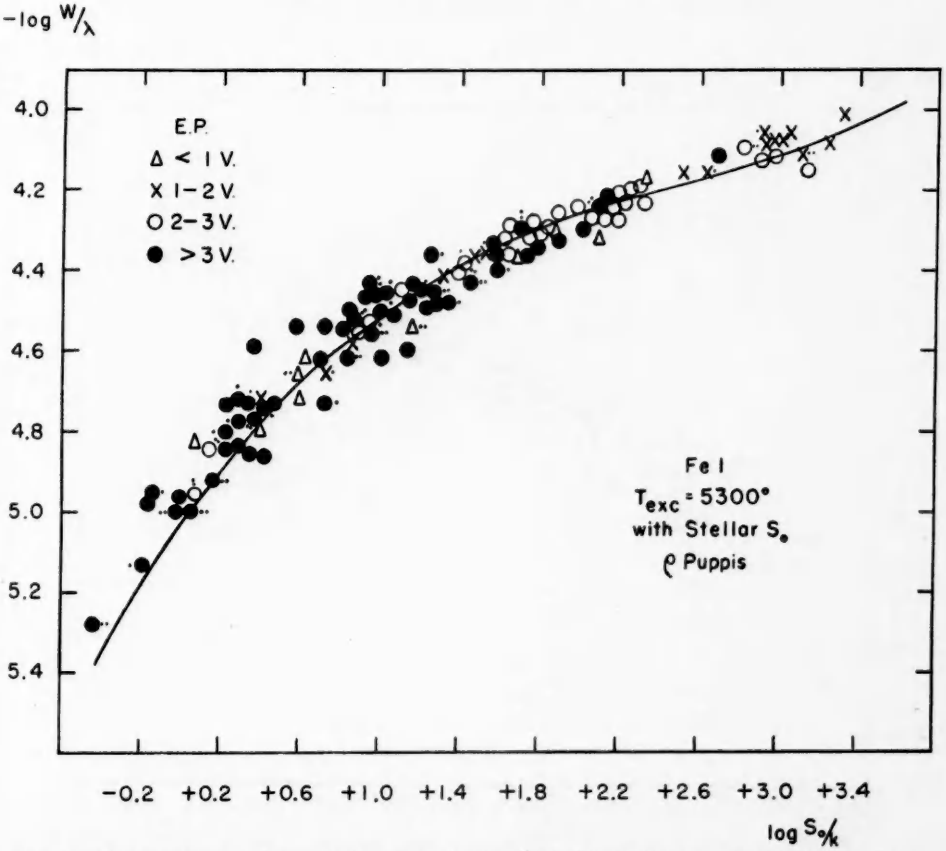

FIG. 6.—The curve of growth for *Fe* I in ρ Pup with the $\eta'_0(\tau)$ of Table 2 as abscissae. Note how the use of stellar values of line strengths reduces the scatter when compared to Fig. 4.

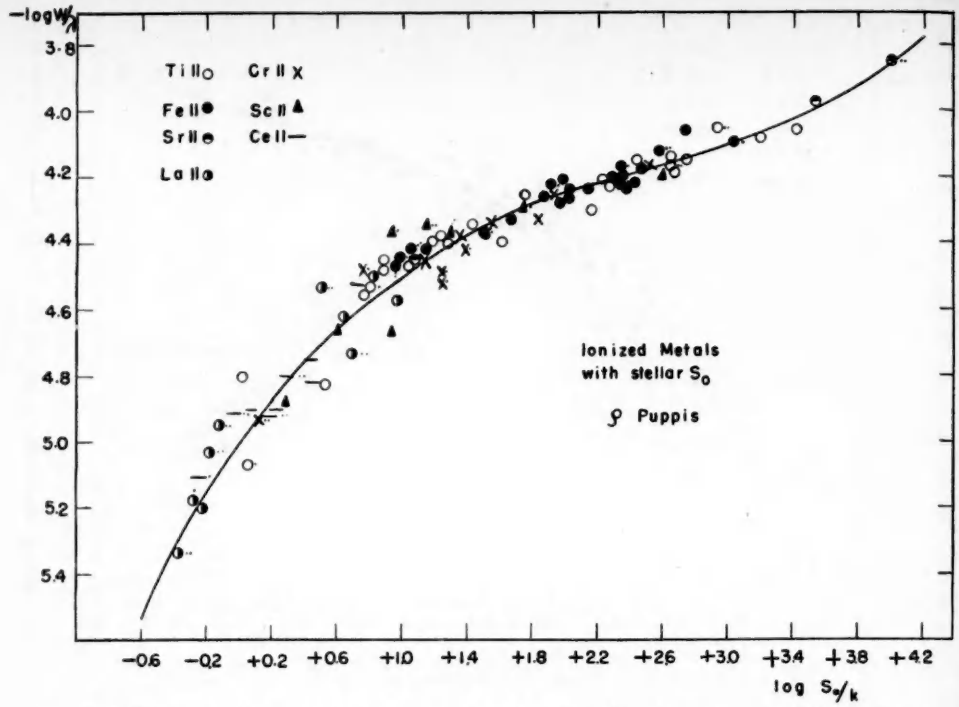

FIG. 7.—The curve of growth for other elements in ρ Pup based on the stellar $\eta_0'(\tau)$. Compare with Fig. 5.

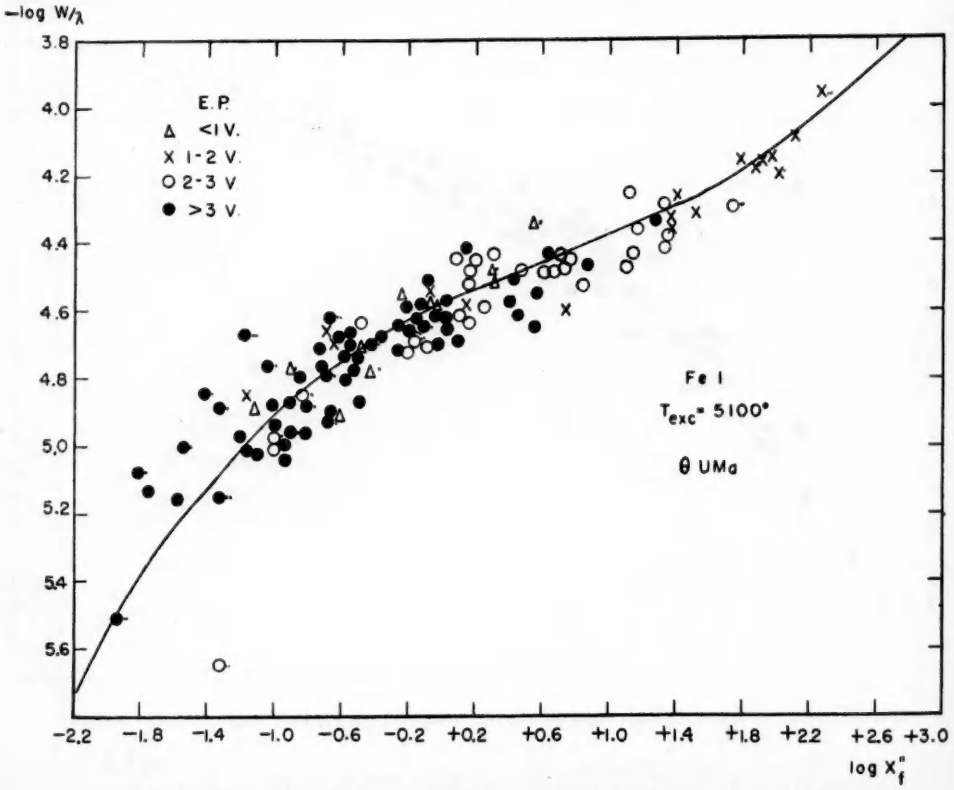

FIG. 8.—The curve of growth of *Fe* I in the giant θ UMa, using solar X_f''

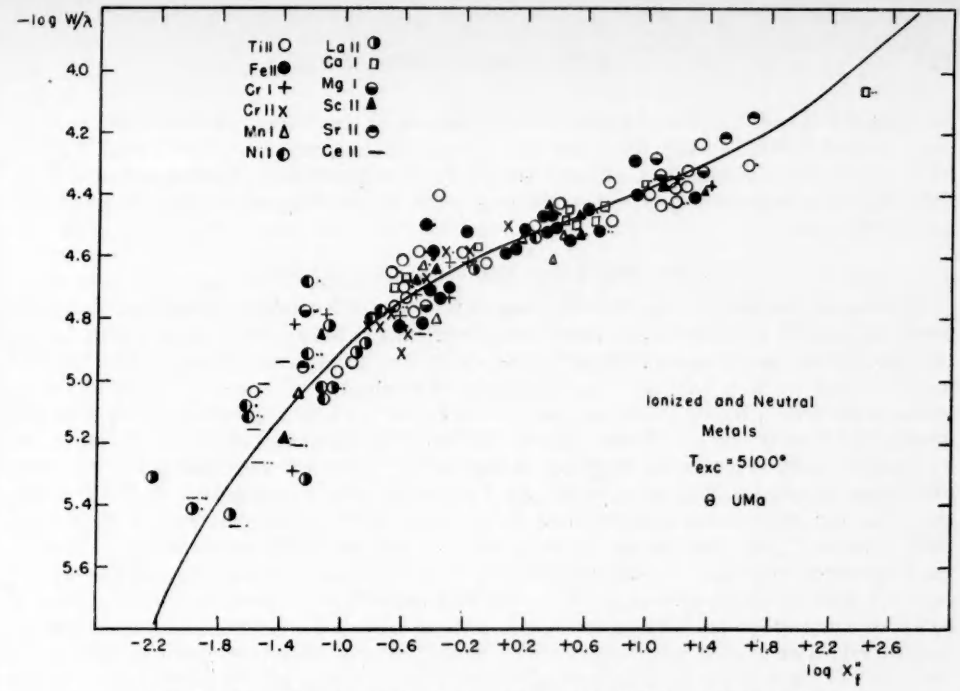

FIG. 9.—The curve of growth of other elements in θ UMa, using solar X_f''

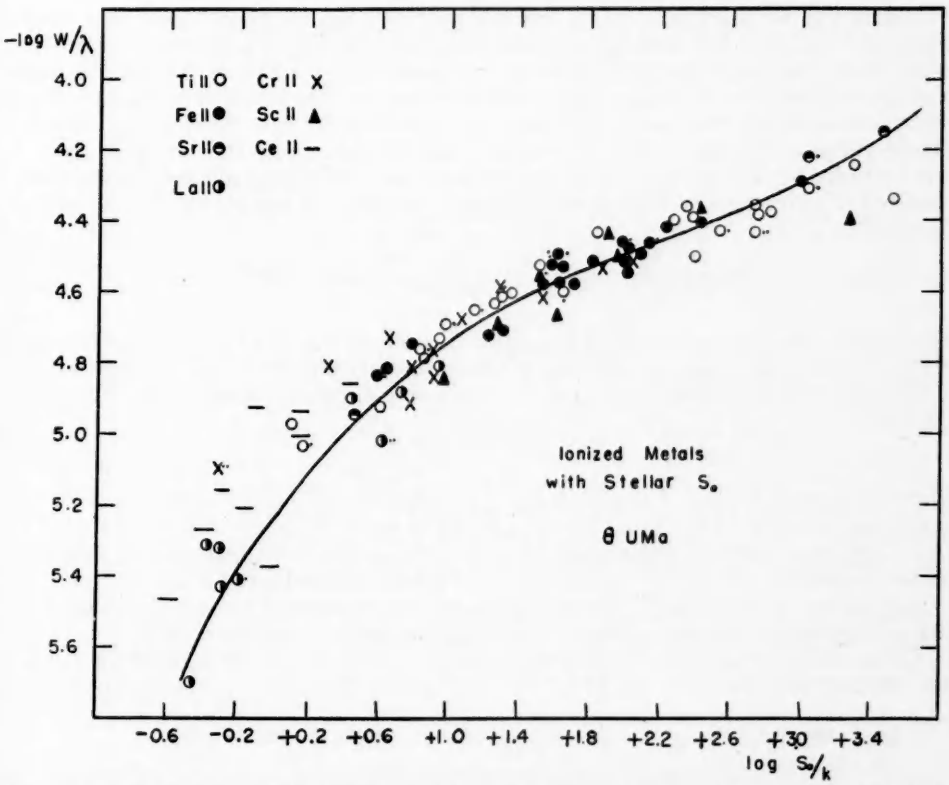

FIG. 10.—The curve of growth for ionized metals in θ UMa, using the stellar $\eta_0'(\tau)$. Compare with Fig. 9

by ionized lines of *V* II, *Fe* II, and *Cr* II. In Plate 31 of the *Atlas* it can be seen that the variations of λ 4172, λ 4178, form one of the most striking luminosity effects in F0 stars. Detailed studies of blending effects, of the type suggested by Pannekoek and van Albada,[16] should prove important in the prediction of low-dispersion spectral and luminosity criteria.

THE PARAMETERS OF THE STELLAR ATMOSPHERES

The major problem of this investigation can be stated as follows: Does the change of curve of growth, temperature, and pressure from star to star completely account for all the changes of line intensity? Or are there actual changes in the abundances of the elements? Since we lack *f*-values for most lines, we evaluated all apparent abundances in terms of the solar abundance of the element in Table 7. These apparent abundances still involve the level of ionization and opacity. The most fundamental approach is that taken by Strömgren in the solar atmosphere, where with a detailed solar model the absolute intensities of certain lines were predicted. For the general investigation of the F stars, the data required for the construction of the model stellar atmospheres is almost completely lacking; only one star has an accurately known mass and luminosity. Eventually the parameters required for such models may be estimated. For example, the color temperature–effective temperature relation will be available from computations by Münch based on the continuous-absorption coefficients of H and H^- (given by Chandrasekhar and Breen[19] and by Chandrasekhar and Münch[20]) and the six-color photoelectric photometry of bright stars. For stars of high luminosity it may not be possible to use the gravitational value of the surface gravity if other mechanisms contribute to the support of these extended atmospheres. The Balmer discontinuity and the color temperatures will ultimately determine both the effective temperature and the electron pressure.

Meanwhile, we must proceed by indirect spectroscopic methods, based on a rough analysis of the star. We shall consider the level of ionization at a representative point in the stellar atmospheres, $\tau_0 = 0.25$; at this point $\theta_{\text{ion}} = 1.10\,\theta_e = 0.92\,\theta_0$. We compare the relative level of ionization of various elements in the star and in the sun. Since we have a model for the solar atmosphere, we know $\theta_{\text{ion}}(\odot) = 0.95$, $\log P_e(\odot) = 0.80$. (These values differ slightly from Strömgren's and fit better with the newer H^- absorption coefficients.) Therefore, in principle, two elements of different ionization potentials, observed in two stages of ionization, determine both $\theta_{\text{ion}}(*)$ and $P_e(*)$. The ionization equation is

$$\log \frac{N_r\,(*)}{\Sigma N\,(*)} - \log \frac{N_r\,(\odot)}{\Sigma N\,(\odot)} = K_r\,(\theta_{\text{ion}}) - \log P_e\,. \tag{30}$$

The ΣN is taken over all stages of ionization. Unfortunately, the simultaneous solution of two relations like equation (30) proves almost indeterminate. In fact the application of equation (30) to the observations results in a single approximately linear relation of the form:

$$\log P_e + c_2\theta_{\text{ion}} = c_1\,, \tag{31}$$

where c_1 depends on the observed $\Delta \log \zeta_i$ and where c_2 is nearly independent of the ionization potential, averaging close to 9.0. While many elements of quite different c_2 and c_1 are observed in a single stage of ionization, in this investigation such elements cannot be used to determine θ_{ion} and P_e, since possible abundance variations from star to star cannot be excluded. In equation (30), even if an element has a gross abundance change from sun to star, both stages of ionization are affected, and no error is introduced.

The actual determination of the level of ionization was carried through for the following elements: *Fe* I/*Fe* II (wt. 2), *Cr* I/*Cr* II (wt. 1), *Ti* I/*Ti* II (wt. 1). The level of ioniza-

[19] *Ap. J.*, **104**, 430, 1946.

[20] *Ap. J.*, **104**, 446, 1946.

tion at the standard point, $\tau_0 = 0.25$, was known in the sun; the $\Delta \log \zeta_i(*)$ gave the ionization in the star, neutral element divided by total. Tables 8 and 9 give the results of these computations. Note in Table 9 the agreement of the observationally determined $\log P_e$ for the three elements. Note also how small the difference between the rate of change of P_e with θ is for *Fe* I and *Cr* I; the constants c_2 in equation (31) are 9.1 and 8.2, respectively.

To obtain a second relation between θ_{ion} and P_e, we make another type of assumption, which would permit changes of relative abundances of various metals to be determined, although not immediately giving their abundances relative to hydrogen. Let us assume that a certain group of heavy elements has the same fractional abundance per gram of

TABLE 8

IONIZATION OF STANDARD ELEMENTS

ELEMENT	$\log \frac{N_I(\odot)}{\Sigma N(\odot)}$	OBSERVED STELLAR IONIZATION $\log \frac{N_I(*)}{\Sigma N(*)}$				
		τ UMa	ρ Pup	θ UMa	α CMi	α Per
Fe I	−1.00	−2.80	−2.58	−1.99	−2.21	−3.00
Cr I	−1.86	−3.36	−3.04	−2.63	−2.66	−3.50
Ti I	−1.98	−3.19	−3.32	−2.66	−3.12	−3.51

TABLE 9

DETERMINATION OF LOG P_e FROM STELLAR IONIZATION

STAR	$\theta_{\text{ion}} = 0.7$				$\theta_{\text{ion}} = 0.8$				$\theta_{\text{ion}} = 0.9$			
	Fe I	*Cr* I	*Ti* I	Mean	*Fe* I	*Cr* I	*Ti* I	Mean	*Fe* I	*Cr* I	*Ti* I	Mean
τ UMa	+1.24	+1.32	+1.63	+1.35	+0.31	+0.50	+0.80	+0.54	−0.60	−0.31	−0.01	−0.38
ρ Pup	+1.46	+1.64	+1.50	+1.51	+0.53	+0.82	+0.67	+0.64	− .38	+ .01	− .14	− .22
θ UMa	+2.05	+2.05	+2.16	+2.08	+1.12	+1.23	+1.33	+1.20	+ .21	+ .42	+ .52	+ .34
α CMi	+1.83	+2.02	+1.70	+1.84	+0.90	+1.20	+0.87	+0.97	− .01	+ .39	+ .06	+ .11
α Per	+1.04	+1.18	+1.31	+1.14	+0.11	+0.36	+0.48	+0.26	−0.80	−0.45	−0.33	−0.60

stellar material in all stars and in the sun. Any gross change of A, the ratio of hydrogen to the metals, invalidates this assumption. The standard elements, together with weighting factors adopted, were: *Ti*(4), *V*(1), *Cr*(2), *Fe*(4), *Ni*(1), *Y*(1), *Ba*(1). These elements prove to be completely in the singly ionized state in F stars. (In τ UMa, *Ti* and *V* were omitted because of their possible slight weakening in that star.) In the analysis of the sun[8] A is equal to the ratio P_g/P_e, since the electrons are contributed by the metals. In the F stars hydrogen is about 1 per cent ionized and provides the electrons; then P_g/P_e varies as P_e. A change of A does not affect P_g/P_e or the opacity and would remain undetected in the following analysis until the absolute strengths of the hydrogen lines were predicted.

We find that the opacity of H and H^- in these stars is a slow function of temperature and nearly proportional to P_e. From the observed $\Delta \log \zeta_i$ for the singly ionized standard elements we obtain a mean ratio of $\log \kappa_\nu(*)/\kappa_\nu(\odot)$ and evaluate $\kappa_\nu(*)$. With a fair degree of approximation we write

$$\log P_e + \phi(\theta) = \log \kappa_\nu , \qquad (32)$$

where $\phi(\theta)$ is nearly a constant. A simultaneous solution of equations (31) and (32) proves highly determinate; the effects of observational errors in the final solution are

$$\Delta\theta_{\text{ion}} \approx 0.1\Delta c_1 - 0.1\Delta \log \kappa_\nu \,. \tag{33}$$

The observational errors are about ± 0.10 (m.e.) in both Δc_1 and $\Delta \log \kappa_\nu$, so that an error of ± 0.015 in θ_{ion} might be expected, with a corresponding error of ± 0.14 in $\log P_e$. The errors in the deduced $\log P_g$ and $\log g_e$ are about ± 0.30. However, while the internal agreement of different elements is good in the determination of $\log \kappa_\nu$, a larger systematic error may arise, owing to the errors of spectrophotometry. For example if our characteristic curve is in error so that all W's are increased by ϵ per cent, lines on the flat part of the curve of growth will give errors in the deduced η_0 of 2 to 4ϵ, appearing in full in κ_ν.

The theoretical κ_ν, including stimulated emission, is determined from the new H^- absorption coefficients of Chandrasekhar and his collaborators.[19, 20]. We evaluate and sum κ_ν at λ 4300 for the H^- absorption and the total H absorption, bound-free and free-free. Detailed tables of $\bar{\kappa}$ and $\kappa_\nu(H^-)$ are available elsewhere; the quantity $\kappa_\nu(H+H^-)$, required in this type of analysis, is given in Table 10. Note that electron scattering is not

TABLE 10

LOG $\kappa_\nu(H + H^-)$

LOG P_e	θ					
	0.5	0.6	0.7	0.8	0.9	1.0
−2	−3.37	−3.05	−2.77	−2.69	−3.25	−3.36
−1	−2.37	−2.05	−1.84	−2.23	−2.51	−2.38
0	−1.37	−1.08	−1.19	−1.66	−1.55	−1.38
+1	−0.38	−0.24	−0.73	−0.75	−0.56	−0.38
+2	+0.53	+0.26	+0.07	+0.24	+0.44	+0.62
+3	+1.25	+0.88	+1.05	+1.24	+1.44	+1.62
+4	+1.74	+1.81	+2.04	+2.24	+2.44	+2.62

included; it would be appreciable in A stars and in supergiants and may slightly affect the results for α Per and τ UMa.

Table 11 gives the individual values of $\Delta \log \zeta_i$ for the standard elements in the ionized state. The level of ionization in F stars and in the sun is such that $\log \zeta_{\text{ion}}(*)/\zeta_{\text{ion}}(\odot)$ averages near $+0.02$. Since

$$\Delta \log \zeta_i = \log \frac{\dfrac{N\,(*)}{\kappa_\nu\,(*)}}{\dfrac{N\,(\odot)}{\kappa_\nu\,(\odot)}}, \tag{34}$$

$$\log \frac{\kappa_\nu\,(*)}{\kappa_\nu\,(\odot)} = +0.02 - \overline{\Delta \log \zeta_i\,(\text{ions})}\,. \tag{35}$$

(In some stars in Table 11 the elements *Y* II and *Ba* II show appreciable ionization.) The value of $\log \kappa_\nu(\odot) = -0.54$; from the mean $\Delta \log \zeta_i$ in Table 11 and from equation (35) we obtain the $\log \kappa_\nu(*)$ in the last row.

The rather complex curves relating $\log P_e$ and $\log \kappa_\nu$ were plotted for various θ; with $\log \kappa_\nu$ in Table 10 we read the $\log P_e$, for each θ, which gives the required opacity. A plot of the $\log P_e$ for each θ required by the ionization (Table 9) and now by the opacity gives θ_{ion} and $\log P_e$ as spectroscopically determined. These are given in Table 7; it is interesting to note that the θ_{ion} agree moderately well with each other and with the

accepted stellar temperature scale and are appreciably smaller than θ_{exc}. This latter fact again suggests that the derived θ_{exc} are not very meaningful parameters of the stars. The detailed stellar models published by Strömgren and his collaborators[14] give the relation between P_g, P_e, and θ for various hydrogen abundances, A. Adopting $\log A = 3.8$, I find the spectroscopic values of P_g given in Table 7. The values of $\bar{\kappa}$ adopted by Strömgren differ slightly from those recently derived by Chandrasekhar, and the range of Strömgren's stellar models is too limited for us to proceed to evaluate the surface gravity exactly. Without exact models, an approximate method can be adopted. Since P_e/P_g is very roughly constant,

$$\frac{\bar{\kappa}(\tau)}{\bar{\kappa}(\tau_0)} = \frac{P_g(\tau)}{P_g(\tau_0)}. \tag{36}$$

TABLE 11

EVALUATION OF STELLAR OPACITY

ELEMENT	WEIGHT	$\Delta \log \zeta_i$				
		τ UMa	ρ Pup	θ UMa	α CMi	α Per
Ti II	4	.....	+0.77	+0.54	+0.71	+0.94
V II	1	.....	+0.63	+ .30	+ .70	+0.79
Cr II	2	+1.20	+0.88	+ .49	+ .57	+1.35
Fe II	4	+1.20	+1.06	+ .56	+ .98	+1.36
Ni II	1	+0.90	+0.50	+ .40	+ .20	+0.77
Y II	1	+0.99	+1.07	+ .45	+ .55	.....
Ba II	1	+0.77	+0.55	+0.23	0.00	.....
Mean	.....	+1.10	+0.84	+0.48	+0.66	+1.12
$\log \kappa_\nu(*)$	.....	−1.62	−1.36	−1.00	−1.18	−1.64

From the hydrostatic equation,

$$\frac{dP_g}{d\tau} = \frac{g_e}{\bar{\kappa}(\tau)}, \tag{37}$$

we obtain

$$g_e = \frac{P_g(\tau_0)\,\bar{\kappa}(\tau_0)}{2\tau_0}. \tag{38}$$

In this range of temperature, I find that $\log \kappa_\nu/\bar{\kappa} \approx -0.2$, from the tables of Chandrasekhar and Münch.[20] By choosing the representative point at $\tau_0 = 0.25$, as before, the g_e given in Table 7 are evaluated from purely spectroscopic data. Any agreement with the expected gravitational values of g, given in the last line of Table 7, is of considerable significance, since it justifies the assumptions made as to the abundance of the metals with respect to hydrogen. The gravitational g are approximately estimated from the masses, luminosities, and temperatures of the F stars. Systematically, $g_e < g$; this is expected for the supergiants, and it is interesting to note that the dwarf τ UMa, in spite of being 6 mag. fainter than ρ Pup, has a lower g_e than that star. This unexpected discrepancy is in line with the large turbulent velocity found for τ UMa (4 km/sec); no dwarfs had previously been found with appreciable turbulence. Another peculiar case is θ UMa, which has a relatively large g_e compared to α CMi, although of about the same luminosity. The weakness of all lines in θ UMa demands the high κ_ν and the consequently large g_e derived. Criticism of the g_e can be made on both observational and theoretical

grounds; photometric errors affect κ_ν directly, and in stars like α CMi the variation of P_g and g with P_e is very steep. Errors of ± 0.3 in the log g_e may be expected.

OBSERVED RELATIVE ABUNDANCES OF THE ELEMENTS

In Table 7 we have tabulated the parameters of the atmospheres required to discuss the relative abundances of the elements. With θ_{ion}, P_e, and κ_ν determined from a small group of standard elements, we compute the level of ionization of all other elements. For each atom of type i in state of ionization r, we write the predicted values of the apparent abundances,

$$\Delta \log \zeta_{i,r} = \log \frac{N_{i,r}(*)}{\sum_r N_{i,r}(*)} - \log \frac{N_{i,r}(\odot)}{\sum_r N_{i,r}(\odot)} - \log \frac{\kappa_\nu(*)}{\kappa_\nu(\odot)} + \log \frac{z_i(*)}{z_i(\odot)}. \quad (39)$$

The quantity $z_i(*)/z_i(\odot)$ represents the abundance ratio, the number of atoms of the element i per gram of material in the star as compared to that ratio in the sun, i.e.,

$$z_i \equiv \sum_r N_{i,r}. \quad (40)$$

If the elements were present in the stars and the sun in the same proportions, all relative abundances $z_i(*)/z_i(\odot)$ would equal unity. From the observed $\Delta \log \zeta_i(*)$ listed in Table 7 and the ionization at θ_{ion} and P_e, equation (39) gives the values of $z_i(*)/z_i(\odot)$ computed for those elements for which the data seem trustworthy. (The results for α Per should throughout be considered of relatively low weight.) If the ionization has been correctly determined, the values of the abundances should be the same in both stages of ionization. This is obvious if there is a true abundance change; it is also true if some peculiar mechanism should ionize an atom, say *Ca* II, more heavily than is predicted by the Saha equation. The ratio *Ca* II/*Ca* I would not be affected by the same mechanism, and *Ca* I would be reduced in the same proportion as *Ca* II; *Ca* would be mainly in the unobservable stage of *Ca* III.

For reasons previously discussed, it was necessary to permit arbitrary zero points, α, in the $\Delta \log \zeta_i$ for *Mg*, *Ca*, *Mn*, *Ni*, and *Eu*. In the first four cases we evaluate these α by requiring that in the mean of the five stars the values of $\log z_i(*)/z_i(\odot)$ should agree for the neutral and ionized elements. This adjustment remains as an unfortunate feature of the abundances of these elements in Table 7. The values determined, $\alpha_1 = -1.7$, $\alpha_2 = +0.74$, $\alpha_3 = +0.9$, $\alpha_4 = +.0.75$, are used in the final $\log z_i(*)/z_i(\odot)$ given in Table 12. The case of *Ca* II may be taken as typical. The observational difficulties have been described. In the sun the collisional damping constant of the K line agreed with the damping found for the average metallic lines in the analysis of the curve of growth. The F stars may not show the same equality, and the deviation observed is in the sense that the K line is too weak in all F stars as compared to the sun. Before adjustment, the abundances of *Ca* indicated by *Ca* II and *Ca* I were as shown in the accompanying tabulation. The systematic nature of the required correction is obvious. (The results for τ UMa

	τ UMa	ρ Pup	α Per	θ UMa	α CMi
Ca I	−1.11	−0.15	0.0	+0.07	+0.25
Ca II	−1.80	−0.97	−0.6	−0.63	−0.63
Difference	−0.69	−0.82	−0.6	−0.70	−0.88

show the great weakening of *Ca* in that star.) It would have been possible to adjust *Ca* I to agree with *Ca* II, but then a large mean negative value of the *Ca* abundance would have resulted. Since the analysis of the K line is subject to greater uncertainties, the adjustment of *Ca* II seems reasonable. In the cases of *Mg* II and *Mn* II the solar X_f is suspect because of the high excitation potential involved. The case of *Ni* II is unsatisfactory; it was adjusted to give an abundance in agreement with *Ni* I, but the mean

TABLE 12

THE RELATIVE ABUNDANCES OF THE ELEMENTS IN UNITS OF THE SOLAR ABUNDANCE
LOG $z_i(*)/z_i(\odot)$

Element	Z	τ UMa	ρ Pup	α Per	θ UMa	α CMi	Qual.	I.P. Volts	
Mg I	.....	−0.8	−0.3	−0.2	+0.01	+0.34	a	.....	.....
Mg II	.....	−0.9	− .2	− .2	+ .34	− .14	d	.....	.....
Mg	12	−0.85	− .25	− .2:	+ .12	+ .18:	b	7.61	14.97
Ca I	.....	−1.06	− .15	.0	+ .07	+ .25	a	.....	.....
Ca II	.....	−0.95	− .23	+ .1	+ .11	+ .11	d	.....	.....
Ca	20	−1.05	− .19	+ .05	+ .09	+ .18	b	6.09	11.82
Sc II	21	−1.65	− 79	− .4:	− .11	− .23	b	.....	12.8
Ti I	.....	−0.30	− .02	+ .08	+ .24	− .05	a	.....	.....
Ti II	.....	−0.61	− .05	− .14	+ .08	+ .07	a	.....	.....
Ti	22	−0.45	− .04	− .03	+ .16	+ .01	a	6.81	13.6
V I	.....	−0.72	− .50	− .7	− .37	− .57	b	.....	.....
V II	.....	−0.52	− .19	− .5	− .43	+ .06	b	.....	.....
V	23	−0.62	− .35	− .6:	− .40	− .25	b	6.71	14.1
Cr I	.....	+0.13	+ .24	+ .2	+ .09	+ .14	a	.....	.....
Cr II	.....	+0.12	+ .06	+ .14	+ .03	− .07	b	.....	.....
Cr	24	+0.13	+ .18	+ .16	+ .07	+ .07	a	6.74	16.6
Mn I	.....	+0.01	− .07	+ .3	− .04	+ .24	a	.....	.....
Mn II	.....	−0.18	+ .08	+ .3	+ .34	− .14	d	.....	.....
Mn	25	−0.05	− .02	+ .3:	+ .09	+ .11	b	7.40	15.6
Fe I	.....	−0.12	+ .10	.00	− .01	+ .19	a	.....	.....
Fe II	.....	+0.12	+ .24	+ .27	+ .10	+ .34	a	.....	.....
Fe	26	0.00	+ .17	+ .14	+ .05	+ .26	a	7.86	16.16
Co I	27	−0.25	− .26	− .3:	− .28	− .08	b	7.85	17.1
Ni I	.....	+0.63	+ .60	+ .3	+ .31	+ .37	b	.....	.....
Ni II	.....	+0.57	+ .43	+ .3	+ .69	+ .32	c	.....	.....
Ni	28	+0.61	+ .54	+ .3:	+ .50	+ .35	c	7.61	18.4
Zn I	30	+0.58	+ .55	+ .1	+ .25	+ .20	b	9.35	17.89
Sr II	38	−0.26	+ .14	− .1	− .44	− .11	b	.....	10.98
Y II	39	+0.06	+ .38	+ .2:	+ .03	− .03	a	.....	12.3
Zr II	40	−0.90	− .13	− .3:	− .31	− .28	a	.....	13.97
Ba II	56	+0.2	+ .2	− .3	− .07	− .62	b	.....	9.96
La II	57	−0.06	− .04	− .1:	− .11	− .27	a	.....	11.38
R.E. II	58–64	0.00	− .03	.0:	− .02:	− .55:	b	.....	11.4
Eu II	63	+0.9	+0.8	+0.1:	0.0	+0.2	d	.....	11.21

residual is left positive in all F stars. The excitation potentials of both *Ni* I and *Ni* II are higher than average.

The final abundances are given in Table 12. The rare earths (except *Eu* II) are lumped together as "R.E. II." Where both stages of ionization are available, the third entry for each element is the adopted mean abundance. The column headed "*Z*" gives the atomic number of the element; "Qual." measures the reliability of the determination, on a scale from "a," good, to "d," very poor. The last two columns give both first and second ionization potentials where relevant. In further discussion of the abundances in Table 12 we shall exclude τ UMa, which will be the subject of Paper III in this series; it apparently shows large abundance changes.

An error of excitation temperature will change some of the derived abundances. If the error of the difference $\theta_{exc}(*) - \theta_{exc}(\odot)$ were as large as 0.1, elements of excitation potential (E.P.) of 5 volts would have errors of $\log z_i(*)/z_i(\odot)$ of 0.5. A weak correlation of abundance differences with excitation potential actually exists, in the sense that elements of high excitation potential have slightly higher abundances in the F stars. Actually, this correlation arises from the more striking low abundance of *Sr*, *Ba*, *Zr*, and *Sc*, which amounts to about -0.2. The lines of these elements have low excitation potential; they are known to be strong at the very low excitation temperatures of K and M giants. Such a low-temperature enhancement may already be present to a slight degree in the sun, because of a steep decrease of η with optical depth. If so, their apparently somewhat low abundance in F stars is unreal.

A curious effect is visible for *Zn* in Table 12; while only two lines are accessible, they are strong and unblended. All F stars show an abundance increase, largest in ρ Pup; in α Per, however, the lines are definitely weakened (to the eye as well), and the abundance is relatively low. Thus *Zn* I seems to show an absolute-magnitude effect with a maximum in the intermediate supergiants.

The element *Eu* II is particularly difficult. The strong lines at λ 4129, λ 4205, are badly blended in all stars, and in the supergiants almost hopelessly blended. All rare-earth lines are strong in ρ Pup, α Per, and τ UMa; and this strengthening is *normal*, not requiring any abundance changes. The strengthening of *Eu* II, however, seems somewhat excessive. A similar excessive strength for *Eu* II lines is noted by Hiltner[21] in β CrB, a peculiar F giant.

Except for τ UMa, it may be said that the four F stars show extremely small abundance changes from the sun. The spectroscopic differences between θ UMa and α Per are enormous to the eye, even on the lowest dispersion. Both differ even more strongly from the sun. Yet for about twenty elements in Table 12, there is no well-established difference of abundance of a factor of 2 between these stars. The accidental errors, especially in α Per, are quite large; to reduce their effect let us group the two "giants," ρ Pup and α Per, and the two "dwarfs," θ UMa and α CMi. Form the differences in abundance, giant divided by dwarf, i.e.,

$$\Delta \log z_i' \equiv \log \frac{\overline{z_i\,(\alpha\ \text{Per},\ \rho\ \text{Pup})}}{z_i\,(\odot)} - \log \frac{\overline{z_i\,(\theta\ \text{UMa},\ \alpha\ \text{CMi})}}{z_i\,(\odot)}. \tag{41}$$

Table 13 gives the mean value of these abundance differences between the F stars. A range of about 6 in absolute magnitude is involved. I have tabulated the elements in the order of their $\Delta \log z_i'$ in Table 13.

The total range of apparent abundance changes is of the order of ± 0.30, and of this at least ± 0.15 may be expected to be observational error. A very unexpected regularity appears in Table 13. The elements deficient in the supergiants are the lighter ones. The median atomic number, Z, is 23 for elements with negative residuals and 39 for those with positive residuals. If real, elements heavier than *Ni* are about 50 per cent more abundant in the supergiants than in the dwarfs and the lighter elements are 50 per cent less abundant. This small difference may have still another origin than in true abundance differences, since lighter elements have, on the average, lower ionization potentials and higher excitation potentials than do the heavy ones.

If the stars are grouped in the same way and are compared to the sun, no systematic effect in atomic weight is apparent. The straight mean $\log z_i(*)/z_i(\odot) = -0.01$ for the giants and -0.03 for the dwarfs. These near-approaches to zero difference between the stars and the sun are only in part forced on the data by the method of reduction. The opacities are determined essentially by the strength of *Ti* II, *Cr* II, and *Fe* II, and the derived abundances of the other elements might well have differed greatly from the solar

[21] *Ap. J.*, **102**, 438, 1945.

values. There is a slight tendency toward positive residuals in the dwarfs for the light-elements. There are many observational and theoretical uncertainties involved, but the predominant evidence shows only small abundance variations of the heavier elements among the "normal" stars of a wide range of luminosity. The abundance of the heavy elements with respect to hydrogen will be treated separately, but a normal value is indicated by the nearly zero mean value of $\log z_i(*)/z_i(\odot)$.

THE HYDROGEN ABUNDANCE

The hydrogen lines are subject to Stark and collisional broadening; because of the high excitation involved, their broadened wings are produced at large depths, and η increases with τ. With detailed model atmospheres, the prediction of the complete line contour can be carried out. If the lines near the Balmer series limit could be observed in F stars as they are in B and A stars, the point of disappearance of individual high series members could be used to estimate P_e. In B and A stars the run of W with series number is also used to estimate the number of excited atoms of hydrogen. Neither method can be applied to F stars, since lines beyond $H\zeta$ are blended with metallic lines. We require estimates of the hydrogen abundance accurate within a factor of 2, and the observational and theoretical difficulties may well produce a greater uncertainty.

TABLE 13

ABUNDANCE DIFFERENCES
SUPERGIANT/DWARF

$\Delta \log z_i'$	Element
< -0.30	*Mg, Sc:*
-0.29 to -0.20	*Ca*
$-.19$ to $-.10$	*Ti, Co:*
$-.09$ to $.00$	*V:, Mn, Fe, Ni*
$+.01$ to $+.10$	*Cr, Zr, Zn*
$+.11$ to $+.20$	*La*
$+0.21$ to $+0.30$	*Sr, Y, Ba, Eu,* rare earths

After some consideration it is apparent that the contours of $H\gamma$ and $H\delta$, available for our F stars, can determine the hydrogen abundance. The equivalent widths of these strong lines cannot be interpreted directly. The type of model atmosphere differs from star to star; the source of broadening may change from collisional damping to Stark effect. If the model changes, a line absorption at distance $\delta\lambda$ from the center of the line $A(\delta\lambda)$ may involve different $\eta(\delta\lambda)$ from star to star. Such an effect should be smallest in the wing of the line. In the wing we also know that Stark effect dominates unless the collisional damping is many times the radiation damping. In the wings the Stark broadening gives a line-absorption coefficient of

$$l(\delta\lambda) = C N_2 P_e T_e^{-1} (\delta\lambda)^{-5/2}, \tag{42}$$

where C is given by the theory of the Stark effect and N_2 is the number of excited hydrogen atoms in the second level. Let us compute η in the star and the sun at wave lengths $\delta\lambda(*)$ and $\delta\lambda(\odot)$:

$$\frac{\eta[\delta\lambda(*)]}{\eta_1 \delta\lambda(\odot)]} = \frac{P_e(*)}{P_e(\odot)} \frac{T_e(\odot)}{T_e(*)} \frac{N_2(*)}{N_2(\odot)} \frac{\kappa_\nu(\odot)}{\kappa_\nu(*)} \left(\frac{\delta\lambda(\odot)}{\delta\lambda(*)}\right)^{5/2}. \tag{43}$$

Our assumption is that the star and the sun follow the same model and that therefore the same observed absorption in the wing of the line corresponds to the same η in star and sun. Measure the width of the line, $\delta\lambda$, in various stars at certain fixed values of the

absorption A; our assumption requires that the left-hand side of equation (43) equal unity. Thus N_2 is determined, and an application of the Boltzmann formula gives the total number of hydrogen atoms, N_0. The abundance then is

$$\log \frac{z_H(*)}{z_H(\odot)} = +\ 10.16[\theta(*)-\theta(\odot)] + \tfrac{5}{2} \log \frac{\delta\lambda(*)}{\delta\lambda(\odot)} + \log \frac{\kappa_\nu(*)\,\theta(\odot) P_e(\odot)}{\kappa_\nu(\odot)\,\theta(*) P_e(*)} . \quad (44)$$

The ionization of hydrogen can be neglected. A fundamental difficulty is to decide at what optical depth to evaluate κ_ν, θ, and P_e for equation (44). Since κ_ν/P_e appears and $\kappa_\nu \propto P_e$, the pressure variation is unimportant. The temperature variation has a large effect, however; we may ask whether the ionization temperature at $\tau_0 = 0.25$ or the excitation temperature (which is usually low) should enter the first term in equation (44). Previous experience[7] has shown that the low excitation temperature found for the metals cannot apply to the hydrogen lines; Strömgren found in the sun[8] that the observed value of N_2 was consistent with the opacity and the hydrogen abundance when the temperature at a rather deep layer ($\tau_0 = 0.53$) was used. However, only the difference $\theta(*) - \theta(\odot)$ appears, and the uncertainties are correspondingly reduced. If η were independent of optical depth, the present analysis would be quite satisfactory. The model dwarf F star, when compared with the sun, in Table 6 fortunately showed only small differences arising from the change of model, except in the extreme wing of the line.

TABLE 14

HYDROGEN LINE WIDTHS AND THE ABUNDANCE OF HYDROGEN

STAR	LOG $\frac{\delta\lambda(*)}{\delta\lambda(\odot)}$			LOG $\frac{z_H(*)}{z_H(\odot)}$	
	Observed	Predicted			
		θ_{ion}	θ_{exc}	θ_{ion}	θ_{exc}
τ UMa	+0.62	+0.46	+0.62	+0.40	0.00
ρ Pup	+ .56	+ .63	+ .53	− .18	+ .08
θ UMa	+ .28	+ .41	+ .34	− .32	− .15
α CMi	+ .49	+ .49	+ .44	.00	+ .12
α Per	+0.57	+0.67	+0.39	−0.22	+0.45

In the application of this analysis of the contours we use the solar contour given in the Utrecht *Atlas*,[17] obtained at the center of the solar disk. The hydrogen lines weaken toward the limb; the observations of $H\gamma$ and $H\delta$ by Royds and Narayan[22] have been criticized by D. S. Evans.[23] While the absolute intensities of the former investigators may be in error, we adopt the scale of decrease toward the limb that they observe. Rather than compute the solar line in the integrated flux, I have arbitrarily weakened the hydrogen lines as observed in the *Atlas* by contracting the wave-length scale by 15 per cent (about −0.06 in log W). The line widths (which range from 2 to 30 A) were measured at absorptions $A = 0.1$, $A = 0.2$, $A = 0.4$ in the sun and in the F stars (Table 4). The ratios $\delta\lambda(*)/\delta\lambda(\odot)$ should be constant and, in fact, do agree moderately well. An unweighted mean is given for each star in Table 14. If the hydrogen abundance is normal, equation (44) gives the predicted values listed in Table 14. Predictions are given in both cases, using the ionization or the excitation temperature. The last two columns give

[22] *Kodaikanal Obs. Bull.*, **109**, 375, 1936.

[23] *M.N.*, **100**, 156, 1939.

the hydrogen abundance deduced from equation (44), using the observed line widths. It is interesting to note that the mean observed ratios of line widths in Table 14 are close to the ratios of equivalent widths in Tables 3 and 4.

Although sensitive to the temperature adopted, the general run of predicted line widths agrees well with the observed values. Most gratifying is the predicted strength of the hydrogen lines in the F supergiants, in agreement with the observations. In the discussion of Table 4 we found that an approximate null absolute-magnitude effect is observed for hydrogen lines in the F stars. The prediction in Table 14 actually suggests that the hydrogen lines should be enhanced in the supergiants (as contrasted to A stars, where the Stark effect results in weakened hydrogen lines in the supergiants). We may hope that eventually the positive absolute-magnitude effect in late-type giants will also be explicable without recourse to deviations from thermodynamic equilibrium.

The scatter of the derived abundances is large; positive residuals have no physical reality, since hydrogen forms substantially all stellar material in the sun. In the mean the two giants show about the same abundance of hydrogen as in the sun. The giant θ UMa has abnormally weak hydrogen lines, probably correlated with the weakness of the metallic lines. Though we endeavored to explain the latter by a large opacity, the predicted hydrogen lines still remain too strong. This star requires further theoretical investigation. A converse small apparent excess of hydrogen may exist in τ UMa; our discussion in Paper III will show that the metallic-line A stars do have somewhat stronger hydrogen lines than their metallic-line type requires. The excitation temperature may be slightly higher in the metallic-line A stars than it is in normal F stars; such an effect may be correlated with the observed turbulence, unusual in dwarfs.

Neglecting these small deviations, we see that the hydrogen abundance in the F stars is compatible with that in the sun within a factor of 2. We have already shown that, on the whole, the metals show about the same relative abundances as in the sun. Large differences of absolute magnitude do not involve any gross changes of abundance. For the first time we may with some confidence say that the spectrum of a star could be predicted in detail from that of the sun. Since we have a satisfactory source of opacity, the color temperature, the Balmer discontinuity, and the absolute intensities of the lines of hydrogen and the metals are all predictable and, with the exception of the first two, have been now proved consistent with observation. One parameter of the stellar atmospheres which is not directly given by the theory is the turbulence, which for some unknown reason increases systematically from dwarfs to giants. With this is correlated abnormally low surface gravity. Only τ UMa, as a dwarf, has unusual turbulence and low surface gravity and shows several apparent abnormal abundances of the metals.

I wish to express my gratitude to Dr. S. Chandrasekhar and to Dr. B. Strömgren for their invaluable discussion of theoretical problems and to Dr. K. O. Wright for providing solar-line strengths in advance of publication.

ON THE RADIATIVE EQUILIBRIUM OF A STELLAR ATMOSPHERE. XXII (*Concluded*)*

S. CHANDRASEKHAR
Yerkes Observatory
Received November 3, 1947

III. SCATTERING IN ACCORDANCE WITH RAYLEIGH'S PHASE FUNCTION

11. *The equations of the problem.*—We have already indicated in Paper XVII, § 6, how the functional equations governing the angular distributions of the reflected and the transmitted radiations from an atmosphere scattering according to a general phase function, expressible as a series in Legendre polynomials, can be reduced to independent systems of functional equations.

In the case of scattering according to Rayleigh's phase function, we can express the reflected and the transmitted intensities in the forms (cf. Paper XIV, eq. [231])

$$I(0; \mu, \varphi; \mu_0, \varphi_0) = \frac{3}{32\mu} F [S^{(0)}(\mu, \mu_0) - 4\mu\mu_0 (1-\mu^2)^{\frac{1}{2}} (1-\mu_0^2)^{\frac{1}{2}} \times S^{(1)}(\mu, \mu_0) \cos(\varphi - \varphi_0) + (1-\mu^2)(1-\mu_0^2) S^{(2)}(\mu, \mu_0) \cos 2(\varphi - \varphi_0)] \tag{214}$$

and

$$I(\tau_1; -\mu, \varphi; \mu_0, \varphi_0) = \frac{3}{32\mu} F [T^{(0)}(\mu, \mu_0) + 4\mu\mu_0 (1-\mu^2)^{\frac{1}{2}} (1-\mu_0^2)^{\frac{1}{2}} \times T^{(1)}(\mu, \mu_0) \cos(\varphi - \varphi_0) + (1-\mu^2)(1-\mu_0^2) T^{(2)}(\mu, \mu_0) \cos 2(\varphi - \varphi_0)], \tag{215}$$

and the functions of the different orders (distinguished by the superscripts) satisfy independent systems of equations. Of these systems, the two governing the functions of order one and two are directly reducible to the standard forms considered in Section I. And the terms in the reflected and the transmitted intensities proportional to $\cos(\varphi - \varphi_0)$ and $\cos 2(\varphi - \varphi_0)$ are of exactly the same forms as those given in Paper XXI, equations (223) and (224); only the functions $X^{(1)}$, $Y^{(1)}$, and $X^{(2)}$, $Y^{(2)}$, must now be redefined in terms of the functional equations which they satisfy. These terms require, therefore, no further consideration.

Turning to the functions $S^{(0)}(\mu, \mu_0)$ and $T^{(0)}(\mu, \mu_0)$ of zero order, we find that these functions must be expressible in the forms (cf. Paper XIV, eqs. [241]–[245])

$$\left(\frac{1}{\mu_0} + \frac{1}{\mu}\right) S^{(0)}(\mu, \mu_0) = \tfrac{1}{3} [\psi(\mu)\psi(\mu_0) - \chi(\mu)\chi(\mu_0)] + \tfrac{8}{3} [\phi(\mu)\phi(\mu_0) - \zeta(\mu)\zeta(\mu_0)] \tag{216}$$

and

$$\left(\frac{1}{\mu_0} - \frac{1}{\mu}\right) T^{(0)}(\mu, \mu_0) = \tfrac{1}{3} [\chi(\mu)\psi(\mu_0) - \psi(\mu)\chi(\mu_0)] + \tfrac{8}{3} [\zeta(\mu)\phi(\mu_0) - \phi(\mu)\zeta(\mu_0)], \tag{217}$$

* Sections I and II of this paper have already appeared in *Ap. J.*, **107**, 48, 1948. The remaining Sections III–V of the paper are published here. The numbering of the sections and equations continue from those of the earlier part.

where

$$\psi(\mu) = 3 - \mu^2 + \tfrac{3}{16}\int_0^1 (3 - \mu'^2)\, S^{(0)}(\mu, \mu')\, \frac{d\mu'}{\mu'}, \tag{218}$$

$$\phi(\mu) = \mu^2 + \tfrac{3}{16}\int_0^1 \mu'^2 S^{(0)}(\mu, \mu')\, \frac{d\mu'}{\mu'}, \tag{219}$$

$$\chi(\mu) = (3 - \mu^2)\, e^{-\tau_1/\mu} + \tfrac{3}{16}\int_0^1 (3 - \mu'^2)\, T^{(0)}(\mu, \mu')\, \frac{d\mu'}{\mu'} \tag{220}$$

and

$$\zeta(\mu) = \mu^2 e^{-\tau_1/\mu} + \tfrac{3}{16}\int_0^1 \mu'^2 T^{(0)}(\mu, \mu')\, \frac{d\mu'}{\mu'}. \tag{221}$$

Further, we must also have

$$\frac{\partial S^{(0)}}{\partial \tau_1} = \tfrac{1}{3}\chi(\mu)\,\chi(\mu_0) + \tfrac{8}{3}\zeta(\mu)\,\zeta(\mu_0) \tag{222}$$

and

$$\left(\frac{1}{\mu_0} - \frac{1}{\mu}\right)\frac{\partial T^{(0)}}{\partial \tau_1} = \frac{1}{\mu_0}\left[\tfrac{1}{3}\psi(\mu)\,\chi(\mu_0) + \tfrac{8}{3}\phi(\mu)\,\zeta(\mu_0)\right] - \frac{1}{\mu}\left[\tfrac{1}{3}\chi(\mu)\,\psi(\mu_0) + \tfrac{8}{3}\zeta(\mu)\,\phi(\mu_0)\right]. \tag{223}$$

Substituting for $S^{(0)}$ and $T^{(0)}$ according to equations (216) and (217) in equations (218)–(221), we obtain the following system of functional equations of fourth order:

$$\psi(\mu) = 3 - \mu^2 + \tfrac{1}{16}\mu\int_0^1 \frac{3 - \mu'^2}{\mu + \mu'}\left[\psi(\mu)\,\psi(\mu') - \chi(\mu)\,\chi(\mu')\right]d\mu' + \tfrac{1}{2}\mu\int_0^1 \frac{3 - \mu'^2}{\mu + \mu'}\left[\phi(\mu)\,\phi(\mu') - \zeta(\mu)\,\zeta(\mu')\right]d\mu', \tag{224}$$

$$\phi(\mu) = \mu^2 + \tfrac{1}{16}\mu\int_0^1 \frac{\mu'^2}{\mu + \mu'}\left[\psi(\mu)\,\psi(\mu') - \chi(\mu)\,\chi(\mu')\right]d\mu' + \tfrac{1}{2}\mu\int_0^1 \frac{\mu'^2}{\mu + \mu'}\left[\phi(\mu)\,\phi(\mu') - \zeta(\mu)\,\zeta(\mu')\right]d\mu', \tag{225}$$

$$\chi(\mu) = (3 - \mu^2)\, e^{-\tau_1/\mu} + \tfrac{1}{16}\mu\int_0^1 \frac{3 - \mu'^2}{\mu - \mu'}\left[\chi(\mu)\,\psi(\mu') - \psi(\mu)\,\chi(\mu')\right]d\mu' + \tfrac{1}{2}\mu\int_0^1 \frac{3 - \mu'^2}{\mu - \mu'}\left[\zeta(\mu)\,\phi(\mu') - \phi(\mu)\,\zeta(\mu')\right]d\mu', \tag{226}$$

and

$$\zeta(\mu) = \mu^2 e^{-\tau_1/\mu} + \tfrac{1}{16}\mu\int_0^1 \frac{\mu'^2}{\mu - \mu'}\left[\chi(\mu)\,\psi(\mu') - \psi(\mu)\,\chi(\mu')\right]d\mu' + \tfrac{1}{2}\mu\int_0^1 \frac{\mu'^2}{\mu - \mu'}\left[\zeta(\mu)\,\phi(\mu') - \phi(\mu)\,\zeta(\mu')\right]d\mu'. \tag{227}$$

12. *The form of the solution.*—In solving systems of functional equations of the type of equations (224)–(227), we shall be guided by the forms of the solutions obtained in the direct solution of the equations of transfer in a general finite approximation and the correspondence enunciated in theorem 9 between the X- and Y-functions occurring in such approximate solutions and the exact functions defined in terms of functional equations they satisfy.

Accordingly, in the present instance, we shall assume that $S^{(0)}(\mu, \mu')$ and $T^{(0)}(\mu, \mu')$ are of the forms (cf. Paper XXI, eqs. [221] and [222])

$$\left(\frac{1}{\mu'}+\frac{1}{\mu}\right) S^{(0)}(\mu, \mu') = X(\mu)\, X(\mu')\,[3 + c_1(\mu+\mu') + \mu\mu'] - Y(\mu)\, Y(\mu')\,[3 - c_1(\mu+\mu') + \mu\mu'] + c_2(\mu+\mu')\,[X(\mu)\, Y(\mu') + Y(\mu)\, X(\mu')] \tag{228}$$

and

$$\left(\frac{1}{\mu'}-\frac{1}{\mu}\right) T^{(0)}(\mu, \mu') = Y(\mu)\, X(\mu')\,[3 - c_1(\mu-\mu') - \mu\mu'] - X(\mu)\, Y(\mu')\,[3 + c_1(\mu-\mu') - \mu\mu'] - c_2(\mu-\mu')\,[X(\mu)\, X(\mu') + Y(\mu)\, Y(\mu')], \tag{229}$$

where c_1 and c_2 are certain constants unspecified for the present, and $X(\mu)$ and $Y(\mu)$ are the *standard solutions* of the equations

$$X(\mu) = 1 + \tfrac{3}{16}\mu \int_0^1 \frac{3-\mu'^2}{\mu+\mu'}\,[X(\mu)\, X(\mu') - Y(\mu)\, Y(\mu')]\, d\mu' \tag{230}$$

and

$$Y(\mu) = e^{-\tau_1/\mu} + \tfrac{3}{16}\mu \int_0^1 \frac{3-\mu'^2}{\mu-\mu'}\,[Y(\mu)\, X(\mu') - X(\mu)\, Y(\mu')]\, d\mu', \tag{231}$$

having the property

$$\tfrac{3}{16}\int_0^1 (3-\mu^2)\, X(\mu)\, d\mu = \tfrac{3}{16}\,(3a_0 - a_2) = 1 \tag{232}$$

and

$$\int_0^1 (3-\mu^2)\, Y(\mu)\, d\mu = (3\beta_0 - \beta_2) = 0 \tag{233}$$

where a_n and β_n have their usual meanings (cf. eq. [11]).

An alternative form of equations (228) and (229) which we shall find useful may be noted here:

$$S^{(0)}(\mu, \mu') = \{(3-\mu^2)\,[X(\mu)\, X(\mu') - Y(\mu)\, Y(\mu')] + (\mu+\mu')\, X(\mu)\,[(c_1+\mu)\, X(\mu') + c_2 Y(\mu')] + (\mu+\mu')\, Y(\mu)\,[c_2 X(\mu') + (c_1-\mu)\, Y(\mu')]\}\, \frac{\mu\mu'}{\mu+\mu'} \tag{234}$$

and

$$T^{(0)}(\mu, \mu') = \{(3-\mu^2)\,[Y(\mu)\, X(\mu') - X(\mu)\, Y(\mu')] - (\mu-\mu')\, X(\mu)\,[(c_1+\mu)\, Y(\mu') + c_2 X(\mu')] - (\mu-\mu')\, Y(\mu)\,[c_2 Y(\mu') + (c_1-\mu)\, X(\mu')]\}\, \frac{\mu\mu'}{\mu-\mu'}. \tag{235}$$

13. *Verification of the solution and a relation between the constants* c_1 *and* c_2.—The verification that the solutions for $S^{(0)}$ and $T^{(0)}$ have the forms assumed in § 12 will consist in first evaluating ψ, ϕ, χ, and ζ according to equations (218)–(221) and then showing that when the resulting expressions for ψ, ϕ, χ, and ζ are substituted back into

equations (216) and (217) we shall recover the form of the solutions assumed. In general, such a procedure will lead to certain conditions which the constants introduced into the solution (such as c_1 and c_2 in the present instance) must satisfy. We shall see that, in the particular case under discussion, the conditions derived in the manner indicated do not suffice to determine c_1 and c_2 without an ambiguity and an arbitrariness. This is a further example of the nonuniqueness of the solution, in conservative cases, of the functional equations incorporating the invariances of the problem. But, again, an appeal to the integrals of the problem resolves the ambiguity and the arbitrariness.

Our first step, then, is to evaluate ψ, ϕ, χ, and ζ according to equations (218)–(221), when $S^{(0)}(\mu, \mu')$ and $T^{(0)}(\mu, \mu')$ have the forms given by equations (234) and (235). The evaluation of the integrals defining ψ, ϕ, etc., is fairly straightforward if appropriate use is made of the various integral properties of the standard solutions of equations (230) and (231). It may be noted that, in addition to equations (232) and (233), use must also be made of the relations (cf. theorem 4, eqs. [44]–[46])

$$\alpha_0 = 1 + \tfrac{3}{32}\left[3\left(\alpha_0^2 - \beta_0^2\right) - \left(\alpha_1^2 - \beta_1^2\right)\right], \tag{236}$$

$$(3-\mu^2)\int_0^1 \frac{X(\mu)\,X(\mu') - Y(\mu)\,Y(\mu')}{\mu+\mu'}\,d\mu' = \frac{X(\mu)-1}{\frac{3}{16}\mu} + (\alpha_1 - \mu\alpha_0)\,X(\mu) - (\beta_1 - \mu\beta_0)\,Y(\mu) \tag{237}$$

and

$$(3-\mu^2)\int_0^1 \frac{Y(\mu)\,X(\mu') - X(\mu)\,Y(\mu')}{\mu-\mu'}\,d\mu' = \frac{Y(\mu) - e^{-\tau_1/\mu}}{\frac{3}{16}\mu} + (\beta_1 + \mu\beta_0)\,X(\mu) - (\alpha_1 + \mu\alpha_0)\,Y(\mu). \tag{238}$$

Evaluating ψ, ϕ, χ, and ζ in the manner indicated, we find that

$$\psi(\mu) = (3 + c_1\mu)\,X(\mu) + c_2\mu\,Y(\mu), \tag{239}$$

$$\chi(\mu) = (3 - c_1\mu)\,Y(\mu) - c_2\mu X(\mu) \tag{240}$$

$$\phi(\mu) = +\mu\left[q_1 X(\mu) + q_2 Y(\mu)\right], \tag{241}$$

and

$$\zeta(\mu) = -\mu\left[q_2 X(\mu) + q_1 Y(\mu)\right] \tag{242}$$

where

$$q_1 = \tfrac{3}{16}\left(c_1\alpha_2 + c_2\beta_2 + 3\alpha_1\right) \tag{243}$$

and

$$q_2 = \tfrac{3}{16}\left(c_1\beta_2 + c_2\alpha_2 - 3\beta_1\right). \tag{244}$$

Using the expressions (239)–(242) for ψ, χ, ϕ, and ζ, we next evaluate $S^{(0)}$ and $T^{(0)}$ according to equations (216) and (217). We find

$$\begin{aligned}\left(\frac{1}{\mu'}+\frac{1}{\mu}\right) S^{(0)}(\mu, \mu') &= X(\mu)\,X(\mu')\left[3 + c_1(\mu+\mu') + \tfrac{1}{3}\left\{c_1^2 - c_2^2 + 8\left(q_1^2 - q_2^2\right)\right\}\mu\mu'\right] \\ &- Y(\mu)\,Y(\mu')\left[3 - c_1(\mu+\mu') + \tfrac{1}{3}\left\{c_1^2 - c_2^2 + 8\left(q_1^2 - q_2^2\right)\right\}\mu\mu'\right] \\ &+ c_2(\mu+\mu')\left[X(\mu)\,Y(\mu') + Y(\mu)\,X(\mu')\right]\end{aligned} \tag{245}$$

and

$$\left(\frac{1}{\mu'}-\frac{1}{\mu}\right)T^{(0)}(\mu,\mu')$$
$$= Y(\mu)\,X(\mu')\left[3-c_1(\mu-\mu')-\tfrac{1}{3}\{c_1^2-c_2^2+8(q_1^2-q_2^2)\}\mu\mu'\right]$$
$$-X(\mu)\,Y(\mu')\left[3+c_1(\mu-\mu')-\tfrac{1}{3}\{c_1^2-c_2^2+8(q_1^2-q_2^2)\}\mu\mu'\right] \tag{246}$$
$$-c_2(\mu-\mu')\left[X(\mu)\,X(\mu')+Y(\mu)\,Y(\mu')\right].$$

A comparison of equations (245) and (246) and (228) and (229) now shows that, among the constants c_1, c_2, q_1, and q_2, we must require that there exist the relation (cf. Paper XIV, eq. [250])

$$c_1^2-c_2^2+8(q_1^2-q_2^2)=3\,. \tag{247}$$

Substituting for q_1 and q_2 according to equations (243) and (244) in equation (247), we obtain

$$32(c_1^2-c_2^2)+9\left[(c_1+c_2)(a_2+\beta_2)+3(a_1-\beta_1)\right]$$
$$\times\left[(c_1-c_2)(a_2-\beta_2)+3(a_1+\beta_1)\right]-96=0\,. \tag{248}$$

After some minor rearranging of the terms, the foregoing equation can be reduced to the form

$$\left[32+9(a_2^2-\beta_2^2)\right](c_1^2-c_2^2)+27(a_1+\beta_1)(a_2+\beta_2)(c_1+c_2)$$
$$+27(a_1-\beta_1)(a_2-\beta_2)(c_1-c_2)+81(a_1^2-\beta_1^2)-96=0\,. \tag{249}$$

On the other hand, according to equations (232), (233), and (236),

$$32+9(a_2^2-\beta_2^2)=32+(9a_0-16)^2-81\beta_0^2$$
$$=288(1-a_0)+81(a_0^2-\beta_0^2) \tag{250}$$
$$=27(a_1^2-\beta_1^2)\,.$$

Equation (249) therefore becomes

$$(a_1^2-\beta_1^2)(c_1^2-c_2^2)+(a_1+\beta_1)(a_2+\beta_2)(c_1+c_2)$$
$$+(a_1-\beta_1)(a_2-\beta_2)(c_1-c_2)+(a_2^2-\beta_2^2)=0\,. \tag{251}$$

Hence

$$\left[(a_1+\beta_1)(c_1+c_2)+(a_2-\beta_2)\right]\left[(a_1-\beta_1)(c_1-c_2)+(a_2+\beta_2)\right]=0\,. \tag{252}$$

It is apparent that one of the two factors in equation (252) must vanish. But within the framework of equations (224)–(227) it is impossible to decide which of the two it must be; and in either case we shall have only one relation between the two constants c_1 and c_2. The problem is therefore characterized by an ambiguity and an arbitrariness. We shall show in the following section how this can be resolved.

14. *The resolution of the ambiguity and the arbitrariness in the solution.*—It can be readily verified that the problem of diffuse reflection and transmission in accordance with Rayleigh's phase function admits, as in the conservative isotropic case, the flux

and the K-integrals. The emergent values of F and K must therefore be given by equations of the form (cf. eqs. [190]–[193])

$$F(0) = \mu_0 F(1+\gamma_1); \qquad F(\tau_1) = \mu_0 F(e^{-\tau_1/\mu_0}+\gamma_1), \tag{253}$$

$$K(0) = \tfrac{1}{4}\mu_0 F(-\mu_0+\gamma_2), \tag{254}$$

and

$$K(\tau_1) = \tfrac{1}{4}\mu_0 F(-\mu_0 e^{-\tau_1/\mu_0}+\gamma_1\tau_1+\gamma_2), \tag{255}$$

where γ_1 and γ_2 are constants.

It is evident that only the azimuth independent terms in the intensity will contribute to F and K. We have, accordingly, to evaluate $F(0)$, $F(\tau_1)$, $K(0)$, and $K(\tau_1)$ for emergent intensities of the forms (cf. eqs. [214], [215], [234], and [235])

$$\begin{aligned} I(0,\mu) = \tfrac{1}{2}\mu_0 F \Big\{ &\tfrac{3}{16}\frac{3-\mu^2}{\mu_0+\mu}[X(\mu_0)X(\mu) - Y(\mu_0)Y(\mu)] \\ &+ \tfrac{3}{16}X(\mu_0)[(c_1+\mu)X(\mu) + c_2 Y(\mu)] \\ &+ \tfrac{3}{16}Y(\mu_0)[c_2 X(\mu) + (c_1-\mu)Y(\mu)]\Big\} \end{aligned} \tag{256}$$

and

$$\begin{aligned} I(\tau_1,-\mu) = \tfrac{1}{2}\mu_0 F \Big\{ &\tfrac{3}{16}\frac{3-\mu^2}{\mu_0-\mu}[Y(\mu_0)X(\mu) - X(\mu_0)Y(\mu)] \\ &- \tfrac{3}{16}X(\mu_0)[c_2 X(\mu) + (c_1-\mu)Y(\mu)] \\ &- \tfrac{3}{16}Y(\mu_0)[(c_1+\mu)X(\mu) + c_2 Y(\mu)]\Big\}. \end{aligned} \tag{257}$$

With $I(0,\mu)$ and $I(\tau_1,-\mu)$ given by equations (256) and (257), the integrals defining $F(0)$, $F(\tau_1)$, $K(0)$, and $K(\tau_1)$ can all be evaluated quite simply by using the various relations given in theorem 8 (eqs. [81]–[86]) and remembering that in the present case

$$x_1 = \tfrac{3}{16}(3a_1 - a_3) \qquad \text{and} \qquad y_1 = \tfrac{3}{16}(3\beta_1 - \beta_3). \tag{258}$$

We thus find

$$F(0) = \mu_0 F\{1 + \tfrac{3}{16}X(\mu_0)(c_1a_1 + c_2\beta_1 + a_2) + \tfrac{3}{16}Y(\mu_0)(c_1\beta_1 + c_2a_1 - \beta_2)\}, \tag{259}$$

$$\begin{aligned} F(\tau_1) = \mu_0 F\{ &e^{-\tau_1/\mu_0} + \tfrac{3}{16}X(\mu_0)(c_1\beta_1 + c_2a_1 - \beta_2) \\ &+ \tfrac{3}{16}Y(\mu_0)(c_1a_1 + c_2\beta_1 + a_2)\}, \end{aligned} \tag{260}$$

$$\begin{aligned} K(0) = \tfrac{1}{4}\mu_0 F\{ &-\mu_0 + \tfrac{3}{16}X(\mu_0)(c_1a_2 + c_2\beta_2 + 3a_1) \\ &+ \tfrac{3}{16}Y(\mu_0)(c_1\beta_2 + c_2a_2 - 3\beta_1)\}, \end{aligned} \tag{261}$$

and

$$\begin{aligned} K(\tau_1) = \tfrac{1}{4}\mu_0 F\{ &-\mu_0 e^{-\tau_1/\mu_0} - \tfrac{3}{16}X(\mu_0)(c_1\beta_2 + c_2a_2 - 3\beta_1) \\ &- \tfrac{3}{16}Y(\mu_0)(c_1a_2 + c_2\beta_2 + 3a_1)\}. \end{aligned} \tag{262}$$

Comparing the reflected and the transmitted fluxes given by equations (259) and (260) with those given by the flux integral (eq. [253]), we find that

$$\gamma_1 = \tfrac{3}{16} X(\mu_0)(c_1\alpha_1 + c_2\beta_1 + \alpha_2) + \tfrac{3}{16} Y(\mu_0)(c_1\beta_1 + c_2\alpha_1 - \beta_2) \tag{263}$$

and also that

$$\gamma_1 = \tfrac{3}{16} X(\mu_0)(c_1\beta_1 + c_2\alpha_1 - \beta_2) + \tfrac{3}{16} Y(\mu_0)(c_1\alpha_1 + c_2\beta_1 + \alpha_2) . \tag{264}$$

We must therefore require that

$$c_1\alpha_1 + c_2\beta_1 + \alpha_2 = c_1\beta_1 + c_2\alpha_1 - \beta_2 , \tag{265}$$

or

$$(c_1 - c_2)(\alpha_1 - \beta_1) + \alpha_2 + \beta_2 = 0 ; \tag{266}$$

but this is one of the factors in equation (252). The appeal to the flux integral has therefore decided which of the two factors in equation (252) must be set equal to zero.

In view of equation (266) we can combine equations (263) and (264) to give

$$\gamma_1 = \tfrac{3}{32}[(c_1 + c_2)(\alpha_1 + \beta_1) + (\alpha_2 - \beta_2)][X(\mu_0) + Y(\mu_0)] . \tag{267}$$

Next, from equations (254) and (261) we find that

$$\gamma_2 = \tfrac{3}{16} X(\mu_0)(c_1\alpha_2 + c_2\beta_2 + 3\alpha_1) + \tfrac{3}{16} Y(\mu_0)(c_1\beta_2 + c_2\alpha_2 - 3\beta_1) . \tag{268}$$

And, finally, from equations (255) and (262) we obtain

$$\gamma_1\tau_1 + \gamma_2 = -\tfrac{3}{16} X(\mu_0)(c_1\beta_2 + c_2\alpha_2 - 3\beta_1) - \tfrac{3}{16} Y(\mu_0)(c_1\alpha_2 + c_2\beta_2 + 3\alpha_1) . \tag{269}$$

Now, substituting for γ_1 and γ_2 according to equations (267) and (268) in equation (269), we find

$$[(\alpha_1 + \beta_1)(c_1 + c_2) + (\alpha_2 - \beta_2)]\tau_1 = -2[(\alpha_2 + \beta_2)(c_1 + c_2) + 3(\alpha_1 - \beta_1)] ; \tag{270}$$

or, solving for $(c_1 + c_2)$, we have

$$c_1 + c_2 = -\frac{(\alpha_2 - \beta_2)\tau_1 + 6(\alpha_1 - \beta_1)}{(\alpha_1 + \beta_1)\tau_1 + 2(\alpha_2 + \beta_2)} . \tag{271}$$

Since we have already shown that (cf. eq. [266])

$$c_1 - c_2 = -\frac{\alpha_2 + \beta_2}{\alpha_1 - \beta_1} , \tag{272}$$

the solution to the problem is completed.

IV. SCATTERING IN ACCORDANCE WITH THE PHASE FUNCTION $\lambda(1 + x \cos \Theta)$

15. *The equations of the problem.*—In the problem of diffuse reflection and transmission according to the phase function $\lambda(1 + x \cos \Theta)(\lambda < 1, 1 \geqslant x \geqslant -1)$ we can

express the reflected and the transmitted intensities in the following forms (cf. Paper XIV, eqs. [196] and [199]):

$$I(0; \mu, \varphi; \mu_0, \varphi_0) = \frac{\lambda}{4\mu} F [S^{(0)}(\mu, \mu_0) + x(1-\mu^2)^{\frac{1}{2}}(1-\mu_0^2)^{\frac{1}{2}} \times S^{(1)}(\mu, \mu_0)\cos(\varphi - \varphi_0)] \tag{273}$$

and

$$I(\tau_1; -\mu, \varphi; \mu_0, \varphi_0) = \frac{\lambda}{4\mu} F [T^{(0)}(\mu, \mu_0) + x(1-\mu^2)^{\frac{1}{2}}(1-\mu_0^2)^{\frac{1}{2}} \times T^{(1)}(\mu, \mu_0)\cos(\varphi - \varphi_0)]. \tag{274}$$

The system of equations governing $S^{(1)}$ and $T^{(1)}$ are directly reducible to the standard forms considered in Section I. And the terms in the emergent intensities proportional to $\cos(\varphi - \varphi_0)$ are of exactly the same forms as those given in Paper XXI, equations (278) and (279); only the functions $X^{(1)}$ and $Y^{(1)}$ must now be redefined in terms of the functional equations which they satisfy.

Turning to the "zero-order" functions $S^{(0)}(\mu, \mu_0)$ and $T^{(0)}(\mu, \mu_0)$, we find that these functions must be expressible in the forms (cf. Paper XIV, eqs. [205]–[209])

$$\left(\frac{1}{\mu_0} + \frac{1}{\mu}\right) S^{(0)}(\mu, \mu_0) = \psi(\mu)\psi(\mu_0) - \chi(\mu)\chi(\mu_0) - x[\phi(\mu)\phi(\mu_0) - \zeta(\mu)\zeta(\mu_0)] \tag{275}$$

and

$$\left(\frac{1}{\mu_0} - \frac{1}{\mu}\right) T^{(0)}(\mu, \mu_0) = \chi(\mu)\psi(\mu_0) - \psi(\mu)\chi(\mu_0) + x[\zeta(\mu)\phi(\mu_0) - \phi(\mu)\zeta(\mu_0)], \tag{276}$$

where ψ, ϕ, χ, and ζ are defined in terms of $S^{(0)}$ and $T^{(0)}$ in the following manner:

$$\psi(\mu) = 1 + \tfrac{1}{2}\lambda \int_0^1 S^{(0)}(\mu, \mu') \frac{d\mu'}{\mu'}, \tag{277}$$

$$\phi(\mu) = \mu - \tfrac{1}{2}\lambda \int_0^1 S^{(0)}(\mu, \mu')\, d\mu', \tag{278}$$

$$\chi(\mu) = e^{-\tau_1/\mu} + \tfrac{1}{2}\lambda \int_0^1 T^{(0)}(\mu, \mu') \frac{d\mu'}{\mu'}, \tag{279}$$

and

$$\zeta(\mu) = \mu e^{-\tau_1/\mu} + \tfrac{1}{2}\lambda \int_0^1 T^{(0)}(\mu, \mu')\, d\mu'. \tag{280}$$

Further, we must also have

$$\frac{\partial S^{(0)}}{\partial \tau_1} = \chi(\mu)\chi(\mu_0) - x\zeta(\mu)\zeta(\mu_0) \tag{281}$$

and

$$\left(\frac{1}{\mu_0} - \frac{1}{\mu}\right) \frac{\partial T^{(0)}}{\partial \tau_1} = \frac{1}{\mu_0}[\psi(\mu)\chi(\mu_0) + x\phi(\mu)\zeta(\mu_0)] - \frac{1}{\mu}[\chi(\mu)\psi(\mu_0) + x\zeta(\mu)\phi(\mu_0)]. \tag{282}$$

Substituting for $S^{(0)}$ and $T^{(0)}$ according to equations (275) and (276) in equations (277)–(280), we obtain the following system of functional equations of fourth order:

$$\psi(\mu) = 1 + \tfrac{1}{2}\lambda\mu\int_0^1 \frac{d\mu'}{\mu+\mu'}[\psi(\mu)\psi(\mu') - \chi(\mu)\chi(\mu')] - \tfrac{1}{2}x\lambda\mu\int_0^1 \frac{d\mu'}{\mu+\mu'}[\phi(\mu)\phi(\mu') - \zeta(\mu)\zeta(\mu')], \tag{283}$$

$$\phi(\mu) = \mu - \tfrac{1}{2}\lambda\mu\int_0^1 \frac{\mu'd\mu'}{\mu+\mu'}[\psi(\mu)\psi(\mu') - \chi(\mu)\chi(\mu')] + \tfrac{1}{2}x\lambda\mu\int_0^1 \frac{\mu'd\mu'}{\mu+\mu'}[\phi(\mu)\phi(\mu') - \zeta(\mu)\zeta(\mu')], \tag{284}$$

$$\chi(\mu) = e^{-\tau_1/\mu} + \tfrac{1}{2}\lambda\mu\int_0^1 \frac{d\mu'}{\mu-\mu'}[\chi(\mu)\psi(\mu') - \psi(\mu)\chi(\mu')] + \tfrac{1}{2}x\lambda\mu\int_0^1 \frac{d\mu'}{\mu-\mu'}[\zeta(\mu)\phi(\mu') - \phi(\mu)\zeta(\mu')], \tag{285}$$

and

$$\zeta(\mu) = \mu e^{-\tau_1/\mu} + \tfrac{1}{2}\lambda\mu\int_0^1 \frac{\mu'd\mu'}{\mu-\mu'}[\chi(\mu)\psi(\mu') - \psi(\mu)\chi(\mu')] + \tfrac{1}{2}x\lambda\mu\int_0^1 \frac{\mu'd\mu'}{\mu-\mu'}[\zeta(\mu)\phi(\mu') - \phi(\mu)\zeta(\mu')]. \tag{286}$$

16. *The form of the solution.*—The solutions for the reflected and the transmitted intensities in a general finite approximation have been found in Paper XXI (eqs. [276] and [277]). Applying to these solutions the correspondence enunciated in theorem 9, we are led to assume for $S^{(0)}(\mu, \mu_0)$ and $T^{(0)}(\mu, \mu_0)$ the following forms:

$$S^{(0)}(\mu,\mu') = \{X(\mu)X(\mu')[1 - x(1-\lambda)c_1(\mu+\mu') - x(1-\lambda)\mu\mu'] - Y(\mu)Y(\mu')[1 + x(1-\lambda)c_1(\mu+\mu') - x(1-\lambda)\mu\mu'] - x(1-\lambda)c_2(\mu+\mu')[X(\mu)Y(\mu') + Y(\mu)X(\mu')]\}\frac{\mu\mu'}{\mu+\mu'} \tag{287}$$

and

$$T^{(0)}(\mu,\mu') = \{Y(\mu)X(\mu')[1 + x(1-\lambda)c_1(\mu-\mu') + x(1-\lambda)\mu\mu'] - X(\mu)Y(\mu')[1 - x(1-\lambda)c_1(\mu-\mu') + x(1-\lambda)\mu\mu'] + x(1-\lambda)c_2(\mu-\mu')[X(\mu)X(\mu') + Y(\mu)Y(\mu')]\}\frac{\mu\mu'}{\mu-\mu'}, \tag{288}$$

where c_1 and c_2 are certain constants unspecified for the present and $X(\mu)$ and $Y(\mu)$ are solutions of the equations

$$X(\mu) = 1 + \tfrac{1}{2}\lambda\mu\int_0^1 \frac{1 + x(1-\lambda)\mu'^2}{\mu+\mu'}[X(\mu)X(\mu') - Y(\mu)Y(\mu')]d\mu' \tag{289}$$

and

$$Y(\mu) = e^{-\tau_1/\mu} + \tfrac{1}{2}\lambda\mu\int_0^1 \frac{1 + x(1-\lambda)\mu'^2}{\mu-\mu'}[Y(\mu)X(\mu') - X(\mu)Y(\mu')]d\mu'. \tag{290}$$

17. *Verification of the solution and the evaluation of the constants in the solution in terms of the moments of* $\mathrm{X}(\mu)$ *and* $\mathrm{Y}(\mu)$.—The verification that the solutions for $S^{(0)}(\mu, \mu')$

and $T^{(0)}(\mu, \mu')$ have the forms assumed in § 16, will consist in first evaluating ψ, ϕ, χ, and ζ according to equations (277)–(280); then requiring that, when the resulting expressions for ψ, ϕ, χ, and ζ are substituted back into equations (275) and (276), we shall recover the form of the solutions assumed; and, finally, showing that the various requirements can be met. In the present case it will appear that the procedure outlined makes the solution determinate.

The evaluation of ψ, ϕ, χ, and ζ according to equations (277)–(280) for $S^{(0)}(\mu, \mu')$ and $T^{(0)}(\mu, \mu')$ given by equations (287) and (288) is straightforward if proper use is made of the integral properties of the functions $X(\mu)$ and $Y(\mu)$. Since these functions are defined in terms of the characteristic function

$$\Psi(\mu) = \tfrac{1}{2}\lambda\,[1 + x\,(1-\lambda)\,\mu^2]\,, \tag{291}$$

we have (cf. theorem 4, eqs. [44]–[46])

$$a_0 = 1 + \tfrac{1}{4}\lambda\,[a_0^2 - \beta_0^2 + x\,(1-\lambda)\,(a_1^2 - \beta_1^2)\,]\,, \tag{292}$$

$$[1 + x\,(1-\lambda)\,\mu^2] \int_0^1 \frac{X(\mu)\,X(\mu') - Y(\mu)\,Y(\mu')}{\mu + \mu'}\,d\mu' = \frac{X(\mu) - 1}{\tfrac{1}{2}\lambda\mu} - x\,(1-\lambda)\,[(a_1 - \mu a_0)\,X(\mu) - (\beta_1 - \mu\beta_0)\,Y(\mu)]\,, \tag{293}$$

and

$$[1 + x\,(1-\lambda)\,\mu^2] \int_0^1 \frac{Y(\mu)\,X(\mu') - X(\mu)\,Y(\mu')}{\mu - \mu'}\,d\mu' = \frac{Y(\mu) - e^{-\tau_1/\mu}}{\tfrac{1}{2}\lambda\mu} - x\,(1-\lambda)\,[(\beta_1 + \mu\beta_0)\,X(\mu) - (a_1 + \mu a_0)\,Y(\mu)]\,. \tag{294}$$

Evaluating ψ, ϕ, χ, and ζ in the manner indicated, we find

$$\psi(\mu) = (1 - q_0\mu)\,X(\mu) - p_0\mu\,Y(\mu)\,, \tag{295}$$

$$\chi(\mu) = (1 + q_0\mu)\,Y(\mu) + p_0\mu\,X(\mu)\,, \tag{296}$$

$$\phi(\mu) = \mu\,[q_1 X(\mu) + p_1 Y(\mu)\,]\,, \tag{297}$$

and

$$\zeta(\mu) = \mu\,[p_1 X(\mu) + q_1 Y(\mu)\,]\,, \tag{298}$$

where

$$q_0 = \tfrac{1}{2}x\lambda\,(1-\lambda)\,(c_1 a_0 + c_2\beta_0 + a_1)\,, \tag{299}$$

$$p_0 = \tfrac{1}{2}x\lambda\,(1-\lambda)\,(c_1\beta_0 + c_2 a_0 - \beta_1)\,, \tag{300}$$

$$q_1 = 1 + \tfrac{1}{2}\lambda\,[x\,(1-\lambda)\,(c_1 a_1 + c_2\beta_1) - a_0]\,, \tag{301}$$

and

$$p_1 = \tfrac{1}{2}\lambda\,[x\,(1-\lambda)\,(c_1\beta_1 + c_2 a_1) + \beta_0]\,. \tag{302}$$

Using the expressions (295)–(298) for ψ, χ, ϕ, and ζ in equations (275) and (276) for $S^{(0)}$ and $T^{(0)}$, we obtain

$$\begin{aligned}\left(\frac{1}{\mu'} + \frac{1}{\mu}\right) S^{(0)}(\mu, \mu') &= X(\mu)\,X(\mu')\,[1 - q_0(\mu + \mu') + \{q_0^2 - p_0^2 - x\,(q_1^2 - p_1^2)\}\,\mu\mu'] \\ &- Y(\mu)\,Y(\mu')\,[1 + q_0(\mu + \mu') + \{q_0^2 - p_0^2 - x\,(q_1^2 - p_1^2)\}\,\mu\mu'] \\ &- p_0(\mu + \mu')\,[X(\mu)\,Y(\mu') + Y(\mu)\,X(\mu')]\end{aligned} \tag{303}$$

and

$$\left(\frac{1}{\mu'}-\frac{1}{\mu}\right)T^{(0)}(\mu,\mu')$$
$$= Y(\mu)\,X(\mu')\,[1+q_0(\mu-\mu')-\{q_0^2-p_0^2-x(q_1^2-p_1^2)\}\mu\mu']$$
$$-X(\mu)\,Y(\mu')\,[1-q_0(\mu-\mu')-\{q_0^2-p_0^2-x(q_1^2-p_1^2)\}\mu\mu'] \tag{304}$$
$$+p_0(\mu-\mu')\,[X(\mu)\,X(\mu')+Y(\mu)\,Y(\mu')]\,.$$

Now, comparing equations (303) and (304) and (287) and (288), we observe that we must have

$$q_0 = x(1-\lambda)\,c_1 \qquad \text{and} \qquad p_0 = x(1-\lambda)\,c_2\,; \tag{305}$$

further, we must also require that

$$q_0^2-p_0^2-x(q_1^2-p_1^2) = -x(1-\lambda)\,. \tag{306}$$

According to equations (299), (300), and (305), we have

$$c_1 = \tfrac{1}{2}\lambda(c_1\alpha_0+c_2\beta_0+\alpha_1) \tag{307}$$

and

$$c_2 = \tfrac{1}{2}\lambda(c_1\beta_0+c_2\alpha_0-\beta_1)\,. \tag{308}$$

Solving these equations for c_1 and c_2, we obtain

$$c_1 = \frac{q_0}{x(1-\lambda)} = \lambda\,\frac{(2-\lambda\alpha_0)\,\alpha_1-\lambda\beta_0\beta_1}{(2-\lambda\alpha_0)^2-\lambda^2\beta_0^2} \tag{309}$$

and

$$c_2 = \frac{p_0}{x(1-\lambda)} = \lambda\,\frac{-(2-\lambda\alpha_0)\,\beta_1+\lambda\beta_0\alpha_1}{(2-\lambda\alpha_0)^2-\lambda^2\beta_0^2}\,. \tag{310}$$

Inserting for c_1 and c_2 from equations (309) and (310) in equation (301) for q_1, we find

$$q_1 = \tfrac{1}{2}(2-\lambda\alpha_0)\left[1+\lambda\,\frac{x\lambda(1-\lambda)(\alpha_1^2-\beta_1^2)}{(2-\lambda\alpha_0)^2-\lambda^2\beta_0^2}\right]. \tag{311}$$

Using the relation (cf. eq. [292])

$$4(\alpha_0-1)-\lambda(\alpha_0^2-\beta_0^2) = x\lambda(1-\lambda)(\alpha_1^2-\beta_1^2)\,, \tag{312}$$

we can now reduce equation (311) to the form

$$q_1 = \frac{2(1-\lambda)(2-\lambda\alpha_0)}{(2-\lambda\alpha_0)^2-\lambda^2\beta_0^2}\,. \tag{313}$$

Similarly,

$$p_1 = \frac{2(1-\lambda)\lambda\beta_0}{(2-\lambda\alpha_0)^2-\lambda^2\beta_0^2}\,. \tag{314}$$

It remains to verify that equation (306) is valid for q_0, p_0, q_1, and p_1 given by equations (309), (310), (313), and (314). To show that this is the case, we first observe that, according to equations (309) and (310),

$$q_0^2-p_0^2 = x^2\lambda^2(1-\lambda)^2\,\frac{\alpha_1^2-\beta_1^2}{(2-\lambda\alpha_0)^2-\lambda^2\beta_0^2}\,, \tag{315}$$

while, according to equations (313) and (314),

$$q_1^2 - p_1^2 = \frac{4\,(1-\lambda)^{\,2}}{(2-\lambda a_0)^{\,2} - \lambda^2\beta_0^2}. \tag{316}$$

Hence

$$q_0^2 - p_0^2 - x\,(q_1^2 - p_1^2) = \frac{x\,(1-\lambda)}{(2-\lambda a_0)^{\,2} - \lambda^2\beta_0^2}\,[\,x\lambda^2\,(1-\lambda)\,(a_1^2 - \beta_1^2) - 4\,(1-\lambda)\,]\,; \tag{317}$$

or, using equation (312), we have

$$\begin{aligned} q_0^2 - p_0^2 - x\,(q_1^2 - p_1^2) &= \frac{x\,(1-\lambda)}{(2-\lambda a_0)^{\,2} - \lambda^2\beta_0^2}\,[\,4\lambda\,(a_0 - 1) - \lambda^2\,(a_0^2 - \beta_0^2) - 4\,(1-\lambda)\,] \\ &= \frac{x\,(1-\lambda)}{(2-\lambda a_0)^{\,2} - \lambda^2\beta_0^2}\,[\,\lambda^2\beta_0^2 - 4 + 4\lambda a_0 - \lambda^2 a_0^2\,] \\ &= -\,x\,(1-\lambda)\,. \end{aligned} \tag{318}$$

The constants q_0, p_0, q_1, and p_1, as defined by equations (309), (310), (313), and (314), are therefore related, as required.

This completes the verification.

V. RAYLEIGH SCATTERING

18. *The equations of the problem.*—When proper allowance is made for the polarization characteristics of the radiation field, the laws of diffuse reflection and transmission are best formulated in terms of a scattering matrix $\boldsymbol{S}$ and a transmission matrix $\boldsymbol{T}$ (cf. Paper XXI, eqs. [533] and [534]). And, as we have already indicated in Paper XVII (the last paragraph of § 5 on p. 455), the equations governing $\boldsymbol{S}$ and $\boldsymbol{T}$ are of the same forms as equations (85)–(88) of Paper XVII, provided that these equations are interpreted as matrix equations in which a *phase matrix* plays the same role as the *phase function* in the more conventional problems. For the particular case of Rayleigh scattering the phase matrix is explicitly known (cf. Paper XIV, eq. [10]), and the required equations for the field quantities I_l, I_r, U, and V[14] can be written down. However, in view of the form of the solutions for U, V, and the azimuth dependent terms in I_l and I_r found in Paper XXI (eqs. [290]–[303] and [548]–[551]) it is evident that the exact solutions for these terms in the scattering and the transmission matrices must be of identically the same forms: only the various X- and Y-functions occurring in the solutions must be redefined in terms of the exact functional equations which they satisfy. Consequently, it is sufficient to confine our detailed considerations to the azimuth independent terms in I_l and I_r which we shall now regard as the components of a *two-dimensional* vector

$$\boldsymbol{I} = (I_l,\, I_r)\,. \tag{319}[15]$$

Let

$$\boldsymbol{F} = (F_l,\, F_r)\,, \tag{320}$$

[14] For a definition of these quantities see Paper XXI, § 15, and the references there given.

[15] Strictly, superscripts (0) should be attached to these and similar azimuth independent quantities describing the diffuse-radiation field. We have suppressed them for the sake of convenience. They should, however, be restored when writing down the complete solution (cf. Paper XXI, § 19, eqs. [540]–[546]).

where πF_l and πF_r are the incident fluxes in the intensities in the meridian plane and at right angles to it,[16] respectively. The reflected and the transmitted intensities can then be expressed in terms of a scattering and a transmission matrix (with two rows and columns) in the forms

$$\boldsymbol{I}(0, \mu) = \frac{3}{16\mu}\boldsymbol{S}(\mu, \mu_0)\boldsymbol{F} \quad \text{and} \quad \boldsymbol{I}(\tau_1, -\mu) = \frac{3}{16\mu}\boldsymbol{T}(\mu, \mu_0)\boldsymbol{F}. \tag{321}$$[15]

The equations governing $\boldsymbol{S}$ and $\boldsymbol{T}$ can be written down in analogy with equations (85)–(88) of Paper XVII by replacing $p(\mu, \varphi; \mu', \varphi')$ by the matrix

$$\tfrac{3}{4}\boldsymbol{J}(\mu, \mu') = \tfrac{3}{4}\begin{pmatrix} 2(1-\mu^2)(1-\mu'^2) + \mu^2\mu'^2 & \mu^2 \\ \mu'^2 & 1 \end{pmatrix}. \tag{322}$$

The resulting equations can be written most compactly by adopting the following notation:

Let the "product" $[\boldsymbol{A}, \boldsymbol{B}]_{\mu,\mu'}$ of two matrices, $\boldsymbol{A}(\mu, \mu')$ and $\boldsymbol{B}(\mu, \mu')$, be defined by the formula

$$[\boldsymbol{A}, \boldsymbol{B}]_{\mu,\mu'} = \frac{3}{8}\int_0^1 \boldsymbol{A}(\mu, \mu'')\boldsymbol{B}(\mu'', \mu')\frac{d\mu''}{\mu''}, \tag{323}$$

where, under the integral sign, the ordinary matrix product is intended. With this product notation, the equations satisfied by $\boldsymbol{S}$ and $\boldsymbol{T}$ take the forms

$$\left(\frac{1}{\mu_0}+\frac{1}{\mu}\right)\boldsymbol{S} + \frac{\partial \boldsymbol{S}}{\partial \tau_1} = \boldsymbol{J} + [\boldsymbol{J}, \boldsymbol{S}] + [\boldsymbol{S}, \boldsymbol{J}] + [[\boldsymbol{S}, \boldsymbol{J}], \boldsymbol{S}], \tag{324}$$

$$\frac{\partial \boldsymbol{S}}{\partial \tau_1} = \exp\left\{-\tau_1\left(\frac{1}{\mu}+\frac{1}{\mu_0}\right)\right\}\boldsymbol{J} + e^{-\tau_1/\mu}[\boldsymbol{J}, \boldsymbol{T}] + e^{-\tau_1/\mu_0}[\boldsymbol{T}, \boldsymbol{J}] + [[\boldsymbol{T}, \boldsymbol{J}], \boldsymbol{T}], \tag{325}$$

$$\frac{1}{\mu_0}\boldsymbol{T} + \frac{\partial \boldsymbol{T}}{\partial \tau_1} = e^{-\tau_1/\mu}\boldsymbol{J} + e^{-\tau_1/\mu}[\boldsymbol{J}, \boldsymbol{S}] + [\boldsymbol{T}, \boldsymbol{J}] + [[\boldsymbol{T}, \boldsymbol{J}], \boldsymbol{S}], \tag{326}$$

and

$$\frac{1}{\mu}\boldsymbol{T} + \frac{\partial \boldsymbol{T}}{\partial \tau_1} = e^{-\tau_1/\mu_0}\boldsymbol{J} + [\boldsymbol{J}, \boldsymbol{T}] + e^{-\tau_1/\mu_0}[\boldsymbol{S}, \boldsymbol{J}] + [[\boldsymbol{S}, \boldsymbol{J}], \boldsymbol{T}]. \tag{327}$$

A discussion of equations (324)–(327) shows that $\boldsymbol{S}$ and $\boldsymbol{T}$ must be expressible in the forms

$$\left(\frac{1}{\mu'}+\frac{1}{\mu}\right)\boldsymbol{S}(\mu, \mu') = \begin{pmatrix} \psi(\mu) & 2^{\frac{1}{2}}\phi(\mu) \\ \chi(\mu) & 2^{\frac{1}{2}}\zeta(\mu) \end{pmatrix}\begin{pmatrix} \psi(\mu') & \chi(\mu') \\ 2^{\frac{1}{2}}\phi(\mu') & 2^{\frac{1}{2}}\zeta(\mu') \end{pmatrix} - \begin{pmatrix} \xi(\mu) & 2^{\frac{1}{2}}\eta(\mu) \\ \sigma(\mu) & 2^{\frac{1}{2}}\theta(\mu) \end{pmatrix}\begin{pmatrix} \xi(\mu') & \sigma(\mu') \\ 2^{\frac{1}{2}}\eta(\mu') & 2^{\frac{1}{2}}\theta(\mu') \end{pmatrix} \tag{328}$$

and

$$\left(\frac{1}{\mu'}-\frac{1}{\mu}\right)\boldsymbol{T}(\mu, \mu') = \begin{pmatrix} \xi(\mu) & 2^{\frac{1}{2}}\eta(\mu) \\ \sigma(\mu) & 2^{\frac{1}{2}}\theta(\mu) \end{pmatrix}\begin{pmatrix} \psi(\mu') & \chi(\mu') \\ 2^{\frac{1}{2}}\phi(\mu') & 2^{\frac{1}{2}}\zeta(\mu') \end{pmatrix} - \begin{pmatrix} \psi(\mu) & 2^{\frac{1}{2}}\phi(\mu) \\ \chi(\mu) & 2^{\frac{1}{2}}\zeta(\mu) \end{pmatrix}\begin{pmatrix} \xi(\mu') & \sigma(\mu') \\ 2^{\frac{1}{2}}\eta(\mu') & 2^{\frac{1}{2}}\theta(\mu') \end{pmatrix}, \tag{329}$$

[16] These directions are referred in the transverse plane containing the electric and the magnetic vectors.

where

$$\psi(\mu) = \mu^2 + \frac{3}{8}\int_0^1 \frac{d\mu'}{\mu'}\left[\mu'^2 S_{11}(\mu, \mu') + S_{12}(\mu, \mu')\right], \tag{330}$$

$$\phi(\mu) = 1 - \mu^2 + \frac{3}{8}\int_0^1 \frac{d\mu'}{\mu'}(1 - \mu'^2) S_{11}(\mu, \mu'), \tag{331}$$

$$\chi(\mu) = 1 + \frac{3}{8}\int_0^1 \frac{d\mu'}{\mu'}\left[\mu'^2 S_{21}(\mu, \mu') + S_{22}(\mu, \mu')\right], \tag{332}$$

$$\zeta(\mu) = \frac{3}{8}\int_0^1 \frac{d\mu'}{\mu'}(1 - \mu'^2) S_{21}(\mu, \mu'), \tag{333}$$

$$\xi(\mu) = \mu^2 e^{-\tau_1/\mu} + \frac{3}{8}\int_0^1 \frac{d\mu'}{\mu'}\left[\mu'^2 T_{11}(\mu, \mu') + T_{12}(\mu, \mu')\right], \tag{334}$$

$$\eta(\mu) = (1 - \mu^2)\, e^{-\tau_1/\mu} + \frac{3}{8}\int_0^1 \frac{d\mu'}{\mu'}(1 - \mu'^2) T_{11}(\mu, \mu'). \tag{335}$$

$$\sigma(\mu) = e^{-\tau_1/\mu} + \frac{3}{8}\int_0^1 \frac{d\mu'}{\mu'}\left[\mu'^2 T_{21}(\mu, \mu') + T_{22}(\mu, \mu')\right], \tag{336}$$

and

$$\theta(\mu) = \frac{3}{8}\int_0^1 \frac{d\mu'}{\mu'}(1 - \mu'^2) T_{21}(\mu, \mu'). \tag{337}$$

Substituting for S_{11}, etc., according to equations (328) and (329) in equations (330)–(337), we shall obtain a simultaneous system of functional equations of order *eight*. It is, however, not necessary to write down these equations explicitly.

19. *The form of the solution.*—The solutions for $\boldsymbol{S}$ and $\boldsymbol{T}$ in a general finite approximation have already been found in Paper XXI (eqs. [539]–[546]). Applying to these solutions the correspondence enunciated in theorem 9, we are led to assume the following forms for $\boldsymbol{S}$ and $\boldsymbol{T}$:

$$\begin{aligned}\left(\frac{1}{\mu'} + \frac{1}{\mu}\right) S_{11}(\mu, \mu') = 2\{ & X_l(\mu)\, X_l(\mu')\left[1 + \nu_4(\mu + \mu') + \mu\mu'\right] \\ & - Y_l(\mu)\, Y_l(\mu')\left[1 - \nu_4(\mu + \mu') + \mu\mu'\right] \\ & - \nu_3(\mu + \mu')\left[X_l(\mu)\, Y_l(\mu') + Y_l(\mu)\, X_l(\mu')\right]\},\end{aligned} \tag{338}$$

$$\begin{aligned}\left(\frac{1}{\mu'} + \frac{1}{\mu}\right) S_{12}(\mu, \mu') = (\mu + \mu')\{ & \nu_1\left[Y_l(\mu)\, X_r(\mu') + X_l(\mu)\, Y_r(\mu')\right] \\ & - \nu_2\left[X_l(\mu)\, X_r(\mu') + Y_l(\mu)\, Y_r(\mu')\right] \\ & + Q(\nu_2 - \nu_1)\,\mu'\left[X_l(\mu) + Y_l(\mu)\right]\left[X_r(\mu') - Y_r(\mu')\right]\},\end{aligned} \tag{339}$$

$$\begin{aligned}\left(\frac{1}{\mu'} + \frac{1}{\mu}\right) S_{21}(\mu, \mu') = (\mu + \mu')\{ & \nu_1\left[X_r(\mu)\, Y_l(\mu') + Y_r(\mu)\, X_l(\mu')\right] \\ & - \nu_2\left[X_r(\mu)\, X_l(\mu') + Y_r(\mu)\, Y_l(\mu')\right] \\ & + Q(\nu_2 - \nu_1)\,\mu\left[X_r(\mu) - Y_r(\mu)\right]\left[X_l(\mu') + Y_l(\mu')\right]\},\end{aligned} \tag{340}$$

$$\left(\frac{1}{\mu'}+\frac{1}{\mu}\right)S_{22}(\mu,\mu') = X_r(\mu)\,X_r(\mu')\,[1-u_4(\mu+\mu')+u_5\mu\mu']$$
$$-Y_r(\mu)\,Y_r(\mu')\,[1+u_4(\mu+\mu')+u_5\mu\mu']$$
$$+u_3(\mu+\mu')\,[X_r(\mu)\,Y_r(\mu')+Y_r(\mu)\,X_r(\mu')]$$
$$-Qu_5\mu\mu'(\mu+\mu')\,[X_r(\mu)-Y_r(\mu)]\,[X_r(\mu')-Y_r(\mu')]$$
$$+Q(u_4-u_3)\,\{\mu^2[X_r(\mu)-Y_r(\mu)]\,[X_r(\mu')+Y_r(\mu')]$$
$$+\mu'^2[X_r(\mu)+Y_r(\mu)]\,[X_r(\mu')-Y_r(\mu')]\}, \tag{341}$$

$$\left(\frac{1}{\mu'}-\frac{1}{\mu}\right)T_{11}(\mu,\mu') = 2\{Y_l(\mu)\,X_l(\mu')\,[1-\nu_4(\mu-\mu')-\mu\mu']$$
$$-X_l(\mu)\,Y_l(\mu')\,[1+\nu_4(\mu-\mu')-\mu\mu'] \tag{342}$$
$$+\nu_3(\mu-\mu')\,[X_l(\mu)\,X_l(\mu')+Y_l(\mu)\,Y_l(\mu')]\},$$

$$\left(\frac{1}{\mu'}-\frac{1}{\mu}\right)T_{12}(\mu,\mu') = (\mu-\mu')\,\{\nu_2[X_l(\mu)\,Y_r(\mu')+Y_l(\mu)\,X_r(\mu')]$$
$$-\nu_1[X_l(\mu)\,X_r(\mu')+Y_l(\mu)\,Y_r(\mu')] \tag{343}$$
$$-Q(\nu_2-\nu_1)\,\mu'\,[X_l(\mu)+Y_l(\mu)]\,[X_r(\mu')-Y_r(\mu')]\},$$

$$\left(\frac{1}{\mu'}-\frac{1}{\mu}\right)T_{21}(\mu,\mu') = (\mu-\mu')\,\{\nu_2[X_r(\mu)\,Y_l(\mu')+Y_r(\mu)\,X_l(\mu')]$$
$$-\nu_1[X_r(\mu)\,X_l(\mu')+Y_r(\mu)\,Y_l(\mu')] \tag{344}$$
$$-Q(\nu_2-\nu_1)\,\mu\,[X_r(\mu)-Y_r(\mu)]\,[X_l(\mu')+Y_l(\mu')]\},$$

and

$$\left(\frac{1}{u'}-\frac{1}{\mu}\right)T_{22}(\mu,\mu') = Y_r(\mu)\,X_r(\mu')\,[1+u_4(\mu-\mu')-u_5\mu\mu']$$
$$-X_r(\mu)\,Y_r(\mu')\,[1-u_4(\mu-\mu')-u_5\mu\mu']$$
$$-u_3(\mu-\mu')\,[X_r(\mu)\,X_r(\mu')+Y_r(\mu)\,Y_r(\mu')] \tag{345}$$
$$+Qu_5\mu\mu'(\mu-\mu')\,[X_r(\mu)-Y_r(\mu)]\,[X_r(\mu')-Y_r(\mu')]$$
$$-Q(u_4-u_3)\,\{\mu^2[X_r(\mu)-Y_r(\mu)]\,[X_r(\mu')+Y_r(\mu')]$$
$$-\mu'^2[X_r(\mu)+Y_r(\mu)]\,[X_r(\mu')-Y_r(\mu')]\},$$

where ν_1, ν_2, ν_3, ν_4, u_3, u_4, and Q are certain constants, unspecified for the present;

$$u_5 = 1+2Q(u_4-u_3)\,; \tag{346}$$[17]

$X_r(\mu)$ and $Y_r(\mu)$ are the solutions of the equations

$$X_r(\mu) = 1+\tfrac{3}{8}\mu\int_0^1 \frac{1-\mu'^2}{\mu+\mu'}\,[X_r(\mu)\,X_r(\mu')-Y_r(\mu)\,Y_r(\mu')]\,d\mu' \tag{347}$$

and

$$Y_r(\mu) = e^{-\tau_1/\mu}+\tfrac{3}{8}\mu\int_0^1 \frac{1-\mu'^2}{\mu-\mu'}\,[Y_r(\mu)\,X_r(\mu')-X_r(\mu)\,Y_r(\mu')]\,d\mu'\,; \tag{348}$$

[17] Cf. Paper XXI, eqs. (512)–(514).

and $X_l(\mu)$ and $Y_l(\mu)$ are the *standard solutions* of the equations

$$X_l(\mu) = 1 + \tfrac{3}{4}\mu \int_0^1 \frac{1-\mu'^2}{\mu+\mu'} [X_l(\mu)\, X_l(\mu') - Y_l(\mu)\, Y_l(\mu')]\, d\mu' \tag{349}$$

and

$$Y_l(\mu) = e^{-\tau_1/\mu} + \tfrac{3}{4}\mu \int_0^1 \frac{1-\mu'^2}{\mu-\mu'} [Y_l(\mu)\, X_l(\mu') - X_l(\mu)\, Y_l(\mu')]\, d\mu', \tag{350}$$

having the property

$$\tfrac{3}{4} \int_0^1 (1-\mu^2)\, X_l(\mu)\, d\mu = \tfrac{3}{4}(\alpha_0 - \alpha_2) = 1 \tag{351}$$

and

$$\int_0^1 (1-\mu^2)\, Y_l(\mu)\, d\mu = (\beta_0 - \beta_2) = 0\,. \tag{352}$$

For the purposes of the various evaluations in §§ 20 and 21, it is convenient to have equations (338)–(345) re-written in the following forms:

$$\begin{aligned} S_{11}(\mu, \mu') = 2\mu\mu' \Big\{ & \frac{1-\mu^2}{\mu+\mu'} [X_l(\mu)\, X_l(\mu') - Y_l(\mu)\, Y_l(\mu')] \\ & + X_l(\mu)\, [(\nu_4 + \mu)\, X_l(\mu') - \nu_3 Y_l(\mu')] \\ & + Y_l(\mu)\, [-\nu_3 X_l(\mu') + (\nu_4 - \mu)\, Y_l(\mu')] \Big\}, \end{aligned} \tag{353}$$

$$\begin{aligned} S_{12}(\mu, \mu') = \mu\mu' \{ & \nu_1 [X_l(\mu)\, Y_r(\mu') + Y_l(\mu)\, X_r(\mu')] \\ & - \nu_2 [X_l(\mu)\, X_r(\mu') + Y_l(\mu)\, Y_r(\mu')] \\ & + Q(\nu_2 - \nu_1)\, \mu' [X_l(\mu) + Y_l(\mu)] [X_r(\mu') - Y_r(\mu')] \}, \end{aligned} \tag{354}$$

$$\begin{aligned} S_{21}(\mu, \mu') = \mu\mu' \{ & \nu_1 [X_r(\mu)\, Y_l(\mu') + Y_r(\mu)\, X_l(\mu')] \\ & - \nu_2 [X_r(\mu)\, X_l(\mu') + Y_r(\mu)\, Y_l(\mu')] \\ & + Q(\nu_2 - \nu_1)\, \mu [X_r(\mu) - Y_r(\mu)] [X_l(\mu') + Y_l(\mu')] \} \end{aligned} \tag{355}$$

$$\begin{aligned} S_{22}(\mu, \mu') = \mu\mu' \Big\{ & \frac{1-\mu^2}{\mu+\mu'} [X_r(\mu)\, X_r(\mu') - Y_r(\mu)\, Y_r(\mu')] \\ & + X_r(\mu)\, [(-u_4 + \mu)\, X_r(\mu') + u_3 Y_r(\mu')] \\ & + Y_r(\mu)\, [u_3 X_r(\mu') - (u_4 + \mu)\, Y_r(\mu')] \\ & - Q u_5 \mu\mu' [X_r(\mu) - Y_r(\mu)] [X_r(\mu') - Y_r(\mu')] \\ & + Q(u_4 - u_3)(\mu + \mu') [X_r(\mu)\, X_r(\mu') - Y_r(\mu)\, Y_r(\mu')] \\ & + Q(u_4 - u_3)(\mu - \mu') [X_r(\mu)\, Y_r(\mu') - Y_r(\mu)\, X_r(\mu')] \Big\}, \end{aligned} \tag{356}[18]$$

$$\begin{aligned} T_{11}(\mu, \mu') = 2\mu\mu' \Big\{ & \frac{1-\mu^2}{\mu-\mu'} [Y_l(\mu)\, X_l(\mu') - X_l(\mu)\, Y_l(\mu')] \\ & - X_l(\mu)\, [-\nu_3 X_l(\mu') + (\nu_4 + \mu)\, Y_l(\mu')] \\ & - Y_l(\mu)\, [(\nu_4 - \mu)\, X_l(\mu') - \nu_3 Y_l(\mu')] \Big\}, \end{aligned} \tag{357}$$

[18] The reduction of eqs. (341) and (345) to the forms (356) and (360) requires the use of eq. (346).

$$T_{12}(\mu, \mu') = \mu\mu'\{\nu_2[X_l(\mu)\, Y_r(\mu') + Y_l(\mu)\, X_r(\mu')] - \nu_1[X_l(\mu)\, X_r(\mu') + Y_l(\mu)\, Y_r(\mu')] - Q(\nu_2-\nu_1)\,\mu'[X_l(\mu) + Y_l(\mu)][X_r(\mu') - Y_r(\mu')]\}, \tag{358}$$

$$T_{21}(\mu, \mu') = \mu\mu'\{\nu_2[X_r(\mu)\, Y_l(\mu') + Y_r(\mu)\, X_l(\mu')] - \nu_1[X_r(\mu)\, X_l(\mu') + Y_r(\mu)\, Y_l(\mu')] - Q(\nu_2-\nu_1)\,\mu[X_r(\mu) - Y_r(\mu)][X_l(\mu') + Y_l(\mu')]\}, \tag{359}$$

and

$$\begin{aligned} T_{22}(\mu, \mu') = \mu\mu' \Big\{ & \frac{1-\mu^2}{\mu-\mu'}[Y_r(\mu)\, X_r(\mu') - X_r(\mu)\, Y_r(\mu')] \\ & - X_r(\mu)[u_3 X_r(\mu') + (-u_4+\mu)\, Y_r(\mu')] \\ & - Y_r(\mu)[-(u_4+\mu)\, X_r(\mu') + u_3 Y_r(\mu')] \\ & + Q u_5 \mu\mu'[X_r(\mu) - Y_r(\mu)][X_r(\mu') - Y_r(\mu')] \\ & - Q(u_4-u_3)(\mu-\mu')[X_r(\mu)\, Y_r(\mu') - Y_r(\mu)\, X_r(\mu')] \\ & - Q(u_4-u_3)(\mu+\mu')[X_r(\mu)\, X_r(\mu') - Y_r(\mu)\, Y_r(\mu')]\Big\}. \end{aligned} \tag{360}$$[18]

20. *The verification of the solution and the expression of the constants* ν_1, ν_2, ν_3, ν_4, u_3, *and* u_4 *in terms of the moments of* $X_l(\mu)$, $Y_l(\mu)$, $X_r(\mu)$, *and* $Y_r(\mu)$ *and a single arbitrary constant* Q.—We shall first evaluate ψ, ϕ, χ, ζ, ξ, η, σ, and θ according to equations (330)–(337) for $\boldsymbol{S}$ and $\boldsymbol{T}$ given by equations (353)–(360); then require that, when the resulting expressions for ψ, ϕ, etc., are substituted back into equations (328) and (329), we shall recover the form of the solutions assumed. As we should expect, this procedure will lead to several conditions[19] among the constants ν_1, ν_2, ν_3, ν_4, u_3, u_4, and Q introduced into the solution. We shall show that all these conditions can be met and that six of the constants (ν_1, ν_2, ν_3, ν_4, u_3, and u_4) can be expressed in terms of Q and the various moments of X_l, Y_l, X_r, and Y_r. The constant Q itself will be found to be left arbitrary. This is a further example of the one-parametric nature of the solutions of the functional equations incorporating the invariances of the problem in conservative cases. In § 21 we shall then finally show how this last arbitrariness in the solutions can be removed by appealing to the K-integrals of the problem.

The evaluation of ψ, ϕ, etc., according to equations (330)–(337) for $\boldsymbol{S}$ and $\boldsymbol{T}$ given by equations (353)–(360) is straightforward if proper use is made of the various integral properties of the functions X_l, Y_l, X_r, and Y_r. In addition to equations (351) and (352), use must also be made of the following relations (cf. theorem 4, eqs. [44]–[46]):

$$\alpha_0 = 1 + \tfrac{3}{8}[(\alpha_0^2 - \beta_0^2) - (\alpha_1^2 - \beta_1^2)], \tag{361}$$

$$(1-\mu^2)\int_0^1 \frac{X_l(\mu)\, X_l(\mu') - Y_l(\mu)\, Y_l(\mu')}{\mu+\mu'}\, d\mu' = \frac{X_l(\mu) - 1}{\tfrac{3}{4}\mu} + (\alpha_1 - \mu\alpha_0)\, X_l(\mu) - (\beta_1 - \mu\beta_0)\, Y_l(\mu), \tag{362}$$

[19] Actually, we shall see that there are twelve of them.

$$(1-\mu^2)\int_0^1 \frac{Y_l(\mu)\,X_l(\mu')-X_l(\mu)\,Y_l(\mu')}{\mu-\mu'}\,d\mu' = \frac{Y_l(\mu)-e^{-\tau_1/\mu}}{\frac{3}{4}\mu} + (\beta_1+\mu\beta_0)\,X_l(\mu)-(\alpha_1+\mu\alpha_0)\,Y_l(\mu)\,, \tag{363}$$

$$A_0 = 1+\tfrac{3}{16}\,[(A_0^2-B_0^2)-(A_1^2-B_1^2)]\,, \tag{364}$$

$$(1-\mu^2)\int_0^1 \frac{X_r(\mu)\,X_r(\mu')-Y_r(\mu)\,Y_r(\mu')}{\mu+\mu'}\,d\mu' = \frac{X_r(\mu)-1}{\frac{3}{8}\mu} + (A_1-\mu A_0)\,X_r(\mu)-(B_1-\mu B_0)\,Y_r(\mu)\,, \tag{365}$$

and

$$(1-\mu^2)\int_0^1 \frac{Y_r(\mu)\,X_r(\mu')-X_r(\mu)\,Y_r(\mu')}{\mu-\mu'}\,d\mu' = \frac{Y_r(\mu)-e^{-\tau_1/\mu}}{\frac{3}{8}\mu} + (B_1+\mu B_0)\,X_r(\mu)-(A_1+\mu A_0)\,Y_r(\mu)\,, \tag{366}$$

where (cf. eq. [11])

$$\alpha_n = \int_0^1 X_l(\mu)\,\mu^n d\mu\,, \qquad \beta_n = \int_0^1 Y_l(\mu)\,\mu^n d\mu\,,$$
$$A_n = \int_0^1 X_r(\mu)\,\mu^n d\mu\,, \quad \text{and} \quad B_n = \int_0^1 Y_r(\mu)\,\mu^n d\mu\,. \tag{367}$$

Evaluating ψ, ϕ, etc., in the manner indicated, we find that

$$\psi(\mu) = +\mu\,[q_1 X_l(\mu)+q_2 Y_l(\mu)]\,, \tag{368}$$

$$\xi(\mu) = -\mu\,[q_2 X_l(\mu)+q_1 Y_l(\mu)]\,, \tag{369}$$

$$\phi(\mu) = (1+\nu_4\mu)\,X_l(\mu)-\nu_3\mu\,Y_l(\mu)\,, \tag{370}$$

$$\eta(\mu) = (1-\nu_4\mu)\,Y_l(\mu)+\nu_3\mu X_l(\mu)\,, \tag{371}$$

$$\chi(\mu) = (1+p_1\mu)\,X_r(\mu)+p_2\mu\,Y_r(\mu)-t\mu^2\,[X_r(\mu)-Y_r(\mu)]\,, \tag{372}$$

$$\sigma(\mu) = (1-p_1\mu)\,Y_r(\mu)-p_2\mu X_r(\mu)+t\mu^2\,[X_r(\mu)-Y_r(\mu)]\,, \tag{373}$$

$$\zeta(\mu) = -\tfrac{1}{2}\mu\,[\nu_2 X_r(\mu)-\nu_1 Y_r(\mu)]+\tfrac{1}{2}Q(\nu_2-\nu_1)\,\mu^2\,[X_r(\mu)-Y_r(\mu)]\,, \tag{374}$$

and

$$\theta(\mu) = +\tfrac{1}{2}\mu\,[-\nu_1 X_r(\mu)+\nu_2 Y_r(\mu)]-\tfrac{1}{2}Q(\nu_2-\nu_1)\,\mu^2\,[X_r(\mu)-Y_r(\mu)]\,, \tag{375}$$

where

$$q_1 = \tfrac{3}{4}\,[\alpha_2\nu_4-\beta_0\nu_3+\alpha_1+\tfrac{1}{2}B_0\nu_1-\tfrac{1}{2}A_0\nu_2+\tfrac{1}{2}Q(\nu_2-\nu_1)(A_1-B_1)]\,, \tag{376}$$

$$q_2 = \tfrac{3}{4}\,[\beta_0\nu_4-\alpha_2\nu_3-\beta_1+\tfrac{1}{2}A_0\nu_1-\tfrac{1}{2}B_0\nu_2+\tfrac{1}{2}Q(\nu_2-\nu_1)(A_1-B_1)]\,, \tag{377}$$

$$p_1 = \tfrac{3}{8}\,[+A_1-A_0u_4+B_0u_3+Q(u_4-u_3)(A_1-B_1)+\beta_0\nu_1-\alpha_2\nu_2]\,, \tag{378}$$

$$p_2 = \tfrac{3}{8}\,[-B_1-B_0u_4+A_0u_3+Q(u_4-u_3)(A_1-B_1)+\alpha_2\nu_1-\beta_0\nu_2]\,, \tag{379}$$

and

$$t = \tfrac{3}{8}Q\,[-(\alpha_2+\beta_0)(\nu_2-\nu_1)-(A_0+B_0)(u_4-u_3)+u_5(A_1-B_1)]\,. \tag{380}$$

We now substitute for ψ, ϕ, etc., according to equations (368)–(375) in equations (328) and (329) and compare them with the solutions (353)–(360), which were originally assumed in the evaluation of ψ, ϕ, etc.

Considering, first, T_{11}, we have

$$\left(\frac{1}{\mu'}-\frac{1}{\mu}\right)T_{11}(\mu,\mu') = \xi(\mu)\psi(\mu') - \psi(\mu)\xi(\mu') + 2[\eta(\mu)\phi(\mu') - \phi(\mu)\eta(\mu')]$$

$$= 2\{Y_l(\mu)X_l(\mu')[1-\nu_4(\mu-\mu') - \{\nu_4^2-\nu_3^2+\tfrac{1}{2}(q_1^2-q_2^2)\}\mu\mu'] \quad (381)$$
$$- X_l(\mu)Y_l(\mu')[1+\nu_4(\mu-\mu') - \{\nu_4^2-\nu_3^2+\tfrac{1}{2}(q_1^2-q_2^2)\}\mu\mu']$$
$$+\nu_3(\mu-\mu')[X_l(\mu)X_l(\mu') + Y_l(\mu)Y_l(\mu')]\}.$$

Comparing this with equation (342), we conclude that we must have

$$\nu_4^2-\nu_3^2+\tfrac{1}{2}(q_1^2-q_2^2) = 1\,. \quad (382)$$

The consideration of S_{11} leads to the same condition, (382).

Considering, next, $S_{21}(\mu,\mu')$, we have

$$\left(\frac{1}{\mu'}+\frac{1}{\mu}\right)S_{21}(\mu,\mu') = \chi(\mu)\psi(\mu') - \sigma(\mu)\xi(\mu') + 2[\zeta(\mu)\phi(\mu') - \theta(\mu)\eta(\mu')]$$

$$= X_r(\mu)Y_l(\mu')[+\nu_1\mu+q_2\mu'+\{p_1q_2-p_2q_1+\nu_2\nu_3-\nu_1\nu_4-Q(\nu_2-\nu_1)\}\mu\mu']$$
$$+ Y_r(\mu)X_l(\mu')[+\nu_1\mu+q_2\mu'-\{p_1q_2-p_2q_1+\nu_2\nu_3-\nu_1\nu_4-Q(\nu_2-\nu_1)\}\mu\mu'] \quad (383)$$
$$+ X_r(\mu)X_l(\mu')[-\nu_2\mu+q_1\mu'+\{p_1q_1-p_2q_2+\nu_1\nu_3-\nu_2\nu_4-Q(\nu_2-\nu_1)\}\mu\mu']$$
$$+ Y_r(\mu)Y_l(\mu')[-\nu_2\mu+q_1\mu'-\{p_1q_1-p_2q_2+\nu_1\nu_3-\nu_2\nu_4-Q(\nu_2-\nu_1)\}\mu\mu']$$
$$+Q(\nu_2-\nu_1)\mu(\mu+\mu')[X_r(\mu)-Y_r(\mu)][X_l(\mu')+Y_l(\mu')]$$
$$+\mu^2\mu'[Q(\nu_2-\nu_1)(\nu_4+\nu_3)+t(q_2-q_1)][X_r(\mu)-Y_r(\mu)][X_l(\mu')-Y_l(\mu')].$$

Comparing equations (340) and (383), we find that we must have

$$q_2=\nu_1\,;\qquad q_1=-\nu_2\,, \quad (384)$$
$$Q(\nu_2-\nu_1)(\nu_4+\nu_3)+t(q_2-q_1) = 0\,, \quad (385)$$
$$p_1q_2-p_2q_1+\nu_2\nu_3-\nu_1\nu_4 = Q(\nu_2-\nu_1)\,, \quad (386)$$

and

$$p_1q_1-p_2q_2+\nu_1\nu_3-\nu_2\nu_4 = Q(\nu_2-\nu_1)\,. \quad (387)$$

The consideration of the other cross-terms, S_{12}, T_{12}, and T_{21}, leads to the same conditions as do equations (384)–(387).

Finally, considering $S_{22}(\mu,\mu')$, we have

$$\left(\frac{1}{\mu'}+\frac{1}{\mu}\right)S_{22}(\mu,\mu') = \chi(\mu)\chi(\mu') - \sigma(\mu)\sigma(\mu') + 2[\zeta(\mu)\zeta(\mu') - \theta(\mu)\theta(\mu')]$$

$$= X_r(\mu)X_r(\mu')[1+p_1(\mu+\mu')+\{p_1^2-p_2^2+\tfrac{1}{2}(\nu_2^2-\nu_1^2)\}\mu\mu']$$
$$- Y_r(\mu)Y_r(\mu')[1-p_1(\mu+\mu')+\{p_1^2-p_2^2+\tfrac{1}{2}(\nu_2^2-\nu_1^2)\}\mu\mu']$$
$$+p_2(\mu+\mu')[X_r(\mu)Y_r(\mu')+Y_r(\mu)X_r(\mu')] \quad (388)$$
$$-\mu\mu'(\mu+\mu')[(p_1-p_2)t+\tfrac{1}{2}Q(\nu_2^2-\nu_1^2)][X_r(\mu)-Y_r(\mu)][X_r(\mu')-Y_r(\mu')]$$
$$-t\{\mu^2[X_r(\mu)-Y_r(\mu)][X_r(\mu')+Y_r(\mu')]$$
$$+\mu'^2[X_r(\mu)+Y_r(\mu)][X_r(\mu')-Y_r(\mu')]\}.$$

From equations (341) and (388) we now obtain the further conditions

$$p_1 = -u_4\,; \qquad p_2 = u_3\,, \tag{389}$$

$$\nu_1^2 - p_2^2 + \tfrac{1}{2}(\nu_2^2 - \nu_1^2) = u_5 = 1 + 2Q(u_4 - u_3)\,, \tag{390}$$

$$(p_1 - p_2)\,t + \tfrac{1}{2}Q(\nu_2^2 - \nu_1^2) = Qu_5\,, \tag{391}$$

and

$$t = -Q(u_4 - u_3)\,. \tag{392}$$

The consideration of $T_{22}(\mu, \mu')$ leads to the same set of conditions as the foregoing.

Collecting all the conditions among the constants that we have found and combining them with equations (376)–(380), we have

$$\nu_1 = q_2 = \tfrac{3}{4}\,[\,-\beta_1 + \beta_0\nu_4 - \alpha_2\nu_3 + \tfrac{1}{2}A_0\nu_1 - \tfrac{1}{2}B_0\nu_2 + \tfrac{1}{2}Q(\nu_2 - \nu_1)(A_1 - B_1)\,] \tag{393}$$

$$-\nu_2 = q_1 = \tfrac{3}{4}\,[\,+\alpha_1 + \alpha_2\nu_4 - \beta_0\nu_3 + \tfrac{1}{2}B_0\nu_1 - \tfrac{1}{2}A_0\nu_2 + \tfrac{1}{2}Q(\nu_2 - \nu_1)(A_1 - B_1)\,]\,, \tag{394}$$

$$u_3 = p_2 = \tfrac{3}{8}\,[\,-B_1 - B_0u_4 + A_0u_3 + \alpha_2\nu_1 - \beta_0\nu_2 + Q(u_4 - u_3)(A_1 - B_1)\,]\,, \tag{395}$$

$$-u_4 = p_1 = \tfrac{3}{8}\,[\,+A_1 - A_0u_4 + B_0u_3 + \beta_0\nu_1 - \alpha_2\nu_2 + Q(u_4 - u_3)(A_1 - B_1)\,]\,, \tag{396}$$

$$\nu_4^2 - \nu_3^2 + \tfrac{1}{2}(\nu_2^2 - \nu_1^2) = 1\,, \tag{397}$$

$$\nu_2(u_3 + \nu_3) - \nu_1(u_4 + \nu_4) = Q(\nu_2 - \nu_1)\,, \tag{398}$$

$$-\nu_1(u_3 - \nu_3) + \nu_2(u_4 - \nu_4) = Q(\nu_2 - \nu_1)\,, \tag{399}$$

$$Q(\nu_2 - \nu_1)(\nu_4 + \nu_3) + t(\nu_2 + \nu_1) = 0\,, \tag{400}$$

$$u_4^2 - u_3^2 + \tfrac{1}{2}(\nu_2^2 - \nu_1^2) = u_5 = 1 + 2Q(u_4 - u_3)\,, \tag{401}$$

$$-t(u_4 + u_3) + \tfrac{1}{2}Q(\nu_2^2 - \nu_1^2) = Qu_5\,, \tag{402}$$

$$t = -Q(u_4 - u_3)\,, \tag{403}$$

and

$$t = \tfrac{3}{8}Q\,[\,-(\nu_2 - \nu_1)(\alpha_2 + \beta_0) - (u_4 - u_3)(A_0 + B_0) + u_5(A_1 - B_1)\,]\,. \tag{404}$$

In considering the foregoing set of twelve equations, we first observe that, according to equation (403), equations (401) and (402) are equivalent. Further (cf. eqs. [400] and [403]),

$$(\nu_2 - \nu_1)(\nu_4 + \nu_3) = (u_4 - u_3)(\nu_2 + \nu_1)\,. \tag{405}$$

Next, adding and subtracting equations (398) and (399), we obtain

$$\nu_2(u_4 + u_3 - \nu_4 + \nu_3) - \nu_1(u_4 + u_3 + \nu_4 - \nu_3) = 2Q(\nu_2 - \nu_1) \tag{406}$$

and

$$\nu_2(\nu_4 + \nu_3 - u_4 + u_3) - \nu_1(\nu_4 + \nu_3 + u_4 - u_3) = 0\,, \tag{407}$$

or

$$(\nu_2 - \nu_1)(u_4 + u_3 - 2Q) = (\nu_2 + \nu_1)(\nu_4 - \nu_3) \tag{408}$$

and

$$(\nu_2 - \nu_1)(\nu_4 + \nu_3) = (\nu_2 + \nu_1)(u_4 - u_3)\,. \tag{409}$$

Equations (405), (408), and (409) can be combined in the form

$$\frac{\nu_2 + \nu_1}{\nu_2 - \nu_1} = \frac{\nu_4 + \nu_3}{u_4 - u_3} = \frac{u_4 + u_3 - 2Q}{\nu_4 - \nu_3} = \frac{1}{\lambda}\,(\text{say})\,. \tag{410}$$

It is now seen that equations (397) and (401) are equivalent; for, according to equation (410),

$$\nu_4^2-\nu_3^2=u_4^2-u_3^2-2Q\,(u_4-u_3)\,; \tag{411}$$

or, using equation (397), we have

$$1-\tfrac{1}{2}\,(\nu_2^2-\nu_1^2)\;=u_4^2-u_3^2-2Q\,(u_4-u_3)\,; \tag{412}$$

but this is the same as equation (401).

Now turning to equations (393)–(396) and rearranging the terms, we can re-write them in the forms

$$(3A_0-8)\,\nu_2-3B_0\nu_1=6\,(\alpha_1+\alpha_2\nu_4-\beta_0\nu_3)\;+3Q\,(\nu_2-\nu_1)\,(A_1-B_1)\,, \tag{413}$$

$$3B_0\nu_2-\;(3A_0-8)\,\nu_1=6\,(-\beta_1+\beta_0\nu_4-\alpha_2\nu_3)\;+3Q\,(\nu_2-\nu_1)\,(A_1-B_1)\,, \tag{414}$$

$$(3A_0-8)\,u_4-3B_0u_3=3\,(A_1+\beta_0\nu_1-\alpha_2\nu_2)\;+3Q\,(u_4-u_3)\,(A_1-B_1)\,, \tag{415}$$

and

$$3B_0u_4-\;(3A_0-8)\,u_3=3\,(-B_1+\alpha_2\nu_1-\beta_0\nu_2)\;+3Q\,(u_4-u_3)\,(A_1-B_1)\,. \tag{416}$$

From these equations the following set can be derived:

$$P_1\,(\nu_2-\nu_1)\;-2\varpi_1\,(\nu_4-\nu_3)\;=a_2\,. \tag{417}$$

$$P_2\,(\nu_2+\nu_1)\;-2\varpi_2\,(\nu_4+\nu_3)\;=a_1\,, \tag{418}$$

$$P_1\,(u_4-u_3)\;+\varpi_1\,(\nu_2-\nu_1)\;=b_2\,, \tag{419}$$

$$P_2\,(u_4+u_3)\;+\varpi_2\,(\nu_2+\nu_1)\;=b_1\,, \tag{420}$$

where we have used the abbreviations

$$\begin{aligned} &6\,(\alpha_1+\beta_1)\;=a_1\,; \qquad 3\,(A_1+B_1)\;=b_1\,; \qquad 3\,(\alpha_2+\beta_0)\;=\varpi_1\,,\\ &6\,(\alpha_1-\beta_1)\;=a_2\,; \qquad 3\,(A_1-B_1)\;=b_2\,; \qquad 3\,(\alpha_2-\beta_0)\;=\varpi_2\,, \end{aligned} \tag{421}$$

$$P_1=3\,(A_0+B_0)\;-8-2Qb_2\,, \qquad \text{and} \qquad P_2=3\,(A_0-B_0)\;-8\,. \tag{422}$$

Using equation (410), we can reduce equations (417)–(420) to the forms

$$P_1\,(\nu_2+\nu_1)\;-2\varpi_1\,(u_4+u_3)\;=\frac{a_2}{\lambda}-4\varpi_1Q\,, \tag{423}$$

$$\varpi_2\,(\nu_2+\nu_1)\;+P_2\,(u_4+u_3)\;=b_1\,, \tag{424}$$

$$P_1\,(\nu_4+\nu_3)\;+\varpi_1\,(\nu_2+\nu_1)\;=\frac{b_2}{\lambda}\,, \tag{425}$$

and

$$-\,2\varpi_2\,(\nu_4+\nu_3)\;+P_2\,(\nu_2+\nu_1)\;=a_1\,. \tag{426}$$

Solving equations (423) and (424) for $(\nu_2+\nu_1)$ and (u_4+u_3), we have

$$\Delta\,(\nu_2+\nu_1)\;=P_2\left(\frac{a_2}{\lambda}-4\varpi_1Q\right)+2\varpi_1b_1 \tag{427}$$

and

$$\Delta\,(u_4+u_3)\;=-\varpi_2\left(\frac{a_2}{\lambda}-4\varpi_1Q\right)+b_1P_1\,, \tag{428}$$

where

$$\Delta=P_1P_2+2\varpi_1\varpi_2\,. \tag{429}$$

Similarly, from equations (424) and (425) we find

$$\Delta\,(\nu_4+\nu_3) = P_2\frac{b_2}{\lambda} - a_1\varpi_1 \tag{430}$$

and

$$\Delta\,(\nu_2+\nu_1) = 2\varpi_2\frac{b_2}{\lambda} + a_1P_1\,. \tag{431}$$

Equations (427) and (431) now determine λ; for, according to these equations, we must have

$$P_2\left(\frac{a_2}{\lambda} - 4\varpi_1 Q\right) + 2\varpi_1 b_1 = 2\varpi_2\frac{b_2}{\lambda} + a_1P_1\,, \tag{432}$$

or

$$\lambda = \frac{P_2a_2 - 2\,b_2\varpi_2}{a_1P_1 - 2\,b_1\varpi_1 + 4\varpi_1P_2Q}\,. \tag{433}$$

It is now seen that equations (410), (427), (or [431]), (428), (430), and (433) determine the six constants ν_1, ν_2, ν_3, ν_4, u_3, and u_4 uniquely in terms of the various moments of $X_l(\mu)$, $Y_l(\mu)$, $X_r(\mu)$, and $Y_r(\mu)$ *and* the constant Q. It remains to verify that, with the constants determined in this fashion, equations (397) and (404) (which we have not used so far) are also satisfied.

Considering, first, condition (397), we observe that, according to equation (410), this is equivalent to

$$(\nu_4+\nu_3)\,\lambda\,(u_4+u_3-2Q) + \tfrac{1}{2}\,(\nu_2+\nu_1)\,\lambda\,(\nu_2+\nu_1) = 1\,. \tag{434}$$

Substituting for $(\nu_4+\nu_3)$, (u_4+u_3), and $(\nu_2+\nu_1)$ from equations (427), (428), (430), and (431) in equation (434), we have

$$\begin{aligned}(b_2P_2 - a_1\varpi_1\lambda)\,(-a_2\varpi_2 + b_1P_1\lambda + 4\varpi_1\varpi_2\lambda Q - 2\lambda Q\Delta)\\ + \tfrac{1}{2}\,(a_2P_2 + 2\varpi_1b_1\lambda - 4\varpi_1\lambda P_2Q)\,(a_1\lambda P_1 + 2\varpi_2b_2) = \lambda\Delta^2\,.\end{aligned} \tag{435}$$

After some straightforward reductions, equation (435) becomes

$$\tfrac{1}{2}\lambda\,(a_1a_2 + 2\,b_1b_2)\,(P_1P_2 + 2\varpi_1\varpi_2) - 2\,b_2\lambda P_2Q\Delta = \lambda\Delta^2\,, \tag{436}$$

or (cf. eq. [429])

$$\tfrac{1}{2}\,(a_1a_2 + 2\,b_1b_2) = \Delta + 2\,b_2P_2Q\,. \tag{437}$$

Hence we have only to verify the truth of equation (437).

Now (cf. eqs. [351], [361], and [364])

$$\begin{aligned}&[3\,(A_0+B_0) - 8]\,[3\,(A_0-B_0) - 8] + 18\,(\alpha_2^2 - \beta_0^2)\\ &\qquad = 9\,(A_0^2 - B_0^2) - 48A_0 + 64 + 18\,(\alpha_2^2 - \beta_0^2)\\ &\qquad = 9\,(A_1^2 - B_1^2) + 16 + 18\,[\,(\tfrac{4}{3} - \alpha_0)^2 - \beta_0^2]\\ &\qquad = 9\,(A_1^2 - B_1^2) + 48 + 18\,(\alpha_0^2 - \beta_0^2) - 48\alpha_0\\ &\qquad = 9\,(A_1^2 - B_1^2) + 18\,(\alpha_1^2 - \beta_1^2) = \tfrac{1}{2}\,(a_1a_2 + 2\,b_1b_2)\,.\end{aligned} \tag{438}$$

Hence

$$\begin{aligned}\tfrac{1}{2}\,(a_1a_2 + 2\,b_1b_2) &= P_2\,(P_1 + 2Qb_2) + 2\varpi_1\varpi_2\\ &= \Delta + 2\,b_2P_2Q\,,\end{aligned} \tag{439}$$

as required.

Finally, considering equation (404), we can re-write this in the form (cf. eq. [403])

$$8\,(u_4-u_3) = 3\,[\,(\nu_2-\nu_1)\,(\alpha_2+\beta_0) + (u_4-u_3)\,(A_0+B_0) - (A_1-B_1)\,\{1+2Q\,(u_4-u_3)\}\,] \tag{440}$$

or

$$(u_4-u_3)\,[3\,(A_0+B_0) - 8 - 6Q\,(A_1-B_1)] + 3\,(\nu_2-\nu_1)\,(\alpha_2+\beta_0) = 3\,(A_1-B_1)\,. \tag{441}$$

With the abbreviations (421) and (422), the foregoing equation is equivalent to

$$P_1\,(u_4-u_3) + \varpi_1\,(\nu_2-\nu_1) = b_2\,. \tag{442}$$

but this is the same as equation (419), which we have already satisfied. With this we have satisfied all the equations (393)–(404).

Substituting for λ according to equation (433) in equations (428), (430), and (431), we find that the solutions for the constants can be expressed in the following forms:

$$\nu_2+\nu_1 = \frac{1}{\lambda}\,(\nu_2-\nu_1) = \frac{a_1a_2-4\varpi_1\varpi_2}{P_2a_2-2b_2\varpi_2}, \tag{443}$$

$$\nu_4+\nu_3 = \frac{1}{\lambda}\,(u_4-u_3) = \frac{a_1b_2-2\varpi_1P_2}{P_2a_2-2b_2\varpi_2}, \tag{444}$$

$$u_4+u_3 = \frac{a_2b_1-2\varpi_2P_1-4\varpi_2b_2Q}{P_2a_2-2b_2\varpi_2}, \tag{445}$$

$$u_4+u_3-2Q = \frac{1}{\lambda}\,(\nu_4-\nu_3) = \frac{a_2b_1-2\varpi_2P_1-2a_2P_2Q}{P_2a_2-2b_2\varpi_2}, \tag{446}$$

$$u_5 = 1+2Q\,(u_4-u_3) = \lambda\,\frac{a_1P_1-2\varpi_1b_1+2a_1b_2Q}{P_2a_2-2b_2\varpi_2}, \tag{447}$$

and

$$\frac{1}{\lambda} = \frac{a_1P_1-2\varpi_1b_1+4\varpi_1P_2Q}{P_2a_2-2b_2\varpi_2}, \tag{448}$$

where it may be recalled that a_1, a_2, b_1, b_2, ϖ_1, ϖ_2, P_1, and P_2 are defined in equations (421) and (422).

The constant Q is, however, left entirely arbitrary.

21. *The removal of the arbitrariness in the solution and the determination of the constant* Q.—In the preceding section we have verified that the solutions for the scattering and the transmission matrices are of the forms given by equations (338)–(345) (or, equivalently, [353]–[360]) and have further shown that the constants, ν_1, ν_2, ν_3, ν_4, u_3, u_4, and u_5, occurring in the solutions can all be expressed in a unique manner in terms of the constant Q (which is left arbitrary) and the moments of the functions $X(\mu)$, $Y_r(\mu)$, $X_l(\mu)$, and $Y_l(\mu)$—the latter two functions being the *standard solutions* of equations (349) and (350). The functional equations governing $\boldsymbol{S}$ and $\boldsymbol{T}$ therefore admit a one-parametric family of solutions. As in the two other cases of conservative scattering that we have considered (Secs. II and III), this arbitrariness in the solution of the equations incorporating the invariances of the problem can be removed by appealing to the flux and the K-integrals. However, in the present instance, there are (formally) two such sets of integrals corresponding to the fact that F_l and F_r can be specified independently of each other. Indeed, starting from the equations of transfer (Paper XIV, System I, p.

153) appropriate to the problem on hand, we can show that the problem admits the integrals

$$F_l(\tau) = 2\int_{-1}^{+1} [I_{ll}(\tau, \mu) + I_{rl}(\tau, \mu)]\, \mu d\mu = \mu_0 F_l [e^{-\tau/\mu_0} + \gamma_l^{(1)}], \tag{449}$$

$$K_l(\tau) = \frac{1}{2}\int_{-1}^{+1} [I_{ll}(\tau, \mu) + I_{rl}(\tau, \mu)]\, \mu^2 d\mu = \tfrac{1}{4}\mu_0 F_l [-\mu_0 e^{-\tau/\mu_0} + \gamma_l^{(1)}\tau + \gamma_l^{(2)}], \tag{450}$$

$$F_r(\tau) = 2\int_{-1}^{+1} [I_{lr}(\tau, \mu) + I_{rr}(\tau, \mu)]\, \mu d\mu = \mu_0 F_r [e^{-\tau/\mu_0} + \gamma_r^{(1)}], \tag{451}$$

and

$$K_r(\tau) = \frac{1}{2}\int_{-1}^{+1} [I_{lr}(\tau, \mu) + I_{rr}(\tau, \mu)]\, \mu^2 d\mu = \tfrac{1}{4}\mu_0 F_r [-\mu_0 e^{-\tau/\mu_0} + \gamma_r^{(1)}\tau + \gamma_r^{(2)}], \tag{452}$$

where $(I_{ll} + I_{rl})$ and $(I_{lr} + I_{rr})$ are the *total* intensities in the diffuse radiation field which are proportional, respectively, to F_l and F_r and where $\gamma_l^{(1)}$, $\gamma_l^{(2)}$, $\gamma_r^{(1)}$, and $\gamma_r^{(2)}$ are constants.

We shall now show how the integrals (449)–(452) enable us to eliminate the arbitrariness in the solution found in § 20 and determine Q explicitly in terms of the moments of $X_r(\mu)$ and $Y_r(\mu)$.

First, we may observe that, according to equations (321),

$$I_{ll}(0, \mu) + I_{rl}(0, \mu) = \frac{3}{16\mu}[S_{11}(\mu, \mu_0) + S_{21}(\mu, \mu_0)]F_l \tag{453}$$

$$I_{ll}(\tau_1, -\mu) + I_{rl}(\tau_1, -\mu) = \frac{3}{16\mu}[T_{11}(\mu, \mu_0) + T_{21}(\mu, \mu_0)]F_l, \tag{454}$$

$$I_{lr}(0, \mu) + I_{rr}(0, \mu) = \frac{3}{16\mu}[S_{12}(\mu, \mu_0) + S_{22}(\mu, \mu_0)]F_r, \tag{455}$$

and

$$I_{lr}(\tau_1, -\mu) + I_{rr}(\tau_1, -\mu) = \frac{3}{16\mu}[T_{12}(\mu, \mu_0) + T_{22}(\mu, \mu_0)]F_r. \tag{456}$$

Considering the part of the emergent intensities proportional to F_l and substituting for the relevant matrix elements of $\boldsymbol{S}$ and $\boldsymbol{T}$ from equations (353)–(360), we have

$$\begin{aligned} I_{ll}(0, \mu) + I_{rl}(0, \mu) = \tfrac{1}{2}\mu_0 \Big\{ & \frac{3}{4}\frac{1-\mu^2}{\mu_0+\mu}[X_l(\mu_0)\, X_l(\mu) - Y_l(\mu_0)\, Y_l(\mu)] \\ & + \tfrac{3}{4} X_l(\mu_0)[(\nu_4+\mu)\, X_l(\mu) - \nu_3 Y_l(\mu) + \tfrac{1}{2}\nu_1 Y_r(\mu) - \tfrac{1}{2}\nu_2 X_r(\mu) \\ & \qquad + \tfrac{1}{2}Q(\nu_2-\nu_1)\,\mu\{X_r(\mu) - Y_r(\mu)\}] \\ & + \tfrac{3}{4} Y_l(\mu_0)[(\nu_4-\mu)\, Y_l(\mu) - \nu_3 X_l(\mu) + \tfrac{1}{2}\nu_1 X_r(\mu) - \tfrac{1}{2}\nu_2 Y_r(\mu) \\ & \qquad + \tfrac{1}{2}Q(\nu_2-\nu_1)\,\mu\{X_r(\mu) - Y_r(\mu)\}]\Big\} F_l \end{aligned} \tag{457}$$

and

$$I_{ll}(\tau_1,-\mu)+I_{rl}(\tau_1,-\mu)=\tfrac{1}{2}\mu_0\left\{\frac{3}{4}\frac{1-\mu^2}{\mu_0-\mu}[\,Y_l(\mu_0)\,X_l(\mu)-X_l(\mu_0)\,Y_l(\mu)\,]\right.$$
$$-\tfrac{3}{4}X_l(\mu_0)[\,(\nu_4-\mu)\,Y_l(\mu)-\nu_3X_l(\mu)+\tfrac{1}{2}\nu_1X_r(\mu)-\tfrac{1}{2}\nu_2Y_r(\mu)$$
$$+\tfrac{1}{2}Q(\nu_2-\nu_1)\,\mu\{X_r(\mu)-Y_r(\mu)\}\,] \tag{458}$$
$$\left.-\tfrac{3}{4}Y_l(\mu_0)[\,(\nu_4+\mu)\,X_l(\mu)-\nu_3Y_l(\mu)+\tfrac{1}{2}\nu_1Y_r(\mu)-\tfrac{1}{2}\nu_2X_r(\mu)\right.$$
$$\left.+\tfrac{1}{2}Q(\nu_2-\nu_1)\,\mu\{X_r(\mu)-Y_r(\mu)\}\,]\right\}F_l\,.$$

Using equations (457) and (458), we can determine the emergent fluxes and the K's by evaluating the various integrals defining these quantities. The evaluations can all be carried out explicitly if proper use is made of the integral properties of the X- and Y-functions.[20] Comparing the resulting expressions for $F_l(0)$, $F_l(\tau_1)$, $K_l(0)$, and $K_l(\tau_1)$ with those given by equations (449) and (450) for $\tau=0$ and $\tau=\tau_1$, we find, respectively,

$$\gamma_l^{(1)}=\tfrac{3}{4}X_l(\mu_0)[\nu_4\alpha_1-\nu_3\beta_1+\alpha_2+\tfrac{1}{2}\nu_1B_1-\tfrac{1}{2}\nu_2A_1+\tfrac{1}{2}Q(\nu_2-\nu_1)(A_2-B_2)\,] \tag{459}$$
$$+\tfrac{3}{4}Y_l(\mu_0)[\nu_4\beta_1-\nu_3\alpha_1-\beta_2+\tfrac{1}{2}\nu_1A_1-\tfrac{1}{2}\nu_2B_1+\tfrac{1}{2}Q(\nu_2-\nu_1)(A_2-B_2)\,],$$

$$\gamma_l^{(1)}=\tfrac{3}{4}X_l(\mu_0)[\nu_4\beta_1-\nu_3\alpha_1-\beta_2+\tfrac{1}{2}\nu_1A_1-\tfrac{1}{2}\nu_2B_1+\tfrac{1}{2}Q(\nu_2-\nu_1)(A_2-B_2)\,] \tag{460}$$
$$+\tfrac{3}{4}Y_l(\mu_0)[\nu_4\alpha_1-\nu_3\beta_1+\alpha_2+\tfrac{1}{2}\nu_1B_1-\tfrac{1}{2}\nu_2A_1+\tfrac{1}{2}Q(\nu_2-\nu_1)(A_2-B_2)\,],$$

$$\gamma_l^{(2)}=\tfrac{3}{4}X_l(\mu_0)[\nu_4\alpha_2-\nu_3\beta_2+\alpha_1+\tfrac{1}{2}\nu_1B_2-\tfrac{1}{2}\nu_2A_2+\tfrac{1}{2}Q(\nu_2-\nu_1)(A_3-B_3)\,] \tag{461}$$
$$+\tfrac{3}{4}Y_l(\mu_0)[\nu_4\beta_2-\nu_3\alpha_2-\beta_1+\tfrac{1}{2}\nu_1A_2-\tfrac{1}{2}\nu_2B_2+\tfrac{1}{2}Q(\nu_2-\nu_1)(A_3-B_3)\,],$$

and

$$\gamma_l^{(1)}\tau_1+\gamma_l^{(2)}$$
$$=-\tfrac{3}{4}X_l(\mu_0)[\nu_4\beta_2-\nu_3\alpha_2-\beta_1+\tfrac{1}{2}\nu_1A_2-\tfrac{1}{2}\nu_2B_2+\tfrac{1}{2}Q(\nu_2-\nu_1)(A_3-B_3)\,] \tag{462}$$
$$-\tfrac{3}{4}Y_l(\mu_0)[\nu_4\alpha_2-\nu_3\beta_2+\alpha_1+\tfrac{1}{2}\nu_1B_2-\tfrac{1}{2}\nu_2A_2+\tfrac{1}{2}Q(\nu_2-\nu_1)(A_3-B_3)\,].$$

It should, first, be observed that equations (459) and (460) are consistent with each other; for, to be consistent,

$$(\nu_4+\nu_3)(\alpha_1-\beta_1)+\alpha_2+\beta_2-\tfrac{1}{2}(\nu_2+\nu_1)(A_1-B_1)=0 \tag{463}$$

must be true. With the abbreviations (421), equation (463) is equivalent to

$$a_2(\nu_4+\nu_3)+2\varpi_1-b_2(\nu_2+\nu_1)=0\,. \tag{464}$$

With the solutions (443) and (444) for $(\nu_2+\nu_1)$ and $(\nu_4+\nu_3)$, it is readily verified that equation (464) is indeed satisfied. We can accordingly combine equations (459) and (460) to give

$$\gamma_l^{(1)}=\tfrac{3}{8}[\,X_l(\mu_0)+Y_l(\mu_0)\,][\,(\nu_4-\nu_3)(\alpha_1+\beta_1)-\tfrac{1}{2}(\nu_2-\nu_1)(A_1+B_1)$$
$$+\alpha_2-\beta_2+Q(\nu_2-\nu_1)(A_2-B_2)\,]\,. \tag{465}$$

[20] In the present context the relations of theorem 8 have to be used.

The factor of $X_l(\mu_0) + Y_l(\mu_0)$ on the right-hand side can be simplified considerably by using equations (443), (446), and (448). Thus

$$\begin{aligned}
&6\,(\nu_4-\nu_3)\,(\alpha_1+\beta_1) - 3\,(\nu_2-\nu_1)\,(A_1+B_1) + 6\,(\alpha_2-\beta_2)\\
&= \lambda\left[a_1\,(u_4+u_3-2Q) - b_1\,(\nu_2+\nu_1) + \frac{2\varpi_2}{\lambda}\right]\\
&= \frac{\lambda}{P_2a_2-2b_2\varpi_2}\,[a_1\,(a_2b_1-2\varpi_2P_1-2a_2P_2Q)\\
&\quad - b_1\,(a_1a_2-4\varpi_1\varpi_2) + 2\varpi_2\,(a_1P_1-2\varpi_1b_1+4\varpi_1P_2Q]\\
&= \frac{2\lambda P_2Q}{P_2a_2-2b_2\varpi_2}\,(-a_1a_2+4\varpi_1\varpi_2)\\
&= -2P_2Q\,(\nu_2-\nu_1) = -2Q\,(\nu_2-\nu_1)\,[3\,(A_0-B_0) - 8]\,.
\end{aligned} \tag{466}$$

Inserting this result in equation (465), we have

$$\gamma_l^{(1)} = -\tfrac{1}{8}Q\,(\nu_2-\nu_1)\,[3\,(A_0-B_0) - 8 - 3\,(A_2-B_2)]\,[X_l(\mu_0) + Y_l(\mu_0)]\,. \tag{467}$$

Next, from equations (461), and (462) we obtain

$$\begin{aligned}
\gamma_l^{(1)}\tau_1 = -\tfrac{3}{4}\,[X_l(\mu_0) + Y_l(\mu_0)]\,[&(\nu_4-\nu_3)\,(\alpha_2+\beta_2) - \tfrac{1}{2}\,(\nu_2-\nu_1)\,(A_2+B_2)\\
&+ (\alpha_1-\beta_1) + Q\,(\nu_2-\nu_1)\,(A_3-B_3)]\,.
\end{aligned} \tag{468}$$

Again, the factor of $X_l(\mu_0) + Y_l(\mu_0)$ can be simplified by using equations (443) and (446); we find

$$\begin{aligned}
\gamma_l^{(1)}\tau_1 = -\tfrac{1}{8}\,(\nu_2-\nu_1)\,[&3\,(A_0-A_2) + 3\,(B_0-B_2) - 8\\
&- 6Q\{(A_1-A_3) - (B_1-B_3)\}]\,[X_l(\mu_0) + Y_l(\mu_0)]\,.
\end{aligned} \tag{469}$$

From equations (467) and (469) we now obtain

$$\tau_1 = \frac{3\,(A_0-A_2) + 3\,(B_0-B_2) - 8 - 6Q\,[(A_1-A_3) - (B_1-B_3)]}{Q\,[3\,(A_0-A_2) - 3\,(B_0-B_2) - 8]}\,. \tag{470}$$

Solving this equation for Q, we have

$$Q = \frac{3\,(A_0-A_2) + 3\,(B_0-B_2) - 8}{[3\,(A_0-A_2) - 3\,(B_0-B_2) - 8]\,\tau_1 + 6\,(A_1-A_3) - 6\,(B_1-B_3)}\,. \tag{471}$$

Introducing the notation (cf. eq. [10])

$$x_n^{(r)} = \frac{3}{8}\int_0^1 (1-\mu^2)\,X_r(\mu)\,\mu^n d\mu \tag{472}$$

and

$$y_n^{(r)} = \frac{3}{8}\int_0^1 (1-\mu^2)\,Y_r(\mu)\,\mu^n d\mu\,, \tag{473}$$

we can re-write equation (471) in the form

$$Q = \frac{x_0^{(r)} + y_0^{(r)} - 1}{[x_0^{(r)} - y_0^{(r)} - 1]\,\tau_1 + 2\,[x_1^{(r)} - y_1^{(r)}]}\,. \tag{474}$$

In this form we recognize the similarity of the present expression for Q with equation (202).

A similar consideration of the integrals (451) and (452) leads to the same value of Q, though the details of the calculation are somewhat more complicated.[21] However, it may be of interest to note that the constant $\gamma_r^{(1)}$ in equations (451) and (452) has the value (cf. eq. [467])

$$\gamma_r^{(1)} = -\tfrac{1}{8}Q\,[3\,(A_0 - A_2) - 3\,(B_0 - B_2) - 8]\,[(u_4 - u_3)\,\{X_r(\mu_0) + Y_r(\mu_0)\} - u_5\mu_0\{X_r(\mu_0) - Y_r(\mu_0)\}]\,. \tag{475}$$

With the foregoing determination of Q in terms of the moments of $X_r(\mu)$ and $Y_r(\mu)$, we have completed the solution of the problem.

22. *Concluding remarks.*—The analysis of the various problems of diffuse reflection and transmission presented in this paper has shown how problems of radiative transfer in plane-parallel atmospheres of finite optical thicknesses can be solved exactly; for, in every case considered, it was possible to reduce the complicated systems of functional equations representing the problem to pairs of equations of the standard form

$$X(\mu) = 1 + \mu\int_0^1 \frac{\Psi(\mu')}{\mu + \mu'}\,[X(\mu)\,X(\mu') - Y(\mu)\,Y(\mu')]\,d\mu' \tag{476}$$

and

$$Y(\mu) = e^{-\tau_1/\mu} + \mu\int_0^1 \frac{\Psi(\mu')}{\mu - \mu'}\,[Y(\mu)\,X(\mu') - X(\mu)\,Y(\mu')]\,d\mu'\,. \tag{477}$$

And, moreover, the expressions (155) and (156) for $X(\mu)$ and $Y(\mu)$, as rational functions involving the points of the Gaussian division and the roots of the characteristic equation

$$1 = \sum_{j=1}^{n} \frac{a_j\Psi(\mu_j)}{1 - k^2\mu_j^2}, \tag{478}$$

provide approximate solutions of equations (476) and (477). Starting with these approximate solutions,[22] we can solve equations (476) and (477) by a process of iteration. Since the iteration will have to be performed for every required value of τ_1, the problem of tabulating the X- and Y-functions is much more elaborate than in the case of the H-functions. However, the existence of the *differential equations* (eqs. [18] and [19]),

$$\frac{\partial X(\mu, \tau_1)}{\partial \tau_1} = Y(\mu, \tau_1)\int_0^1 \frac{d\mu'}{\mu'}\Psi(\mu')\,Y(\mu', \tau_1) \tag{479}$$

and

$$\frac{\partial Y(\mu, \tau_1)}{\partial \tau_1} = -\frac{Y(\mu, \tau_1)}{\mu} + X(\mu, \tau_1)\int_0^1 \frac{d\mu'}{\mu'}\Psi(\mu')\,Y(\mu', \tau_1)\,, \tag{480}$$

simplifies the tabulation problem considerably, since corrections for small changes in τ_1 can always be found with the aid of these equations.[23]

[21] In the reductions, use must be made of eqs. (13)–(16).

[22] For $\tau_1 \to 0$, a generalization of the method described by van de Hulst (*Ap. J.*, **107**, 220, 1948) in the context of the simpler equations (172) and (173) can also be used with considerable advantage. While the necessary generalizations of van de Hulst's method will be considered in a later paper of this series, it may be remarked here that the method is essentially one of solving equations (476) and (477) by an iteration scheme which is started with the "trial solutions" $X(\mu) = 1$ and $Y(\mu) = e^{-\tau_1/\mu}$.

[23] Expressions for the second- and higher-order derivatives can be easily derived from eqs. (479) and (480), so that Taylor expansions with as many terms as may be desired could be used.

In view of the importance of the problem and its long-standing nature, it is worthy of comment here that the basic problem underlying the theories relating to the illumination and polarization of the sunlit sky has now been solved exactly. The solution presented in Section V assumes that beyond $\tau = \tau_1$ there is a vacuum (or, equivalently, that there is a perfect absorber at $\tau = \tau_1$). However, the solution for the case in which there is a "ground" can be reduced to the "standard problem" considered in this paper.[24]

Again, while attention was concentrated in this paper on problems of diffuse reflection and transmission, it is evident that solutions for other problems in which there is a distribution of external sources through the medium can also be reduced to the X- and Y-functions of this paper.[25] We shall consider such problems in later papers of this series.

Finally, it should be remarked that, while the present paper solves the mathematical problem of the transfer equations, the practical use of the solutions must await the construction of tables of the X- and Y-functions appropriate for the various problems. The preparation of these tables is now being undertaken by Mrs. Frances Breen and the writer.

[24] Cf. van de Hulst, *op. cit.*

[25] E.g., a case in the theory of formation of stellar absorption lines leads to an equation of transfer with an external source function which increases linearly with the optical depth (cf. Paper XX, *Ap. J.*, **106**, 145, eq. [5], 1947). The exact solution for this problem can, nevertheless, be reduced to an H-function and its moments (Paper XX, eq. [47]).

ON THE RADIATIVE EQUILIBRIUM OF A STELLAR ATMOSPHERE. XXIII

S. CHANDRASEKHAR AND FRANCES H. BREEN
Yerkes Observatory
Received January 2, 1948

ABSTRACT

In this paper the exact H-functions governing the law of diffuse reflection by a semi-infinite plane-parallel atmosphere in accordance with the phase function $\lambda(1 + x \cos \Theta)$ are tabulated. The functions were determined numerically by solving the exact functional equations which they satisfy.

The cases $(1 + x \cos \Theta)$ ($x = -1.0, -0.8, -0.6, -0.4, -0.2, 0.2, 0.4, 0.6, 0.8$, and 1.0) and $\lambda(1 + \cos \Theta)$ ($\lambda = 0.975, 0.950, 0.925, 0.9, 0.8, 0.7, 0.6, 0.5, 0.4, 0.3, 0.2$, and 0.1) are covered by the tabulations.

In continuation of Papers XVI[1] and XIX,[2] in which we have tabulated the exact solutions for several problems in the theory of radiative transfer, we provide in this paper tables of H-functions governing the law of diffuse reflection by a semi-infinite plane-parallel atmosphere in accordance with the phase function $\lambda(1 + x \cos \Theta)$.

DIFFUSE REFLECTION IN ACCORDANCE WITH THE PHASE FUNCTION $\lambda(1 + x \cos \Theta)$

The law of diffuse reflection by a semi-infinite plane-parallel atmosphere.—

$$I(\mu, \varphi; \mu_0, \varphi_0) = \tfrac{1}{4}\lambda F [H^{(0)}(\mu) H^{(0)}(\mu_0) \{1 - c(\mu + \mu_0) - x(1 - \lambda)\mu\mu_0\} + x(1 - \mu^2)^{\frac{1}{2}}(1 - \mu_0^2)^{\frac{1}{2}} H^{(1)}(\mu) H^{(1)}(\mu_0) \cos(\varphi - \varphi_0)] \frac{\mu_0}{\mu_0 + \mu}.$$

The characteristic functions in terms of which $H^{(0)}(\mu)$ and $H^{(1)}(\mu)$ are defined, are, respectively,

$$\Psi^{(0)}(\mu) = \tfrac{1}{2}\lambda [1 + x(1 - \lambda)\mu^2]$$

and

$$\Psi^{(1)}(\mu) = \tfrac{1}{4} x\lambda (1 - \mu^2).$$

The constant, c, is given by

$$c = x\lambda (1 - \lambda) \frac{a_1}{2 - \lambda a_0},$$

where a_0 and a_1 are the moments of order zero and one of $H^{(0)}(\mu)$.

An alternative way of expressing the law of diffuse reflection is

$$I(\mu, \varphi; \mu_0, \varphi_0) = \tfrac{1}{4}\lambda F [\psi(\mu)\psi(\mu_0) - x\phi(\mu)\phi(\mu_0) + x(1 - \mu^2)^{\frac{1}{2}}(1 - \mu_0^2)^{\frac{1}{2}} H^{(1)}(\mu) H^{(1)}(\mu_0) \cos(\varphi - \varphi_0)] \frac{\mu_0}{\mu_0 + \mu},$$

where

$$\psi(\mu) = H^{(0)}(\mu)(1 - c\mu), \qquad \phi(\mu) = q\mu H^{(0)}(\mu)$$

and

$$q = \frac{2(1 - \lambda)}{2 - \lambda a_0}.$$

[1] *Ap. J.*, **105**, 435, 1947. [2] *Ibid.*, **106**, 143, 1947.

TABLE 1

THE FUNCTIONS $H^{(0)}(\mu)$ OBTAINED AS SOLUTIONS OF THE EXACT FUNCTIONAL EQUATIONS THEY SATISFY

(The Case $x = 1$)

μ	$\lambda=0.1$	$\lambda=0.2$	$\lambda=0.3$	$\lambda=0.4$	$\lambda=0.5$	$\lambda=0.6$
0	1.0000	1.0000	1.0000	1.0000	1.0000	1.0000
0.05	1.0089	1.0183	1.0280	1.0383	1.0492	1.0608
0.10	1.0145	1.0297	1.0459	1.0632	1.0817	1.1020
0.15	1.0188	1.0388	1.0602	1.0832	1.1084	1.1361
0.20	1.0224	1.0463	1.0722	1.1003	1.1311	1.1656
0.25	1.0254	1.0528	1.0825	1.1151	1.1511	1.1918
0.30	1.0280	1.0584	1.0916	1.1281	1.1689	1.2153
0.35	1.0303	1.0634	1.0996	1.1398	1.1850	1.2366
0.40	1.0324	1.0678	1.1069	1.1504	1.1996	1.2562
0.45	1.0343	1.0719	1.1135	1.1600	1.2129	1.2742
0.50	1.0359	1.0755	1.1194	1.1688	1.2252	1.2908
0.55	1.0375	1.0788	1.1249	1.1769	1.2365	1.3063
0.60	1.0389	1.0819	1.1300	1.1844	1.2470	1.3207
0.65	1.0401	1.0847	1.1346	1.1913	1.2568	1.3342
0.70	1.0413	1.0873	1.1389	1.1978	1.2659	1.3468
0.75	1.0424	1.0897	1.1429	1.2038	1.2745	1.3587
0.80	1.0434	1.0919	1.1467	1.2094	1.2825	1.3699
0.85	1.0444	1.0940	1.1502	1.2147	1.2900	1.3805
0.90	1.0453	1.0960	1.1535	1.2196	1.2972	1.3905
0.95	1.0461	1.0978	1.1566	1.2243	1.3039	1.4000
1.00	1.0469	1.0995	1.1595	1.2287	1.3103	1.4090

TABLE 1—*Continued*

μ	$\lambda=0.7$	$\lambda=0.8$	$\lambda=0.9$	$\lambda=0.925$	$\lambda=0.95$	$\lambda=0.975$
0	1.0000	1.0000	1.0000	1.0000	1.0000	1.0000
0.05	1.0735	1.0876	1.1045	1.1096	1.1153	1.1223
0.10	1.1244	1.1501	1.1819	1.1917	1.2029	1.2169
0.15	1.1673	1.2038	1.2500	1.2645	1.2814	1.3027
0.20	1.2049	1.2516	1.3120	1.3313	1.3539	1.3830
0.25	1.2387	1.2951	1.3695	1.3936	1.4222	1.4593
0.30	1.2693	1.3351	1.4233	1.4523	1.4869	1.5323
0.35	1.2973	1.3722	1.4740	1.5079	1.5487	1.6026
0.40	1.3233	1.4068	1.5220	1.5608	1.6078	1.6706
0.45	1.3473	1.4392	1.5677	1.6114	1.6647	1.7365
0.50	1.3697	1.4697	1.6112	1.6598	1.7195	1.8005
0.55	1.3907	1.4985	1.6528	1.7063	1.7724	1.8627
0.60	1.4103	1.5257	1.6926	1.7510	1.8235	1.9234
0.65	1.4288	1.5515	1.7308	1.7941	1.8730	1.9826
0.70	1.4462	1.5760	1.7674	1.8356	1.9210	2.0403
0.75	1.4627	1.5993	1.8027	1.8757	1.9675	2.0967
0.80	1.4783	1.6216	1.8367	1.9144	2.0127	2.1519
0.85	1.4931	1.6428	1.8694	1.9519	2.0567	2.2058
0.90	1.5072	1.6631	1.9010	1.9882	2.0994	2.2586
0.95	1.5206	1.6825	1.9315	2.0233	2.1409	2.3103
1.00	1.5334	1.7011	1.9610	2.0574	2.1814	2.3609

The constants, q and c, are further related according to

$$q^2 - \frac{c^2}{x} = 1 - \lambda .$$

When $\lambda = 1$, the characteristic function $\Psi^{(0)}(\mu)$ becomes $\frac{1}{2}$, independently of x. The corresponding H-function is therefore the one tabulated in Paper XIX (Table 1, the case $\tilde{\omega}_0 = 1$).

The H-functions tabulated in this paper were computed by the iteration method described in Paper XVI.

TABLE 2

THE MOMENTS a_0 AND a_1 AND THE CONSTANTS q AND c

λ	a_0	a_1	q	c	q^2-c^2
0.1	1.032729	0.519588	0.949003	0.024654	0.899999
.2	1.068832	.541348	.895740	.048491	.799998
.3	1.109034	.565767	.839686	.071260	.699995
.4	1.154378	.593541	.780108	.092605	.599993
.5	1.206366	.625686	.715914	.111984	.499992
.6	1.267352	.663798	.645375	.128520	.399992
.7	1.341368	.710639	.565482	.140649	.299987
.8	1.436535	.771792	.470161	.145147	.199984
.9	1.574492	.862276	.343079	.133123	.099981
.925	1.623024	.894620	.300780	.124451	.074981
.950	1.683484	.935277	.249569	.110873	.049992
0.975	1.767379	0.992380	0.180632	0.087387	0.024992

TABLE 3

THE FUNCTIONS $H^{(1)}(\mu)$ OBTAINED AS SOLUTIONS OF THE EXACT FUNCTIONAL EQUATIONS THEY SATISFY

μ	$x\lambda=1.0$	$x\lambda=0.8$	$x\lambda=0.6$	$x\lambda=0.4$	$x\lambda=0.2$	$x\lambda=-0.2$	$x\lambda=-0.4$	$x\lambda=-0.6$	$x\lambda=-0.8$	$x\lambda=-1.0$
0	1.0000	1.0000	1.0000	1.0000	1.0000	1.0000	1.0000	1.0000	1.0000	1.0000
0.05	1.0359	1.0281	1.0206	1.0135	1.0066	0.9936	0.9875	0.9815	0.9758	0.9702
0.10	1.0561	1.0436	1.0319	1.0207	1.0101	0.9903	0.9811	0.9722	0.9637	0.9555
0.15	1.0711	1.0550	1.0400	1.0259	1.0126	0.9880	0.9766	0.9657	0.9553	0.9453
0.20	1.0832	1.0642	1.0466	1.0301	1.0146	0.9862	0.9731	0.9607	0.9488	0.9375
0.25	1.0933	1.0718	1.0520	1.0335	1.0162	0.9847	0.9703	0.9566	0.9436	0.9313
0.30	1.1019	1.0783	1.0565	1.0364	1.0176	0.9835	0.9679	0.9533	0.9393	0.9261
0.35	1.1093	1.0838	1.0604	1.0388	1.0187	0.9825	0.9660	0.9504	0.9358	0.9219
0.40	1.1157	1.0886	1.0638	1.0409	1.0197	0.9816	0.9643	0.9480	0.9327	0.9182
0.45	1.1214	1.0928	1.0667	1.0428	1.0206	0.9808	0.9628	0.9459	0.9300	0.9150
0.50	1.1265	1.0966	1.0694	1.0444	1.0214	0.9801	0.9615	0.9441	0.9277	0.9122
0.55	1.1311	1.1000	1.0718	1.0459	1.0221	0.9795	0.9604	0.9424	0.9256	0.9097
0.60	1.1353	1.1031	1.0739	1.0472	1.0227	0.9789	0.9593	0.9409	0.9237	0.9075
0.65	1.1391	1.1059	1.0759	1.0484	1.0232	0.9784	0.9584	0.9396	0.9220	0.9055
0.70	1.1426	1.1085	1.0776	1.0495	1.0238	0.9780	0.9575	0.9384	0.9205	0.9037
0.75	1.1458	1.1108	1.0792	1.0505	1.0242	0.9776	0.9568	0.9373	0.9191	0.9020
0.80	1.1487	1.1130	1.0807	1.0514	1.0246	0.9772	0.9560	0.9363	0.9179	0.9005
0.85	1.1514	1.1150	1.0821	1.0523	1.0250	0.9769	0.9554	0.9354	0.9167	0.8992
0.90	1.1540	1.1168	1.0834	1.0531	1.0254	0.9765	0.9548	0.9345	0.9156	0.8979
0.95	1.1563	1.1185	1.0846	1.0538	1.0258	0.9762	0.9542	0.9338	0.9146	0.8967
1.00	1.1585	1.1201	1.0857	1.0545	1.0261	0.9760	0.9537	0.9330	0.9137	0.8956

An idea of the accuracy reached in our calculations can be obtained by the comparisons made in Table 4 and 5 between the values of the integrals

$$\int_0^1 H^{(0)}(\mu)\,[1 + x\,(1-\lambda)\,\mu^2]\,d\mu \qquad \text{and} \qquad \int_0^1 H^{(1)}(\mu)\,(1-\mu^2)\,d\mu\,,$$

evaluated numerically with the aid of the tabulated functions and their exact values, given by the formulae

$$\int_0^1 H^{(0)}(\mu)\,[1 + x\,(1-\lambda)\,\mu^2]\,d\mu = \frac{2}{\lambda}\,[1 - \sqrt{(1-\lambda)\,(1-\tfrac{1}{3}x\lambda)}\,]$$

and

$$\int_0^1 H^{(1)}(\mu)\,(1-\mu^2)\,d\mu = \frac{4}{x\lambda}\,[1 - \sqrt{1-\tfrac{1}{3}x\lambda}\,]\,.$$

The values of $q^2 - c^2$ listed in Table 2 may also be compared with $1 - \lambda$ in this connection.

TABLE 4

COMPARISON OF THE INTEGRALS $\int_0^1 H^{(0)}(\mu)[1 + (1-\lambda)\mu^2]d\mu$ WITH THE AID OF THE TABULATED FUNCTIONS WITH THEIR EXACT VALUES $2[1 - \sqrt{(1-\lambda)(1-\frac{1}{3}\lambda)}]\lambda^{-1}$

λ	Iterated	Exact	λ	Iterated	Exact
0.1	1.34523	1.345242	0.7	1.48688	1.486905
.2	1.35900	1.359012	.8	1.54253	1.542573
.3	1.37514	1.375164	.9	1.63422	1.634277
.4	1.39442	1.394449	.925	1.66964	1.669706
.5	1.41799	1.418011	.950	1.71609	1.716122
0.6	1.44770	1.447715	0.975	1.78476	1.784813

TABLE 5

COMPARISON OF THE INTEGRALS $\int_0^1 H^{(1)}(\mu)\,(1-\mu^2)d\mu$ WITH THE AID OF THE TABULATED FUNCTIONS WITH THEIR EXACT VALUES $4[\,1 - \sqrt{1-\frac{1}{3}x\lambda}\,](x\lambda)^{-1}$

$x\lambda$	Iterated	Exact	$x\lambda$	Iterated	Exact
+1.0	0.73397	0.734014	−0.2	0.65592	0.655910
+0.8	.71822	.718256	−0.4	.64583	.645813
+0.6	.70379	.703819	−0.6	.63632	.636301
+0.4	.69049	.690507	−0.8	.62734	.627314
+0.2	0.67816	0.678164	−1.0	0.61884	0.618802

SCATTERING IN A PLANETARY ATMOSPHERE

H. C. VAN DE HULST
Yerkes Observatory
Received November 7, 1947

ABSTRACT

In this paper the problem of multiple scattering in a planetary atmosphere, both with and without a diffusely reflecting bottom surface, is discussed. We assume that the atmospheric scattering is isotropic, with an albedo a, and that the ground surface reflects the radiation according to Lambert's law, with an albedo b.

Sections II–IV are devoted to the *standard problem*, i.e., to the problem of a finite atmosphere without a ground surface. After the exact expressions for single and double scattering have been obtained in Section II by direct integration, we show in Section III that an indirect method gives the same result in a more elegant way. This method is based on the use of Chandrasekhar's equations by which the intensities of the reflected and transmitted radiation can be expressed in terms of two functions, $X(s)$ and $Y(s)$. A new feature in the present discussion is that physical meanings are assigned to these functions. With these meanings the general relations are newly derived; and the expressions for single and double scattering are obtained in a simple manner. Section IV completes these calculations by adding an approximate expression for the third-order scattering. A numerical example shows that in this way an accuracy of 0.1 per cent is reached for an atmosphere with $\tau = 0.1$.

Section V discusses the *planet problem*, i.e., the problem of an atmosphere with a bottom surface. The solution of this problem is expressed in a general way in terms of the solution of the standard problem. The exact solution for the case of an isotropically scattering atmosphere involves the functions $X(s)$ and $Y(s)$ and their moments. Formulae suitable for the case of a thin atmosphere are also given and illustrated by a numerical example.

A comprehensive discussion of the *mathematical functions* occurring in these calculations is given in the appendix. They are of three types: The functions $E_n(x)$ are the ordinary exponential integrals. The functions $F_n(b, x)$ are definite integrals, of which the integrand is the product of an E-function and an exponential function. The functions $G_{nm}(x)$ and $G'_{nm}(x)$ are definite integrals, of which the integrand is the product of two E-functions. Only the last type of functions cannot be expressed in terms of known functions. For their calculation a new elementary function, the exponential integral of the second order, is introduced. Numerical values of all functions needed are given in four tables.

Quantitative knowledge about the composition and depth of planetary atmospheres can be gained only from photometric observations. The term "photometry" has here to be taken in its most general sense: the intensity being specified according to the position on the disk of the planet, the wave length, and the state of polarization. The atmosphere of the earth can be investigated by other than optical methods, but general photometry of the sky light still provides an important source of information.

The interpretation of any observation in this general field has to deal with scattering problems. The most well known of these problems is that of explaining the brightness and polarization of the blue daylight sky. L. V. King[1] and others have made approximate calculations on this subject. Much attention has further been given to the limb darkening of the outer planets, in particular by E. Schoenberg[2] and V. C. Fessenkoff.[3] Other allied problems are those of the polarization of the planets, the escape of the heat radiation of the planet through its atmosphere, and the formation of absorption lines in the process of diffuse reflection by the planetary atmospheres. Finally, the theory of reflection nebulae and undoubtedly various problems occurring in physical experiments may also be treated by the same formalism.

The analysis of the problems that we have mentioned presents difficulties of two sorts. First, the formulae describing the *elementary processes* of scattering by a single air mole-

[1] *Phil. Trans. R. Soc. London, A*, **212**, 375, 1913.

[2] *Handb. d. Ap.*, **2**, Part I, 221, 1929.

[3] *Astr. J. Sovjet Union*, **21**, 257, 1944.

cule, or fog droplet, and of diffuse reflection by an area of the ground may already have a fairly complex form. Second, the *multiple scattering* in the atmosphere, combined with the diffuse reflection by the ground, introduces further mathematical difficulties of an essentially different nature.

In the present paper we shall concentrate on the second difficulty. We shall, therefore, make, throughout this paper, the simplest possible assumptions about the elementary processes. In particular we shall assume that (1) the scattering by a volume element of the atmosphere is *isotropic scattering with an albedo* a and (2) the reflection by the ground is *reflection according to Lambert's law with an albedo* b. Both *a* and *b* are defined in the usual way:

$$\text{Albedo} = \frac{\text{Energy scattered in all directions}}{\text{Energy removed from original direction}}.$$

The lost fraction, 1-albedo, will be called the "absorbed energy." Of course, it may reappear as radiation in some other wave length. For the present calculation, however, this does not make any difference.

A calculation based on these simple assumptions will bring out most clearly what kind of mathematical difficulties occur in the theory of multiple scattering. The problems that arise if the scattering is of a more complex type, for instance, Rayleigh scattering with exact account of the polarization of the incident and scattered light, are mostly of a similar nature. The calculations of S. Chandrasekhar[4] have shown that the solution in that case will consist of a larger number of terms but that the forms of the separate terms closely resemble the form for isotropic scattering.

I. METHODS OF SOLUTION

We may first remark that the presence of a diffusely reflecting ground beneath the atmosphere does not introduce any new difficulties. We shall refer to the problem in which the bottom surface is absent as the "standard problem" and to the case in which it is present as the "planet problem." It will be shown in Section V that the second problem can be reduced to the first one. Most of our discussion will therefore be devoted to the standard problem.

The methods by which these problems may be solved can be divided into three types. In methods of type I, one tries to follow the career of an incident quantum of radiation. It may be scattered 0, 1, 2, or any number of times. The emerging intensities, including all such possibilities, would together give the required result. However, the calculations are too complex to be pursued beyond $n = 2$. Therefore, this method is useful only in cases in which the series converges very rapidly.

In methods of type II the radiation field inside the atmosphere is introduced as an unknown function of the optical depth and the angles. This function has to satisfy an integrodifferential equation, *the equation of transfer*, and certain boundary conditions. Approximate solutions of this equation may be obtained by various methods. The most widely known method is the Milne-Eddington approximation. A more effective one is the method of Gaussian subdivisions and characteristic roots recently used extensively by Chandrasekhar.[5]

In methods of type III, only the reflected and transmitted intensities are introduced as unknown functions. Using certain invariances that must hold if, for instance, a layer $d\tau$ is removed from the top and added to the bottom of the atmosphere, one can show that these functions must satisfy certain *functional equations*. These equations have the

[4] A series of papers entitled "On the Radiative Equilibrium of a Stellar Atmosphere," starting in *Ap. J.*, **99**, 180, 1944. These papers will be referred to as "Paper I," etc. Chandrasekhar has given a comprehensive account of these investigations in his Gibbs lecture, *Bull. Amer. Math. Soc.*, **53**, 641, 1947.

[5] Paper II, *Ap. J.*, **100**, 76, 1944, and following papers.

form of nonlinear integral equations. This method was introduced by Ambarzumiam and has been made into a very powerful tool by Chandrasekhar.[6] In particular, Chandrasekhar has proved that the solutions can be separated into products of a function of the angle of incidence only *times* a function of the angle of emergence only. These functions satisfy separate functional equations. The equations can be easily solved with an accuracy of five or more decimals, provided that a fairly good approximation is already known to start with. If, however, such a starting solution was not known, the nonlinearity of these equations would virtually forbid their solution by trial and error.

In choosing the appropriate method for our present problem we may be guided by the following considerations. The devices of type III will prove useful in any case, both as a check on the general form of the solution and as the only means of reaching the utmost accuracy. But, first, an approximate solution has to be found by means of either method I or method II. Now in problems of planetary illumination we are primarily interested in thin atmospheres. Thus the optical thickness, τ, of the terrestrial atmosphere at λ 5000 A is 0.14. Since the sources of scattered radiation are about evenly distributed in such an atmosphere, the intensities in vertical direction are of the order of τ times the intensities in horizontal direction. It has been found that the methods of type II that assume an intensity distribution expressible in a few spherical harmonics are not always satisfactory in this case. Fortunately, the thin atmospheres just provide a case in which methods of type I are useful. For the flux of $n + 1$ times scattered light is of the order of $a\tau$ times the flux of n times scattered light, so that the series converges rapidly.

It should be noted that the idea of applying a method of this kind is not new. The well-known law of Lommel-Seeliger is, for example, the single-scattering term for a semi-infinite atmosphere. King's calculations,[1] though presented in the form of type II, are actually of type I. Further, L. S. Ornstein[7] and A. Hammad and S. Chapman[8] have suggested this method. However, it gains sufficient power only in the present context, where the result can be used in conjunction with the formulae obtained by method III and thus be transformed into a completely rigorous solution, if so desired.

II. THE STANDARD PROBLEM

Definitions.—Let the atmosphere be bounded by two parallel planes that for convenience we shall call "horizontal." The cosine of the angle between any direction and the downward vertical will be denoted by μ. The radiation that is incident on the top of the atmosphere has a direction for which μ has a positive value, μ'. Let $s' = 1/\mu'$. The radiation field inside the atmosphere will contain both upward- and downward-directed radiations. For the upward radiation, $\mu < 0$, we shall put $s = -1/\mu$; for the downward radiation, $\mu > 0$, we shall put $s = 1/\mu$; s is therefore always positive.

The intensities of upward- and downward-directed radiations at a depth x below the top boundary will be denoted by $I^-(s, s', x)$ and $I^+(s, s', x)$, respectively. We shall denote the reflected and transmitted intensities by

$$R(s, s') = I^-(s, s', 0)$$

and

$$T(s, s') = I^+(s, s', \tau),$$

respectively. Here τ is the total optical thickness of the atmosphere.

We shall further normalize the functions R and T by requiring that the flux incident on a unit area of the top boundary be π. Diffuse reflection according to Lambert's law, would then make $R(s, s')$ identically 1. We may therefore say that $R(s, s')$ is the *Re-*

[6] Paper XIV, *Ap. J.*, **105**, 164, 1946, and following papers.

[7] *M.N.*, **97**, 207, 1937.

[8] *Phil. Mag.*, **28**, 99, 1939.

flected intensity expressed in terms of the intensity that would obtain in the case of Lambert reflection.

Let πr and πt denote the flux of radiation that emerges from a unit area of the top boundary or the bottom boundary, respectively. Then

$$r(s') = 2\int_1^\infty R(s, s')\frac{ds}{s^3}, \qquad t(s') = 2\int_1^\infty T(s, s')\frac{ds}{s^3}. \tag{1}$$

Recursion formulae for the intensities of n *times scattered light.*—We shall now use a subscript n to denote the various quantities pertaining to the light which has been

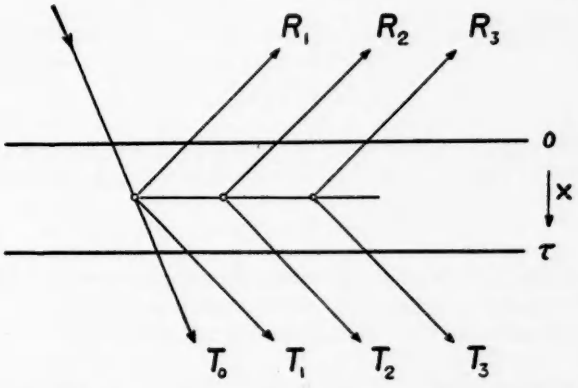

FIG. 1.—Schematic diagram of multiple scattering in the standard problem

scattered exactly n times (cf. Fig. 1). Scattering of the intensity, I_n, will then give rise to a source function, J_{n+1}, of the $n+1$ times scattered light as follows:[9]

$$J_{n+1}(x) = \frac{a}{2}\int_1^\infty \{I_n^+(s, x) + I_n^-(s, x)\}\frac{ds}{s^2}. \tag{2}$$

This source function, in turn, gives rise to the intensities,

$$I_{n+1}^-(s, x) = s\int_x^\tau J_{n+1}(z)\, e^{(x-z)s}dz, \qquad I_{n+1}^+(s, x) = s\int_0^x J_{n+1}(z)\, e^{(z-x)s}dz. \tag{3}$$

Equations (2) and (3) form a recursion scheme from which the entire radiation field may, in principle, be derived. Eliminating the I's, we find the recursion formula,

$$\begin{aligned} J_{n+1}(x) &= \frac{a}{2}\int_0^\tau J_n(z)\, E_1(|x-z|)\, dz \\ &= \frac{a}{2}\int_0^x J_n(x-y)\, E_1(y)\, dy + \frac{a}{2}\int_0^{\tau-x} J_n(x+y)\, E_1(y)\, dy, \end{aligned} \tag{4}$$

[9] The additional arguments, s' and τ, on which all these functions depend, need not be written down.

where $E_1(y)$ denotes the exponential integral (appen., sec. 2).[10] The corresponding emergent intensities are

$$R_n = s\int_0^\tau J_n(x)\, e^{-xs}dx\,,$$
$$T_n = s\int_0^\tau J_n(x)\, e^{-(\tau-x)s}dx\,. \tag{5}$$

Further, according to equations (1), the emerging fractions of the incident flux are

$$r_n = 2\int_0^\tau J_n(x)\, E_2(x)\, dx\,,$$
$$t_n = 2\int_0^\tau J_n(\tau - x)\, E_2(x)\, dx\,. \tag{6}$$

Finally, we shall denote by f_n the fraction of the incident flux that is scattered *at least* n times. Then

$$f_n = 4\int_0^\tau J_n(x)\, dx\,. \tag{7}$$

The factor 4 in this equation arises from the fact that a unit point source emits the flux 4π, i.e., 4 times the incident flux. If no radiation is lost by absorption ($a = 1$) we must further have

$$f_{n+1} = f_n - r_n - t_n\,. \tag{8}$$

The correctness of this equation can be verified by means of equations (4), (6), and (7).

Exact expressions for first- and second-order scattering.—After these preliminaries we can write down the formulae for the light that is scattered not at all, once, twice, etc., by straightforward integrations.

n = *0*.—The incident radiation is confined to a small solid angle, $\Delta\omega$, about one direction. In order that the flux on a unit area of the top of the atmosphere may be π, the specific intensity inside this solid angle must be $s'\pi/\Delta\omega$. This gives for the direct radiation the intensities,

$$I_0^-(x) = \frac{s'\pi}{\Delta\omega}\, e^{-s'x} \qquad \text{and} \qquad T_0 = \frac{s'\pi}{\Delta\omega}\, e^{-s'\tau}\,.$$

The transmitted fraction of the total flux is

$$t_0 = e^{-s'\tau}\,.$$

Further, the source density for primary scattering is

$$J_1(x) = \frac{a\,s'}{4}(1 - e^{-s'\tau})\,,$$

and the fraction of the flux that is scattered once is

$$f_1 = a\,(1 - e^{-s'\tau})\,.$$

n = *1*.—Equations (5) give to the reflected and transmitted intensities the expressions

$$R_1 = a\,\frac{s\,s'}{4\,(s + s')}\{1 - e^{-\tau(s+s')}\}$$

and

$$T_1 = a\,\frac{s\,s'}{4\,(s - s')}\{e^{-\tau s'} - e^{-\tau s}\,.$$

[10] The mathematical formulae needed in these integrations have been collected in an appendix (pp. 240–46).

The corresponding flux integrals are

$$r_1 = a\,\frac{s'}{2}\,F_2(-s',\tau)$$

and

$$t_1 = a\,\frac{s'}{2}\,F_2(s',\tau)\,e^{-s'\tau}.$$

Further, the new source density derived from equation (4) is

$$J_2(x) = a^2\,\frac{s'}{8}\,e^{-xs'}\{F_1(s',x) + F_1(-s',\tau - x)\}.$$

The functions $F_n(b, x)$ that occur in these expressions are defined by the integral,

$$F_n(b,x) = \int_0^x e^{bt}E_n(t)\,dt.$$

The properties of these functions have been discussed in the appendix (secs. 3 and 4).

Finally, using equation (7), we find the flux of radiation scattered twice to be (appen., sec. 5):

$$f_2 = \frac{a^2}{2}[(1 - e^{-\tau s'})\{1 - E_2(\tau)\} + F_1(-s',\tau) - e^{-\tau s'}F_1(s,\tau)].$$

Using the recursion formula for the F-functions, we can easily verify equation (8),

$$f_2 = f_1 - r_1 - t_1,$$

for the case $a = 1$ as a check.

n = *2.*—The reflected and transmitted intensities of light that is scattered twice follow from equations (5) by substituting for $J_2(x)$ the expression just derived and by using the definite integrals of the appendix, section 5. The resulting expressions are

$$R_2 = \frac{a^2 s s'}{8(s+s')}[F_1(-s,\tau) + F_1(-s',\tau) - e^{-(s+s')\tau}\{F_1(s,\tau) + F_1(s',\tau)\}]$$

and

$$T_2 = \frac{a^2 s s'}{8(s-s')}[e^{-\tau s'}\{F_1(-s,\tau) + F_1(s',\tau)\} - e^{-\tau s}\{F_1(-s',\tau) + F_1(s,\tau)\}].$$

At this stage in our calculation the same thing happens as has happened in all earlier investigations of this kind: the integrations become too complex. Neither the new source function, $J_3(x)$, nor the flux integrals, r_2, t_2, and f_3, can be expressed in terms of simple functions involving the exponential integrals. However, we shall presently see that the terms with $n = 1$ and $n = 2$ already form a suitable approximation that can be introduced into the general equations of Chandrasekhar and thus lead to significant results.

Separation of the solution.—Chandrasekhar has proved that the rigorous solution must have the form (Paper XXII, § 7)

$$R = \frac{a s s'}{4(s+s')}\{X(s)X(s') - Y(s)Y(s')\},$$

$$T = \frac{a s s'}{4(s-s')}\{X(s)Y(s') - Y(s)X(s')\} + T_0. \qquad (9)$$

These equations follow from the paper referred to[11] by noting that the s and s' used here are the inverse values of the μ and μ_0 used there and that the functions derived there are, by definition, $F\mu\mu_0$ times the R and T used in the present paper.

[11] Paper XXII, *Ap. J.*, **107**, 48, 188, 1948.

The results derived above can be re-written in the form,

$$\begin{aligned} R &= R_1 + R_2 + \text{terms of the order of } (a\tau)^3 , \\ T &= T_0 + T_1 + T_2 + \text{terms of the order of } (a\tau)^3 . \end{aligned} \tag{10}$$

By an inspection of the formulae for R_1, T_1, R_2, and T_2, we find that equations (10) can indeed be written in the form (9), if we assume that $X(s)$ and $Y(s)$ have the following values:

$$\begin{aligned} X(s) &= 1 + \tfrac{1}{2} a F_1(-s, \tau) , \\ Y(s) &= e^{-\tau s} \{ 1 + \tfrac{1}{2} a F_1(s, \tau) \} . \end{aligned} \tag{11}$$

This solution is still an approximate one. Terms of the order of $(a\tau)^2$ and higher are still lacking. However, for any small value of $a\tau$ equations (11) already give a satisfactory approximation. Depending on the accuracy required, this approximation may be used as it stands, or it may be used as a "starting solution" in Chandrasekhar's functional equations and in that way lead to a numerical solution of any desired degree of accuracy.

III. ALTERNATIVE DEDUCTION; PHYSICAL EXPLANATION OF THE FUNCTIONS $X(s)$ AND $Y(s)$

Although the results of the preceding section are satisfactory, the method by which they were derived is not elegant. In particular, we combined two entirely different points of view, between which there is no apparent relation. The recursion formulae and the consequent expressions for R_1, R_2, T_1, and T_2 were based on a visualization of the multiple scattering; the final separation of the solution, however, was based on the general equations derived by Chandrasekhar from the equations of transfer and certain invariances characterizing the angular distribution of the emergent radiation.

It appeared worth while, therefore, to make an effort to resolve this duality and place the entire deduction on the basis of a visual understanding of the problem. We shall show that it is, in fact, possible to assign definite physical meanings to the functions $X(s)$ and $Y(s)$. In terms of these meanings the formulae become very transparent and the relevant equations can be written down almost immediately.

Physical meaning of X(s) *and* Y(s).—Basic to the present deduction is the physical meaning to be attached to these functions. We shall start by defining these functions as follows: Let a point source of unit brightness (emitting the total flux 4π) be placed at some distance above the plane-parallel atmosphere. Part of the light of this light-source will suffer multiple scattering, resulting in transmission and reflection by the atmosphere. Now the same point source together with the illuminated part of the atmosphere will from a very large distance again appear as a point source. The *brightness of this combined source* will be denoted by $X(s)$ for directions on the same side as the illuminating source and by $Y(s)$ for directions on the opposite side (see Fig. 2). In either case, s is the positive secant of the angle with the normal.

The following, equivalent, definition is a little more convenient. Let a homogeneously emitting, but completely transparent, layer be placed above the atmosphere. Then $X(s)$, respectively $Y(s)$, is the ratio of the intensity emitted by the luminous layer together with the atmosphere to the intensity that would be emitted by the luminous layer alone.

We shall now use this definition in order to express X and Y in terms of the reflection and transmission functions, $R(s, s')$ and $T(s, s')$, defined in the preceding section. Earlier we adopted the normalization that the flux reaching a unit area of the top of the atmosphere is π. If the incident radiation comes from various directions, s', its intensity, $I(s')$, must therefore satisfy the equation

$$2\int_1^\infty I(s') \frac{ds'}{s'^3} = 1 . \tag{12}$$

Accordingly, the intensities of reflected and transmitted radiation emerging in a direction s are

$$2\int_1^\infty R(s, s')\, I(s')\, \frac{ds'}{s'^3} \quad \text{and} \quad 2\int_1^\infty T(s, s')\, I(s')\, \frac{ds'}{s'^3}, \tag{13}$$

respectively. Only the function $T_0(s, s')$, representing the direct transmission, has to be defined more precisely than we did before. Equation (13) shows that the correct intensity, $I(s)\ e^{-s\tau}$, of the directly transmitted light is obtained if $T_0(s, s')$ has the form

$$T_0(s, s') = \tfrac{1}{2} s^3 e^{-s\tau} \delta(s, s'), \tag{14}$$

where $\delta(s, s')$ is the usual δ-function.

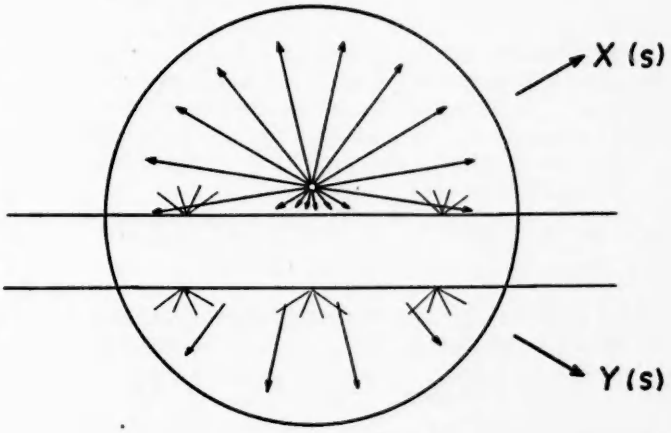

FIG. 2.—Physical meaning of $X(s)$ and $Y(s)$. The combined brightness of the light-source and the illuminated atmosphere in a given direction is $X(s)$, or $Y(s)$, times the brightness of the source alone.

Now the intensity of the thin luminous layer is proportional to s'. According to equation (12), we must therefore put

$$I(s') = \frac{s'}{2}. \tag{15}$$

Substituting this value in equation (13) and dividing the result by the intensity, $s/2$, of the layer alone, we obtain at once

$$\begin{aligned} X(s) &= 1 + \frac{2}{s}\int_1^\infty R(s, s')\, \frac{ds'}{s'^2}, \\ Y(s) &= \frac{2}{s}\int_1^\infty T(s, s')\, \frac{ds'}{s'^2}. \end{aligned} \tag{16}$$

The term 1 on the right-hand side for $X(s)$ stands for the unmodified radiation that is emitted by the luminous layer in directions away from the atmosphere. Using equation (14), we find that a similar term, $e^{-s\tau}$, is included in $Y(s)$ as the term due to the directly transmitted light.

Reciprocal meaning of X(s) *and* Y(s).—Now it should be noted that any function occurring in scattering problems has two reciprocal meanings, corresponding to the different senses of direction of the light-rays. The reciprocal meaning of $X(s)$ and $Y(s)$, suggested by inverting the direction of the radiation in Figure 2, is the following:

Considering again the standard problem, wherein the radiation is incident from one direction, s', we observe that the *density of radiation* above the atmosphere divided by the density of radiation of the incident light is $X(s')$. The corresponding density below the atmosphere in terms of the same units is $Y(s')$; for the integrals that define these radiation densities are identical with those in equations (16).

Expression of R *and* T *in terms of* X *and* Y.—We shall now derive some equations by which $R(s, s')$ and $T(s, s')$ can be expressed in terms of $X(s)$ and $Y(s)$. Let us consider again the standard case, with incident radiation in the direction s' and emergent radiation in the direction s. Now we add a layer with thickness $d\tau$ to the top of the atmosphere. The source density of scattered radiation inside this layer is proportional to the radiation density. In fact, equation (2) shows that

$$J = \frac{a s'}{4} X(s')$$

inside this layer. If this layer were alone, it would emit the intensities $sJd\tau$, according to equation (5). Because of the presence of the atmosphere, however, these intensities have to be multiplied by $X(s)$ or $Y(s)$. Further, we have to allow for the fact that the layer scatters, or absorbs, a small part of the radiation that would be reflected, or transmitted, otherwise. We find therefore that the addition of this thin layer increases the intensities, $R(s, s')$ and $T(s, s')$, by the amounts,

$$dR(s, s') = -(s' + s) R(s, s')\, d\tau + \tfrac{1}{4} a s s' X(s')\, X(s)\, d\tau$$

and

$$dT(s, s') = -s' T(s, s')\, d\tau + \tfrac{1}{4} a s s' X(s')\, Y(s)\, d\tau .$$

Instead of adding a layer to the top, we may equally add a layer to the bottom of the atmosphere. In the latter case the source density in this layer becomes

$$J = \frac{a s'}{4} Y(s') ,$$

and the reflected and transmitted intensities are increased by

$$dR(s, s') = \tfrac{1}{4} a s s' Y(s')\, Y(s)\, d\tau$$

and

$$dT(s, s') = -sT(s, s')\, d\tau + \tfrac{1}{4} a s s' Y(s')\, X(s)\, d\tau .$$

Since the net effect of an additional layer at top or bottom must be the same, we may equate the two expressions for $dR(s, s')$ and those for $dT(s, s')$. The result is that, identically with equations (9),

$$R(s, s') = \frac{a s s'}{4(s + s')} \{ X(s)\, X(s') - Y(s)\, Y(s') \}$$

$$T(s, s') = \frac{a s s'}{4(s - s')} \{ X(s)\, Y(s') - Y(s)\, X(s') \} + T_0(s, s') . \tag{17}$$

The value of the transmission term, $T_0(s, s')$, of the direct light is not found by means of this deduction because it vanishes except for $s - s' = 0$. Therefore, we have added this term as a separate term.

Functional equations for X *and* Y.—Substituting equations (17) in equations (16), we obtain the functional equations,

$$X(s) = 1 + \frac{a}{2s} \int_1^\infty \frac{s s'}{s + s'} \{ X(s)\, X(s') - Y(s)\, Y(s') \} \frac{ds'}{s'^2} ,$$

$$Y(s) = e^{-\tau s} + \frac{a}{2s} \int_1^\infty \frac{s s'}{s - s'} \{ X(s)\, Y(s') - Y(s)\, X(s') \} \frac{ds'}{s'^2} . \tag{18}$$

These relations are the basic equations in the mathematical treatment given in Chandrasekhar's paper (Paper XXII, eqs. [172] and [173]). For a detailed discussion we may refer to that paper.

Integrodifferential equations for X *and* Y.—By similar reasoning we can derive integrodifferential equations for $X(s)$ and $Y(s)$. Let us place a luminous layer, emitting the intensity s', above an atmosphere of optical thickness τ. The intensity emerging at the bottom is then, by definition, $s\,Y(s)$. Now add to the bottom a layer of thickness $d\tau$. The source density in this layer, according to equation (2), will be

$$\frac{a}{2}\int_1^\infty Y(s)\,\frac{ds}{s} \equiv y_{-1}\,. \tag{19}$$

The emergent intensities due to this additional source density will be, again by definition, $y_{-1}sd\tau Y(s)$ for upward radiation and $y_{-1}sd\tau X(s)$ for downward radiation. Further, the radiation transmitted by the original atmosphere loses a fraction $sd\tau$ of its amount because of the additional layer. Equating the new intensities thus found to $s(X + dX)$ and $s(Y + dY)$, we obtain at once the equations

$$\begin{aligned} \frac{dX(s)}{d\tau} &= y_{-1}Y(s)\,, \\ \frac{dY(s)}{d\tau} + sY(s) &= y_{-1}X(s)\,. \end{aligned} \tag{20}$$

These equations have also been derived by Chandrasekhar (*ibid.*, eqs. [175] and [176]).

Series expansion of X(s) *and* Y(s).—The physical interpretation of the functions $X(s)$ and $Y(s)$ has the great advantage of suggesting a rapid method for calculating them. Thus, let us consider the scattering of light emitted by a luminous layer on top of the atmosphere. We may use the same formulae for multiple scattering that were used in Section II.

Let the source density inside the luminous layer be

$$J_0 = \delta(x, 0)\,.$$

The source density for the scattering of any order may then be computed by means of equation (4). In particular, we obtain

$$J_1 = \frac{a}{2}E_1(x)\,.$$

The next term will be

$$J_2 = \frac{a^2}{4}\int_0^x E_1(x-y)\,E_1(y)\,dy + \frac{a^2}{4}\int_0^{\tau-x} E_1(x+y)\,E_1(y)\,dy\,,$$

in which the first integral is identical to $G'_{11}(x)$ (appen., sec. 9) and the second integral has a similar nature. It does not seem profitable to go further into the calculations of these integrals, except by means of approximations or by numerical methods.

The corresponding intensities of emergent light follow from equations (5). Their values, divided by the intensities, s, that the luminous layer itself would emit, give the functions $X_n(s)$ and $Y_n(s)$, so that

$$\begin{aligned} X_n(s) &= \int_0^\tau J_n(x)\,e^{-xs}dx\,, \\ Y_n(s) &= e^{-\tau s}\int_0^\tau J_n(x)\,e^{xs}dx\,. \end{aligned} \tag{21}$$

By adding the functions due to scattering of any order we have

$$X(s) = X_0(s) + X_1(s) + X_2(s) + \dots,$$
$$Y(s) = Y_0(s) + Y_1(s) + Y_2(s) + \dots. \tag{22}$$

These functions follow from the total source density,

$$J(x) = J_0(x) + J_1(x) + J_2(x) + \dots, \tag{23}$$

by

$$X(s) = \int_0^\tau J(x)\, e^{-xs} dx,$$
$$Y(s) = e^{-\tau s} \int_0^\tau J(x)\, e^{xs} dx. \tag{24}$$

Thus, writing only the terms of order 0 and 1 and using the expressions for $J_0(x)$ and $J_1(x)$ given above, we find

$$X(s) = 1 + \frac{a}{2} F_1(-s, \tau),$$
$$Y(s) = e^{-s\tau} \left\{ 1 + \frac{a}{2} F_1(s, \tau) \right\}. \tag{25}$$

These equations are identical with equations (11), found in Section II only after a lengthy calculation.

Equations (24) further explain the existence of one more formula derived by Chandrasekhar:

$$Y(s) = e^{-\tau s} X(-s). \tag{26}$$

This relation, however, is only a formal one, because only the values of $s > 1$ have physical significance. The actual functions $X(s)$ and $Y(s)$ to be computed are two entirely different functions.

It should be noted that the indices, $n = 0, 1, 2, \dots$, occurring in the present deduction do not exactly correspond to the indices n used in Section II. There the index n denoted the nth-order term in a series expansion of $R(s, s')$ and $T(s, s')$ in powers of a. Here, however, they denote the same in an expansion of $X(s)$ and $Y(s)$. The exact relation, equations (24), shows that there is no simple correspondence. It is easily seen, however, that formulae for $X(s)$ and $Y(s)$ complete to the nth order, when substituted in equations (24), will give $R(s, s')$ and $T(s, s')$ complete up to the $n + 1$th order plus further incomplete terms. Thus the first-order approximation of X and Y, equations (11) or equations (25), was sufficient to obtain the second-order approximation of R and T.

IV. CALCULATION OF THE THIRD-ORDER TERM

It is not the object of the present paper to go into the numerical computations that are needed for reaching the utmost accuracy. The relative simplicity of the formulae prompts us, however, to calculate at least one further term of the solutions. This calculation will give us the second-order terms of $X(s)$ and $Y(s)$ and, accordingly, the third-order terms of $R(s, s')$ and $T(s, s')$.

It is not feasible to calculate the exact values of these terms; for we have seen, both in Section II and in Section III, that the source functions from which these terms have to be derived already involve integrals of too complex a type. It is possible, however, to find satisfactory approximations if $s\tau$ is not too large.

New terms of X *and* Y.—We shall first derive the values that would hold in the (physically impossible) case of $s = 0$. Equations (21) become for that case

$$X_2(0) = Y_2(0) = \int_0^\tau J_2(x)\, dx.$$

This integral can be calculated exactly. Expressing $J_2(x)$ by an integral according to equation (4) and inverting the order of integration, we obtain

$$\int_0^\tau J_2(x)\,dx = \frac{a}{2}\int_0^\tau \{2 - E_2(z) - E_2(\tau - z)\} J_1(z)\,dz .$$

With the substitution $J_1(z) = \frac{1}{2}aE_1(z)$ in the foregoing equation, the result becomes

$$X_2(0) = Y_2(0) = \frac{a^2}{4} g(\tau), \tag{27}$$

where

$$g(\tau) = 2 - 2E_2(\tau) - G_{12}(\tau) - G'_{12}(\tau). \tag{28}$$

The functions

$$G_{mn}(\tau) = \int_0^\tau E_m(z) E_n(z)\,dz \quad \text{and} \quad G'_{mn}(\tau) = \int_0^\tau E_m(z) E_n(\tau - z)\,dz$$

occurring in this expression are discussed in the appendix, sections 7–10.

The same result may be derived in several other ways. For example, we may use the differential equations (20). We shall denote the approximate solution expressed by equations (25) by $X^*(s)$ and $Y^*(s)$. This solution may be used as a starting solution. The value of y_{-1} corresponding to this solution is (cf. appen., sec. 6):

$$\begin{aligned} y^*_{-1} &= \frac{a}{2}\int_1^\infty \left\{ e^{-\tau s} + \frac{a}{2} e^{-\tau s} F_1(s, \tau) \right\} \frac{ds}{s} \\ &= \frac{a}{2} E_1(\tau) + \frac{a^2}{4} G'_{11}(\tau). \end{aligned} \tag{29}$$

After substituting this expression and the expression for $Y^*(s)$ in the right-hand side of equation (20), we obtain an expression for $dX(s)/d\tau$ which is correct up to terms of the order of $a^2\tau$, inclusive. Again we find that integration is feasible only for the case $s = 0$. The integration for that case can be made after some reduction and gives, indeed, a result identical with equation (27).

In the derivation of equation (27) we have been forced to assume that $s = 0$. We shall now derive an approximate expression, useful for any value of s, by assuming that the source function $J_2(x)$ is approximately constant. It follows, then, from equations (21) that $X_2(0)$ and $Y_2(0)$ have to be multiplied by

$$\frac{1}{\tau}\int_0^\tau e^{-sx} dx = \frac{1}{s\tau}(1 - e^{-s\tau})$$

in order to obtain the values for $X_2(s)$ and $Y_2(s)$. So we have

$$X - X^* = Y - Y^* = \frac{a^2}{4} g(\tau) \frac{1}{s\tau}(1 - e^{-s\tau}). \tag{30}$$

It should be noted that the approximate values of X and Y defined by this equation exactly satisfy the relation expressed by equation (26).

Final expressions for R *and* T.—We may finally investigate the consequences of this additional term for the reflected and transmitted intensities, $R(s, s')$ and $T(s, s')$. Let the values of R and T obtained by substituting the approximate solutions X^* and Y^* in equations (17) be denoted by R^* and T^*. The improved values of R and T will then be found by substituting in the same equation the improved solutions,

$$X(s) = X^*(s) + U(s)$$

and

$$Y(s) = Y^*(s) + U(s).$$

Here $U(s)$ has been written for the right-hand member of equation (30).

For convenience of notation we shall for a moment omit the asterisks from X^* and Y^* and denote the argument s' by adding a prime to the symbols $X, Y,$ and U. The quantities in braces in equations (17) can then be reduced as follows:

$$(X+U)(X'+U') - (Y+U)(Y'+U') = XX' - YY' + U'(X-Y) + U(X'-Y'),$$

and

$$(X+U)(Y'+U') - (Y+U)(X'+U') = XY' - YX' + U'(X-Y) - U(X'-Y').$$

The first two terms on the right-hand side of these equations give rise to the original values, R^* and T^*. Now we may neglect terms that are of the order of $a\tau$ times the term we seek to derive. Therefore,

$$X(s) - Y(s) = 1 - e^{-s\tau}.$$

Thus it appears that the remaining terms of the expressions just derived have the factor

$$(1 - e^{-s\tau})(1 - e^{-s'\tau})$$

in common. A simple reduction now gives:

$$R - R^* = T - T^* = \frac{a^3}{16\tau} g(\tau)(1 - e^{-\tau s})(1 - e^{-\tau s'}). \tag{31}$$

The result that the correction terms of R and T turn out to be the same is not unexpected; for the derivation of equation (31) holds strictly only if we assume that both τs and $\tau s'$ are small compared to 1. This assumption amounts to saying that we consider only angles for which the atmosphere is transparent. In that case the intensity emerging at either side of the atmosphere must be the same function of the angle of emergence. If, on the other hand, τs is large, the factor $1 - e^{-\tau s}$ gives correctly the effective depth of the atmosphere in the direction s, but the assumption that the average source density in that layer equals the average source density in the entire atmosphere is no longer correct.

It should be noted that the earlier approximation, R^* and T^*, is useful in a much wider range than is the correction term just derived; for the terms of X^* and Y^* are the rigorous expressions for the first two terms in series expansions of X and Y in powers of a. Therefore, these expressions provide a useful approximation as soon as $a\tau \ll 1$. The correction term given by equation (31), however, is subject to the further restriction that $s\tau \ll 1$, i.e., that τ itself must be $\ll 1$. Thus, in the case of a thick atmosphere with heavy absorption (so that $a\tau$ is small), the approximations R^* and T^* are still useful, but the expression for the correction term cannot be trusted.

Practical computation.—Recapitulating the relevant formulae, we may state, first, that the values of X^* and Y^* have to be computed according to equations (25). Then, in accordance with equations (17), the values of R^* and T^* follow from

$$R^*(s, s') = \frac{a s s'}{4(s+s')}\{X^*(s)\,X^*(s') - Y^*(s)\,Y^*(s')\},$$

$$T^*(s, s') = \frac{a s s'}{4(s-s')}\{X^*(s)\,Y^*(s') - Y^*(s)\,X^*(s')\} + T_0. \tag{32}$$

Finally, the correction term to be added to both these values can be computed from equation (31), where $g(\tau)$ is given by equation (28).

One further remark of a practical nature may be made. Equation (32) leaves T^* in-

determinate for $s = s'$. We can easily find a correct formula for this case by putting $s' = s - ds$ and letting ds approach 0. The formula thus obtained is

$$T(s, s) = \frac{a s^2}{4} \left\{ \frac{dX}{ds} Y(s) - \frac{dY}{ds} X(s) \right\}. \tag{33}$$

The derivatives corresponding to equations (25) are (appen., sec. 3)

$$\frac{dX}{ds} = \frac{a}{2}\left[\frac{1}{s+1} \{ e^{-(s+1)\tau} - 1 \} + F_2(-s, x) \right]$$

and (34)

$$\frac{dY}{ds} = -\tau Y(s) + \frac{a}{2} e^{-s\tau}\left[\frac{1}{s-1} \{ e^{(s-1)\tau} - 1 \} - F_2(s, x) \right].$$

The substitution of these expressions, and of equations (25) themselves, in equation (33) does not lead to any particularly simple result. It would therefore seem that formula (33) is best used directly for numerical computations.

Numerical example.—The use of the foregoing formulae may be illustrated by a numerical example. Let $\tau = 0.10$, $s = s' = 2$, and $a = 1$. Equations (25) then give

$$X^* = 1.1280 \quad \text{and} \quad Y^* = 0.9423 .$$

The corresponding derivatives, found from equations (34), are

$$\frac{dX^*}{ds} = -0.0051 \quad \text{and} \quad \frac{dY^*}{ds} = -0.08891 .$$

The approximate values of R and T are then found from equations (32) and (33), respectively:

$$R^* = 0.09611 \quad \text{and} \quad T^* = 0.09548 .$$

The correction term, computed by means of equation (31), is equal to 0.00184; so the values are:

$$R = 0.09795 \quad \text{and} \quad T = 0.09732 .$$

In this computation the tables of the E-, F-, and G-functions given at the end of this paper have been used.

It is thus seen that, even without any process of further numerical improvement, the formulae give results that are satisfactory for most purposes. A rough estimate of the higher-order terms by means of the rule that subsequent terms are in the ratio $ac(\tau) = 0.163$ (eq. [60]) shows that the values just computed are still too low by about 0.00045. This final correction is 0.5 per cent; the remaining uncertainty is less than 0.1 per cent.

V. THE PLANET PROBLEM

We shall now discuss the problem of scattering by a homogeneous atmosphere under which is a diffusely reflecting surface with an albedo b. We shall assume that the diffuse reflection follows Lambert's law, i.e., that the reflected radiation has the same intensity in all (outward) directions. The scattering properties of the atmosphere need not be specified beyond the general requirement that its reflection and transmission in the absence of a ground surface be described by the symmetrical functions $R(s, s')$ and $T(s, s')$. The symmetry of these functions is required because of the "reciprocity principle" of Helmholtz.

General formulae.—We may first compute the angular distribution with which the diffuse radiation that comes from the ground surface is transmitted or reflected to the

bottom again. In this case the intensity, $I(s')$, of the radiation incident on the atmosphere from below is a constant, C, say. The intensities of transmitted and reflected light are, then, according to equations (13),

$$2C\int_1^\infty R(s, s')\frac{ds'}{s'^3} = C\,r(s)$$

and (35)

$$2C\int_1^\infty T(s, s')\frac{ds'}{s'^3} = C\,t(s)\,,$$

respectively. Here $r(s)$ and $t(s)$ are the same integrals as occurred in the calculation of the flux in the standard problem; for their definition by means of equations (35) is equivalent to their definition by means of equations (1), because of the symmetry of R and T.

Further, the total flux of the transmitted and reflected light will be denoted by

$$2\pi C\int_1^\infty r(s)\frac{ds}{s^3} = \pi C\,r_c$$

and (36)

$$2\pi C\int_1^\infty t(s)\frac{ds}{s^3} = \pi C\,t_c\,,$$

where r_c and t_c are constants.

Equations (35) and (36) are all we need in order to solve the planet problem entirely. In the following we shall treat two slightly different cases. In case A we assume that the radiation is incident from outside; this case corresponds to the illumination of the planet by the sun. In case B we assume diffuse emission by the ground surface; this case corresponds to the scattering and absorption of the planet's own radiation.

A. Let the radiation be incident from one direction, s'. We assume, as in the standard case, that the flux incident on a unit area of the top of the atmosphere is π. The constant surface brightness, C, of the bottom surface can then be computed by considering the flux equation at this level.

The flux incident on the bottom surface consists of two parts: a part, $\pi t(s')$, of radiation that has never reached this surface before and a part, $\pi C r_c$, of radiation that has been reflected by this surface before and is now reflected to the bottom again. The flux emitted by the bottom surface is simply πC. Since the emitted flux must be b times the incident flux, we have

$$\pi C = \pi b\{C\,r_c + t(s')\}\,.$$

Hence

$$C = \frac{b\,t(s')}{1 - b\,r_c}\,. \tag{37}$$

The intensity reflected by the entire system of atmosphere plus ground surface consists also of two parts. The part that comes from the atmosphere will be denoted by $R(s, s')$, as in the standard problem. The part that comes, directly or indirectly, from the bottom is given by equation (35), where C has the value given by equation (37). Thus we obtain

$$R_{\text{planet}}(s, s') = R(s, s') + \frac{b}{1 - b\,r_c}\,t(s)\,t(s')\,. \tag{38}$$

This is the final formula by means of which any problems of phase-function, limb darkening, etc., of a planet may be solved, once a satisfactory solution of the standard problem has been obtained.

There is no "transmitted light" in the present case. However, we may inquire what the angular intensity distribution, measured by an observer at the base of the at-

mosphere, would be. The intensity in any outward direction is equal to C, as stated above. In any downward direction it is obviously

$$I^{+}_{\text{planet}}(s, \tau) = T(s, s') + \frac{b}{1 - b r_c} t(s')\, r(s). \tag{39}$$

The first term of this expression is simply the transmission function for the standard case; it includes the term T_0 of the direct sunlight. The second term is the light from the ground scattered back by the air.

If all our assumptions were correct, equation (39) would give the intensity distribution of the daylight sky. Several modifications have to be made, however, before this is true. First, the standard problem for a finite atmosphere with Rayleigh scattering has to be solved. Chandrasekhar (Paper XXII, Sec. V) has obtained the solution of this problem; the functions occurring in this solution (equivalent to $X[s]$ and $Y[s]$ in the case of isotropic scattering) can probably be determined with sufficient accuracy by means of a method similar to that used in the present paper. Next, the solution should be substituted in equation (39). Because of the polarization, however, we have scattering matrices R and T instead of scattering functions; equation (39) will have to be modified accordingly. Finally, measurements might show that the ground reflects light according to a law different from Lambert's law. This would necessitate a further modification of equation (39), which is also of a fairly simple nature. All these modifications would make the calculations longer but not much more difficult. It would seem, therefore, that the calculation of brightness and polarization of the daylight sky, correctly within 0.1 per cent, is now distinctly within reach of the theory.

B. The converse problem can be solved in a similar way. Let the bottom surface be self-luminous and emit an intensity 1 in all outward directions. The atmosphere will then change both the angular distribution and the amount of the emitted radiation. Again we shall put the *total* surface brightness of the bottom equal to C. This surface brightness consists partly of the original emission and partly of radiation scattered back by the atmosphere and then reflected by the bottom surface again. Therefore,

$$C = 1 + bC r_c;$$

whence

$$C = \frac{1}{1 - b r_c}. \tag{40}$$

The intensity emerging in a direction s from the top of the atmosphere is then

$$I^{-}(s, 0) = \frac{t(s)}{1 - b r_c}. \tag{41}$$

The energy balance.—In some applications one may want to know what happens to the incident *energy*. There are three possibilities: part of the energy may escape into space, another part may be absorbed by the atmosphere, and a third part may be absorbed by the bottom surface. We shall denote these fractions of the incident energy by f_s, f_a, and f_b, respectively.

A. In the case of incident radiation from a direction s' we find by substituting equations (38) in equations (1) that

$$f_s = r(s') + \frac{b t_c}{1 - b r_c} t(s'). \tag{42}$$

Further, the amount absorbed by the bottom is $(1 - b)/b$ times the amount reflected by the bottom, so

$$f_b = \frac{1 - b}{1 - b r_c} t(s'). \tag{43}$$

And, finally, by the conservation of energy we have

$$f_a = 1 - f_s - f_b \,. \tag{44}$$

If the albedo of the atmospheric particles is 1 (this is called a "conservative case"), we have in the standard problem $r(s') + t(s') = 1$ and therefore also $r_c + t_c = 1$. It can be easily verified that in that case $f_a = 0$.

B. A similar calculation for the case of emission by the ground surface leads to the following expression for the distribution of the energy:

$$f_s = \frac{t_c}{1 - o\, r_c}, \qquad f_b = \frac{(1-b)\, r_c}{1 - b\, r_c}, \qquad f_a = 1 - f_s - f_b \,. \tag{45}$$

Again we can verify that $f_a = 0$ in conservative cases.

Isotropic scattering.—The solution of the planet problem given above holds for any scattering properties of the atmosphere. We shall now assume that the atmosphere consists of isotropically scattering particles with an albedo a. The solution of the standard problem for such an atmosphere, given in Sections II–IV, has resulted in the determination of the two functions, $R(s, s')$ and $T(s, s')$. We now have to perform the integrations shown by equations (35) and (36) in order to determine also the functions $r(s)$ and $t(s)$ and the constants r_c and t_c.

Let the *moments* of the functions $X(s)$ and $Y(s)$ be defined by

$$\begin{aligned} x_p &= \frac{a}{2} \int_1^\infty X(s)\, s^{-p-2} ds \,, \\ y_p &= \frac{a}{2} \int_1^\infty Y(s)\, s^{-p-2} ds \,. \end{aligned} \tag{46}$$

The factor $a/2$ here takes the place of the more general "characteristic function," $\Psi(\mu)$, in Chandrasekhar's formulae.

Now we shall show that the functions $r(s)$ and $t(s)$ can be expressed in terms of $X(s)$ and $Y(s)$ and their moments. By substituting in equations (35) equations (17) for $R(s, s')$ and $T(s, s')$, we obtain:

$$r(s) = \frac{a}{2} \int_1^\infty \frac{s}{s+s'} \{ X(s)\, X(s') - Y(s)\, Y(s') \} \frac{ds'}{s'^2}$$

and

$$t(s) = \frac{a}{2} \int_1^\infty \frac{s}{s-s'} \{ X(s)\, Y(s') - Y(s)\, X(s') \} \frac{ds'}{s'^2} + t_0(s) \,.$$

The integrands can be separated by means of the relations,

$$\frac{1}{s'(s+s')} = \frac{1}{ss'} - \frac{1}{s(s+s')}$$

and

$$\frac{1}{s'(s-s')} = \frac{1}{ss'} + \frac{1}{s(s-s')} \,.$$

The first terms on the right-hand side of these equations give rise to products containing the moments x_0 and y_0. The second terms give integrals identical with those in equations (18). Thus we obtain (cf. Paper XXII, eqs. [13] and [14])

$$\begin{aligned} r(s) &= x_0 X(s) - y_0 Y(s) - X(s) + 1 \,, \\ t(s) &= y_0 X(s) - x_0 Y(s) + Y(s) \,. \end{aligned} \tag{47}$$

The term $t_0 = \exp(-\tau s)$ that is contained in $t(s)$ cancels out against the same term with negative sign occurring in the other part of the integral.

By substituting this result in equations (37) we further find directly:

$$r_c = \frac{4}{a}(x_0 - 1)\, x_1 - \frac{4}{a}\, y_0 y_1 + 1\,,$$
$$t_c = \frac{4}{a}\, y_0 x_1 - \frac{4}{a}(x_0 - 1)\, y_1\,. \tag{48}$$

Equations (47) and (48) give the exact expressions for $r(s)$, $t(s)$, r_c, and t_c in terms of the exact functions $X(s)$ and $Y(s)$. However, since we have only the approximate solutions of $X(s)$ and $Y(s)$ derived in the preceding sections, the following calculation is only approximate.

The expressions we derived for $X(s)$ and $Y(s)$ consist of three terms: the first two terms are given by equations (25) and the third one, which is the same for X and Y, by equation (30). Integrating term by term, we find that the corresponding moments are

$$x_p = \frac{a}{2}\frac{1}{p+1} + \frac{a^2}{4} G_{p+2,1}(\tau) + \frac{a^3}{8}\frac{g(\tau)}{p+1}\,,$$
$$y_p = \frac{a}{2} E_{p+2}(\tau) + \frac{a^2}{4} G'_{p+2,1}(\tau) + \frac{a^3}{8}\frac{g(\tau)}{p+1}\,. \tag{49}$$

Here the first terms follow from an elementary integration. The second terms have been found as shown in section 6 of the appendix. A rigorous expression for the third term cannot be derived, because we do not have expressions for the corresponding terms of $X(s)$ and $Y(s)$ that are correct for large values of $s\tau$. Equation (30) would give

$$\frac{a^3}{8}\frac{g(\tau)}{\tau}\left\{\frac{1}{p+2} - E_{p+3}(\tau)\right\} \tag{50}$$

for the third terms of x_p and y_p. The more convenient form shown in equations (49) was found by integrating equation (27) instead of equation (30). This amounts to the assumption that $X_2(s)$ and $Y_2(s)$ may be put equal to $X_2(0)$ and $Y_2(0)$ in the entire integration interval. Since the third-order term is already a small correction term, the difference between the forms shown by equations (49) and (50) is not important.

In particular we find that the moments of order 0 are

$$x_0 = \frac{a}{2} + \frac{a^2}{4} G_{12}(\tau) + \frac{a^3}{8}\, g(\tau)\,,$$
$$y_0 = \frac{a}{2} E_2(\tau) + \frac{a^2}{4} G'_{12}(\tau) + \frac{a^3}{8}\, g(\tau)\,. \tag{51}$$

Further, the moments of order 1 are

$$x_1 = \frac{a}{4} + \frac{a^2}{4} G_{13}(\tau) + \frac{a^3}{16}\, g(\tau)\,,$$
$$y_1 = \frac{a}{2} E_3(\tau) + \frac{a^2}{4} G'_{13}(\tau) + \frac{a^3}{16}\, g(\tau)\,. \tag{52}$$

Chandrasekhar has shown that there are various relations between the moments x_p and y_p. These relations can be used for a check on the approximate expressions just derived. For example, if $a \neq 1$, x_0 and y_0 satisfy the relation (Paper XXII, eq. [37])

$$(1 - x_0)^2 = 1 - a + y_0^2\,. \tag{53}$$

When equations (51) are substituted in this equation, the coefficients of 1, a, and a^2 satisfy the equation rigorously, but the coefficients of a^3 show a discrepancy. This illustrates once more the fact that the third-order terms in these equations are not exact. The relation for $a = 1$ is

$$x_0 + y_0 = 1 \, . \tag{54}$$

Using the definition of $g(\tau)$, equation (28), we find that this equation is exactly satisfied. A further consequence of this relation is, for $a = 1$,

$$r(s) + t(s) = 1 \, ; \tag{55}$$

this equation expresses the conservation of energy in the standard problem.

Practical computation.—Although we have now a complete set of equations for solving the planet problem, we have not yet arrived at the formulae that are most suitable for numerical computation. First, we may remark that, if the atmosphere is thick or if a solution of very high accuracy is required, the method outlined above needs only little change. This change consists in the first step: the moments x_0, y_0, x_1, and y_1 have to be computed by direct integration from the exact X- and Y-functions rather than from the approximate equations (51) and (52). The further steps remain the same: by substituting the moments in equations (47) and (48), we find $r(s)$, $t(s)$, r_c, and t_c. Finally, these functions and constants, when substituted in any of the equations (38)–(45), will give the solution of some problem in planetary illumination.

If, however, the atmosphere is thin, accurate results may be obtained in a much more rapid way. In particular, it is then possible to avoid the moments entirely. In fact, in Section II we have already found the exact forms for the terms of $r(s)$ and $t(s)$ that correspond to the direct light and to single scattering. These formulae together give the equations,

$$\begin{aligned} r^*(s) &= \frac{a s}{2} F_2(-s, \tau) \, , \\ t^*(s) &= e^{-\tau s} + \frac{a s}{2} e^{-\tau s} F_2(s, \tau) \, . \end{aligned} \tag{56}$$

Here the asterisk is used to indicate that these expressions are incomplete, the higher-order terms being still absent. Integrating these equations according to equations (36), we further find

$$\begin{aligned} r_c^* &= a G_{22}(\tau) \, , \\ t_c^* &= 2E_3(\tau) + a G'_{22}(\tau) \, . \end{aligned} \tag{57}$$

Equivalent formulae may be derived by substituting equations (51) and (52) in equations (47) and (48). If we use recursion formulae for the F- and G-functions, the expressions thus found can be greatly simplified; the result is that the terms of order 0 and 1 become identical with those in equations (56) and (57).

The higher-order terms cannot be expressed in elementary functions. The derivation of formulae suitable for finding the approximate values of these terms is, therefore, to some extent a matter of taste. It appears most practicable to go back to the calculations in Section II, in which the physical meaning is most evident.

The method proceeds by calculating successively the amounts of radiation that are scattered 0, 1, 2, etc., times. Let the incident amount be 1. Briefly repeating the first steps, we have an amount, t_0, which is directly transmitted. A fraction $1 - a$ of the remainder is absorbed, and the fraction

$$f_1 = a(1 - t_0) \tag{58}$$

is scattered. The amounts of radiation emerging after this first scattering are r_1 and t_1. Again, a fraction $1 - a$ of the remainder is absorbed, and the further fraction, which equals

$$f_2 = a\,(f_1 - r_1 - t_1)\,, \tag{59}$$

is scattered for the second time. This is as far as the rigorous calculation goes.

Now we shall dispose of the remaining energy by assuming that the source density of second- and higher-order scattering may be considered constant through the atmosphere. According to equations (6) and (7), we then have

$$r_n = t_n = \frac{1}{2\tau}\{\tfrac{1}{2} - E_3(\tau)\}\, f_n\,,$$

so that

$$f_{n+1} = a\,c\,(\tau)\, f_n\,, \tag{60}$$

where

$$c\,(\tau) = \frac{1}{2\tau}\{2\tau - 1 + 2E_3(\tau)\}\,. \tag{61}$$

It is seen that in every step $ac(\tau)$ may be described as "the fraction of the scattered flux which will be scattered another time." It is now easy to add all the emergent amounts of radiation in a geometrical series. Thus we obtain

$$r_2 + r_3 + \ldots = t_2 + t_3 + \ldots = \frac{1}{2}\,\frac{1 - c\,(\tau)}{1 - a\,c\,(\tau)}\, f_2\,. \tag{62}$$

Likewise, the total amount of radiation that is absorbed by the atmosphere after being scattered one or more times is

$$\frac{(1 - a)\,c\,(\tau)}{1 - a\,c\,(\tau)}\, f_2\,. \tag{63}$$

These equations can be used for computing the functions $r(s)$ and $t(s)$ as well as the constants r_c and t_c. The exact expressions of t_0, r_1, and t_1 for either case have already been given in equations (56) and (57). Equations (58) and (59) then give f_2; and equations (62) and (63) show how much of this remainder emerges and how much is absorbed.

Numerical example.—These formulae may be illustrated by a numerical example. Let $\tau = 0.1$, $a = 1$, and $s = 2$. We then have

$$\left.\begin{aligned} r^*\,(s) &= 0.0762 \\ t^*\,(s) &= 0.8187 + 0.0755 = 0.8942 \end{aligned}\right\} \text{with} \left\{\begin{aligned} f_1 &= 0.1813\,, \\ f_2 &= 0.0296\,; \end{aligned}\right.$$

and, further,

$$\left.\begin{aligned} r_c^* &= 0.0707 \\ t_c^* &= 0.8326 + 0.0695 = 0.9021 \end{aligned}\right\} \text{with} \left\{\begin{aligned} f_1 &= 0.1674\,, \\ f_2 &= 0.0272\,. \end{aligned}\right.$$

The ratio f_2/f_1 in both cases is 0.163, i.e., practically equal to $c(\tau) = 0.1630$. This is a sufficient guaranty that the computation of the further terms by means of equation (62) is correct.

Since $a = 1$, we have to divide f_2 equally between the reflected and the transmitted light. The final results are

$$r\,(s) = 0.0910\,, \qquad r_c = 0.0843\,,$$

$$t\,(s) = 0.9090\,, \qquad t_c = 0.9157\,.$$

Combining these results with the results of Section IV, we find that equation (38) for $s = s' = 2$, $\tau = 0.1$, $a = 1$, and $b = 0.1$, gives

$$R_{\text{planet}}(s, s') = 0.09795 + 0.08333 = 0.18128 .$$

This result shows that, under the specified conditions, 54 per cent of the planetary light comes from the atmosphere and 46 per cent directly or indirectly from the bottom surface; the entire surface brightness is 0.180 times the brightness of a surface reflecting according to Lambert's law. Problems of limb darkening, visibility of surface markings, formation of absorption lines, etc., can be investigated by means of similar computations.

Under the same conditions, equation (39) yields the following result:

$$I^{+}_{\text{planet}}(s, \tau) = 0.09732 + 0.00834 = 0.10566 .$$

This means that, under the specified conditions, about 8 per cent of the brightness of the daylight sky at 30° above the horizon would arise from reflection by the ground.

This investigation was made in connection with the Symposium on Planetary Atmospheres held at Yerkes Observatory, September 8–10, 1947. With pleasure I recall the stimulating discussions with several members of the Yerkes staff. In particular, I wish to record my thanks to Dr. Chandrasekhar, without whose encouraging interest this paper would not have been written.

Appendix: On Certain Functions Related to the Exponential Integral

1. The exponential integral,

$$Ei(x) = \int_{-\infty}^{x} \frac{e^t}{t}\, dt ,$$

is the elementary function to which most of the following functions can be reduced. Only one further elementary function will be needed; this function will be introduced in section 9.

2. It has been customary for a long time to introduce in problems of radiative transfer the set of functions

$$E_n(x) = \int_1^{\infty} \frac{e^{-xt}}{t^n}\, dt \qquad (x \geq 0,\ n = \text{integer} \geq 1) ,$$

which satisfy the recurrence relation,

$$nE_{n+1}(x) = e^{-x} - xE_n(x)$$

and the differential relation,

$$\frac{d}{dx} E_{n+1}(x) = -E(x) .$$

An easy substitution shows that

$$E_1(x) = -Ei(-x) ,$$

so that all the E-functions can be computed from tables of the exponential integral.

3. Further, we define the set of functions,

$$F_n(b, x) = \int_0^x e^{bt} E_n(t)\, dt \qquad (n \text{ and } x \text{ as above, } b \text{ any real value}) .$$

By using the recurrence relation for the E-functions, we find the relation

$$bF_{n+1}(b, x) = e^{bx} E_{n+1}(x) - \frac{1}{n} + F_n(b, x) .$$

The partial derivatives are

$$\frac{\partial F_n(b, x)}{\partial x} = e^{bx}E_n(x),$$

which follows directly from the definition, and

$$\frac{\partial F_n(b, x)}{\partial b} = \frac{1}{b-1}\{e^{(b-1)x} - 1\} - nF_{n+1}(b, x),$$

which is obtained by differentiating the integrand and using the recursion formulae for the E-functions.

The calculation of $F_1(b, x)$ is not so obvious. Replacing $E_1(t)$ by its definition and inverting the order of integration, we find

$$F_1(b, x) = \int_1^\infty \frac{du}{u}\int_0^x e^{(b-u)t}dt = \frac{1}{b}\int_1^\infty \left(\frac{1}{u} + \frac{1}{b-u}\right)\{e^{(b-u)x} - 1\}\,du.$$

In this way the function is reduced to exponential integrals, but it is necessary to distinguish carefully between the various cases. The various formulae are:

$$F_1(b, x) = \frac{1}{b}\{e^{bx}E_1(x) - E_1(x - bx) - \ln(1 - b)\} \qquad (b < 1 \text{ but } \neq 0);$$

$$F_1(b, x) = \frac{1}{b}\{e^{bx}E_1(x) + Ei(bx - x) - \ln(b - 1)\} \qquad (b > 1);$$

$$F_1(0, x) = 1 - E_2(x);$$

$$F_1(1, x) = e^x E_1(x) + l, \qquad \text{where } l = \gamma + \ln x.$$

In the last formula $\gamma = 0.577216$ is Euler's constant. Essentially the same formulae have been derived by King.[1]

4. If $x = \infty$, the F-integrals converge only for $b < 1$. The recursion formula for that case is

$$bF_{n+1}(b, \infty) = -\frac{1}{n} + F_n(b, \infty);$$

and the formulae for F_1 are

$$F_1(b, \infty) = -\frac{1}{b}\ln(1 - b) \qquad (b < 1 \text{ but } \neq 0)$$

$$F_1(0, \infty) = 1.$$

5. The following integral can be reduced by replacing F_n by its definition and inverting the order of integration as follows:

$$\int_0^x e^{-at}F_n(b, t)\,a\,dt = \int_0^x e^{-at}a\,dt\int_0^t e^{bu}E_n(u)\,du$$

$$= \int_0^x e^{bu}E_n(u)\,du\int_u^x e^{-at}a\,dt = \int_0^x e^{bu}(e^{-au} - e^{-ax})E_n(u)\,du$$

$$= F_n(b - a, x) - e^{-ax}F_n(b, x).$$

6. In a similar way we can derive the following equations:

$$\int_1^\infty F_n(-s, x)\frac{ds}{s^m} = \int_0^x E_n(u)E_m(u)\,du \equiv G_{nm}(x)$$

and

$$\int_1^\infty e^{-xs}F_n(s, x)\frac{ds}{s^m} = \int_0^x E_n(u)E_m(x - u)\,du \equiv G'_{nm}(x).$$

The functions $G_{nm}(x)$ and $G'_{nm}(x)$ are symmetrical in n and m; they will be further discussed in sections 7, 8, and 10.

7. The integral,

$$G_{mn}(x) = \int_0^x E_m(t) E_n(t)\, dt,$$

can be reduced to known functions. By using the recursion formula for E_m and E_n, we obtain

$$(m-1) G_{mn}(x) = F_n(-1, x) - \int_0^x tE_{m-1}(t) E_n(t)\, dt$$

and

$$(n-1) G_{mn}(x) = F_m(-1, x) - \int_0^x tE_{n-1}(t) E_m(t)\, dt;$$

further, one partial integration gives

$$G_{mn}(x) = xE_m(x) E_n(x) + \int_0^x tE_{m-1}(t) E_n(t)\, dt + \int_0^x tE_{n-1}(t) E_m(t)\, dt.$$

By adding these expressions, we obtain

$$(m+n-1) G_{mn}(x) = xE_m(x) E_n(x) + F_m(-1, x) + F_n(-1, x).$$

In the particular case of $m = n-1$ this formula admits of a further reduction. Using the recursion formulae for the E- and F-functions, we find

$$2G_{n,n-1}(x) = \frac{1}{(n-1)^2} - \{E_n(x)\}^2;$$

this result can also be found directly by partial integration.

8. The integral,

$$G'_{mn}(x) = \int_0^x E_m(t) E_n(x-t)\, dt,$$

is *not* expressible in terms of the ordinary exponential integral. By reducing it in a manner similar to that adopted for $G_{mn}(x)$, we first obtain

$$(m-1) G'_{mn}(x) = e^{-x} F_n(1, x) - \int_0^x tE_{m-1}(t) E_n(x-t)\, dt$$

and

$$(n-1) G'_{mn}(x) = e^{-x} F_m(1, x) + \int_0^x tE_m(t) E_{n-1}(x-t)\, dt - xG_{m,n-1}(x),$$

and then

$$G'_{mn}(x) = \frac{xE_m(x)}{n-1} + \int_0^x tE_{m-1}(t) E_n(x-t)\, dt - \int_0^x tE_m(t) E_{n-1}(x-t)\, dt.$$

Hence

$$(m+n-1) G'_{mn}(x) = \frac{xE_m(x)}{n-1} - xG'_{m,n-1}(x) + e^{-x}\{F_n(1, x) + F_m(1, x)\}.$$

The recurrence formula thus derived can serve to reduce any integral $G'_{mn}(x)$ to the integral $G'_{11}(x)$, discussed in section 10.

By differentiating $G'_{mn}(x)$ under the integral sign, we further obtain

$$\frac{dG'_{mn}(x)}{dx} = \frac{E_m(x)}{n-1} - G'_{m,n-1}(x),$$

so that the recurrence formula gives rise to the differential equation,

$$(m+n-1) G'_{mn}(x) = x \frac{d}{dx} G'_{mn}(x) + e^{-x}\{F_n(1, x) + F_m(1, x)\}.$$

9. In preparation of the next section we shall define a new set of functions, $E_1^{(p)}(x)$, for which the name "exponential integrals of the pth order" would seem suitable. They are defined by

$$E_1^{(p+1)}(x) = \int_x^\infty E_1^{(p)} \frac{dx}{x} \quad \text{and} \quad E_1^{(0)}(x) = e^{-x}.$$

None of these functions can be reduced to the other ones, so that for each of them a separate numerical table has to be constructed. Their series expansions are

$$E_1^{(p)}(x) = P - \sum_{n=1}^{\infty} \frac{(-x)^n}{n^{p-1} n!},$$

where P is an even, or odd, polynomial in $l = \ln x + \gamma$, the highest term of which is $(-l)^p/p!$. I have not investigated what rule the further coefficients of these polynomials obey.

In the present calculations we need only the exponential integrals of the orders $p = 1$ and $p = 2$. The first one, $E_1^{(1)}(x)$, is identical with the function $E_1(x)$ discussed above. The second one,

$$E_1^{(2)}(x) = \int_x^\infty E_1(x) \frac{dx}{x},$$

seems to be new; I have found no reference to any such function in the literature. Its series expansion,

$$E_1^{(2)}(x) = \tfrac{1}{2}(\ln x + \gamma)^2 + \frac{\pi^2}{12} - x + \frac{x^2}{2^2 \cdot 2!} - \frac{x^3}{3^2 \cdot 3!} + \cdots,$$

is very suitable for numerical computation. The integration constant, $\pi^2/12$, appears in the form, $-\frac{1}{2}\gamma^2 + \frac{1}{2}\Gamma''(1)$. A check computation of $E_1^{(2)}(5)$, using twenty terms of this expansion, gave 0.0001728, while an asymptotic expansion gave 0.000172.

10. Now we can express the integral,

$$G'_{11}(x) = \int_0^x E_1(t) E_1(x-t)\, dt,$$

and, accordingly, all integrals $G'_{mn}(x)$ in terms of known functions. Let us briefly denote this integral by y. The differential equation derived in section 7 takes for $m = n = 1$ the form,

$$y = x \frac{dy}{dx} + 2e^{-x} F_1(1, x).$$

After dividing by x^2 and replacing $F_1(1, x)$ by its expression derived in section 3, we obtain

$$-\frac{d}{dx}\left(\frac{y}{x}\right) = \frac{2}{x^2}\{E_1(x) + l e^{-x}\}.$$

The function that satisfies this differential equation and vanishes for $x = \infty$ is

$$y = G'_{11}(x) = 2\{E_1(x) + l E_2(x) - x E_1^{(2)}(x)\}.$$

The correctness of this formula can be verified by direct differentiation. I do not see any obvious way of deriving this formula; I actually found it by using the series expansions for $E_1(t)$ and $E_1(x-t)$ in the integrand of the defining integral and integrating term by term. The result of a fairly tedious reduction[12] then is

$$G'_{11}(x) = \left(l^2 - 2l + 2 + \frac{\pi^2}{6}\right) x + 2 \sum_{n=1}^{\infty} \frac{(-x)^{n+1}}{n(n+1)!}\left(-l + \frac{1}{n} + \frac{1}{n+1}\right),$$

which is identical with the series expansion of the formula given above.

[12] In this reduction I used integrals from Tables 1, 30, and 106 of D. Bierens de Haan, *Nouvelles tables d'intégrales définies* (Leyden: P. Engels, 1867).

It should further be noted that the differential equation from which we started does not follow strictly from the equations of section 8, because the demonstration given there does not hold for $m = n = 1$. Again, series expansion shows that the equation is indeed correct. On the whole, the functions discussed in sections 9 and 10 would seem to require a more thorough investigation. The discussion given here has not been extended beyond what was strictly needed for making the numerical computations.

11. All functions discussed above can be expanded in series in powers of x, with the understanding that some of the coefficients may contain

$$l = \ln x + \gamma \qquad (x > 0),$$

besides constant terms. The following formulae present the first few terms of those functions that occurred in the preceding calculations. All have been derived in several ways, e.g., by integration of separate terms, by expansion of recurrence formulae, etc.

$$Ei(x) = l + x + \tfrac{1}{4}x^2 + \tfrac{1}{18}x^3;$$

$$E_1(x) = -l + x - \tfrac{1}{4}x^2 + \tfrac{1}{18}x^3,$$

$$E_2(x) = 1 + (l-1)\,x - \tfrac{1}{2}x^2 + \tfrac{1}{12}x^3,$$

$$E_3(x) = \tfrac{1}{2} - x + \tfrac{1}{2}(-l + \tfrac{3}{2})\,x^2 + \tfrac{1}{6}x^3;$$

$$F_1(b, x) = (-l+1)\,x + \tfrac{1}{2}(-bl + \tfrac{1}{2}b + 1)\,x^2,$$

$$F_2(b, x) = x + \tfrac{1}{2}(l + b - \tfrac{3}{2})\,x^2;$$

$$G_{11}(x) = (l^2 - 2l + 2)\,x + (-l + \tfrac{1}{2})\,x^2,$$

$$G_{12}(x) = (-l+1)\,x - \tfrac{1}{2}(l^2 - 2l)\,x^2,$$

$$G_{13}(x) = \tfrac{1}{2}(-l+1)\,x + \tfrac{1}{2}lx^2,$$

$$G_{22}(x) = x + (l - \tfrac{3}{2})\,x^2;$$

$$G'_{11}(x) = \left(l^2 - 2l + 2 - \frac{\pi^2}{6}\right)x + (-l + \tfrac{3}{2})\,x^2,$$

$$G'_{12}(x) = (-l+1)\,x - \tfrac{1}{2}\left(l^2 - 3l + \tfrac{5}{2} - \frac{\pi^2}{6}\right)x^2,$$

$$G'_{13}(x) = \tfrac{1}{2}(-l+1)\,x + \tfrac{1}{2}(l-1)\,x^2,$$

$$G'_{22}(x) = x + (l - \tfrac{3}{2})\,x^2.$$

These formulae are useful both for approximate computation and for checking the correctness of any equation involving these functions.

Finally, the function

$$g(x) = 2 - 2E_2(x) - G_{12}(x) - G'_{12}(x)$$

has as its dominant term

$$g(x) = \tfrac{1}{2}\left(2l^2 - 5l + \tfrac{9}{2} - \frac{\pi^2}{6}\right)x^2;$$

and the function

$$c(x) = \frac{x - \frac{1}{2} + E_3(x)}{x}$$

has the expansion

$$c(x) = \tfrac{1}{2}(-l + \tfrac{3}{2})\, x + \tfrac{1}{6}x^2 + \ldots.$$

12. *Tables.*—Numerical values of the functions needed have been computed for fifteen selected values of x and—in the case of the F-functions—for four selected values of s. These values are given in Tables 1–4. Table 1 gives the E-functions: the functions $\ln x$, e^{-x}, and $E_1(x)$ were taken from the *New York Mathematical Tables Project* tables; E_2 and E_3 were computed by means of the recurrence relation; $E_1^{(2)}(x)$ was computed from

TABLE 1

EXPONENTIAL INTEGRALS OF THE FIRST AND SECOND ORDER

x	l	e^{-x}	$E_1(x)$	$E_2(x)$	$2E_3(x)$	$E_1^{(2)}(x)$
0.01	−4.027954	0.990050	4.037930	0.949671	0.98055	8.924688
0.02	−3.334807	.980199	3.354708	.913105	.96194	6.362987
0.05	−2.418517	.951229	2.467898	.827834	.90984	3.697389
0.1	−1.725369	.904837	1.822924	.722545	.83259	2.212149
0.2	−1.032222	.818731	1.222651	.574201	.70389	1.160064
0.3	−0.626757	.740818	0.905677	.469115	.60008	0.729650
0.4	−0.339075	.670320	0.702380	.389368	.51457	0.498831
0.6	+0.066390	.548812	0.454380	.276184	.38310	0.265984
0.8	+0.354072	.449329	0.310597	.200852	.28865	0.156636
1.0	+0.577216	.367879	0.219384	.148496	.21938	0.097843
1.5	+0.982681	.223130	0.100020	.073101	.11348	0.034517
2.0	+1.270363	.135335	0.048901	.037534	.06027	0.014265
2.5	+1.493506	.082085	0.024915	.019798	.03259	0.006250
3.0	+1.675828	0.049787	0.013048	0.010642	0.01786	0.002879
∞	∞	0	0	0	0	0

TABLE 2

THE FUNCTIONS $F_1(b, x)$

x	$F_1(-s, x)$				$e^{-sx}F_1(s, x)$				
	$s=10$	$s=5$	$s=2$	$s=1$	$s=0$	$s=1$	$s=2$	$s=5$	$s=10$
0.01	0.0482	0.0492	0.0499	0.0501	0.0503	0.0501	0.0498	0.0490	0.0477
0.02	.0797	.0832	.0854	.0861	0.0869	.0859	.0849	.0823	.0779
0.05	.1404	.1551	.1650	.1685	0.1722	.1673	.1627	.1496	.1308
0.1	.1913	.2281	.2560	.2663	0.2775	.2617	.2471	.2091	.1612
0.2	.2270	.3001	.3667	.3945	0.4258	.3775	.3359	.2417	.1500
0.3	.2362	.3309	.4309	.4766	0.5309	.4414	.3698	.2283	.1200
0.4	.2387	.3450	.4707	.5329	0.6106	.4751	.3747	.2005	.0935
0.6	.2397	.3551	.5132	.6022	0.7238	.4908	.3432	.1428	.0583
0.8	.2398	.3576	.5321	.6399	0.7991	.4697	.2913	.0987	.0386
1.0	.2398	.3582	.5409	.6613	0.8515	.4317	.2379	.0685	.0266
1.5	.2398	.3584	.5479	.6839	0.9269	.3193	.1322	.0294	.0118
2.0	.2398	.3584	.5491	.6903	0.9625	.2208	.0698	.0138	.0057
2.5	.2398	.3584	.5493	.6922	0.9802	.1475	.0363	.0068	.0029
3.0	.2398	.3584	.5493	.6929	0.9894	0.0965	0.0188	0.0035	0.0015
∞	0.2398	0.3584	0.5493	0.6931	1.0000	0	0	0	0

its series expansion. Tables 2 and 3 give the F-functions. Since $F_1(s, x)$ occurs always with the factor e^{-sx}, we have tabulated in Table 2 the functions $F_1(-s, x)$ and $e^{-sx}F_1(s, x)$. The central column shows their common value for $s = 0$. Table 3 is arranged in the

TABLE 3

THE FUNCTIONS $F_2(b, x)$

x	$F_2(-s, x)$					$e^{-sx}F_2(s, x)$			
	$s=10$	$s=5$	$s=2$	$s=1$	$s=0$	$s=1$	$s=2$	$s=5$	$s=10$
0.01	0.0093	0.0095	0.0096	0.0097	0.0097	0.0097	0.0096	0.0095	0.0092
0.02	.0173	.0181	.0187	.0188	.0190	.0188	.0186	.0181	.0172
0.05	.0358	.0400	.0430	.0440	.0451	.0439	.0428	.0397	.0352
0.1	.0543	.0667	.0762	.0799	.0837	.0795	.0755	.0650	.0516
0.2	.0695	.0977	.1242	.1354	.1481	.1330	.1199	.0896	.0589
0.3	.0740	.1129	.1558	.1759	.2000	.1697	.1450	.0948	.0539
0.4	.0754	.1205	.1772	.2061	.2427	.1941	.1574	.0909	.0464
0.6	.0760	.1262	.2018	.2462	.3084	.2182	.1591	.0738	.0332
0.8	.0760	.1277	.2136	.2699	.3557	.2212	.1452	.0563	.0239
1.0	.0760	.1281	.2195	.2840	.3903	.2123	.1256	.0421	.0175
1.5	.0760	.1283	.2242	.2998	.4433	.1693	.0778	.0204	.0084
2.0	.0760	.1283	.2251	.3046	.4699	.1230	.0445	.0103	.0043
2.5	.0760	.1283	.2253	.3061	.4837	.0852	.0247	.0053	.0023
3.0	.0760	.1283	.2253	.3066	.4911	0.0573	0.0134	0.0028	0.0012
∞	0.0760	0.1283	0.2253	0.3069	0.5000	0	0	0	0

TABLE 4

THE FUNCTIONS $G_{mn}(x)$, $G'_{mn}(x)$, $g(x)$, AND $c(x)$

x	$G_{11}(x)$	$G_{12}(x)$	$G_{22}(x)$	$G'_{11}(x)$	$G'_{12}(x)$	$G'_{22}(x)$	$g(x)$	$c(x)$
0.01	0.26325	0.04906	0.00946	0.24690	0.04882	0.00945	0.0028	0.0277
0.02	0.39734	.08312	.01812	.36484	.08229	.01810	0.0084	0.0484
0.05	0.64160	.15735	.04076	.56180	.15329	.04054	0.0337	0.0984
0.1	0.86500	.23896	.07065	.71010	.22624	.06951	0.0897	0.1630
0.2	1.08798	.33515	.11223	.79587	.29795	.10709	0.2185	0.2597
0.3	1.19924	.38997	.13926	.78552	.32354	.12766	0.3483	0.3335
0.4	1.26318	.42420	.15760	.74165	.32676	.13777	0.4703	0.3932
0.6	1.32825	.46186	.17942	.62625	.30294	.14011	0.6828	0.4859
0.8	1.35697	.47983	.19066	.51281	.26329	.13083	0.8552	0.5554
1.0	1.37081	.48897	.19670	.41451	.22448	.11624	0.9896	0.6097
1.5	1.38276	.49733	.20255	.24016	.13917	.07980	1.2173	0.7045
2.0	1.38540	.49930	.20401	.13611	.08472	.05056	1.3409	0.7651
2.5	1.38605	.49980	.20441	.07772	.05036	.03134	1.4102	0.8065
3.0	1.38622	.49994	.20452	.04449	.02975	.01912	1.4490	0.8363
∞	1.38629	0.50000	0.20457	0.00000	0.00000	0.00000	1.5000	1.0000

same way. Table 4 gives the G-functions computed from the values in the preceding tables. However, six-place values instead of four-place values of the functions $F_n(-1, x)$ and $F_n(1, x)$ were used in this computation.

The computations were made with a Marchant machine. Apart from possible computational errors, all given decimals should be correct. Only the F-functions for $s = \pm 2$ may be in error by a full unit of the last decimal.

THE SCHUSTER PROBLEM FOR AN EXTENDED ATMOSPHERE

ANNE B. UNDERHILL*
Yerkes Observatory
Received December 26, 1947

ABSTRACT

The Schuster problem has been solved for a stellar atmosphere with spherical symmetry. It is assumed that $l\rho = c/r^2$, where $l\rho$ is the line-scattering coefficient, c is a constant, and r is the radius. A table of residual intensity in the line is given for a series of optical thicknesses of the atmosphere. The effect of the sphericity of the stellar atmosphere is to make the cores of the absorption lines, where the optical depth is large, shallower and to make the wings, where the optical depth is small, deeper than for a line formed in a plane-parallel atmosphere.

The interpretation of the observed shapes of lines in supergiants is discussed on the assumption of extended atmospheres for these stars. The effect on line shape of continuous electron scattering in the envelope is briefly considered. The data may also be used to interpret the change in line intensity when a star with an extended atmosphere is eclipsed by a compact body, since the calculations indicate that the fraction of the emergent flux which arises from the scattering in the envelope is appreciable.

1. *Introduction.*—In theoretical discussions of line formation the stellar atmosphere is usually considered to be stratified in parallel planes. However, observations indicate that some stars have a very extensive atmosphere, the extent of the atmosphere being comparable to the radius of the star itself. For such stars the assumption of plane-parallelism is inadequate, and the varying curvature of the outer layers should be allowed for. The purpose of this paper is to solve a simple problem in the theory of line formation for an atmosphere with spherical symmetry and, from a comparison of the results obtained with those obtained for a plane-parallel atmosphere, to estimate the effects of the sphericity of the atmosphere on the line shape.

The Schuster problem in its standard form idealizes the problem of line formation in a stellar atmosphere in the following manner. The photospheric surface emits continuous radiation with an angular distribution specified by

$$I_{ph}(\vartheta) = I_0(1 + \beta \cos \vartheta), \tag{1}$$

where β is related to the coefficient of darkening. Above this surface lies an atmosphere which scatters isotropically with a mass-scattering coefficient, l_ν, which is appreciably different from zero only for a small range of frequencies about the center of the line. For radiation of frequency ν within the line the angular distribution of the intensity emerging from the atmosphere is determined by the solution of the equation of transfer. Integration of this intensity over the outward hemisphere gives the emergent flux, F_ν, in the frequency ν. The ratio of this flux to the flux from the photosphere, F, gives the residual intensity in the line, since the flux in frequencies outside the line is the photospheric flux.

Let the intensity of radiation in frequency ν at depth z in the atmosphere and in a direction ϑ to the outward normal be denoted by $I_\nu(z, \vartheta)$. Then the equation of transfer appropriate to the problem is

$$\cos \vartheta \frac{dI_\nu(z, \vartheta)}{dz} = -l_\nu \rho I_\nu(z, \vartheta) + \tfrac{1}{2} l_\nu \rho \int_0^\pi I_\nu(z, \vartheta') \sin \vartheta' d\vartheta'. \tag{2}$$

The boundary conditions are that there is no incident radiation on the atmosphere at

* This work was completed during tenure of a scholarship from the Canadian Federation of University Women.

$z = z_1$, and that at the base of the atmosphere $z = 0$, where the optical thickness in the frequency ν is

$$\tau_\nu = \int_0^{z_1} l_\nu \rho \, dz , \tag{3}$$

the outward intensity has the value given by equation (1). The emergent flux in frequency ν is

$$F_\nu = 2 \int_0^{\pi/2} I_\nu (0, \vartheta) \sin \vartheta \cos \vartheta \, d\vartheta , \tag{4}$$

and the emergent flux in the continuum is

$$F = 2 \int_0^{\pi/2} I_{ph} (\vartheta) \sin \vartheta \cos \vartheta \, d\vartheta . \tag{5}$$

The ratio of these fluxes gives the residual intensity in the line:

$$R_\nu = \frac{F_\nu}{F} . \tag{6}$$

Chandrasekhar's solution of this problem[1] in his "second approximation" is

$$R_\nu = \frac{1 + \frac{2}{3}\beta\chi(\tau_\nu)}{1.04253 + \frac{2}{3}\beta} \cdot \frac{1}{\chi(\tau_\nu) + \frac{3}{4}\tau_\nu} , \tag{7}$$

where $\chi(\tau_\nu)$ is a certain function of τ_ν and is close to unity.

The Schuster problem in a spherical atmosphere can be formulated similarly. There is a spherical photospheric surface which is surrounded concentrically by an atmosphere extending to infinity. The photosphere emits radiation with an angular distribution that is given by equation (1). The mass-scattering coefficient in the atmosphere is l_ν as before, and the emergent intensity in any frequency ν must be found from the equation of transfer which allows for the curvature of the atmosphere. The residual intensity in the line is found from the ratio of the net emergent flux in the line to the flux in the continuum.

The equation of transfer is

$$\cos \vartheta \frac{\partial I_\nu}{\partial r} - \frac{\sin \vartheta}{r} \frac{\partial I_\nu}{\partial \vartheta} = - l_\nu \rho I_\nu + \tfrac{1}{2} l_\nu \rho \int_0^\pi I_\nu (r, \vartheta') \sin \vartheta' \, d\vartheta' , \tag{8}$$

where r is the distance measured outward from the center of symmetry of the atmosphere and ϑ is the angle measured from the positive direction of the radius vector. This equation must be solved under the boundary conditions that there is no incident radiation on the outside boundary of the atmosphere and that at the base of the atmosphere, where the radial optical depth in frequency ν is

$$\tau_\nu = - \int_\infty^r l_\nu \rho \, dr , \tag{9}$$

the outward intensity equals the photospheric intensity, I_{ph}.

The solution of equation (8) in the "second approximation" for the case $l_\nu \rho \propto r^{-n}$ $(n > 1)$ and under the boundary conditions that all quantities vanish as $r \to \infty$ (this is equivalent in this case to the condition that there is no incident radiation) and that none of the quantities involved increase exponentially as $r \to 0$ has been obtained by Chandrasekhar.[2] The present discussion is based on his work. We shall assume, as he did, that $l_\nu \rho \propto r^{-n} (n > 1)$.

[1] Unpublished.

[2] *Ap. J.*, **101**, 95, 1945. This paper will be referred to as "Paper V."

2. *Solution of the equation of transfer and application of the boundary conditions.*—For the sake of convenience we shall suppress the subscript ν in this part of the discussion. The arguments in Paper V are valid up to the introduction of the boundary conditions. Hence, following the analysis of Paper V, we introduce the abbreviations (cf. Paper V, eqs. [34]–[43]):

$$J = \tfrac{1}{2}\Sigma a_i I_i , \qquad L = \tfrac{1}{2}\Sigma a_i \mu_i^3 I_i ,$$
$$H = \tfrac{1}{2}\Sigma a_i \mu_i I_i , \qquad M = \tfrac{1}{2}\Sigma a_i \mu_i^4 I_i . \tag{10}$$
$$K = \tfrac{1}{2}\Sigma a_i \mu_i^2 I_i ,$$

The second approximation is equivalent to the condition

$$35M - 30K + 3J = 0 .$$

Hence the independent quantities are J, H, K, and L. The flux is

$$H = \tfrac{1}{4} F_0 r^{-2} , \tag{11}$$

where F_0 is a constant of integration. After introducing the quantities

$$X = 3K - J , \tag{12}$$
$$Y = 5L - 3H ,$$

and expressing all fluxes in units of the emergent flux, F_0/R^2, at the radius R, where $\tau = 1$, we find that the equation of transfer reduces to the pair of simultaneous differential equations (cf. Paper V, eqs. [62] and [63]),

$$\tfrac{7}{3} Y = \frac{dX}{d\tau} + \frac{2}{(n-1)\tau} X \tag{13}$$

and

$$\tfrac{5}{3} X - \frac{1}{(n-1)} \tau^{(3-n)/(n-1)} = \frac{dY}{d\tau} - \frac{4}{(n-1)\tau} Y . \tag{14}$$

Since we assume that $l\rho = cr^{-n} (n > 1)$, it follows from equation (9) that

$$\tau = \frac{c}{n-1} r^{-(n-1)} , \tag{15}$$

where c is a constant.

When the substitutions,

$$z = q\tau \qquad \text{with} \qquad q = \sqrt{35}/3 = 1.9720$$

and

$$\nu = \frac{n+5}{2(n-1)} , \qquad \mu = \frac{3-n}{2(n-1)} ,$$

are made, it is found that the differential equation to be solved is (cf. Paper V, eq. [70])

$$z^2 \frac{d^2\phi}{dz^2} + z \frac{d\phi}{dz} - (z^2 + \nu^2)\phi = - z^{\mu+1} . \tag{16}$$

If $\phi(z)$ is a solution of equation (16), then it follows that (cf. Paper V, eqs. [71] and [72])

$$X = \frac{7}{3(n-1)} q^{-(n+1)/(n-1)} z^{(n+1)/2(n-1)} \phi(z) \tag{17}$$

and

$$K = q^{-(n+1)/(n-1)} \left[\frac{7}{3(n-1)^2} \int_0^z z^{(3-n)/2(n-1)} \phi(z)\, dz + \frac{n-1}{4(n+1)} z^{(n+1)/(n-1)} \right] . \tag{18}$$

Since the homogeneous part of equation (16) is Bessel's equation for a purely imaginary argument, it can be shown that (cf. Paper V, eq. [80])

$$\phi(z) = I_\nu(z) \int_z^{c_1} z^\mu K_\nu(z)\, dz + K_\nu(z) \int_{c_2}^{z} z^\mu I_\nu(z)\, dz, \tag{19}$$

where $I_\nu(z)$ and $K_\nu(z)$ are the fundamental solutions of this type of Bessel's equation. To satisfy the boundary condition as $r \to \infty$, it is necessary to put $c_2 = 0$, since no quantity may have a singularity at $z = 0$. The constant, c_1, remains arbitrary and must be determined from the other boundary condition of the problem.

In order to do this, we write

$$\phi = \Phi - a I_\nu(z), \tag{20}$$

where

$$\Phi = I_\nu(z) \int_z^{\infty} z^\mu K_\nu(z)\, dz + K_\nu(z) \int_0^{z} z^\mu I_\nu(z)\, dz \tag{21}$$

is the function found as a solution in Paper V for an atmosphere of infinite depth, and

$$a = \int_{c_1}^{\infty} z^\mu K_\nu(z)\, dz. \tag{22}$$

The constant a is to be determined from the boundary condition at $z = z_1$.

From equation (17) we have, upon use of equation (20),

$$X = \frac{7}{3(n-1)}\, q^{-(n+1)/(n-1)}\, z^{(n+1)/2(n-1)}\Phi - a\,\frac{7}{3(n-1)}\, q^{-(n+1)/(n-1)}\, z^{(n+1)/2(n-1)} I_\nu(z)$$

or

$$X = X_\infty - a\,\frac{7}{3(n-1)}\, q^{-(n+1)/(n-1)}\, z^{(n+1)/2(n-1)} I_\nu(z), \tag{23}$$

where

$$X_\infty = \frac{7}{3(n-1)}\, q^{-(n+1)/(n-1)}\, z^{(n+1)/2(n-1)}\Phi$$

is the quantity calculated in Paper V for an infinitely deep atmosphere. The subscript ∞ on any quantity will be used to denote that quantity as it is calculated in Paper V. From equation (18) we find that

$$K = K_\infty - a\beta(z), \tag{24}$$

where

$$\beta(z) = \frac{7}{3(n-1)^2}\, q^{-(n+1)/(n-1)} \int_0^{z} z^{(3-n)/2(n-1)} I_\nu(z)\, dz. \tag{25}$$

From equations (12) we then have

$$J = J_\infty - a\gamma(z), \tag{26}$$

where

$$\gamma(z) = 3\beta(z) - \frac{7}{3(n-1)}\, q^{-(n+1)/(n-1)}\, z^{(n+1)/2(n-1)} I_\nu(z). \tag{27}$$

From equation (13) we find

$$Y = Y_\infty - a\,\delta(z), \tag{28}$$

where

$$\delta(z) = q^{-2/(n-1)}\,\frac{1}{(n-1)}\left[z^{(n+1)/2(n-1)}\,\frac{dI_\nu(z)}{dz} + \frac{n+5}{2(n-1)}\, z^{[(n+1)/2(n-1)]-1} I_\nu(z) \right]. \tag{29}$$

Using the recurrence properties[3] of $I_\nu(z)$, we find

$$\delta(z) = q^{-2/(n-1)} \frac{1}{(n-1)} [\, z^{(n+1)/2(n-1)} I_{\nu-1}(z) \,]. \tag{30}$$

The quantities X, Y, J, and K are expressed in units of F_0/R^2; hence from equation (11) we see that H in the same units is

$$H = \tfrac{1}{4} \left(\frac{R}{r}\right)^2. \tag{31}$$

In Paper V (cf. eq. [60]) it is shown that

$$\tau = \frac{z}{q} = \left(\frac{R}{r}\right)^{n-1};$$

hence it follows that

$$H = \tfrac{1}{4} q^{-2/(n-1)} z^{2/(n-1)}. \tag{32}$$

Since

$$L = \tfrac{1}{5} (Y + 3H),$$

we have

$$L = \tfrac{1}{5} [\, Y_\infty + 3H - \alpha \delta(z) \,]. \tag{33}$$

The next step is to solve equations (10) for I_{+1} and I_{+2} at $z = z_1$ (z_1 is the radial optical thickness of the atmosphere) and to apply the boundary condition that the outward intensity in the atmosphere at depth z_1 must equal that from the photosphere. We have, since we are working in the "second approximation,"

$$a_1 (I_1 + I_{-1}) + a_2 (I_2 + I_{-2}) - 2J = 0,$$

$$a_1\mu_1 (I_1 - I_{-1}) + a_2\mu_2 (I_2 - I_{-2}) - 2H = 0,$$

$$a_1\mu_1^2 (I_1 + I_{-1}) + a_2\mu_2^2 (I_2 + I_{-2}) - 2K = 0,$$

and

$$a_1\mu_1^3 (I_1 - I_{-1}) + a_2\mu_2^3 (I_2 - I_{-2}) - 2L = 0,$$

where we have used the properties of the Gaussian division that $a_i = a_{-i}$ and $u_{-i} = -u_i$. Solution of these four simultaneous equations gives

$$I_1 = \frac{\mu_2^2 (J\mu_1 + H) - (K\mu_1 + L)}{a_1\mu_1 (\mu_2^2 - \mu_1^2)} \tag{34}$$

and

$$I_2 = \frac{-\mu_1^2 (J\mu_2 + H) + (K\mu_2 + L)}{a_2\mu_2 (\mu_2^2 - \mu_1^2)}. \tag{35}$$

These intensities are expressed in units of

$$\frac{F_0}{R^2} = f. \tag{36}$$

[3] Watson, *Treatise on the Theory of Bessel Functions* (Cambridge, England, 1922), p. 79.

When we convert to the usual units and apply the boundary condition at $z = z_1$, we find that

$$\frac{\mu_2^2(J\mu_1+H) - (K\mu_1+L)}{a_1\mu_1(\mu_2^2-\mu_1^2)} = \frac{I_0}{f}(1+\beta\mu_1) \tag{37}$$

and

$$\frac{-\mu_1^2(J\mu_2+H) + (K\mu_2+L)}{a_2\mu_2(\mu_2^2-\mu_1^2)} = \frac{I_0}{f}(1+\beta\mu_2)\,, \tag{38}$$

where the quantities K, J, H, and L are evaluated at $z = z_1$ according to equations (24), (26), (32), and (33).

There are two constants to be determined from the pair of simultaneous equations (37) and (38): a, which is contained in the expression for K, J, and L, and f/I_0. Since the value of these constants depends on z_1, they may be written as $a(z_1)$ and $f(z_1)$. In the case of an infinite atmosphere $a(z_1) = 0$, and $f(z_1)$ is a free parameter; but, for a finite atmosphere, $f(z_1)$ depends on the unknown net flux, for only the outward flux is given and the inward flux (or back-radiation) is determined by the "envelope" which is attached.

The result of substituting the expressions for K, J, H, and L and of solving equations (37) and (38) simultaneously for $a(z_1)$ and $f(z_1)$ is

$$a(z_1) = \frac{\mathfrak{E}(z_1)\,a_1\mu_1(1+\beta\mu_1) + \mathfrak{B}(z_1)\,a_2\mu_2(1+\beta\mu_2)}{\mathfrak{D}(z_1)\,a_1\mu_1(1+\beta\mu_1) + \mathfrak{A}(z_1)\,a_2\mu_2(1+\beta\mu_2)} \tag{39}$$

and

$$f(z_1) = \frac{(\mu_2^2-\mu_1^2)[\mathfrak{D}(z_1)\,a_1\mu_1(1+\beta\mu_1) + \mathfrak{A}(z_1)\,a_2\mu_2(1+\beta\mu_2)]}{\mathfrak{B}(z_1)\,\mathfrak{D}(z_1) - \mathfrak{A}(z_1)\,\mathfrak{E}(z_1)}\,, \tag{40}$$

where

$$\mathfrak{A}(z_1) = \mu_1\mu_2^2\gamma(z_1) - \mu_1\beta(z_1) - \tfrac{1}{5}\delta(z_1)\,, \tag{41}$$

$$\mathfrak{D}(z_1) = \mu_1^2\mu_2\gamma(z_1) - \mu_2\beta(z_1) - \tfrac{1}{5}\delta(z_1)\,, \tag{42}$$

$$\mathfrak{B}(z_1) = [\mu_1\mu_2^2 J_\infty + (\mu_2^2-\tfrac{3}{5})H - \tfrac{1}{5}Y_\infty - \mu_1 K_\infty]_{z=z_1}\,, \tag{43}$$

and

$$\mathfrak{E}(z_1) = [\mu_1^2\mu_2 J_\infty + (\mu_1^2-\tfrac{3}{5})H - \tfrac{1}{5}Y_\infty - \mu_2 K_\infty]_{z=z_1}\,. \tag{44}$$

(The function $\beta(z)$, defined in eq. [25], should not be confused with the constant β, which depends on the coefficient of darkening of the photosphere.)

For any value of the coefficient of darkening of the photosphere a series of $a(z_1)$ and $f(z_1)$ can be calculated from equations (39) and (40) for selected values of z_1, the total optical thickness of the envelope for radiation of any given frequency. Once $a(z_1)$ is known, the source function $J(z)$ may be found from equation (26) for any optical depth $z \leq z_1$ in the atmosphere. Table 1 gives the quantities $a(z_1)$ and $f(z_1)$ when $\beta = 2$.

3. *The formation of lines.*—In order to find the residual intensity at any frequency ν, it is necessary to find the emergent flux in that frequency. In the Schuster problem each frequency of radiation is characterized by a unique total optical thickness of the atmosphere. We have

$$l_\nu\rho = \frac{c_\nu}{r^n}\,, \tag{45}$$

where c is a constant for any frequency. The variation of c with ν corresponds to the variation of the scattering coefficient with ν. In the following discussion it is assumed that the variation of l_ν with frequency is constant with depth, making the discussion the same for all frequencies, hence the suffix ν may be suppressed. The case with $n = 2$ will be studied. Then

$$l\rho = \frac{c}{r^2}. \tag{46}$$

The adoption of $n = 2$ gives a fairly steep gradient for the scattering coefficient, for, if at $r = r_1$, $l\rho$ has a given value, at $2r_1$ it will have one-quarter this value, at $3r_1$, one-ninth this value, and so on. For the case[4] in which ρ varies as r^{-2}, it means that l, the scattering coefficient per atom, is independent of r. How true this is in an actual star depends on the variation of temperature and pressure with radius, and hence of the ionization and excitation equilibria. Although the radius of the star is allowed to extend

TABLE 1

THE CONSTANTS $a(z_1)$ AND $f(z_1)$

z_1	$a(z_1)$	$f(z_1)$	z_1	$a(z_1)$	$f(z_1)$
0.0			1.6	2.19883	0.54190
0.1	9925.773	11.02985	1.8	1.48005	.47068
0.2	1267.721	5.40606	2.0	1.02960	.41462
0.3	358.8193	4.02397	2.2	0.73517	.36949
0.4	159.98997	2.60939	2.4	0.57907	.33398
0.5	82.02384	2.04822	2.6	0.39761	.30188
0.6	47.38368	1.67583	2.8	0.29933	.27548
0.7	29.47683	1.42230	3.0	0.22817	.25322
0.8	19.76638	1.21408	3.5	0.12043	.20949
0.9	13.85398	1.04572	4.0	0.06645	.17763
1.0	9.92324	0.94072	4.5	0.03774	.15343
1.2	5.59178	0.76119	5.0	0.02192	.13448
1.4	3.40860	0.63800	5.5	0.01293	0.11924

to infinity, it is seen that with $n = 2$ the effective atmosphere in which $l\rho$ is significantly large is not exorbitantly extended.

The emergent flux from a spherical atmosphere is

$$F = 2\pi \int_0^\infty p\, I\,(p)\, dp\,, \tag{47}$$

where $I(p)$ is the emergent intensity along a line OA at a perpendicular distance p from the center of the star (see Fig. 1). The quantity p varies from 0 to ∞, since the radius of the star extends to infinity. If $I(\theta, p)$ refers to the intensity of radiation at a point P on the line OA, then, quite generally,[5]

$$I\,(\theta, p) = e^{p\int_0^\theta l\rho \operatorname{cosec}^2\theta d\theta} \int_\theta^{\theta_1} e^{-p\int_0^\varphi l\rho \operatorname{cosec}^2\varphi d\varphi} J\,(\varphi, p)\, pl\rho \operatorname{cosec}^2\varphi\, d\varphi\,, \tag{48}$$

where $J(\varphi, p)$ is the source function at a point on OA characterized by the angle φ and θ_1 is the maximum angle that φ can reach. In our case we have a photosphere of radius r_1; hence when $p > r_1$, θ_1 is π; when $p \leq r_1$, θ_1 is $\sin^{-1} p/r_1$. To obtain the emergent intensity, we must set $\theta = 0$.

[4] Cf. N. A. Kosirev, *M.N.* **94**, 430, 1934.

[5] S. Chandrasekhar, *Proc. Cambridge Phil. Soc.* **31**, 390, 1935.

Thus for all $p > r_1$ the emergent intensity arising from light scattered in the envelope is

$$I_1(p) = \left[\int_0^{\pi} e^{-p\int_0^{\varphi} l\rho \operatorname{cosec}^2\varphi d\varphi} J(\varphi, p)\, pl\rho \operatorname{cosec}^2\varphi d\varphi\right]_{p>r_1}, \tag{49}$$

while for all $p \leq r_1$ it is

$$I_2(p) = \left[\int_0^{\sin^{-1}p/r_1} e^{-p\int_0^{\varphi} l\rho \operatorname{cosec}^2\varphi d\varphi} J(\varphi, p)\, pl\rho \operatorname{cosec}^2\varphi d\varphi\right]_{p\leq r_1}. \tag{50}$$

For all $p \leq r_1$ there is also an emergent intensity arising from the transmitted light of the photosphere. This is

$$I_3(p) = e^{-p\int_0^{\theta_1} l\rho \operatorname{cosec}^2\varphi d\varphi} I_0(1+\beta\cos\theta_1) \tag{51}$$

where

$$\theta_1 = \sin^{-1}\frac{p}{r_1}. \tag{52}$$

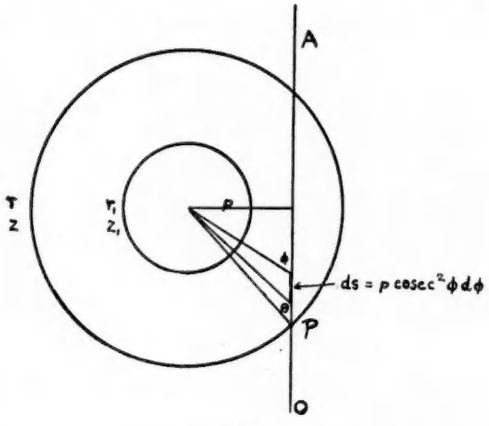

FIG. 1

In equations (49), (50), and (51) $l\rho$ is a function of p and φ, for

$$l\rho = \frac{c}{r^2} = \frac{c}{p^2\operatorname{cosec}^2\varphi}. \tag{53}$$

The introduction of equation (53) into equations (49), (50), and (51) gives

$$I_1(p) = \frac{c}{p}\int_0^{\pi} e^{-c\varphi/p} J(\varphi, p)\, d\varphi, \tag{54}$$

$$I_2(p) = \frac{c}{p}\int_0^{\sin^{-1}p/r_1} e^{-c\varphi/p} J(\varphi, p)\, d\varphi, \tag{55}$$

and

$$I_3(p) = e^{-c\theta_1/p} I_0(1+\beta\cos\theta_1). \tag{56}$$

The net flux in any frequency of the line is then given by

$$F_\nu = 2\pi\int_{r_1}^{\infty} p\, I_1(p)\, dp + 2\pi\int_0^{r_1} p\, I_2(p)\, dp + 2\pi\int_0^{r_1} p\, I_3(p)\, dp. \tag{57}$$

Let F_1, F_2, and F_3 be, respectively, the first, second, and third parts of F_ν. The dependence on frequency of each of these fluxes is given by the constant, c, which enters the expressions for $I_1(p)$, $I_2(p)$, and $I_3(p)$.

The flux from the photosphere is

$$F = 2\pi r_1^2 I_0 \int_0^{\pi/2} (1+\beta\cos\theta)\sin\theta\cos\theta\, d\theta\,, \tag{58}$$

which gives us

$$F = 2\pi r_1^2 I_0 (\tfrac{1}{2}+\tfrac{1}{3}\beta)\,. \tag{59}$$

Accordingly, we find that the residual intensity in the line is

$$R_\nu = \frac{F_\nu}{F} = R_1 + R_2 + R_3\,, \tag{60}$$

where

$$R_1 = \frac{F_1}{F}\,, \qquad R_2 = \frac{F_2}{F}\,, \qquad \text{and} \qquad R_3 = \frac{F_3}{F}\,. \tag{61}$$

The fluxes F_1, F_2, and F_3 must be evaluated explicitly as functions of z_1, the total optical thickness of the atmosphere in radiation of frequency ν.

Let

$$p = \xi r_1\,. \tag{62}$$

Then, after some simple substitutions, we find that

$$R_1 = \frac{z_1}{I_0(\frac{1}{2}+\frac{1}{3}\beta)\,q}\int_1^\infty d\xi \int_0^\pi e^{-z_1\varphi/q\xi} J(\varphi,\xi)\, d\varphi \tag{63}$$

and

$$R_2 = \frac{z_1}{I_0(\frac{1}{2}+\frac{1}{3}\beta)\,q}\int_0^1 d\xi \int_0^{\sin^{-1}\xi} e^{-z_1\varphi/q\xi} J(\varphi,\xi)\, d\varphi\,. \tag{64}$$

The source function $J(\varphi, \xi)$ is evaluated at the point characterized by the co-ordinates φ and ξ. Since

$$z = q\tau = \frac{z_1 r_1}{c}\cdot\frac{c}{r}\,,$$

we have

$$z = z_1\frac{\sin\varphi}{\xi} \tag{65}$$

hence any pair of values of φ and ξ characterize an optical depth, z, thus:

$$J(\varphi,\xi) \equiv J(z)\,. \tag{66}$$

We have shown in equation (26) how to calculate the source function, $J(z)$, in units of $I_0 f(z_1)$. Equation (40) enables us to calculate the quantity $f(z_1)$; hence, in the usual units,

$$J(\varphi,\xi) \equiv I_0 f(z_1) J(z)\,. \tag{67}$$

When we substitute this expression for $J(\varphi, \xi)$ in equations (63) and (64), we find that

$$R_1 = \frac{z_1}{q}\frac{f(z_1)}{(\frac{1}{2}+\frac{1}{3}\beta)}\int_1^\infty d\xi\int_0^\pi e^{-z_1\varphi/q\xi} J(z)\, d\varphi \tag{68}$$

and

$$R_2 = \frac{z_1}{q}\frac{f(z_1)}{(\frac{1}{2}+\frac{1}{3}\beta)}\int_0^1 d\xi\int_0^{\sin^{-1}\xi} e^{-z_1\varphi/q\xi} J(z)\, d\varphi\,. \tag{69}$$

The expression for R_3 is

$$R_3 = \frac{\int_0^{r_1} p\, e^{-c\theta_1/p}\,(1+\beta\cos\theta_1)\,dp}{r_1^2\,(\frac{1}{2}+\frac{1}{3}\beta)}. \tag{70}$$

Since $p = r_1 \sin\theta_1$, we shall transform to the variable θ_1; we also note that $c/r_1 = z_1/q$. Then we have

$$R_3 = (\tfrac{1}{2}+\tfrac{1}{3}\beta)^{-1}\int_0^{\pi/2} e^{-z_1\theta_1/q\sin\theta_1}\,(1+\beta\cos\theta_1)\sin\theta_1\cos\theta_1 d\theta_1. \tag{71}$$

Referring to equations (68), (69), and (71), we see that the residual intensity, $R_\nu = R_1 + R_2 + R_3$, can be found explicitly if the quantity z_1 is known. This solves the Schuster problem in a spherical atmosphere.

4. *Numerical work.*—According to equation (26),

$$J(z) = J_\infty(z) - a(z_1)\,\gamma(z).$$

In Paper V we saw that (cf. eq. [83]), for the case $n = 2$,

$$J_\infty(z) = q^{-3}[\tfrac{1}{4}z^3 + \Delta_\infty(z)], \tag{72}$$

where

$$\Delta_\infty(z) = [J_\infty(z)]_{\text{2d approx}} - [J_\infty(z)]_{\text{1st approx}}. \tag{73}$$

The quantity $\Delta_\infty(z)$ can be evaluated numerically from the tables in Paper V. If we write the source function as

$$q^3 J(z) = \tfrac{1}{4}z^3 + \epsilon(z, z_1), \tag{74}$$

where

$$\epsilon(z, z_1) = \Delta_\infty(z) - a(z_1)\,q^3\gamma(z), \tag{75}$$

and substitute equation (74) in equations (68) and (69), we find that

$$R_1 = \frac{z_1}{q^4}\frac{f(z_1)}{(\frac{1}{2}+\frac{1}{3}\beta)}[\Im_1' + \Im_2''] \tag{76}$$

and

$$R_2 = \frac{z_1}{q^4}\frac{f(z_1)}{(\frac{1}{2}+\frac{1}{3}\beta)}[\Im_2' + \Im_2''], \tag{77}$$

where

$$\Im_1' = \frac{1}{4}\int_1^\infty d\xi \int_0^\pi d\varphi\, e^{-z_1\varphi/q\xi} z^3, \tag{78}$$

$$\Im_1'' = \int_1^\infty d\xi \int_0^\pi d\varphi\, e^{-z_1\varphi/q\xi}\epsilon(z, z_1), \tag{79}$$

$$\Im_2' = \frac{1}{4}\int_0^1 d\xi \int_0^{\sin^{-1}\xi} d\varphi\, e^{-z_1\varphi/q\xi} z^3, \tag{80}$$

and

$$\Im_2'' = \int_0^1 d\xi \int_0^{\sin^{-1}\xi} d\varphi\, e^{-z_1\varphi/q\xi}\epsilon(z, z_1). \tag{81}$$

The integrals $\Im_1''$ and $\Im_2''$ may be neglected, since $\epsilon(z, z_1)$ is small compared to $\frac{1}{4}z^3$. Some typical values of $\epsilon(z, z_1)$ are given in Table 2. Although, with large z, $\epsilon(z, z_1)$ becomes comparable to $\frac{1}{4}z^3$, the product $\epsilon(z, z_1)\exp(-z_1\varphi/q\xi]$, which enters the integrals

$\mathfrak{I}_1''$ and $\mathfrak{I}_2''$, always remains small, for equation (65) shows that, for any given z_1/q and ξ, the term $z_1\varphi/q\xi$ increases with increasing z. The neglect of $\mathfrak{I}_1''$ and $\mathfrak{I}_2''$ means that we are using the source function in the first approximation.

The integral $\mathfrak{I}_1'$ may be evaluated as follows: From equations (65) and (78) we have

$$\mathfrak{I}_1' = \tfrac{1}{4} z_1^3 \int_1^\infty d\xi \int_0^\pi d\varphi \, e^{-z_1\varphi/q\xi} \frac{\sin^3 \varphi}{\xi^3}. \tag{82}$$

If we put $z_1\varphi/q = a$ and invert the order of integration, we obtain

$$\mathfrak{I}_1' = \tfrac{1}{4} z_1^3 \int_0^\pi d\varphi \sin^3 \varphi \int_1^\infty d\xi \, e^{-a/\xi} \xi^{-3}. \tag{83}$$

TABLE 2

TYPICAL $\epsilon(z, z_1)$

z	$\frac{1}{4}z^3$	$\epsilon(z, z_1)$		z	$\frac{1}{4}z^3$	$\epsilon(z, z_1)$
		$z_1=1$	$z_1=5$			$z_1=5$
0.0	0.0000000	0.0000000	0.0000000	1.6	1.02400	0.08322
0.1	.0002500	.0000008	.0000000	1.8	1.45800	0.13100
0.2	.0020000	.0000323	.0000097	2.0	2.0000	0.1973
0.3	.0067500	.0002372	.0000658	2.2	2.6620	0.2781
0.4	.016000	.000967	.000240	2.4	3.4560	0.3827
0.5	.031250	.002881	.000645	2.6	4.3940	0.5112
0.6	.054000	.007044	.001432	2.8	5.4880	0.6667
0.7	.085750	.013699	.002789	3.0	6.7500	0.8524
0.8	.12800	.02910	.00493	3.5	10.7188	1.4760
0.9	.18225	.05224	.00811	4.0	16.0000	2.4060
1.0	.25000	0.08843	.01258	4.5	22.7813	3.8246
1.2	.43200		.02656	5.0	31.2500	6.0446
1.4	0.68600		0.04926			

Then we make the substitution $x = 1/\xi$ and evaluate the integral over x, getting

$$\mathfrak{I}_1' = \tfrac{1}{4} z_1^3 \int_0^\pi d\varphi \sin^3 \varphi a^{-2} [1 - e^{-a}(a+1)]. \tag{84}$$

We then replace a by $z_1\varphi/q$ and substitute $\mu = \cos\varphi$, which gives us

$$\mathfrak{I}_1' = \frac{q^2 z_1}{4} \int_{-1}^{+1} d\mu (1-\mu^2) \left\{ \frac{1}{\varphi^2} - \frac{1}{\varphi^2} e^{-z_1\varphi/q} - \frac{z_1}{q\varphi} e^{-z_1\varphi/q} \right\}. \tag{85}$$

This integral may be evaluated numerically by using Gauss's quadrature formula; thus,

$$\mathfrak{I}_1' = \frac{q^2 z_1}{4} \left[\sum_{j=-n}^{+n} \frac{a_j}{\varphi_j^2}(1-\mu_j^2) - \sum_{j=-n}^{+n} \frac{a_j}{\varphi_j^2}(1-\mu_j^2) e^{-z_1\varphi_j/q} - \frac{z_1}{q} \sum_{j=-n}^{+n} \frac{a_j}{\varphi_j}(1-\mu_j^2) e^{-z_1\varphi_j/q} \right], \tag{86}$$

where the a_j's are Gaussian weights,[6] the μ_j's are the roots of Legendre polynomial of order $2n+1$, and the summation is carried out over both positive and negative roots. Also we have

$$\varphi_j = \cos^{-1} \mu_j. \tag{87}$$

[6] *Bull. Am. Math. Soc.*, **48**, 741, 1942.

A five-point formula, j running from -2 to $+2$, was found to yield sufficiently accurate results.

The integral $\mathfrak{I}_2'$ is evaluated in a similar manner. We have

$$\mathfrak{I}_2' = \frac{z_1^3}{4}\int_0^1 d\xi \int_0^{\sin^{-1}\xi} d\varphi\, e^{-z_1\varphi/q\xi}\,\frac{\sin^3\varphi}{\xi^3}. \tag{88}$$

If we invert the order of integration and substitute $a = z_1\varphi/q$, we obtain

$$\mathfrak{I}_2' = \frac{z_1^3}{4}\int_0^{\pi/2} d\varphi\,\sin^3\varphi \int_{\sin\varphi}^1 d\xi\, e^{-a/\xi}\xi^{-3}. \tag{89}$$

The integral over ξ is evaluated as in the previous case, with the result that

$$\mathfrak{I}_2' = \frac{z_1^3}{4}\int_0^{\pi/2} d\varphi\,\sin^3\varphi\, a^{-2}\left[\, e^{-a}(a+1) - e^{-a/\sin\varphi}\left(\frac{a}{\sin\varphi}+1\right)\right]. \tag{90}$$

Then a is replaced by $z_1\varphi/q$, the terms are collected, and $\mu = \cos\varphi$ is introduced, giving us

$$\mathfrak{I}_2' = \frac{q^2 z_1}{4}\int_0^1 d\mu\,(1-\mu^2)\left[\frac{1}{\varphi^2}\left\{\, e^{-z_1\varphi/q} - e^{-z_1\varphi/q(1-\mu^2)^{1/2}}\right\}\right.$$
$$\left. + \frac{z_1}{q\varphi}\left\{\, e^{-z_1\varphi/q} - (1-\mu^2)^{-1/2}\, e^{-z_1\varphi/q(1-\mu^2)^{1/2}}\right\}\right]. \tag{91}$$

We again evaluate this integral by Gauss's formula, the roots of a Legendre polynomial of order $2n$ being now used and the summation being extended over the positive j-values. Thus we get

$$\mathfrak{I}_2' = \frac{q^2 z_1}{4}\left[\sum_{j=1}^{n}\frac{a_j}{\varphi_j^2}(1-\mu_j^2)\left\{\, e^{-z_1\varphi_j/q} - e^{-z_1\varphi_j/q(1-\mu^2)^{1/2}}\right\}\right.$$
$$\left. + \frac{z_1}{q}\sum_{j=1}^{n}\frac{a_j}{\varphi_j}(1-\mu_j^2)\left\{\, e^{-z_1\varphi_j/q} - (1-\mu_j^2)^{-1/2}\, e^{-z_1\varphi_j/q(1-\mu_j^2)^{1/2}}\right\}\right]. \tag{92}$$

A five-point formula—$j = 1, 2, 3, 4, 5$—is used.

Let the integral in the expression for R_3 (eq. [70]) be $\mathfrak{I}_3$, then

$$\mathfrak{I}_3 = \int^{\pi/2} e^{-z_1\theta_1/q\sin\theta_1}(1+\beta\cos\theta_1)\sin\theta_1\cos\theta_1 d\theta_1. \tag{93}$$

Let $\mu = \cos\theta_1$, and evaluate the integral by an even Gaussian division, as for integral $\mathfrak{I}_2'$. Then we have

$$\mathfrak{I}_3 = \sum_{j=1}^{n} a_j\mu_j(1+\beta\mu_j)\exp\left[-\frac{z_1\theta_j}{q(1-\mu_j^2)^{1/2}}\right]. \tag{94}$$

It is sufficient to use a five-point formula.

Table 3 gives R_1, R_2, R_3, and R, calculated according to equations (68), (69), and (71) for various values of z_1, and hence of τ_1, the total optical thickness of the atmosphere for radiation of frequency ν. Table 4 gives a table of residual intensities for a plane-parallel Schuster atmosphere calculated according to equation (7).

Evaluation of the integrals $\mathfrak{I}_1''$ and $\mathfrak{I}_2''$ will increase the values of R_1 and R_2 by a few per cent. In view of the uncertainty with which our idealized model fits a real star, it does not seem worth while to evaluate $\mathfrak{I}_1''$ and $\mathfrak{I}_2''$.

TABLE 3

SPHERICAL ATMOSPHERE

z_1	$\tau_1=z_1/q$	R_1	R_2	R_3	R
0.0	0.0000	0.0000	0.0000	1.0000	1.0000
0.1	0.0507	.0018	.0004	0.9479	0.9501
0.2	0.1014	.0065	.0022	0.8957	0.9044
0.3	0.1521	.0155	.0039	0.8462	0.8656
0.4	0.2028	.0228	.0058	0.7997	0.8283
0.5	0.2536	.0332	.0085	0.7556	0.7973
0.6	0.3043	.0444	.0114	0.7140	0.7698
0.7	0.3550	.0570	.0147	0.6747	0.7464
0.8	0.4057	.0692	.0180	0.6376	0.7248
0.9	0.4564	.0809	.0210	0.6025	0.7044
1.0	0.5071	.0935	.0248	0.5694	0.6877
1.2	0.6085	.1214	.0318	0.5086	0.6618
1.4	0.7099	.1470	.0384	0.4544	0.6398
1.6	0.8114	.1715	.0448	0.4059	0.6222
1.8	0.9128	.1947	.0508	0.3627	0.6082
2.0	1.0142	.2165	.0562	0.3241	0.5968
2.2	1.1156	.2368	.0611	0.2896	0.5875
2.4	1.2170	.2567	.0658	0.2589	0.5814
2.6	1.3185	.2731	.0694	0.2314	0.5739
2.8	1.4199	.2887	.0725	0.2069	0.5681
3.0	1.5213	.3032	.0753	0.1849	0.5634
3.5	1.7748	.3341	.0802	0.1398	0.5541
4.0	2.0284	.3584	.0826	0.1058	0.5468
4.5	2.2819	.3770	.0829	0.0800	0.5399
5.0	2.5355	.3913	.0817	0.0606	0.5336
5.5	2.7890	0.4018	0.0794	0.0459	0.5271

TABLE 4

PLANE-PARALLEL ATMOSPHERE

τ_1	R	τ_1	R	τ_1	R	τ_1	R
0.00	1.000	0.35	0.7780	0.90	0.5859	2.00	0.3954
.05	0.9588	.40	.7547	1.00	.5612	2.20	.3734
.10	0.9219	.50	.7129	1.20	.5176	2.40	.3538
.15	0.8888	.60	.6760	1.40	.4804	2.60	.3360
.20	0.8576	.70	.6428	1.60	.4483	2.80	.3200
.25	0.8285	0.80	0.6127	1.80	0.4202	3.00	0.3055
0.30	0.8024						

5. *Discussion of the results.*—Figure 2 gives the data of Tables 3 and 4 plotted against τ_1. For very small τ_1—$\tau_1 < 0.05$—the two curves are practically identical, as might be expected, since for very small τ_1 the effect of the curvature of the atmosphere will be negligible. For $0.05 < \tau_1 < 0.8$ the residual intensity in the plane-parallel atmosphere is greater than that in the spherical atmosphere. For $\tau_1 > 0.8$ the residual intensity in the spherical atmosphere becomes greater than that in the plane-parallel atmosphere. The effect of this is shown in Figure 3, which gives line profiles calculated for a spherical

Schuster atmosphere and for a plane-parallel Schuster atmosphere. Figure 3, *a*, is obtained when it is assumed that $\tau = \tau_0 e^{-(\Delta\lambda)^2}$, Figure 3, *b*, when $\tau = \tau_0[1 + (\Delta\lambda)^2]^{-1}$. In both cases the same $\tau_0 = 2.7890$ was used. The following conclusions are evident from inspection of the line profiles:

1. The cores of the lines are blunter and more shallow in a spherical atmosphere than in a plane-parallel atmosphere.
2. The wings of the lines are deeper in a spherical atmosphere than in a plane-parallel atmosphere.
3. When the absorption coefficient has a Gaussian form (Fig. 3, *a*), the equivalent width of the line formed in the spherical atmosphere is less than that of the line formed in a plane-parallel atmosphere.

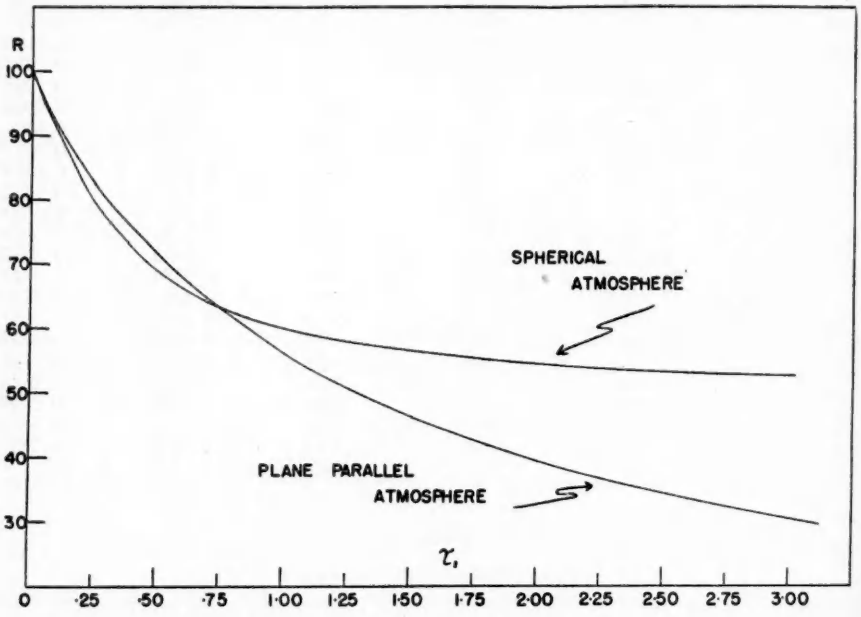

FIG. 2.—The variation of residual intensity with τ_1 for a spherical and a plane-parallel atmosphere. R is given in percentage of the continuum.

4. When the absorption coefficient has a damping form (Fig. 3, *b*), the equivalent width in the two cases may remain much the same, as the reduction in equivalent width caused by the shallowing of the core of the line formed in a spherical atmosphere is largely compensated by the deepening of the extensive wings of this line.

The most significant result of the curvature of the atmosphere is that, for $\tau_1 > 2$, the residual intensity in the spherical atmosphere is much greater than that in the plane-parallel atmosphere. Thus the cores of the lines formed in a spherical atmosphere will be shallower than those of lines formed in a plane-parallel atmosphere. This effect might be observed in some lines of supergiant stars. For the elements other than *H* or *He*, τ_0 is not very large and may fall in the range of values in Tables 3 and 4. If this is true and the curvature of the atmosphere is important for supergiants, the lines in supergiants should have blunter, shallower cores than the lines in main-sequence stars. However, rotation and mass motion of the atmosphere also shallow the lines. Thus it may be dif-

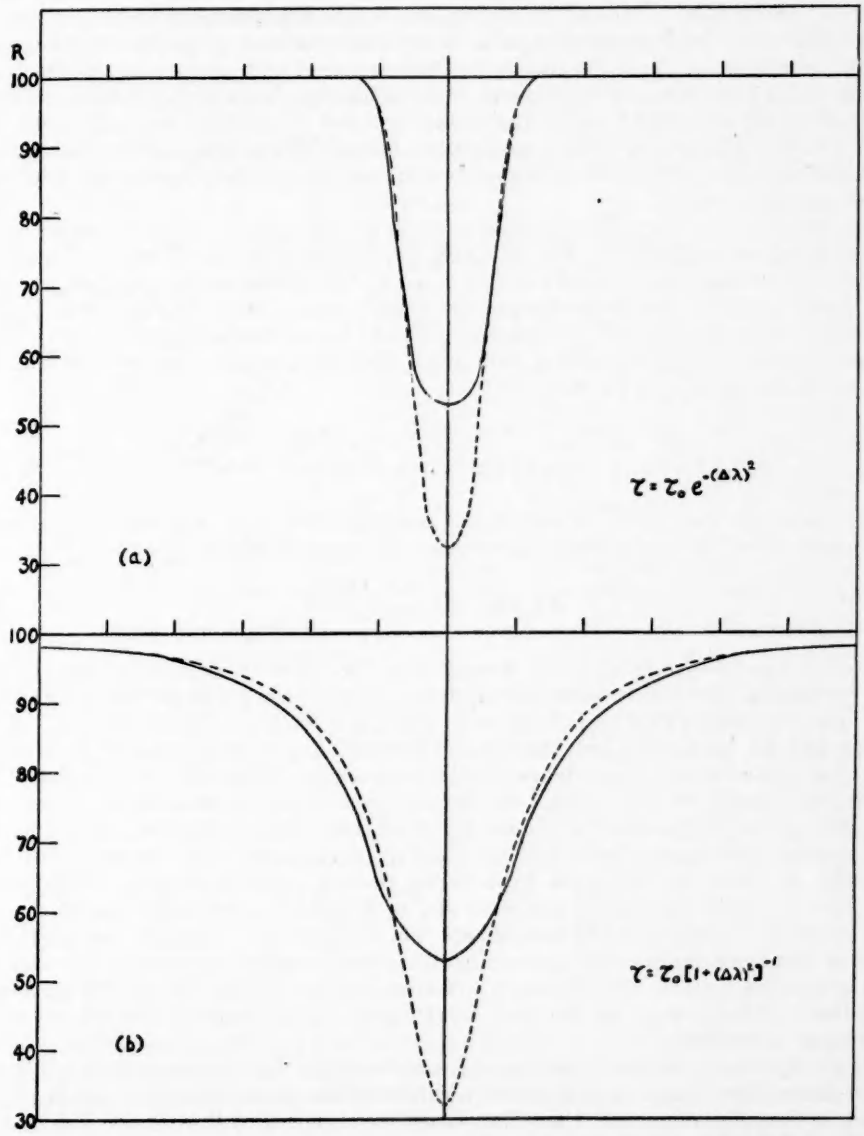

FIG. 3.—Line shapes in a spherical and a plane-parallel atmosphere, (*a*) when the absorption coefficient has Gaussian form, (*b*) when the absorption coefficient has damping form. The solid curve gives the profile in a spherical atmosphere; the broken curve gives the profile in a plane-parallel atmosphere. The residual intensity is given in percentage of the continuum. The wave-length scale is arbitrary.

ficult to interpret shallow lines in supergiants directly as a result of sphericity. Although rotation of the star broadens the lines, it does not change their relative equivalent widths. Uniform mass motion of the atmosphere causes displacements of the lines (which will be difficult to separate from the peculiar motion of the star except when there is some outside indication of the star's true radial velocity) and may also cause certain asymmetries of all lines.[7] On the other hand, the shallowing effects of the sphericity of the atmosphere depend greatly upon the strength of the line, that is upon τ_0. Only for $\tau_0 > 2$ will the shallowing of the cores be conspicuous. Thus a comparison of strong and weak lines in supergiant and main-sequence stars may reveal the effects of the sphericity of the atmosphere.

If a similar comparison is to be made for the hydrogen lines, the tables must be extended to larger values of τ_1. The following asymptotic form for R results if only the terms with the highest power of z are included in the expression for $f(z_1)$ (see eq. [40]) and if only the first term in the integral $\mathfrak{J}_1'$ is used (see eq. [86]). The figures in Table 3 show that the integrals $\mathfrak{J}_2'$ and $\mathfrak{J}_3$, which give R_2 and R_3, become negligible with increasing z. Furthermore, the computations show that, with large z, only the first term in the integral $\mathfrak{J}_1'$ is significant. We find

$$R\ (\text{large}\ z_1) = \frac{(\mu_2^2-\mu_1^2)}{(\frac{1}{2}+\frac{1}{3}\beta)} \frac{[a_1\mu_1(1+\beta\mu_1)+a_2\mu_2(1+\beta\mu_2)]}{[\frac{1}{4}(\mu_1\mu_2^2-\mu_2\mu_1^2)-\frac{1}{2}(\mu_1-\mu_2)]} \frac{1}{4}\frac{q}{z_1}\sum_j a_j(1-\mu_j^2)\frac{1}{\theta_j^2}, \quad (95)$$

where the summation over j is carried out over the zeros of a Legendre polynomial of odd order. When the appropriate numerical values are introduced, we obtain

$$R\ (\text{large}\ z_1) = \frac{5.587}{\tau_1}, \quad (96)$$

where q/z_1 has been replaced by τ_1, according to the definition of τ_1. Equation (7) may still be used to give the residual intensity for large τ_1 in a plane-parallel atmosphere. The use of equations (96) and (7) gives us the values shown in Table 5.

We see that, for large τ_1 also, the residual intensity in a spherical atmosphere is larger than the residual intensity in a plane-parallel atmosphere. However, the detection of this difference from observations would require very careful photometry. If the curvature of the atmosphere is important in the formation of the hydrogen lines of supergiants, the line profiles for these stars should show sharp, deep cores with comparatively high "shoulders," since, according to Table 3, the residual intensity in the "shoulders" of the lines, where τ_1 might be of the order of 2 or 3, will be considerably higher than for lines formed in a plane-parallel atmosphere. The comparisons which are discussed above assume that the Schuster idealization represents the formation of lines in main-sequence and in supergiant stars. Although such an assumption may not be justified, it is probable that the main features of the argument would carry over if a more detailed theory of line formation were used.

If the sphericity of the atmosphere is important in determining the line shape in supergiants, the change in equivalent width that may ensue will have an important effect on the curve of growth. Consideration of the variation of R with τ_1 in Tables 3 and 4 and of Figure 3 leads to the following conclusions. If the line is very weak, i.e., τ_0 small, the equivalent width will be somewhat larger in a spherical atmosphere than in a plane-parallel atmosphere. For such lines $\log W/\lambda \propto N$ would likely be true. As τ_0 increases, the absorption coefficient being still predominantly Gaussian in form, the case of Figure 3, *a*, is reached. Then W in the spherical atmosphere is less than W in the plane-parallel atmosphere; hence the curve of growth for such a star will begin to flatten out sooner than it would for a star with a plane-parallel atmosphere. However, in the

[7] *Ap. J.*, **106**, 128, 1947.

supergiant stars turbulence is important and tends to lift the flat part of the curve of growth,[8] the line-absorption coefficient remaining Gaussian in form. The net result of the opposing effects of sphericity and turbulence will be to show a reduced lifting of the flat portion of the curve of growth. Hence a smaller turbulent velocity than is actually the case will be deduced. The damping portion of the curve of growth might remain much the same in a spherical and plane-parallel atmosphere, since Figure 3, *b*, shows that, when the absorption coefficient has a damping form, there may be little difference in equivalent width between the two cases.

TABLE 5

RESIDUAL INTENSITIES FOR LARGE τ_1

τ_1	Spherical Atmosphere R	Plane-parallel Atmosphere R
50	0.112	0.026
100	.056	.013
1000	0.006	0.001

TABLE 6

THE EFFECT OF CONTINUOUS SCATTERING IN THE ATMOSPHERE*

$z_{1\nu}$	SPHERICAL ATMOSPHERE			PLANE-PARALLEL ATMOSPHERE		
	$z_{1\sigma}=0.0$	$z_{1\sigma}=0.1$	$z_{1\sigma}=2.0$	$z_{1\sigma}=0.0$	$z_{1\sigma}=0.1$	$z_{1\sigma}=2.0$
0.0	1.000	1.000	1.000	1.000	1.000	1.000
0.2	0.904	0.911	0.983	0.921	0.926	0.960
0.4	0.828	0.839	0.974	0.856	0.863	0.920
0.6	0.770	0.785	0.961	0.800	0.810	0.888
0.8	0.725	0.741	0.952	0.752	0.763	0.854
1.0	0.688	0.711	0.943	0.710	0.722	0.826
2.0	0.597	0.623	0.916	0.558	0.571	0.703
3.0	0.563	0.585	0.895	0.461	0.473	0.612
4.0	0.547	0.570	.....	0.393	0.405	.....
5.0	0.534	0.556	.....	0.342	0.352	.....

* The table gives R'_ν.

These remarks emphasize again the necessity of the study of line profiles in supergiant stars rather than deriving information from curves of growth only, since so many opposing tendencies, whose effects are obliterated in a mere study of equivalent widths, may be at work.

From Tables 3 and 4 we can also estimate the effect of the occurrence of continuous scattering in the atmosphere, as well as line scattering. Such scattering might arise from the presence of electrons. The continuous scattering coefficient, σ, is independent of frequency. Let the optical depth in the atmosphere due to continuous scattering be τ_σ. Then the flux emerging from the atmosphere in frequencies outside a line is

$$F_c = R(\tau_\sigma) F , \tag{97}$$

[8] *Ap. J.*, **79**, 409, 1934.

where F is the photospheric flux. The emergent flux for any frequency in the line is

$$F_\nu = R(\tau_\sigma + \tau_\nu) F , \tag{98}$$

where τ_ν is the optical thickness of an atmosphere without continuous scattering for radiation of frequency ν; hence $\tau_\sigma + \tau_\nu$ is the total optical thickness in the frequency ν. The residual intensity of the line will be

$$R'_\nu = \frac{F_\nu}{F_c} = \frac{R(\tau_\sigma + \tau_\nu)}{R(\tau_\sigma)} . \tag{99}$$

Table 6 gives the results for a spherical and a plane-parallel atmosphere when the optical depth due to electron scattering corresponds to $z_{1\sigma} = 0, 0.1$, and 2.0. The residual intensity is calculated according to equation (99) for a series of total optical depths $z_{1\sigma} + z_{1\nu}$ corresponding to the values of $z_{1\nu}$ given in the first column. We see that the effect of superposed electron scattering is to shallow the line in all cases, the effects of electron scattering being enhanced in a spherical atmosphere.

Table 3 offers an interesting opportunity for considering possible line-intensity changes during the eclipse of an extended star by a dark or faintly luminous compact body. The quantity R_1 is the part of the residual intensity in the line arising from the integrated flux over all the envelope except that part immediately in front of the disk; R_2 is the part of the residual intensity in the line arising from that part of the envelope in front of the disk; R_3 is the part of the residual intensity in the line arising from the transmitted photospheric light. These numbers are proportional to the corresponding fluxes from these portions of the star, since these fluxes are obtained by multiplying R_1, R_2, and R_3 by the flux from the photosphere. Estimation of how the total residual intensity $R = R_1 + R_2 + R_3$ will change as different parts of the star are eclipsed then follows from Table 3.

My sincere thanks are due to Dr. S. Chandrasekhar for his criticism and guidance throughout this study, and to Dr. J. L. Greenstein for helpful discussions of the application of the theory to observation.

THE EFFECT OF NONGRAYNESS ON THE TEMPERATURE DISTRIBUTION OF THE SOLAR ATMOSPHERE

GUIDO MÜNCH
Yerkes Observatory
Received November 13, 1947

ABSTRACT

In this paper the temperature distribution in the solar atmosphere is determined by making proper allowance for its departures from grayness. The variation of temperature with optical depth is determined in the second approximation of the method developed by S. Chandrasekhar to solve the problem of radiative transfer in a stellar atmosphere in which the continuous absorption coefficient depends on the frequency. The difference between this temperature and the gray atmospheric value is found to be sufficiently small to justify the use of the temperature distribution of the gray body as a good first approximation.

1. *Introduction.*—In the solution to the problem of radiative transfer in a nongray atmosphere developed by S. Chandrasekhar,[1] the temperature, T, prevailing at the depth, τ, in a first approximation is related to the effective temperature, T_e, through the standard equation,

$$T^4 = \tfrac{3}{4}T_e^4 [\tau + q(\tau)], \tag{1}$$

provided that the mean absorption coefficient, $\bar{\kappa}$, in terms of which τ is measured, is defined as a weighted mean of the monochromatic absorption coefficient, κ_ν, where the weight function is the flux, $F_\nu^{(1)}(\tau)$, of a gray atmosphere of the same effective temperature, T_e. However, in a higher approximation, certain corrections are introduced to the temperature distribution (1), which are entirely determined by the departures from grayness, measured by the quantity

$$\delta_\nu = \frac{\kappa_\nu}{\bar{\kappa}} - 1, \tag{2}$$

and certain invariants of the gray atmospheres.

It is the object of this paper to evaluate the temperature distribution of a model solar atmosphere in a second approximation, making proper allowance for nongrayness, following the method developed in Paper VII. To be specific, we shall consider the model solar atmosphere defined by the hydrogen-metal ratio $A = 10^{3.8}$, considered earlier by the author,[2] although the quantity $\delta_\nu = \delta_\nu(\tau)$, defined by equation (2), is, in the case of solar atmospheres, practically independent of the value of A, in the relevant range of τ.

2. *The temperature distribution of a nongray atmosphere in the (2, 2) approximation.*—If equation (1) is accepted to be valid in a first approximation, then the integrated Planck function, $B^{(2)}(\tau)$, in the second approximation is given by

$$B^{(2)} = J^{(2)} + \frac{1}{4}\int_0^\infty \delta_\nu \frac{dF_\nu^{(1)}}{d\tau}\, d\nu = J^{(2)} + \frac{\bar{\delta}_1}{2}, \tag{3}$$

where $J^{(2)}$ stands for the mean intensity in the second approximation. However, in this case $J^{(2)}$ does not have the gray atmospheric value, $J^{(1)}$. Indeed, it is given by the equation

$$J^{(2)} = J^{(1)} + \Delta J, \tag{4}$$

[1] *Ap. J.*, **101**, 328, 1945. This paper will be referred to as "Paper VII."

[2] *Ap. J.*, **106**, 217, 1947.

where ΔJ, in units of the integrated net flux, F, is given by[3]

$$\Delta J = -0.1664\,(2+0.2301\,e^{-k_1\tau})\int_0^\infty e^{-k_1\tau}\left(\bar{\delta}_3-\frac{\bar{\delta}_1}{3}+k_1\bar{\delta}_4\right)d\,(k_1\tau)$$
$$+\tfrac{3}{4}\,e^{-k_1\tau}\int_0^\tau e^{+k_1\tau}\left(\bar{\delta}_3-\frac{\bar{\delta}_1}{3}-k_1\bar{\delta}_4\right)d\,(k_1\tau) \qquad (5)$$
$$+\tfrac{3}{4}\,e^{+k_1\tau}\int_\tau^\infty e^{-k_1\tau}\left(\bar{\delta}_3-\frac{\bar{\delta}_1}{3}+k_1\bar{\delta}_4\right)d\,(k_1\tau)\,.$$

In equation (5), k_1 is a numerical constant having the value $\sqrt{35}/3 = 1.9703$, and $\bar{\delta}_m$ $(m = 1, 3, 4)$ is defined by the equation

$$\bar{\delta}_m = \bar{\delta}_m(\tau) = \int_0^\infty W_m(\nu,\tau)\,\delta_\nu(\tau)\,d\nu\,, \qquad (6)$$

where

$$W_m(\nu,\tau) = \int_{-1}^{+1}\frac{dI_\nu^{(1)}}{d\tau}\,\mu^m d\mu\,. \qquad (7)$$

Moreover, in equation (7) $I_\nu^{(1)} = I_\nu^{(1)}(\tau,\mu)$ refers to the monochromatic intensities in a gray atmosphere. The weight functions, $W_3(\nu,\tau)$ and $W_4(\nu,\tau)$, have been evaluated and given in numerical form by S. Chandrasekhar and Mrs. Breen in Paper XVIII (Table 11), for values of τ in the range $0 \leqslant \tau \leqslant 2$ and values of a $(=h\nu/kT_e)$ in the range $1 \leqslant a \leqslant 12$. The weight function, $W_1(a,\tau)$, is given in numerical form for the same ranges of the arguments in Paper VII (Table 3). The averages $\bar{\delta}_m$, therefore, can be readily evaluated by a numerical procedure, once we have a table of $\delta_\nu(\tau)$.

3. *The temperature distribution of the solar atmosphere in a second approximation.*—The values of $\delta_\nu(\tau)$ in the case of the solar atmosphere were obtained from the tables given by the author[4] and the values of the monochromatic absorption coefficient of the negative ion of hydrogen given by Chandrasekhar and Breen.[5] It should be mentioned, however, that, in order to be able to evaluate the averages $\bar{\delta}_m$, it is necessary to know accurately the values of the weight functions, $W_m(a,\tau)$, for values of a in the neighborhood of $a = 0$, since $K_\nu(H^-) \to \infty$ as ν^{-2} when $\nu \to 0$. In order to evaluate $W_m(a,\tau)$ for small values of a, it is sufficient to know the values of $F_a^{(1)}(\tau)$.[6] This may be accomplished, without going into lengthy numerical work, by writing $F_a^{(1)}(\tau)$ in the form

$$F_a^{(1)}(\tau) = 2B_a(0)\,f_a(\tau)\,, \qquad (8)$$

where $B_a(0)$ stands for the Planck function of the boundary temperature, $T_0 = (\sqrt{3}/4)^{1/4}T_e$, and $f_a(\tau)$ is a function which has a nonvanishing finite value at $a = 0$, and which can be obtained with sufficient accuracy by interpolating between the values $a = 0$ and $a = 1$ given in Table 1 of Paper VII. On the other hand, the Planck function, $B_a(\tau=0)$, for $a < 2\pi(\sqrt{3}/4)^{1/4}$, may be developed in a power series of a, in the form

$$B_a(0) = \frac{15}{\pi^4}\left(\frac{\sqrt{3}}{4}\right)^{1/4}\left[a^2-\frac{1}{2}\left(\frac{\sqrt{3}}{4}\right)^{-1/4}a^3+\frac{B_1}{2!}\left(\frac{\sqrt{3}}{4}\right)^{-2/4}a^4\right.$$
$$\left.-\frac{B_2}{4!}\left(\frac{\sqrt{3}}{4}\right)^{-4/4}a^6+\ldots\right], \qquad (9)$$

[3] *Ap. J.*, **105**, 461, eq. (21), 1947. This paper is hereafter referred to as "Paper XVIII."

[4] Cf. *op. cit.*, Table 3.

[5] *Ap. J.*, **104**, 430, 1946.

[6] Cf. Paper XVIII, eqs. (23), (26), (27), and (28).

where $B_1, B_2, \ldots$, are the Bernoullian numbers. According to series (9), $B_\alpha(0) \to 0$ as α^2 when $\alpha \to 0$; and therefore the products $\delta_\nu(\tau)W_m(\nu, \tau)$ tend to a finite limit, different from zero, when the frequency approaches zero.

The averages $\bar{\delta}_m$ were evaluated at the depths $\tau = 0, 0.1, 0.2, 0.4, 0.7, 1.0, 1.4$, by graphical integrations, and the results of the calculation are given in Table 1. Once the averages $\bar{\delta}_m$ have been obtained, it is a simple matter to obtain the integrated Planck function, $B^{(2)}(\tau)$, from equations (3), (4), and (5). The result of this calculation is also given in Table 1.

4. *Discussion of the results.*—It should be recalled here that in Paper VII attention was drawn to the different character of the corrections which must be made to the temperature distribution derived on the assumption of grayness, in order to be valid in a

TABLE 1*

THE TEMPERATURE DISTRIBUTION $T_2(\tau)$ IN A NONGRAY MODEL SOLAR ATMOSPHERE

τ	$\bar{\delta}_1$	$\bar{\delta}_3$	$\bar{\delta}_4$	ΔJ	$\frac{B^{(1)}}{J^{(1)}} =$	$J^{(2)}$	$B^{(2)}$	T_1	T_2
0	−0.0357	−0.0156	+0.0011	−0.0025	0.4330	0.4305	0.4127	4634° K	4579° K
0.05	− .0397	.....	.....	− .0030	0.4787	0.4757	0.4559	4752	4694
0.1	− .0416	− .0191	+ .0005	− .0035	0.5236	0.5201	0.4993	4860	4802
0.2	− .0440	− .0216	.0000	− .0045	0.6116	0.6071	0.5851	5052	4996
0.3	− .0461	.....	.....	− .0054	0.6971	0.6917	0.6687	5220	5166
0.4	− .0477	− .0242	− .0002	− .0060	0.7808	0.7748	0.7510	5370	5318
0.5	− .0482	.....	.....	− .0065	0.8629	0.8564	0.8323	5506	5457
0.6	− .0482	.....	.....	− .0068	0.9437	0.9369	0.9128	5631	5584
0.7	− .0481	− .0262	+ .0007	− .0069	1.0235	1.0166	0.9926	5746	5702
0.8	− .0479	.....	.....	− .0069	1.1024	1.0955	1.0716	5854	5813
1.0	− .0471	− .0261	+ .0021	− .0065	1.2584	1.2519	1.2283	6051	6014
1.2	− .0457	.....	.....	− .0058	1.4123	1.4065	1.3837	6228	6196
1.4	− .0441	−0.0258	+0.0031	− .0048	1.5650	1.5602	1.5381	6390	6362
2.0	−0.0388	.....	.....	−0.0018	2.0188	2.0170	1.9976	6810	6792

* The values of T_2 at $\tau = 0.05, 0.3, 0.5, 0.6, 0.8$, and 1.2 were obtained by interpolating the values of $\bar{\delta}_1$ and ΔJ, while the value of T_2 at $\tau = 2.0$ is an extrapolation.

nongray atmosphere. These corrections arise from two sources: first, the integrated Planck intensity, B, is not equal to the mean integrated intensity, and, second, the energy density of the radiation does not have the gray atmospheric value. The former is represented by the term $\bar{\delta}_1/2$ in equation (2), which in Table 1 is seen to be much larger than the correction arising from the second effect, which is measured by ΔJ. A comparison of the temperatures, T_1 and T_2, derived on the assumptions of grayness and nongrayness, respectively, given in the last two columns of Table 1, shows that the difference between the two is maximum at the boundary and steadily decreases as we go into deeper layers. It is important to notice, in particular, that temperature T_2 is systematically lower than T_1. This fact provides another reason[7] to expect the actual boundary temperature of the solar atmosphere to be lower than the gray atmospheric value is.

When the comparison of the temperatures T_1 and T_2 is made, we should have in mind that, although both temperatures refer to the same optical depth, they do not correspond to the same geometrical depth, because the mean absorption coefficients $\bar{\kappa}$, in terms of which we measure τ, are different in both cases. In connection with this point, it should be noticed also that the way in which the calculations have been made is not strictly con-

[7] The author (*Ap. J.*, **104**, 87, 1946) has shown that the process in which the Fraunhofer lines arise has also the effect of lowering the boundary temperature.

sistent with the theoretical foundations of the method, because we have used the fourth approximation of the gray atmospheric temperature distribution to compute our model solar atmosphere, instead of the second approximation, $J^{(1)}$, as required by the theory. However, considering that the differences between the second and fourth approximations for the function $q(\tau)$ of equation (1) are quite small,[8] we should expect the corrections for nongrayness to be of the same order of magnitude in both approximations. In any case, it is important to remark that the corrections for nongrayness are, indeed, small and that therefore the gray atmospheric values for the temperature distribution provide an approximation quite accurate when dealing with atmospheres of the solar type.

In view of the results obtained in this paper, it would be profitable to consider, next, an atmosphere with higher effective temperature, since in such case the variation of the continuous absorption coefficient with wave length would be more pronounced than in the case of the sun, with which we were concerned here. It is our intention to examine this problem in the near future.

It is a pleasure again to record my indebtedness to Professor Chandrasekhar for helpful advice.

[8] *Ap. J.*, **100**, 76, Table 1, 1944.

COLOR INDICES OF PROPER-MOTION STARS

W. J. Luyten and P. D. Jose
University of Minnesota and McDonald Observatory
Received December 6, 1947

ABSTRACT

The color indices are given for 139 single stars and for the components of 214 wide doubles with common proper motion, as determined from eye estimates made on blue and yellow plates. Among the double stars, 6 new white dwarfs were found.

The present paper is a continuation of an earlier one, which gave the color indices for 309 stars in the northern hemisphere whose proper motions had been found with the blink microscope.[1] The material now reported on consists of (*a*) 139 single stars between declinations −48° and 0° and with proper motions mainly between 0".1 and 0".3 annually. These stars were found during the regular Bruce proper-motion survey, and their motions were measured in advance of the systematic program of measurement. Since none of these motions have been published before, the data given in Table 1 include the star's designation, the position for 1900, the photographic magnitude, the annual proper motion and its direction, and the adopted color index, which is the average of the estimates made by Jose and Luyten separately. (*b*) 214 wide double stars with common proper motion. Since data for these have been published before,[2] they are identified in Table 2 only by their LDS numbers. However, for a large number of them, new estimates of the photographic magnitudes were made from the Tucson plates, and hence the values for magnitudes given in the columns of Table 2 are largely independent of those given before in the LDS catalogue. The color indices of the components are given in the fourth and fifth columns.

All observations were made with the 36-inch telescope of the Steward Observatory during the years 1944–46 in the same manner as before; and reference may be made to our earlier paper for a description of the method used.

Past experience has shown that the color indices obtained in this way are generally reliable to within 0.3 except in heavily obscured regions. It is possible, therefore, that some stars for which we find color indices of around +0.3 or even +0.4 may actually be white dwarfs (as was the case with W 457). However, the probability of such occurrence is not high, and it is thus disappointing to find that, among the 139 single stars observed, no white dwarf has been found. On the other hand, among 424 components of the wide doubles observed, which have proper motion no larger than those of the single stars, at least seven white dwarfs occur. This confirms again the indication obtained before that white dwarfs appear to be more common among components of binaries than among single stars.

[1] *Ap. J.*, **101**, 87, 1945.

[2] *Pub. Astr. Obs. Minnesota*, **3**, 33, 1941.

TABLE 1

Name	α(1900)	δ(1900)	m_{pg}	μ	p°	IC (Mag.)
L 362-21	0^h07^m1	−40° 57′	12.1	0.10	111	0.8
866-22	0 12.6	− 9 15	12.8	.27	83	1.3
434-30	0 13.8	−36 54	13.0	.22	235	1.7
795-39	0 25.3	−12 21	15.1	.28	79	1.6
868-2	0 55.8	− 5 01	15.0	.22	67	1.4
L 580-71	1 01.1	−28 10	15.2	.27	107	0.3
725-14	1 10.5	−16 05	14.4	.42	124	1.6
725-12	1 12.3	−16 09	10.8	.23	67	1.0
725-26	1 16.8	−16 43	13.3	.24	75	1.4
654-21	1 28.2	−21 59	15.6	.23	87	1.7
L 367-53	1 38.2	−42 42	14.4	.13	106	1.7
510-38	1 40.6	−32 36	13.1	.20	89	0.5
510-37	1 41.1	−32 36	12.5	.15	108	1.0
801-20	2 31.1	−11 21	14.5	.11	64	1.5
801-19	2 31.2	−11 22	13.7	.10	21	0.9
L 801-54	2 35.3	−14 00	12.0	.27	73	1.0
730-40	2 47.4	−18 34	14.4	.20	180	1.9
730-9	2 52.7	−16 17	14.7	.28	120	1.9
515-20	3 06.2	−32 18	14.3	.12	102	1.7
515-19	3 06.3	−32 18	13.2	.06	115	0.6
L 443-43	3 10.1	−38 14	14.8	.27	38	1.6
876-35	3 30.1	− 7 54	14.9	.24	120	1.6
444-21	3 30.2	−37 54	14.3	.24	104	1.8
876-39	3 36.2	− 8 09	14.1	.26	164	0.7
589-17	3 41.2	−28 12	9.7	.27	51	0.8
L 589-18	3 41.2	−28 10	13.1	.13	34	1.1
517-12	3 56.1	−31 15	15.4	.15	25	1.5
517-13	3 56.1	−31 15	14.9	.08	104	1.0
446-17	4 05.9	−36 29	13.5	.14	120	0.6
446-14	4 06.0	−36 21	13.3	.17	180	1.9
L 446-13	4 06.4	−36 25	12.2	.24	102	1.0
951-48	4 25.2	− 3 16	14.7	.29	146	0.7
807-9	4 29.9	−11 02	15.2	.28	258	1.5
736-7	4 44.0	−15 55	14.8	.25	134	1.4
449-48	5 12.6	−38 53	15.3	.20	20	1.6
L 453-31	6 36.2	−36 53	13.5	.29	167	1.2
742-24	6 48.9	−16 07	12.8	.30	121	0.2
455-39	7 18.8	−36 33	14.5	.27	166	0.9
315-97	8 31.8	−47 02	13.2	.24	164	1.1
963-53	8 33.3	− 3 34	12.6	.34	187	1.1
L 532-12	8 49.9	−30 29	14.4	.25	265	1.3
676-34	8 51.6	−22 35	14.9	.26	316	1.3
604-111	8 59.8	−28 05	14.0	.28	121	1.4
461-137	9 05.2	−38 43	15.6	.23	139	1.2
461-163	9 05.4	−39 34	14.4	.24	213	1.2
L 461-56	9 14.7	−36 39	15.3	.16	142	1.3
461-53	9 17.0	−36 31	12.4	.26	106	0.7
533-116	9 17.1	−33 05	14.7	.27	186	1.3
750-58	9 36.1	−17 54	15.5	.18	313	1.6
679-50	9 45.7	−22 05	14.3	0.26	156	1.3

TABLE 1—*Continued*

Name	α(1900)	δ(1900)	m_{pg}	μ	p°	IC (Mag.)
L 895-9	9^h45^m9	− 6° 16′	14.5	0.29	137	1.0
463-15	9 53.4	−35 40	13.0	.26	268	1.4
463-7	9 53.7	−35 25	15.6	.21	271	0.3
751-43	9 54.4	−16 57	14.7	.24	177	1.4
464-13	10 09.2	−35 28	14.4	.25	277	1.5
L 465-40	10 28.1	−36 12	13.1	.30	268	1.2
897-47	10 30.0	− 8 53	14.8	.28	125	1.5
465-43	10 36.6	−36 22	12.2	.27	133	1.0
537-90	10 39.0	−33 13	15.2	.18	272	1.4
538-18	10 47.3	−31 30	12.5	.26	282	1.2
L 754-6	10 57.4	−15 23	14.4	.30	300	1.2
898-23	11 01.6	− 6 53	14.7	.24	244	1.3
900-32	11 25.8	− 7 26	14.1	.25	152	1.1
758-76	12 04.7	−18 10	15.2	.22	300	1.7
471-28	12 37.8	−37 11	13.2	.16	237	0.9
L 471-27	12 38.2	−37 09	13.7	.18	288	1.2
544-38	12 41.4	−32 47	12.5	.22	181	0.8
832-12	12 47.0	−11 32	15.5	.25	202	1.2
545-55	13 10.7	−33 16	12.9	.20	176	1.4
834-11	13 32.2	−10 18	13.2	.21	152	1.3
L 834-9	13 32.3	−10 16	11.7	.16	139	1.1
834-103	13 36.2	−13 30	14.5	.30	168	1.5
546-142	13 39.4	−31 51	13.7	.27	252	0.7
619-49	13 45.7	−27 05	13.9	.24	168	1.4
619-50	13 45.7	−27 05	15.2	.24	168	0.0
L 547-60	13 46.6	−32 06	14.8	.28	225	1.5
764-24	14 05.9	−16 13	14.6	.26	315	1.6
764-6	14 12.2	−15 21	13.8	.25	160	1.3
980-19	14 16.3	− 1 25	12.8	.30	228	0.8
764-29	14 17.0	−16 35	14.0	.08	262	1.6
L 764-28	14 17.1	−16 35	16.0	.25	232	1.4
836-24	14 20.3	−11 23	15.2	.28	268	1.6
980-76	14 22.9	− 0 41	11.8	.27	295	0.9
549-52	14 26.1	−31 26	11.5	.27	256	0.8
333-48	14 28.6	−45 42	16.5	.29	238	1.2
L 621-64	14 39.4	−27 09	15.2	.15	259	1.3
550-19	14 46.2	−31 19	12.3	.28	248	0.4
766-90	14 52.5	−19 17	15.5	.27	207	1.5
910-91	14 55.2	− 8 59	12.3	.35	203	0.8
623-7	15 05.8	−24 58	12.7	.28	278	1.3
L 407-39	15 16.9	−41 52	13.6	.29	232	1.1+
912-65	15 26.6	− 8 09	13.9	.27	214	1.3
984-17	15 38.3	− 1 14	15.4	.24	216	0.7+
984-25	15 40.5	− 1 56	12.3	.29	249	0.9
553-105	15 49.3	−31 44	14.5	.13	240	1.3
L 553-14	15 49.4	−31 40	13.0	.13	240	1.2
553-30	15 58.0	−32 46	13.2	.26	258	0.9
555-95	16 36.4	−33 03	12.2	.29	206	0.8
555-94	16 36.6	−33 07	12.8	.21	215	0.6
916-36	16 45.5	− 8 14	14.0	0.28	223	0.9+

TABLE 1—*Continued*

Name	$\alpha(1900)$	$\delta(1900)$	m_{pg}	μ	p°	IC (Mag.)
L 1060-54	16^h52^m3	− 0°01′	13.4	0.32	187	1.1
556-6	16 53.7	−30 26	15.3	.24	197	0.9+
701-19	17 03.1	−22 49	13.4	.28	235	0.3+
989-21	17 04.1	− 1 50	11.5	.24	205	0.4+
629-108	17 05.8	−27 39	14.7	.27	246	1.1+
L 413-148	17 05.9	−43 12	12.4	.28	176	0.9+
629-77	17 15.7	−27 02	13.5	.27	236	1.2
413-74	17 15.9	−41 46	15.6	.24	214	1.1+
774-66	17 24.6	−18 48	16.0	.24	113	1.1+
846-51	17 34.6	−13 42	14.7	.29	217	1.1+
L 486-135	17 36.8	−38 40	14.3	.15	149	1.0
559-103	17 48.1	−32 30	15.9	.17	195	1.2
559-63	17 51.8	−31 39	16.4	.08	240	0.9
559-68	17 51.9	−31 48	15.6	.26	162	1.0
560-36	18 00.4	−32 32	17.3	.16	193	1.1
L 560-64	18 08.1	−33 19	13.0	.29	190	0.9
419-73	19 02.9	−41 40	15.2	.26	159	1.3
419-91	19 03.8	−41 57	13.8	.07	201	0.7
995-20	19 15.5	− 2 09	15.3	.30	181	0.4
996-72	19 33.3	− 3 04	12.5	.29	114	0.6
L 708-33	19 34.3	−22 58	14.7	.18	180	1.3
708-32	19 34.4	−22 58	11.0	.26	183	0.6
926-41	20 09.1	− 7 35	12.3	.28	179	1.0
926-12	20 17.7	− 6 38	13.7	.14	246	1.2
926-11	20 17.8	− 6 39	11.8	.13	206	0.6
L 569-25	21 10.0	−31 17	15.7	.16	150	1.5
785-30	21 12.3	−17 20	14.6	.09	148	1.3
785-31	21 12.3	−17 21	15.6	.19	106	1.4
1002-14	21 28.5	− 0 02	13.2	.21	94	0.5
356-20	21 56.4	−45 39	12.8	.13	210	1.1
L 356-19	21 56.6	−45 40	12.4	.29	122	1.0
787-64	22 00.2	−17 02	12.2	.27	232	1.1
356-17	22 05.9	−45 39	14.5	.26	143	1.6
574-53	22 45.7	−33 09	14.4	.26	140	1.2
935-25	23 07.8	− 6 04	13.3	.23	101	1.2
L 431-35	23 11.1	−41 45	14.4	.30	89	1.7
791-74	23 12.9	−19 28	13.6	.21	165	1.4
935-80	23 13.4	− 8 38	16.2	.28	103	1.6
937-17	23 55.5	− 7 03	13.9	0.25	228	1.4

TABLE 2

LDS	m_A	m	IC_A	IC_B	LDS	m_A	m_B	IC_A	IC_B
1	12.6	14.7	0.2	0.5*	145	12.8	14.0	0.9	1.4
2	13.5	13.9	1.3	1.7	150	15.0	15.2	1.7	1.7
5	11.1	11.6	1.0	1.1	151	11.6	11.7	1.0	1.1
7	11.6	14.4	1.0	1.7	153	13.6	14.6	1.2	1.3
9	11.0	11.6	1.1	1.2	156	13.6	14.9	0.8	1.0
10	12.8	14.5	0.8	1.1	160	11.2	13.8	0.8	1.4
14	14.8	15.5	1.6	1.8	161	8.5	14.8	0.5	1.4
18	14.2	14.4	1.7	1.8	162	7.5	12.7	0.3	1.4
19	11.4	14.9	1.1	1.7	163	14.7	15.3	1.5	1.5
23	10.6	11.4	0.3	1.0	165	11.6	12.4	0.5	0.7
24	12.7	13.5	1.4	1.6	167	9.5	13.8	0.8	1.5
26	12.3	14.0	0.9	1.4	168	11.4	15.7	0.7	1.4
27	14.3	15.3	1.4	1.8	170	12.7	13.3	1.0	1.2
29	11.7	14.1	0.5	1.2	172	13.8	15.5	0.6	0.8*
30	13.7	14.4	1.6	1.4	173	9.0	10.7	0.5	0.5
32	13.3	14.6	1.5	1.9	176	12.7	14.8	0.6	0.9
33	14.0	14.7	1.6	2.0	177	13.7	15.1	1.3	1.2
34	10.0	12.4	0.9	1.6	180	9.6	9.9	0.8	0.9
35	12.4	14.1	0.8	1.5	184	12.8	13.2	0.4	0.9
37	12.2	13.4	1.1	0.7	197	9.7	13.9	0.5	1.3
38	14.4	15.2	1.6	2.0	200	14.0	14.1	1.1	1.3
41	14.3	14.7	1.8	1.8	205	11.5	14.8	0.3	1.1
48	14.0	14.5	1.4	1.3	207	12.1	14.9	0.7	1.3
54	13.6	14.2	1.2	1.2	212	10.9	15.4	0.4	1.3
55	11.5	11.9	1.5	1.5	213	14.9	15.3	1.0	1.1
61	8.5	14.7	0.5	1.8	224	10.8	14.8	0.7	1.4
62	12.5	13.0	1.0	1.1	225	13.5	13.5	1.3	1.4
65	15.0	15.5	1.8	2.0	226	13.8	14.3	1.0	1.3
66	14.0	15.0	1.4	1.4	230	9.4	14.3	0.6	1.3
72	13.2	13.9	0.8	1.0	235	12.4	15.1	0.9	−0.2
73	15.5	15.7	2.0	1.8	240	13.3	15.2	0.7	0.8*
76	13.5	14.0	1.3	1.3	247	14.6	14.9	0.9	1.2
80	9.5	13.2	.....	1.4	253	11.0	12.6	0.7	1.2
84	12.3	16.0	1.1	.....	259	12.6	12.8	0.8	0.8
87	12.8	13.0	1.2	1.4	261	13.9	14.1	1.4	1.5
89	11.0	13.9	0.9	1.4	262	11.0	14.4	0.7	1.4
90	11.9	14.3	1.0	1.6*	263	14.4	15.4	1.1	1.0
107	13.0	15.1	0.5	0.7	273	14.2	14.4	1.1	1.2
108	12.9	14.0	1.6	1.8	281	9.7	12.2	0.8	1.0
112	13.9	14.2	1.3	1.4	283	12.5	13.2	1.0	1.1
124	13.1	13.4	1.3	1.3	290	12.3	15.4	1.0	1.4
125	13.6	13.8	1.7	1.8	293	13.8	15.0	1.2	1.4
126	9.0	12.9	0.4	1.4	296	13.6	15.7	1.4	1.7
128	13.4	13.7	1.0	1.1	297	13.3	15.7	1.1	1.5
129	10.8	13.2	1.4	1.7	300	14.2	15.0	1.6	1.5
134	13.9	14.4	1.8	1.8	307	14.3	15.3	0.8	1.0*
136	11.4	11.5	0.9	1.0	308	11.5	15.2	0.7	1.4
137	10.4	10.9	0.7	0.8	313	13.2	15.0	1.2	1.4
138	13.9	14.1	1.4	1.5	315	12.0	14.5	0.5	0.9
141	11.4	15.0	1.2	1.6	317	10.7	15.2	0.7	1.4

TABLE 2—*Continued*

LDS	m_A	m_B	IC_A	IC_B	LDS	m_A	m_B	IC_A	IC_B
318	14.0	14.4	1.3	1.4	533	13.1	15.7	0.5	1.5
320	11.9	14.7	0.9	1.2	535	11.8	13.9	0.6	1.2
323	13.0	15.0	1.0	1.6	539	15.0	15.3	1.2	0.3*
330	10.0	14.0	1.0	1.5	547	9.9	14.7	0.7	1.3
340	14.9	15.6	1.6	1.5	554	13.8	15.8	0.8	0.7
347	7.4	15.0	.....	1.5	563	12.3	13.0	1.1	1.2
348	10.7	13.0	1.1	1.5	564	14.7	15.0	0.9	0.7
349	15.0	15.1	1.6	1.6	571	13.6	13.8	0.9	1.1
354	10.8	15.3	0.6	1.3	575	13.8	14.7	1.1	1.0
368	13.0	14.5	1.3	1.7	576	11.9	12.7	0.5	0.6*
384	13.5	13.9	0.3	0.9	580	13.3	13.6	1.2	1.3
385	9.4	14.9	0.7	1.4	593	14.0	14.1	1.1	1.1
388	14.2	15.0	0.8	1.0	602	14.3	15.1	0.8	0.9
389	13.8	15.4	0.9	1.6	605	14.3	14.6	0.6	0.6
390	13.6	14.9	1.5	1.5	607	16.1	16.2	0.6	0.6*
391	12.5	14.2	1.2	1.3	611	11.3	12.2	1.0	1.2
393	15.1	15.4	1.6	1.7	613	15.4	15.7	0.4	0.7
399	11.7	16.2	0.9	1.8	617	12.5	12.8	0.3+	0.3+
403	13.9	14.0	1.7	1.7	621	15.1	15.7	0.5+	0.6+
406	11.8	15.2	0.8	1.4*	629	11.4	12.6	0.4	0.7
407	13.6	14.0	1.3	1.3*	640	13.1	13.8	0.8	0.7*
409	12.1	14.5	0.6	1.3	641	9.7	11.4	0.5	0.7
413	9.5	14.0	0.9	1.2*	651	12.3	13.4	0.5	0.8
414	13.4	13.9	1.2	1.4	653	14.3	14.5	1.2	1.3
418	10.0	15.1	0.6	1.1	678	12.0	13.5	−0.3	1.4
424	15.5	16.3	1.2	1.0	682	10.7	14.2	0.6	1.3
426	12.6	13.1	1.3	1.3	683	15.1	15.4	1.1	0.0
428	14.2	14.3	1.3	1.5	685	10.7	13.6	0.4	0.8
431	13.5	14.8	1.1	1.6	694	12.0	14.5	0.5	1.4
437	12.8	14.3	1.4	1.6	709	13.0	14.3	1.0	1.4
440	15.0	15.4	1.7	1.6	715	14.1	15.5	1.6	1.7*
451	12.8	15.6	0.8	1.4	716	11.0	14.3	0.7	1.5
455	14.7	15.0	0.0	1.6*	717	13.5	14.1	1.4	1.6
459	14.5	16.5	1.4	1.5*	722	13.7	14.7	0.5	0.5
466	11.1	14.9	0.9	1.6	724	13.5	14.0	0.9	1.2
469	12.3	14.8	0.8	1.4	725	12.5	14.4	1.2	1.4
477	13.8	14.0	1.6	1.6	727	14.7	15.3	1.2	1.4
480	15.3	15.5	1.7	1.7	729	14.8	15.5	1.6	1.7*
483	11.9	15.5	0.9	1.8	731	14.3	15.2	1.4	1.5
486	13.6	15.5	1.3	.....*	737	14.2	15.0	0.7+	1.1+
487	12.1	14.3	0.8	1.5	738	8.1	15.4	0.8	1.6
488	14.0	14.3	1.0	1.1*	741	14.3	15.5	1.6	1.3
492	14.6	15.5	1.4	1.5	743	14.5	15.2	1.4	1.5
493	16.0	16.2	1.8	1.9	744	14.6	14.8	1.2	1.3
498	13.5	15.0	0.7	1.6	745	11.4	14.6	0.5	1.4
500	13.4	14.9	0.3	0.3	748	9.7	15.0	0.6	1.5
503	9.5	14.2	0.6	1.3*	749	11.2	14.4	0.9	−0.1
507	7.5	14.5	0.3	0.9	750	10.6	13.9	0.5	1.6
510	15.0	16.0	1.4	1.4	751	12.1	12.3	1.0	0.9
527	13.2	15.2	0.5	1.5*	752	15.0	16.2	1.6	1.7

TABLE 2—*Continued*

LDS	m_A	m_B	IC_A	IC_B	LDS	m_A	m_B	IC_A	IC_B
756.....	11.6	14.3	0.5	1.5	820.....	10.8	13.6	1.1	1.5
761.....	12.9	14.9	1.3	1.6	821.....	12.2	12.7	0.6	0.7
766.....	14.2	15.5	−0.1	1.3	828.....	14.4	15.8	1.1	1.3
768.....	12.3	13.7	0.9	1.6	830.....	14.6	14.8	1.5	1.5
776.....	11.0	15.5	0.9	1.3					
779.....	12.6	15.5	0.7	1.4					
780.....	13.1	14.2	1.0	1.4					
785.....	14.7	14.7	1.6	0.2					
793.....	13.3	14.6	1.5	1.6					
810.....	11.8	13.0	1.2	1.2					

NOTES TO TABLE 2

1 See also *Harvard Ann. Card*, No. 712 (1945).
90 Declination of this star should read −31:25 instead of −30:25.
172 Magnitude of *B* should read 15.5 instead of 13.5.
240 B is nf instead of preceding.
307 B is np instead of sp.
406 B is south instead of sp.
407 B is sp instead of nf.
413 B is sf instead of np.
455 B is sp instead of nf.
459 B is nf instead of sp.
486 Separation is 5″ instead of 10″.
488 Declination should read −29:26 instead of −27:26; separation is 93″.
503 B is nf instead of sf.
527 B is north instead of nf.
539 B is pr instead of fo.
576 This is the same pair as LDS 577.
607 B is fo instead of pr.
640 This is the same pair as LDS 639, whose declination should read −25:07 instead of −24:07.
715 B is sf instead of np.
729 For direction of proper motion read 263 instead of 221.

NOTES

THE VELOCITY-CURVE OF THE CLUSTER-TYPE VARIABLE UY BOOTIS

The variability of UY Bootis was discovered by C. Hoffmeister[1] in 1935. He noted that it went through its light-variations rapidly, from 9.5 to 10.5 mag., and concluded that it must be an RR Lyrae star. G. Lange[2] observed it in July and August of the same year and gave the elements

$$\text{Maximum} = \text{JD } 2427988.22 + 0^d.2822\,E\,.$$

This period was later found to be in error,[3] and the following new elements were given by Gurjev:

$$\text{Maximum} = \text{JD } 2429025.433 + 0^d.65079\,E\,.$$

An investigation by R. Prager,[4] on the basis of the Harvard plate material, revealed that an apparently abrupt change in the period—from 0.6508552 to 0.6507849 day—took place in 1928. After that date he found that the elements held:

$$\text{Maximum} = \text{JD } 2425688.836 + 0^d.6507849\,E\,.$$

UY Bootis has not hitherto been investigated spectroscopically, because of its faintness (9.5–10.5 mag. photographic) and rapid changes in light. The period is so short, however, that it was possible to cover the curve almost completely in two successive nights of observing. In this way the effects of a possible change in the velocity-curve or in the period during observation were minimized. Two plates taken a week earlier, however, gave velocities that agreed with those taken during the two-night run.

Eighteen spectrograms were obtained with a two-prism spectrograph and a 3½-inch camera at the 36-inch refractor, the combination giving a dispersion of 130 A/mm at $H\gamma$. Sixteen of these plates were taken in a continuous series during two nights in May, 1947, when the star was above the horizon all night. Exposure times ranging from 22 to 88 minutes were determined by estimates of the brightness of the variable in the finder and on the slit of the spectrograph.

Eight plates of four standard stars of known velocity were observed with the same adjustments of the spectrograph, in order to set up a dispersion table.

Table 1 gives a list of the spectrograms; JD of mid-exposure; geocentric phases in fractional parts of the period from maximum, computed with the epoch given in the next paragraph and with Prager's period of 0.6507849 day; and the radial velocities in kilometers per second.

One maximum was observed at JD 2432306.759 (heliocentric) by G. H. Herbig with the 6-inch refractor at the Students' Observatory in Berkeley. This maximum was 2 hours and 11 minutes late according to Prager's post-1928 elements. This difference checked with the estimates of magnitude made while the spectrograms were being taken.

The velocities are plotted in Figure 1. The observations indicate that minimum velocity lags about 0.10 or 0.15 period behind maximum light, in approximate agreement with observations of similar variables, such as RR Lyrae[5] and W Canum Venaticorum.[6]

[1] *A.N.* **255**, 401, 1935.

[2] *Tadjik Circ.*, No. 11, 1935.

[3] *Tadjik Circ.*, No. 40, 1938.

[4] *Harvard Bull.*, No. 911, 1939.

[5] Kiess, *Lick Obs. Bull.*, **7**, 140, 1913 (No. 232); Sanford, *Ap. J.*, **67**, 319, 1928; *Mt. W. Contr.*, No. 351.

[6] Joy, *Ap. J.*, **88**, 408, 1938; *Mt. W. Contr.*, No. 595.

The velocity range is approximately 100 km/sec. The mean probable error of a plate calculated from the agreement of individual lines on a spectrogram is ±11 km/sec. The normal velocity of the star is +145 km/sec.

The measurements were based principally on the hydrogen lines ($H\beta$, $H\gamma$, $H\delta$) and on the K line of *Ca* II, although λλ 4045 (*Fe* I), 4226 (*Ca* I), and 4383 (*Fe* I) were used on some of the plates.

TABLE 1

RADIAL VELOCITIES OF UY BOOTIS

Plate No.	JD 2432300+	Phase (Period)	Velocity (Km/Sec)	Plate No.	JD 2432300+	Phase (Period)	Velocity (Km/Sec)
31643	12.788	0.264	+106	31657	19.852	0.119	+ 99
31644	12.826	.323	+119	31658	19.874	.153	+112
31650	19.684	.861	+140	31659	19.912	.211	+107
31651	19.718	.913	+177	31660	19.932	.242	+102
31652	19.746	.956	+155	31661	20.687	.402	+122
31653	19.768	.990	+139	31662	20.737	.479	+160
31654	19.783	.013	+138	31663	20.803	.580	+167
31655	19.800	.039	+124	31664	20.858	.665	+212
31656	19.830	0.085	+ 98	31665	20.915	0.752	+175

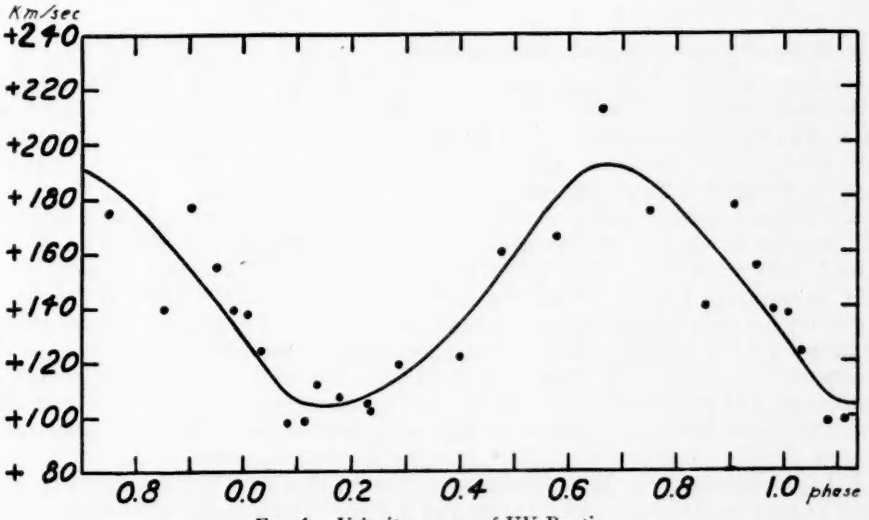

FIG. 1.—Velocity-curve of UY Bootis

The spectrum of UY Bootis, as estimated from K and the metallic lines, varies between about A1 and A8, the earlier type appearing when the star is bright. The hydrogen lines, in general, correspond to a somewhat later type; they suddenly become wider and stronger at maximum light.

I wish to express my gratitude to George H. Herbig for his suggesting and outlining this work, and to Harold F. Weaver for his co-operation.

A. VIRGINIA FARQUHAR

LICK OBSERVATORY
December 10, 1947

THE METHOD OF "COLOR-DIFFERENCE"

In *Ap. J.*, **104**, 403, 1946, J. L. Greenstein described a method of distinguishing between interstellar reddened B stars and normal stars of later spectral type without knowledge of the spectral types. The method is based on the entirely different distribution of energy in the spectra of these two groups. I proposed the same method in 1938[1] and later in 1942[2] and used it in several papers, all of which are not yet published. The difficulty of international exchange of scientific results has prevented them from being known in the United States; therefore, the following short note may be presented.

The method is a part of a more general method, which I called the method of "Color-Difference" (*CD*). *CD* is the difference between a short-wave color index and a long-wave color index, for instance, the difference *CI* λ 3700/λ 4800 minus *CI* λ 4800/λ 6300. The method may be applied in principle in the following problems:

1. Distinction between reddened B stars and normal stars of later spectral types without knowledge of spectral type.
2. Classification of stars in four or five spectral "groups" without knowledge of spectral type and without the disturbing influence of interstellar reddening.
3. Separation of giants and dwarfs in the later spectral types, partly without knowledge of spectral type.
4. Study of the Balmer jump in B and A stars.
5. Distinction between physical and nonphysical members of open star clusters.

Some observational examples may be listed.

1. Let us compare the *CD* of 9 strongly reddened B stars and 4 unclassified red stars in the open cluster NGC 6910 (Table 1). In the long-wave *CI* (and also in the International *CI*) the groups could not be separated, but the *CD* (by means of an additional short-wave *CI*) demonstrates the entirely different intensity distribution in the two groups. The stars in the second group must be normal K stars.

2. By appropriate selection of wave lengths, the *CD* is independent of interstellar reddening; it shows only the deviation of black-body radiation of stars. This deviation depends systematically on spectral type. For a mixture of giants and dwarfs the mean *CD* is as shown in Table 2. By using a fourth wave length near λ 4200, we are able also to distinguish between A-type stars and F and G stars. The method is proposed particularly for faint stars, for it allows the classification especially of the later-type stars, besides the early types. In connection with this, it would be interesting to ascertain whether the numerous additional stars found by Baade[3] on red-sensitive plates in Milky Way star clouds are faint reddened B stars or normal K dwarfs in the neighborhood of the sun. The *CD* differs about 1 mag. or more for the two cases.

3. In the open cluster M 37 there are seventeen G giants, besides many G dwarfs. The *CD* for the two groups are as shown in Table 3. The long-wave *CI* is the same for giants and dwarfs, but the *CD* is quite different. For K stars the effect is still greater. Here we have a useful variation of the well-known spectroscopic method of Adams and Kohlschütter, based on the temperature difference between giants and dwarfs. It should be of importance for the determination of the star-density function.

4. The *CD* is a measure of the Balmer jump, which may be easily derived from it. The method applied to A-type stars in open clusters gives the following result: In 4

[1] *Zs. f. Ap.*, **15**, 225, 1938.

[2] *A.N.*, **272**, 179, 1942.

[3] *Trans. I.A.U.*, **6**, 452, 1938.

clusters studied up to now the brightest A stars show an abnormally strong Balmer jump, while the A stars, $1^m.0$ or $1^m.5$ fainter, are normal. The brighter A-cluster stars are separated from the normal A-cluster stars by a minimum in the luminosity function.

TABLE 1

	CI λ 4800/λ 6300	*CI* λ 3700/λ 4800	*CD*
9 B stars	$+0^m.98$	$+1^m.20$	$+0^m.22$
4 red stars	+1.19	+2.57	+1.38

TABLE 2

	B0	A0	F0	G0	K0	K5
CD	$0^m.00$	$+0^m.7$	$+0^m.8$	$+0^m.8$	$+1^m.4$	$+1^m.8$

These are the same stars for which Trumpler found an abnormally high absolute luminosity. Obviously, they are surrounded by an extended *H* envelope.

5. In many cases the field stars in open clusters (especially in reddened clusters) cannot be distinguished from physical members because they are exactly on the main

TABLE 3

	CI λ 4800/λ 6300	*CI* λ 3700/λ 4800	*CD*
dG	$+0^m.88$	$+1^m.65$	$+0^m.77$
gG	+0.92	+2.33	+1.41

TABLE 4

BALMER JUMP OF BRIGHTEST A STARS

	Obs.	Norm.	Obs.−Norm.
NGC 7654*	$1^m.7$	$1^m.2$	$+0^m.5$
NGC 663	1.3	0.9	+ .4
NGC 6811	1.8	1.2	+ .6
M 37	1.9	1.2	+0.7

* *Veröff. d. Univ. Sternw. Göttingen*, No. 82, 1946.

ranch of the color-magnitude diagram. But generally this is the case only in either the long-wave *CI* or the short-wave *CI*, but not both. Therefore, field stars may be selected by means of the diagram of *CD* and magnitude. In this way 63 field stars in four open clusters were recognized. Half of these could not be distinguished from physical members in a simple color-magnitude diagram of International *CI*.

These results induced me to propose a reform of the astronomical integral photometry.[4] The main point is the need to use the wave lengths for photometry in such a way that the resulting magnitudes represent as far as possible the intensity distribution in

[4] *Veröff. d. Univ. Sternw. Göttingen*, Nos. 79–81, 1946.

stellar spectra commonly known from spectral-photometric work on bright stars. The International wave lengths of m_{pv} and m_{pg} are not consistent with this requirement and therefore are unsuitable for work in connection with the method of Color-Difference. They should be replaced by the wave lengths proposed above. There may be a better selection of wave lengths (except for λ 4800), especially in the ultraviolet. The ultraviolet, as far as I can see, will be the most important spectral region for further work in astronomical integral photometry. Any progress in this direction will be very useful for stellar statistical purposes.

W. BECKER

HAMBURG-BERGEDORF
October 1947